The descriptions of sites, cores and data included in these site reports were completed within one year of the cruise, but many of the topical chapters that follow were completed at a later date. More data were acquired and authors' interpretations matured during this interval, so readers may find some discrepancies between site reports and topical papers. The timely publication of the *Initial Reports* series, which is intended to report the early results of each leg, precludes incurring the delays that would allow the site reports to be revised at a later stage of production.

3. SITE 612[1]

Shipboard Scientific Party[2]

HOLE 612

Date occupied: 2332 hr., 25 August 1983

Date departed: 0525 hr., 31 August 1983

Time on hole: 5 days, 6 hr., 25 min.

Position: 38°49.21′N, 72°46.43′W

Water depth (sea level; corrected m, echo-sounding): 1386

Water depth (rig floor; corrected m, echo-sounding): 1396

Bottom felt (m, drill pipe): 1414.3

Penetration (m): 675.3

Number of cores: 72

Total length of cored section (m): 675.3

Total core recovered (m): 580.66

Core recovery (%): 86.0

Oldest sediment cored:
Depth sub-bottom (m): 675.3
Nature: Black, glauconitic, foraminiferal, marly shale
Age: late Campanian
Measured velocity (km/s): 2.03

Basement: Not attempted

GEOLOGIC SETTING AND OBJECTIVES

Hole 612

Site 612 is on the middle part of the New Jersey continental slope in 1404 m water depth. The surface of the continental slope in this region is characterized by a complex series of submarine canyons and associated smaller channels whose axes trend southeastward downslope. Site 612 is located in one of the smaller channels, which is subsidiary to Carteret Canyon (see Figure 7 of Background and Objectives chapter, this volume). The northwestern edge of a broad (~10 km maximum width) seafloor outcrop belt of middle Eocene strata is approximately 2 km southeast of Site 612. Site 612 is positioned approximately 0.7 km northwest of the intersection of U.S.G.S. multichannel seismic Lines 25 and 34. The COST B-3 well is 10 km north of Site 612; ASP 14 is 6 km to the west; ASP 15 is 6.4 km to the southwest.

Structurally, Site 612 occupies the crest of a gently dipping anticline. The arching of this structure appears to be related to differential compaction and faulting of sedimentary beds deposited in front of and behind a buried Late Jurassic–Early Cretaceous shelf-edge reef (Poag, 1985). The arched geometry has been accentuated by severe erosion, particularly of middle Eocene strata, that has significantly thinned the sedimentary sequence in the landward direction, toward the COST B-3 well projection (see Figure 5 of Background and Objectives chapter, this volume). The landward dip of strata between the COST B-3 projection and Site 612 persisted until the early Miocene, when the depositional trough beneath the COST B-3 projection was filled with terrigenous deposits. This infilling initiated a seaward dip, which has been maintained to the present.

Another apparent consequence of differential compaction along Line 25 is the development of a series of normal faults, some of which display the characteristic downward-increasing throw of growth faults. A prominent system of such normal faults is manifest on Line 25 approximately 2 km southeast of Site 612, at the edge of the middle Eocene outcrop belt (see Figure 5 of Background and Objectives chapter, this volume).

Mapping the top of the Cretaceous strata has shown that the post-Cretaceous structural closure beneath Site 612 is only apparent. In fact, the structural closure on the top of the Cretaceous is a few kilometers northwest of the COST B-3 well. Since no hydrocarbon accumulations other than methane gas were encountered in the B-3 well (Scholle et al., 1980), drilling at Site 612 was not considered to be geologically hazardous.

The location for Site 612 was selected to provide a reasonably complete Cenozoic and Upper Cretaceous stratigraphic section in a middle continental slope setting that would link the sections drilled at the COST B-3 well and at Site 605. It also provides a western Atlantic counterpart to Site 548 on Goban Spur (upper continental slope of Ireland; Graciansky, Poag et al., 1985) and Site 369 off Morocco (Lancelot, Seibold, et al., 1978). The general objectives of Site 612 are the same as those of the other New Jersey margin sites (see Background and Objectives chapter, this volume).

---

[1] Poag, C. W., Watts, A. B., et al., *Init. Repts. DSDP*, 95: Washington (U.S. Govt. Printing Office).

[2] Addresses: C. Wylie Poag (Co-Chief Scientist), U.S. Geological Survey, Woods Hole, MA 02543; Anthony B. Watts (Co-Chief Scientist), Lamont-Doherty Geological Observatory, Palisades, NY 10964; Michel Cousin, Laboratoire de Géodynamique Sous-Marine, Université Pierre et Marie Curie VI, B. P. 48, 06230 Villefranche-sur-Mer, France; David Goldberg, Lamont-Doherty Geological Observatory, Palisades NY 10964; Malcolm B. Hart, Department of Geological Sciences, Plymouth Polytechnic, Plymouth PL4 8AA, Devon, United Kingdom; Kenneth G. Miller, Lamont-Doherty Geological Observatory, Palisades, NY 10964; Gregory S. Mountain, Lamont-Doherty Geological Observatory, Palisades, NY 10964; Yuji Nakamura, Laboratory for Earthquake Chemistry, University of Tokyo, Tokyo 113, Japan; Amanda Palmer, Department of Geology and Geophysical Sciences, Princeton University, Princeton, NJ 08544 (present address: Ocean Drilling Program, 1000 Discovery Drive, Texas A&M University, College Station, TX 77840); Paul A. Schiffelbein, Deep Sea Drilling Project, Scripps Institution of Oceanography, La Jolla, California 92093 (present address: E. I. duPont de Nemours, Louviers Bldg., Wilmington, DE 19898); B. Charlotte Schreiber, Department of Earth and Environmental Sciences, Queens College (CUNY), Flushing, NY 11367; Martha Tarafa, Chemistry Department, Woods Hole Oceanographic Institution, Woods Hole, MA 02543; Jean E. Thein, Geologisches Institut, Universität Bonn, D-53 Bonn 1, Federal Republic of Germany (present address: Fachrichtung 15.5, Angewandte Geochemie, Universität des Saarlandes, D6600 Saarbrucken, Federal Republic of Germany); Page C. Valentine, U.S. Geological Survey, Woods Hole, MA 02543; Roy H. Wilkins, Department of Earth and Planetary Sciences, Massachusetts Institute of Technology, Cambridge, MA 02139.

OPERATIONS

St. John's Port Call

Leg 95 began officially at 1851 hr., 17 August 1983, when *Glomar Challenger* docked at Pier 9, St. John's, Newfoundland, Canada. The port call was a brief one involving the routine operations of changing crews and on-loading supplies and equipment. The major accomplishments were

1. A full Tuboscope drill pipe inspection was completed. No suspect joints of pipe were identified.
2. We loaded and checked out Schlumberger logging equipment.
3. We inspected Cat Engine No. 9 in preparation for overhaul in Ft. Lauderdale.
4. We topped off fresh water.
5. A representative from Pressure Coring, Inc. schooled the drill crew on drilling procedures with a pair of new Polycrystalline Diamond Compact bits, which had been brought aboard for use at Site 603.

All scheduled work items had been completed and the vessel was ready to get underway at 2000 hr. on Saturday, 20 August. However, departure was delayed until midnight while awaiting a shipment of ^{14}C and ^{35}S isotopes ordered by Organic Geochemist Martha Tarafa. The isotopes arrived on a delayed flight from Montreal and were delivered to the ship at 2310 hr.

St. John's to Site 612

Glomar Challenger departed St. John's at 0007 hr., Sunday, 21 August. On board were 45 Global Marine Inc. (GMI) and 29 Scripps personnel. The first 2 days of steaming were in poor weather with high seas and some fog and drizzle. Speed was reduced to 7 knots at times. The following 2 days were passed in exceptionally fine weather with temperatures becoming more pleasant as the vessel proceeded southwest toward the first site of the voyage, about 100 miles off the New Jersey coast. Following winds improved the ship's speed so that by the time the turn was made to approach the site on the fifth day, the ship was back on schedule.

Site 612 (NJ-2) was approached from the northeast on the evening of 25 August 1983. Following a good satellite navigation fix at 2040 hr., the ship crossed control siesmic Line 25 (U.S.G.S.) at shot point 3670, then proceeded northwestward in an attempt to achieve a high-resolution seismic survey (water gun) along Line 25 to its intersection with Line 34 (U.S.G.S.; see Fig. 1, Background and Objectives chapter, this volume). The intent was also to cross DSDP Sites 604 and 605 en route. A good satellite fix at 2125 hr., coupled with LORAN fixes, brought the vessel directly over Site 604. The presence of several commercial seismic survey vessels in the area, one of which was occupying Line 25 ahead of *Challenger*, necessitated several small course changes. Thus, despite navigational fixes the track deviated from Line 25. The vessel passed 0.6 n. mi. southwest of Site 605, and upon crossing Line 34, dropped the beacon at 2332 hr., 0.2 n. mi. northwest of it and 0.6 n. mi. northwest of the intended NJ-2 location. In order to drill closer to Line 25, *Challenger* offset from the beacon location 0.6 n. mi. to the southwest before spud-in. Subsequent satellite fixes placed the mean position of Site 612 approximately 0.45 n. mi. northwest of the intended NJ-2 location, but the water depth and subsurface stratigraphy are nearly identical to NJ-2.

Site 612

The site plans called for piston coring, rotary coring to the Upper Cretaceous, and logging. The most time-effective way to do this was with a single hole utilizing the advanced piston corer/extended core barrel (APC/XCB) system. Since the bit would have a 3.88-in. diameter core guide and the logging tools all were required to pass through a 3.75-in. opening, the possibility existed that logging could be accomplished without having to release this bit. This would be feasible if (1) the Baker Float Valve was deleted from the bottom-hole assembly (BHA) and (2) the logging tools could be shown to have no trouble re-entering the bottom of the drill string through the bit itself. This plan had several significant advantages over the conventional technique of logging only after releasing the bit. First, there would be no bit release mechanism in the BHA, thus no possibility of either a premature release or failure to release on command. Second, no time would be wasted on a potentially balky release operation. Third, the bit would remain on the string for the benefit of wiper trips or drilling out bridges or fill. And last, if, following logging, a second hole were desired for spot coring unconformities or heavily sampled intervals, that operation would be carried out immediately without a pipe round trip for a new bit. Thus, a test assembly of logging tools was hung from a cablehead and lowered through the bit with a tugger line. The assembly included the in-line caliper tool and the density tool with its one-sided bow spring. These were expected to be the most troublesome tool sections in re-entering. The bit was located at the moon pool platform to enable observation as the tool moved into and out of the bit. The procedure was carried off smoothly and the Schlumberger logging engineer on board was convinced that the technique would be successful.

The pipe was run as normal to just above the seafloor as indicated by a precision depth recorder (PDR) reading of 1371 m. Past experience in this region had shown actual depths to be consistently greater than PDR depth, however, so the bit was slowly lowered to feel for bottom. No clear weight indication was encountered, so when the bit had reached a depth of 1413 m the APC was run in on the wireline and a shot was taken from 1410 m in hopes of encountering the mud line. Core 1H was recovered with 4.85 m of core, thus establishing the mud line at 1414.3 m by drill pipe measurement. The hole was spudded at 1836 hours, 26 August.

The new APC, first deployed on Leg 94, was used to take the first seven cores. At this point, the partial stroke of the corer and the very firm nature of the glauconitic clay being recovered defined the limit of piston core penetration. The APC was laid down to rig up a pair of XCB tools.

Starting with Core 612-8, the XCB was deployed using sawtooth Soft Formation Cutting Shoes. These shoes

proved to be adequate to drill the entire hole. Cores 612-8 through 612-35 were taken in firm glauconitic clay changing to siliceous nannofossil ooze. Penetration and recovery rates were excellent, with some cores measured at greater than 100% recovery—most likely because of minor swelling of the cored material. Cores arrived on deck at 45-min. intervals as the XCB functioned flawlessly, maintaining minimum core disturbance.

At Core 612-36, a change in lithology was encountered, an abrupt solidification of the ooze combined with the first appearance of small chert nodules. The chert had no deleterious effect on coring except for causing localized disturbance in the cores. The solidification, however, was apparently responsible for a dramatic reduction in core diameter. Sections of some of the next 16 cores had diameters of less than 2 in. This "broomstick" phenomenon was traced to the XCB cutting shoes. An adjustment was made to the trimmers inside the throats of the XCB cutting shoes and the subsequent cores were considerably improved, although still roughly trimmed. The large-throat cutting shoes were used to drill the rest of the hole.

The scientific objective of reaching the Upper Cretaceous was achieved at a shallower depth than expected. The anticipated Paleocene section did not appear and the Maestrichtian was observed at about 550 m BSF. A dozen more XCB cores were taken, terminating with Core 612-72 at 2089.3 m total depth in the upper Campanian sediments. The hole remained clean and trouble free. A maximum drift angle of 2½° was measured. Virtually no gas was detected.

Anticipating a large diameter hole resulting from 11-7/16 in. XCB/HPC bit, the hole was filled with 420 barrels of 10.5 ppg barite mud. The bit was pulled to the logging depth of 104.5 m BSF. The air spinner tool rather than the rotary table was used to break the drill pipe connections during the pipe trip. This prevented disturbing the hole by rotating the bit, which had not been released.

Two problem-free Schlumberger logging runs were made in just over 13 hr. The first run combined dual induction, gamma ray, caliper, and sonic tools and the section was repeated for sonic waveforms. The second run included bulk density, neutron, and NGT. In both runs the logged interval was from 1489.2 m (74.9 m BSF) to total depth.

The hole remained open during the entire logging operation, although the caliper tool indicated that the hole had contracted to less than the bit diameter over most of its length. The hole diameter was as small as 6+ in. in some sections. This was thought to result from certain clays that swelled in the presence of the fresh water barite mud standing in the hole.

Following the Schlumberger logging operation, a 6- to 8-hr. period was used by the downhole tools specialist from Lamont-Doherty, David Goldberg, to deploy his 12-channel sonic tool. The sonic tool was lowered into the hole and run to total depth and back to the bit, but software problems in the on-deck monitoring equipment for the tool prevented it from completing the exercise. The allotted time was consumed troubleshooting and testing the equipment. No data were taken.

After the Lamont sonic tool was retrieved, the drill pipe was pulled out of the hole. The bit arrived on deck at 0525 hr. and the vessel got underway at 0554 hr., August 31.

The coring summary for Site 612 appears in Table 1. A superlog for Hole 612 is found in the back pocket.

SEDIMENT LITHOLOGY

At Site 612, 675.3 m of sediment was continuously cored by advanced piston corer (Cores 612-1 to 612-7: seafloor to 52.1 m sub-bottom) and by rotary drilling with the extended core barrel (Cores 612-8 to 612-72: 52.1–675.3 m sub-bottom). The sedimentary sequence is divided into five lithologic units (Fig. 1) of Pleistocene to late Campanian age, all having been deposited on the continental slope or outer shelf in open marine environments. Lithologic Unit I (0–135.3 m), comprising Pleistocene to upper Miocene sediments, is composed of glauconitic muds and sands, which reflect high terrigenous input. Below an upper Miocene to lower Oligocene unconformity, lithologic Unit II extends from the lower Oligocene down to nearly the base of the middle Eocene section (135.3–323.4 m). Unit II consists of radiolarian–diatomaceous nannofossil ooze and chalk, containing variable amounts of foraminifers and sponge spicules. The lower boundary of lithologic Unit II is a diagenetic change ~8 m above the middle/lower Eocene contact. Lithologic Unit III (323.4–550.3 m) is a sequence of porcellanitic foraminifer–nannofossil chalks containing diffuse cements, in addition to sporadic layers and nodules, largely of porcellanitic composition. There was no recovery in the 9.1 m between 550.3 and 559.4 m. This gap at the base of Core 612-60 divides lithologic Unit III from Unit IV. Lithologic Unit IV is of early to middle Maestrichtian age, and is composed of marly foraminifer nannofossil chalks and nannofossil–foraminifer chalks (559.4–639.6 m). Lithologic Unit V is composed of foraminiferal mudstone and shale (639.6–675.3 m) and was deposited during the late Campanian.

Nearly all the contacts between chronostratigraphic units match sedimentary breaks (unconformities), which interrupted normal pelagic and hemipelagic sedimentation. The post-Oligocene sedimentary breaks are marked by possible debris flows. Relatively long hiatuses (10 Ma or more) are represented by the unconformities that separate upper Miocene from lower Oligocene and lower Eocene from middle Maestrichtian strata. None of the unconformities that have been identified are represented by hardgrounds or other signs of prolonged exposure. Nonetheless, scoured contacts and biostratigraphic discontinuities mark many of the unconformities (Fig. 2). It is important to note that sedimentary environments did not always change dramatically across these unconformities and that little coarse-grained transported material rests atop some of the erosion surfaces.

One of the most significant sedimentary changes observed in Hole 612 does not coincide with an evident unconformity, but is instead a marked diagenetic front

Table 1. Coring summary, Site 612.

Core no.[a]	Date (August 1983)	Time	Depth from drill floor (m)	Depth below Seafloor (m)	Length cored (m)	Length recovered (m)	Amount recovered (%)
1H	26	1050	1414.3–1419.1	0.0–4.8	4.8	4.85	101
2H	26	1210	1419.1–1428.7	4.8–14.4	9.6	8.89	93
3H	26	1310	1428.7–1438.3	14.4–24.0	9.6	8.89	93
4H	26	1450	1438.3–1447.9	24.0–33.6	9.6	9.30	93
5H	26	1525	1447.9–1454.9	33.6–40.6	7.0	6.70	96
6H	26	1600	1454.9–1458.9	40.6–44.6	4.0	3.80	95
7H	26	1715	1458.9–1466.4	44.6–52.1	7.5	6.42	85
8X	26	1945	1466.4–1473.3	52.1–59.0	6.9	4.72	68
9X	26	2035	1473.3–1483.0	59.0–68.7	9.7	7.09	73
10X	26	2100	1483.0–1492.7	68.7–78.4	9.7	6.00	62
11X	26	2130	1492.7–1502.4	78.4–88.1	9.7	6.00	62
12X	26	2220	1502.4–1512.1	88.1–97.8	9.7	8.54	88
13X	26	2258	1512.1–1521.8	97.8–107.5	9.7	9.61	99
14X	26	2335	1521.8–1531.5	107.5–117.2	9.7	9.68	100
15X	27	0000	1531.5–1541.0	117.2–126.7	9.5	9.65	102
16X	27	0100	1541.0–1550.5	126.7–136.2	9.5	9.60	101
17X	27	0200	1550.5–1560.0	136.2–145.7	9.5	9.57	101
18X	27	0230	1560.0–1569.5	145.7–155.2	9.5	8.77	92
19X	27	0345	1569.5–1579.0	155.2–164.7	9.5	9.63	101
20X	27	0430	1579.0–1588.5	164.7–174.2	9.5	8.87	93
21X	27	0545	1588.5–1598.1	174.2–183.8	9.6	9.59	100
22X	27	0630	1598.1–1607.7	183.8–193.4	9.6	9.43	98
23X	27	0740	1607.7–1617.3	193.4–203.0	9.6	9.22	96
24X	27	0800	1617.3–1626.9	203.0–212.6	9.6	9.35	97
25X	27	0845	1626.9–1636.5	212.6–222.2	9.6	9.41	98
26X	27	0945	1636.5–1646.1	222.2–231.8	9.6	9.54	99
27X	27	1015	1646.1–1655.7	231.8–241.4	9.6	9.33	97
28X	27	1055	1655.7–1665.3	241.4–251.0	9.6	9.00	94
29X	27	1140	1665.3–1674.9	251.0–260.6	9.6	9.51	99
30X	27	1240	1674.9–1684.5	260.6–270.2	9.6	9.64	100
31X	27	1335	1684.5–1694.1	270.2–279.8	9.6	9.58	100
32X	27	1415	1694.1–1703.7	279.8–289.4	9.6	9.50	99
33X	27	1455	1703.7–1713.4	289.4–299.1	9.7	9.58	99
34X	27	1520	1713.4–1723.1	299.1–308.8	9.7	2.27	23
35X	27	1630	1723.1–1732.8	308.8–318.5	9.7	9.47	98
36X	27	1730	1732.8–1742.4	318.5–328.1	9.6	9.50	99
37X	27	1840	1742.4–1752.0	328.1–337.7	9.6	9.57	100
38X	27	2005	1752.0–1761.6	337.7–347.3	9.6	1.64	17
39X	27	2110	1761.6–1771.3	347.3–357.0	9.7	6.10	63
40X	27	2240	1771.3–1781.0	357.0–366.7	9.7	5.64	58
41X	27	2353	1781.0–1790.7	366.7–376.4	9.7	9.48	98
42X	27	0050	1790.7–1800.3	376.4–386.0	9.6	8.48	88
43X	27	0200	1800.3–1809.9	386.0–395.6	9.6	9.57	100
44X	27	0315	1809.9–1819.5	395.6–405.2	9.6	9.57	100
45X	27	0410	1819.5–1829.2	405.2–414.9	9.7	9.12	94
46X	27	0630	1829.2–1838.9	414.9–424.6	9.7	9.55	98
47X	27	0750	1838.9–1848.6	424.6–434.3	9.7	9.64	99
48X	27	0925	1848.6–1858.3	434.3–444.0	9.7	9.37	97
49X	27	1115	1858.3–1868.0	444.0–453.7	9.7	9.56	99
50X	27	1310	1868.0–1877.7	453.7–463.4	9.7	9.49	98
51X	27	1440	1877.7–1887.4	463.4–473.1	9.7	7.97	82
52X	27	1650	1887.4–1897.1	473.1–482.8	9.7	9.68	100
53X	27	1900	1897.1–1906.8	482.8–492.5	9.7	0.63	6
54X	27	2025	1906.8–1916.3	492.5–502.0	9.5	7.43	78
55X	27	2230	1916.3–1925.8	502.0–511.5	9.5	9.53	100
56X	27	0000	1925.8–1935.3	511.5–521.0	9.5	9.55	101
57X	27	0145	1935.3–1944.9	521.0–530.6	9.6	9.40	98
58X	27	0525	1944.9–1954.5	530.6–540.2	9.6	0.30	3
59X	27	0800	1954.5–1964.1	540.2–549.8	9.6	9.53	99
60X	27	0845	1964.1–1973.7	549.8–559.4	9.6	0.79	8
61X	27	0940	1973.7–1983.3	559.4–569.0	9.6	9.24	96
62X	27	1055	1983.3–1992.9	569.0–578.6	9.6	8.80	92
63X	27	1210	1992.9–2002.6	578.6–588.3	9.7	9.31	96
64X	27	1335	2002.6–2012.3	588.3–598.0	9.7	8.60	89
65X	27	1500	2012.3–2022.0	598.0–607.7	9.7	2.22	23
66X	27	1610	2022.0–2031.6	607.7–617.3	9.6	9.46	98
67X	27	1705	2031.6–2041.2	617.3–626.9	9.6	9.58	100
68X	27	1825	2041.2–2050.8	626.9–636.5	9.6	9.43	98
69X	27	1940	2050.8–2060.5	636.5–646.2	9.7	9.07	94
70X	27	2100	2060.5–2070.2	646.2–655.9	9.7	4.28	44
71X	27	2205	2070.2–2079.9	655.9–665.6	9.7	8.42	87
72X	27	2315	2079.9–2089.6	665.6–675.3	9.7	9.56	99
					675.3	580.66	86

[a] Core type is indicated as follows: H = hydraulic piston core, X = extended core barrel.

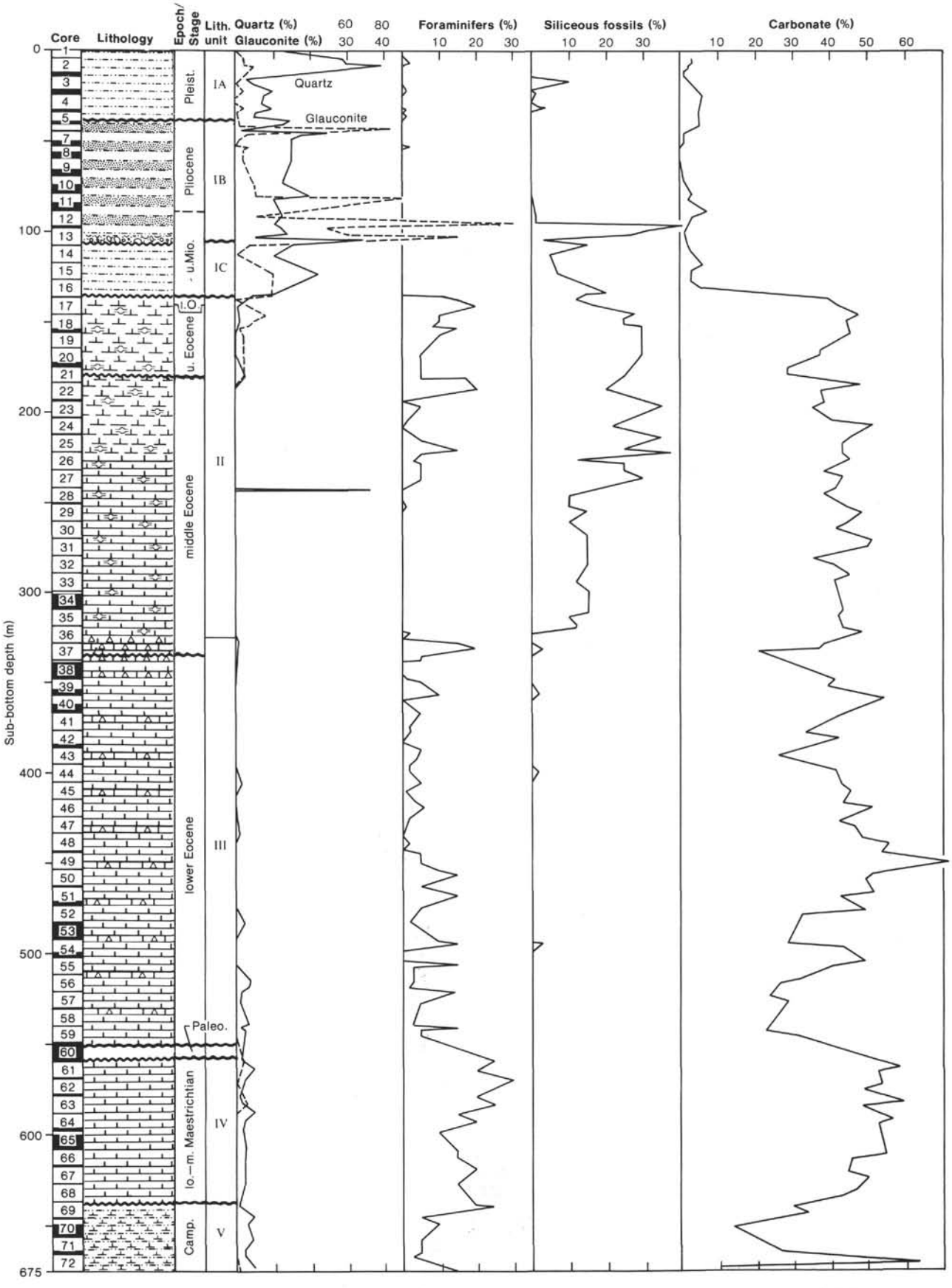

Figure 1. Percentage of quartz, glauconite, foraminifers, siliceous fossils (diatoms and radiolarians), and $CaCO_3$ in Hole 612.

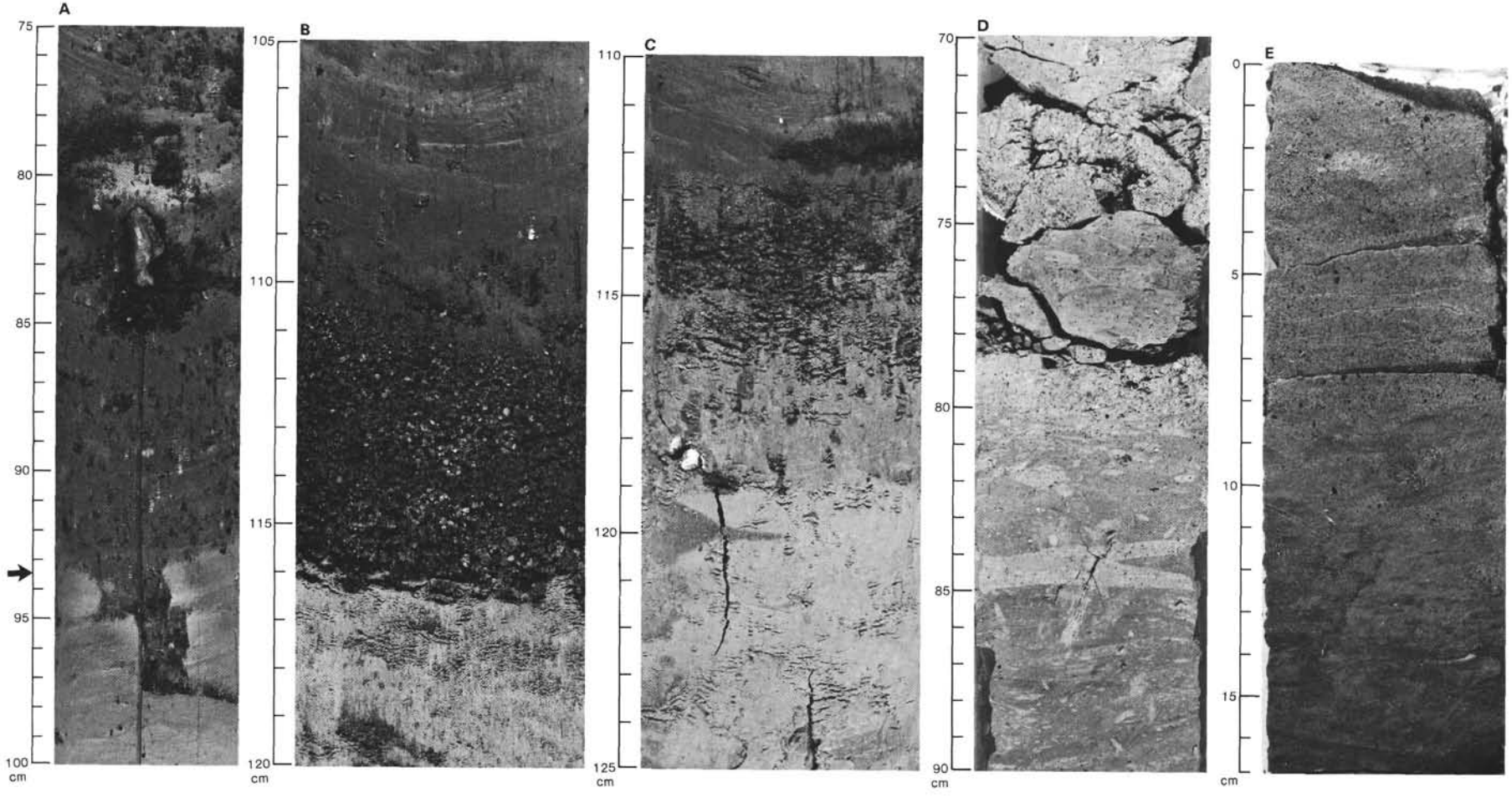

Figure 2. A. Tortonian/Messinian contact (612-13-6, 75–100 cm). Note truncated surface at arrow and mass-flow zone containing a bone fragment located 10 cm above contact. B. Miocene/lower Oligocene contact (612-16-6, 105–120 cm). Note unconformable surface overlain by a 5-cm-thick glauconite-quartz sand. C. Upper/middle Eocene contact marked by a thin glauconite layer (612-21-5, 110–125 cm). A slight color change is seen below contact. Note the small gypsum nodules at 118.5 cm. D. Middle/lower Eocene contact (612-37-3, 70–90 cm). Note burrows within lower Eocene section filled with mid-Eocene sediment. Burrow fill contains glauconite-rich mud. E. Maestrichtian/Campanian contact, with eroded and burrowed surface (612-69-3, 0–17 cm). Burrow filling and overlying sediments are glauconite-rich muds.

(Section 612-36-3; 323.4 m below seafloor). This front divides the Oligocene–Eocene sequence of siliceous nannofossil oozes and chalks into two parts. The upper part, lithologic Unit II, contains ooze and chalk in which compaction is the most significant postdepositional factor. The lower part, lithologic Unit III, has been affected by the dissolution of siliceous components and the reprecipitation of some of this silica as opal-CT in the form of porcellanitic cements. Diagenetic alteration has generated a 226.9-m-thick zone of relatively dense, partially cemented porcellanitic chalk. These two totally different types of lithologic "boundaries," erosional and diagenetic, form marked impedence contrasts and consequently may both be evident on seismic reflection profiles.

Lithologic Unit I

Interbedded dark gray to olive gray mud and very dark gray glauconitic sand (Fig. 3). Top of Core 612-1 to 612-16-6, 115 cm; 0–135.3 m below seafloor (BSF), Pleistocene to upper Miocene. Thickness: 135.3 m.

Subunit IA (Core 612-1 to 612-5-3, 35 cm)

In the upper three cores this unit consists of dark gray (2.5YR 4/1) homogeneous mud containing numerous black, pyritic mottles produced by endobenthos. Core 612-1 and the upper part of Core 612-3 contain numerous irregular burrows, filled with sand and silt that, on the basis of smear slide analysis, are composed of quartz (60 to 80%), glauconite (5%), and relatively large quantities of mixed heavy minerals (as much as 14%) (Plate 1). The mud matrix consists of clay (approximately 70–90%), quartz sand (20%), heavy minerals (8%), and feldspars (3%), together with traces of glauconite, iron sulfides, and disseminated organic matter. Foraminifers, unspecified carbonate (shell debris) and siliceous skeletal debris are present in quantities greater than 5% throughout the upper part of Subunit IA.

Several sharp color changes to reddish gray (5YR 5/2) occur between 612-4-6, 97 cm and the bottom of Subunit IA at 612-5-3, 35 cm. Quartz- and glauconite-bearing silty laminae are common in this interval. Disturbed bedding suggests that much of this is a debris flow. The bottom of Subunit IA is a distinct, eroded surface that corresponds to the upper Pleistocene/upper Pliocene contact.

Subunit IB (612-5-3, 35 cm to 612-13-6, 95 cm)

The distinctive lithologic feature of Subunit IB is the abundance of glauconite and quartz sand layers (Fig. 1). Faintly developed graded bedding is seen in some layers, especially in Sections 612-8-2 and -3. The thickness of the sand layers is variable and ranges from 1.5 m (in Section 612-6-3) to centimeter-thick laminae (in Section 612-7-3). Thicker sand beds contain thin interlayered mud stringers. Some sands are composed of as much as 70% glauconite grains, which are fresh and mostly rounded.

The thicker mud sections are extensively burrowed so that thinner sand interlayers are churned and intermixed, giving a patchy aspect to the mud from Cores 612-9 to 612-13 (Fig. 3).

In Core 612-9 and below, the first nannofossils were observed in smear slides, but do not exceed 10% of the sediment. Total carbonate content, measured by the shipboard carbonate "bomb" method, does not rise above 7% and is consistently lower than estimates based on smear slide observation. This difference can be explained by the fact that smear slide observations are areal estimates, and in the case of flat-lying nannofossils, this overemphasizes their total volume.

Core 612-13 contains a 2.3-m section that is probably a single debris flow (612-12-5, 15 cm to 612-13-6, 95 cm). The flow is made up of a mix of centimeter-sized light-gray clay fragments, dark chert pebbles, and one 3-cm bone fragment (Fig. 2). These materials are contained in a mixed matrix of mud, glauconitic sand, and diverse clasts of older strata. The base of this flow is a very sharp scoured boundary and coincides approximately with the Tortonian/Messinian contact (see Poag and Low, this volume).

Subunit IC (612-13-6, 95 cm to 612-16-6, 115 cm)

Subunit IC differs from Subunit IB by the lack of well-developed sand layers (Fig. 1). The mud is much less burrowed and contains centimeter-sized, light brown, irregularly-dispersed barite concretions (Sections 612-14-5, 612-14-6, 612-14-7, and 612-14,CC). Core 612-15 may contain another debris flow, with a sharply scoured lower contact (612-15-4, 110 cm), as indicated by light patches of reworked nannofossil ooze and deformed bedding. In Core 612-16 the sediment color becomes olive gray (5Y 4/2). Subunit IC is entirely late Miocene in age. It is bounded by a very sharp lower contact (612-16-6, 115 cm) that is overlain by a 5-cm-thick, coarse-grained glauconite–quartz sand (Fig. 2). In contrast to Subunit IB, Subunit IC consistently contains 5–10% siliceous microfossils and up to 10% nannofossils. This moderate percentage of biogenic components indicates that surface productivity at this site (perhaps because of stronger upwelling or current flow) may have been higher in the late Miocene than it was in the Pliocene and Pleistocene.

The weakly graded glauconite-bearing sand layers of Subunit IB indicate that frequent reworking from a relatively short distance updip on the slope and outer shelf contributed sediment to this site. High original organic content in those environments provided an excellent site for glauconite formation—glauconite being a synsedimentary diagenetic product in organic-rich sands and silts.

Lithologic Unit II

Light gray siliceous nannofossil oozes and chalks. 612-16-6, 115 cm to 612-36-4, 15 cm; 135.3–323.4 m BSF. Lower Oligocene to middle Eocene. Thickness: 188.1 m.

Lithologic Unit II consists of light greenish gray (5G 8/1) to grayish yellow green (5GY 7/2) siliceous, foraminifer–nannofossil oozes and chalks or siliceous nannofossil oozes and chalks. Bioturbation throughout Unit II is generally pervasive and produces light olive gray (5Y 8/1, 5Y 6/1) mottles. No significant change in sediment character can be detected throughout this unit.

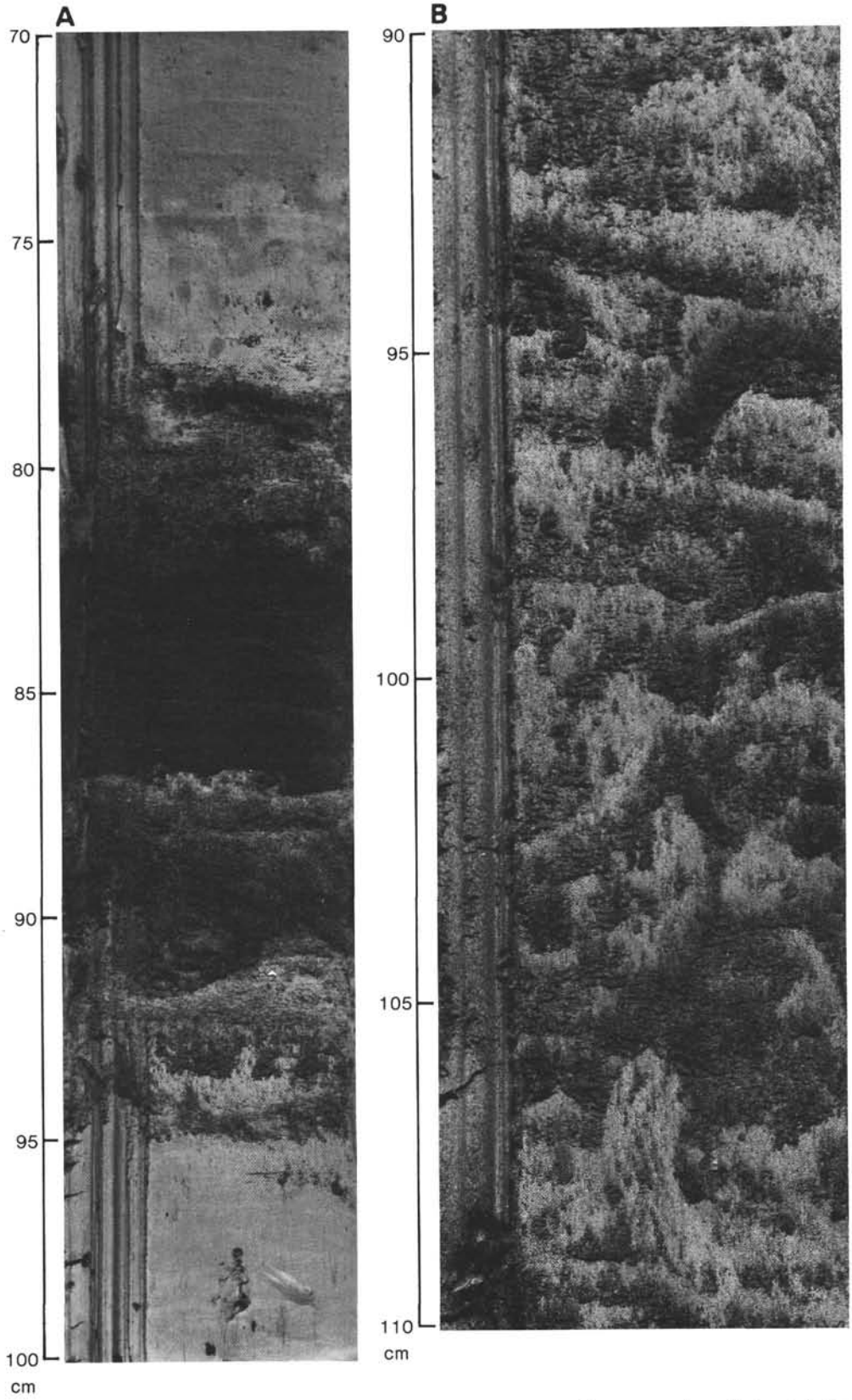

Figure 3. A. Lithologic Unit IA (612-8-2, 70–100 cm). Reddish gray mud (upper part is mottled and darker gray) with dark gray glauconitic sand layers. Base of upper thick bed is muddy, deformed by rapid influx of sand onto the soft sediment. B. Lithologic Unit 1B (612-12-2, 90–110 cm). Thin layers of glauconitic mud and sand, completely intermixed by burrowing.

The top of Unit II coincides with the sharp upper Miocene/lower Oligocene erosional contact as described above (612-16-6, 115 cm). The sediment is mainly composed of calcareous nannofossils (30–50% in smear slides). Planktonic foraminifers, which make up to 20% of the oozes in the upper part of Unit II (down to Core 612-25), decrease rapidly to mere traces in Core 612-28 and below. Similarly, radiolarians, diatoms, and sponge spicules drop from a total of 25% in the upper parts (on average) to 10 to 15% below Core 612-28. The bulk calcium carbonate content provided by "bomb" analysis varies between 30 and 50% with an average of about 40%. The rest of the sediment is composed of an unspecified mixture of terrigenous clay or authigenic clay material (approximately 5–10%) and (early) amorphous opal from dissolved biogenic silica. This mixture is specially symbolized in the graphic lithology column of the barrel sheets (see Explanatory Notes, this volume). Detrital quartz is limited to the upper two cores of this unit (Cores 612-17 and 612-18), in which values are below 5%. Fish scales were observed, but are rare. A layer of apparent microtektites occurs in Sample 612-21-5, 111–114 cm (Plate 1, fig. 2; see also Thein, this volume and Cousin and Thein, this volume).

The sediment is intensely burrowed throughout. A large variety of burrow types are especially visible in Core 612-32 (Fig. 4), and below, where cores were cut by the saw and thus are much less deformed than those above. The olive gray burrows and dwelling structures, filled by weakly glauconitic and pyritic nannofossil ooze and chalk, range from frequent horizontal, diagonal, and vertical large spreiten to horizontal, diagonal, bifurcated and pear-shaped vertical dwellings to small Chondrites-like burrows.

Sediments are soft to firm oozes in the upper cores of lithologic Unit II. Cores 612-24 to 612-30 show a marked "biscuit" deformation which coincides with the first downhole occurrence of moderately lithified chalks interlayered with firm oozes. Shipboard sonic velocity values rise slightly and irregularly from Cores 612-24 to 612-28, following the trend in increasing lithification. Velocities increase sharply below the lower boundary of Unit II. Below Core 612-28, chalks make up the main part of Unit II; drilling disturbance disappears below 612-30. In the lowest part of Unit II (Cores 612-33 to 612-36) the first traces of opal-CT were detected by X-ray diffraction, and values increase toward the bottom where the first porcellanite nodules mark the boundary with lithologic Unit III.

The striking homogeneity of Unit II is interrupted at two levels. The first is an unconformity that coincides with the contact between the upper and middle Eocene in 612-21-5, 120 cm (181.3 m BSF) (Fig. 2C). This unconformity is overlain by a 5-cm-thick sand layer with abundant, nearly spherical to pear-shaped glass grains. Many of these grains contain round gas bubbles. The 20 cm above this erosion surface are darker gray.

The other layer that interrupts the homogeneity of lithologic Unit II is found in 612-28-2, 85 cm (243.7 m BSF). It consists of medium-size quartz sand with 10% heavy minerals and considerable amounts of idiomorphous pyrite. This interval is highly disturbed by drilling. It coincides with the aforementioned decrease in both foraminifers and siliceous fossil content, although no biostratigraphic gap is noted. It also closely matches an increase of 10 GAPI units on the gamma ray log.

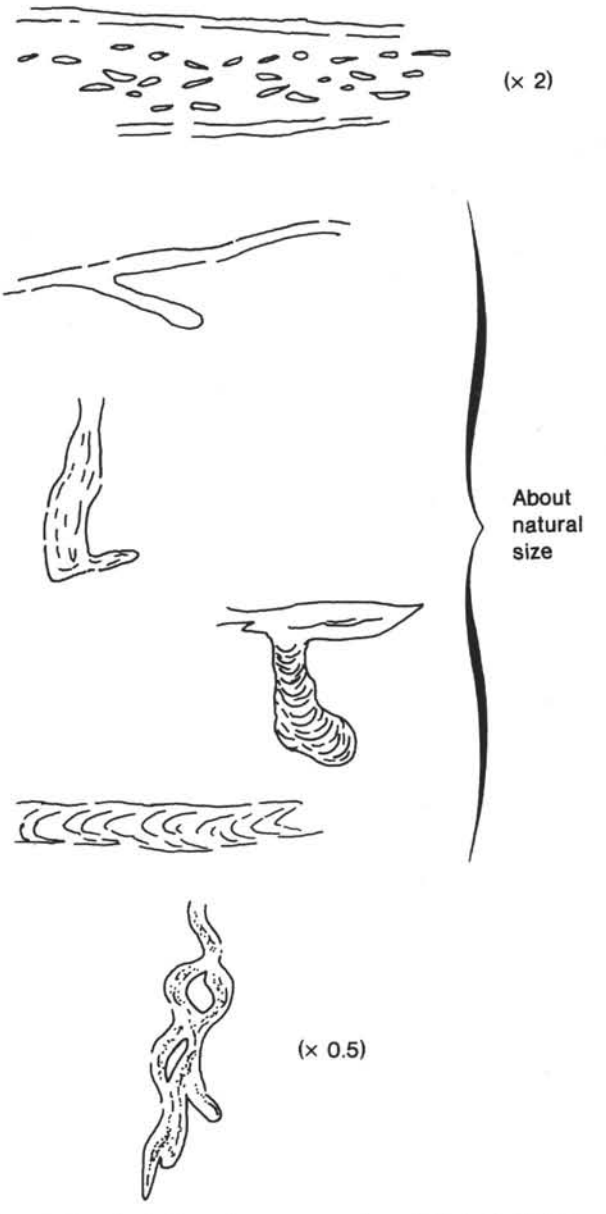

Figure 4. Sketch of diverse burrow types from Lithologic Unit II.

The nannofossil oozes and chalks of lithologic Unit II were deposited on a continental slope much like the present under continuously well-oxygenated conditions and with high surface productivity. The gradual disappearance of siliceous fossils toward the bottom of Unit II and the appearance of porcellanite at the top of Unit III result from diagenetic processes. The diagenetic front at the top of Unit III forms a marked horizon in shipboard physical property measurements and in downhole wireline logs, and coincides with a strong seismic reflector (Tucholke, 1979; Poag and Low, this volume; Poag and Mountain, this volume).

Lithologic Unit III

Laminar to intensely burrowed, light greenish gray, light olive to brownish gray, porcellanitic foraminifer-nannofossil chalk to porcellanite, partially zeolitic. 612-36-4, 15 cm to 612-60,CC; 323.4–550.3 m BSF. Middle to lower Eocene. Thickness: 226.9 m.

Lithologic Unit III consists of a light greenish gray (5GY 7/1), greenish gray (5GY 6/1) or olive gray (5Y 5/1) porcellanitic nannofossil chalk to porcellanite (Fig. 1; Plate 1, fig. 3). Burrows and mottles are marked by light olive gray (5Y 6/2) and light brownish gray (2.5Y 6/2). The unit is monotonous, usually burrowed, but sporadically laminated. These laminated zones are slightly darker (olive gray 5Y 5/1), and appear as part of several cyclic successions in Cores 612-50, 612-55, and 612-56 (Fig. 5). The remainder of Unit III is extensively burrowed. Most burrows are oriented subparallel to original bedding. The variety of burrows and related features is similar to that in Unit II and includes delicate spreiten, sporadic Zoophycos, and several relatively large burrows, as much as 10 cm deep (Fig. 6).

The induration observed in lithologic Unit III, coupled with the development of opal-CT, is variable and does not follow a smooth downward increase. The degree of lithification ranges from zones that are nearly cherty to those that are only weakly cemented. The carbonate content of the sediment in lithologic Unit III (measured aboard ship) ranges from 21% (Section 612-37-4) to 71% (Section 612-49-4) and does not seem to be related to the degree of induration. Subsequent studies (this volume) distinguish between the involvement of carbonate and opal C-T cementation in the process of lithification.

Porcellanitic lithification, coupled with carbonate cementation, provides the major differentiation of lithologic Unit III from Unit II. The original composition of the bioturbated intervals in these units appears to have been the same. The laminated intervals in Unit III may have accumulated under moderately low-oxygen conditions, during periods of impingement of an oxygen-minimum zone on the continental slope.

Although traces of opal-CT were detected by X-ray diffraction in Cores 612-33 to 612-36 of Unit II, it is the first downhole appearance of thoroughly cemented porcellanite nodules as well as the sharp change in numerous physical properties (Wilkens et al., this volume; Goldberg et al., this volume) that leads us to place the Unit II/III boundary in Section 612-36-4. The occurrence of chert lithification has been reported in other holes from the western North Atlantic (Jansa et al., 1979) and despite various enclosing lithologies, burial depths, and depositional environments, it frequently occurs in lower to middle Eocene sediment. At Site 612, this diagenetic boundary occurs approximately 8 m above the middle/lower Eocene contact; at Site 613 it occurs approximately 2 m below the biostratigraphic contact. We think that the diagenetic front is a fossil front and is not advancing upward at present. The factors controlling the location of this front and the stratigraphic distribution of the porcellanite lithification throughout Unit III remain unknown.

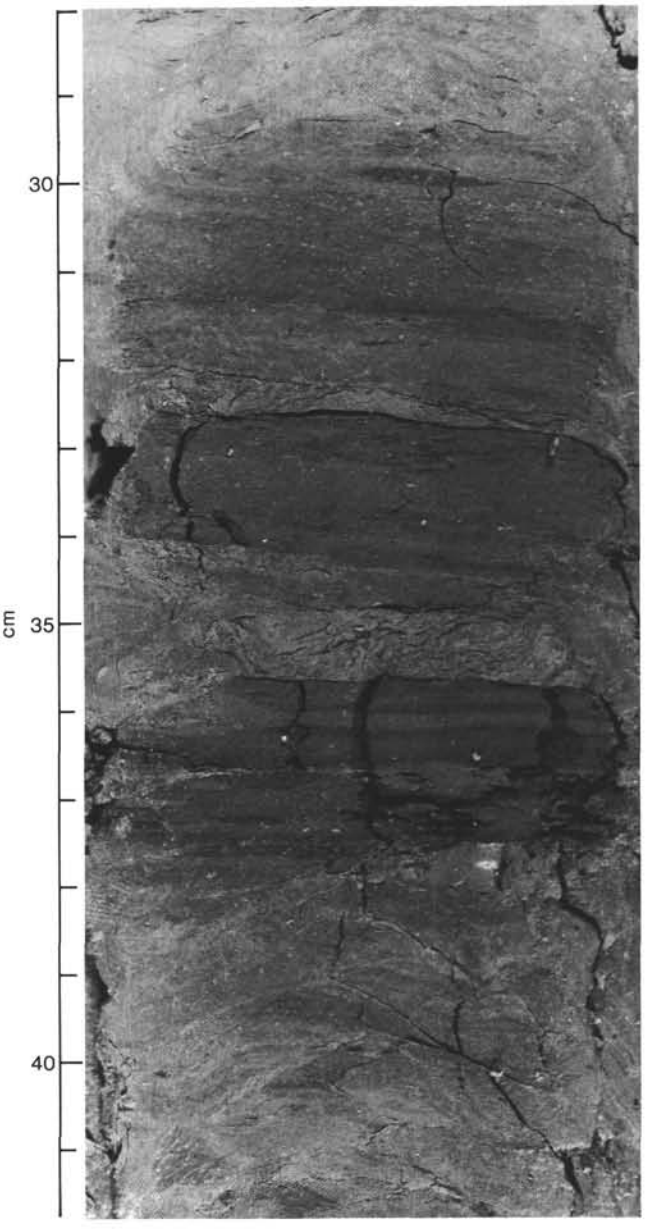

Figure 5. Lithologic Unit III (612-56-3, 28–42 cm). Even, laminar bedding in porcellanite-cemented nannofossil chalk. Note oozy clay between segments, probably a drilling artifact.

Lithologic Unit IV

Dark gray marly foraminifer–nannofossil or nannofossil–foraminifer chalks. Top of Core 612-61 to 612-69-3, 8 cm; 559.4 m to 639.6 m BSF. Lower to middle Maestrichtian. Thickness: 80.2 m.

Unit IV consists of marly foraminifer–nannofossil chalks (Cores 612-61, 612-63 to 612-66, and 612-69) and marly nannofossil–foraminifer chalks (Cores 612-62, 612-67 and 612-68) containing some layers of lithified limestone (e.g., Section 612-68-4; Fig. 1). Colors are inter-

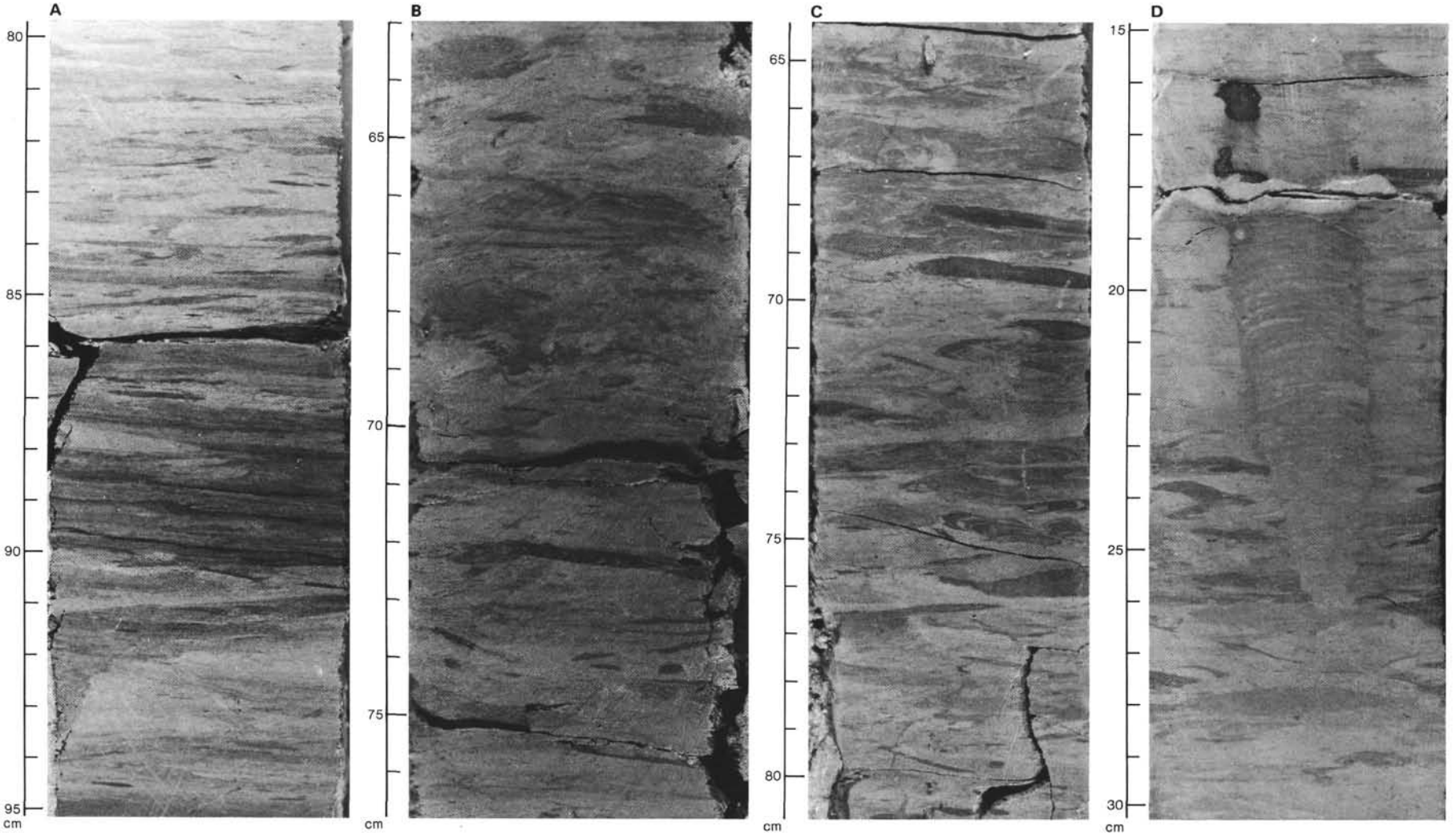

Figure 6. Lithologic Unit III A. (612-55-1, 80–95 cm). Horizontal to low angle burrows commonly with cross-cutting relationships in a moderately lithified nannofossil chalk. B. 612-56-3, 63–77 cm. Horizontally burrowed well-indurated chalk, with spreiten between 72 and 73 cm. C. 612-52-3, 64–81 cm. Horizontal to low-angle oblique burrows with Zoophycos between 73 and 75 cm. D. 612-57-3, 15–30 cm. Horizontal to low-angle burrows in siliceous nannofossil chalk, with a deep (10 cm) burrow cross-cutting the earlier burrows.

layered dark gray (10YR 4/1) or dark olive gray (5Y 3/2) and intensely burrowed light gray (10YR 5/1), darker gray (10YR 3/1), or very dark olive gray (5Y 3/1).

The contact between lithologic Units III and IV was not recovered, but on the basis of biostratigraphic data an unconformity representing 10 m.y. may separate lower Eocene (612-60-1, 70 cm, lithologic Unit III) from middle Maestrichtian strata (Core 612-61). A similar unconformable contact between Eocene and Maestrichtian strata has been reported in shelf and coastal plain localities of the United States Atlantic margin (Poag, 1985).

The $CaCO_3$ content (as measured by the carbonate "bomb" method) decreases from the top to the bottom of lithologic Unit IV: values of 50 to 60% measured in Cores 612-61 to 612-65, 40 to 50% in Cores 612-66 to 612-68, and 30 to 35% near the base of the unit in Core 612-69. On the basis of smear slides, the terrigenous components are quartz sand or silt (5–10%) and clay (30–50%). Framboidal pyrite is frequent; fine sand-sized glauconite grains appear at the top (Cores 612-61 and 612-62) and at the bottom (Cores 612-68 and 612-69) of the unit. They are not as abundant as in lithologic Unit I except at the basal contact with Campanian strata (94% in Sample 612-69-3, 1 cm).

The sediment in lithologic Unit IV is massive, with irregular and discontinuous bedding, and is intensely burrowed showing spreiten, dwellings, and frequent Chondrites (Fig. 7). Well-preserved foraminifers are often concentrated in these burrows. Numerous large fragments of *Inoceramus* shells occur in thin layers throughout the unit. Depositional conditions were open marine and bathyal.

Lithologic Unit V

Black foraminifer or nannofossil mudstone or chalk (Fig. 8). 612-69-3, 8 cm to 612-72,CC; 639.6–675.3 m BSF. Upper Campanian. Thickness: 35.7 m.

Lithologic Unit V is composed of black (5Y 2.5/2), interlayered, foraminifer (Core 612-69), foraminifer–nannofossil (Core 612-70), or nannofossil mudstone and chalk (Cores 612-71 and 612-72; Fig 1). The black color is interrupted by pinkish gray (5YR 8/1) foraminifer specks, shell fragments, and small burrow mottles. Sporadic, thin, foraminifer-rich layers occur in this unit and explain the high $CaCO_3$ content of some samples (64% in Sample 612-72-2, 70–73 cm).

Lithologic Unit V unconformably underlies lithologic Unit IV. The contact is sharp, and the top of the Campanian strata is scoured and deeply burrowed (612-69-3, 8 cm; see Fig. 2E).

The variable carbonate content (more or less than 30%, as measured aboard ship by the carbonate "bomb" method) agrees with the observed interlayering of mudstone and chalk. In general, the major component is fine-grained terrigenous detritus, which from smear slide analysis is clay (up to 60%), quartz sand or silt (5–10%), and mica (2–5%). Pyritic nodules are common; organic matter is pervasive (up to 2.68% total organic carbon) and consists mainly of detrital plant debris. Large fragments of *Inoceramus* shells are found in layers in Core 612-71.

The bedding in lithologic Unit V is usually irregular and discontinuous, containing sporadic, thin, foraminifer-rich layers. Bioturbation is common and occurs in the form of horizontal or oblique burrows and frequent Chondrites. The unburrowed intervals in Core 612-69 and 612-70 are fissile shales.

The benthic/planktonic foraminifer ratio in Unit V is higher than at any other level at Site 612 (according to shipboard analysis) suggesting that this sediment was deposited in the shallowest water environment of this site. However, the co-occurrence of detrital quartz and plant debris indicates that part of this sediment was transported from even shallower water. The extensive burrowing shows that bottom conditions periodically were open marine and well oxygenated.

BIOSTRATIGRAPHY

General Summary

At Site 612, 580.66 m of sediment was recovered in 72 cores, ranging in age from Pleistocene to late Campanian (see Fig. 9). Sediment recovery in most cores was good to excellent, averaging 86% for the site. Unfortunately, some stratigraphically critical levels yielded poor recovery. Throughout much of the succession, faunas and floras are abundant and preservation is moderate to good, although the radiolarians are either poorly preserved or completely absent from Cretaceous sediments and from some intervals of the lower to lower middle Eocene. The foraminifers were also poorly preserved in the lower to lower middle Eocene, and biostratigraphic zonal determinations from those intervals are provisional, pending shore-based studies.

This report is based on core catcher material from Cores 612-1 through 612-72, although some additional samples were used at specific levels to locate biostratigraphic boundaries. Calcareous nannofossils, radiolarians, and the planktonic and benthic foraminifers were examined on the ship. Throughout the succession there was good agreement between the nannofossil, radiolarian, and foraminiferal age assignments.

Cretaceous sediments were recovered from Cores 612-72 through 612-61, all of which contained calcareous faunas and floras. However, the radiolarians were poorly preserved and of little stratigraphic value. Cores 612-72 through 612-69-3, 8 cm (675.30–639.60 m) contain a distinctive upper Campanian assemblage, and these are overlain by the Maestrichtian in Cores 612-69-3, 8 cm through 612-61 (639.60–559.40 m). There is a reasonably marked faunal and floral hiatus between the Campanian and the Maestrichtian. Nannofossil and foraminiferal data suggest that a large part of the Cretaceous succession is of early (?) to middle Maestrichtian age, although the precise zonation of the stage will require further work.

Recovery near the Cretaceous/Tertiary contact (Core 612-60) was poor; only the core catcher contained any sediment. The overlying strata are lowermost Eocene (P6b or CP9) according to all the fossil groups. This would indicate a possible hiatus of some 10 m.y. between the mid-Maestrichtian and the lower Eocene. There is no paleontological evidence to suggest the presence of Pa-

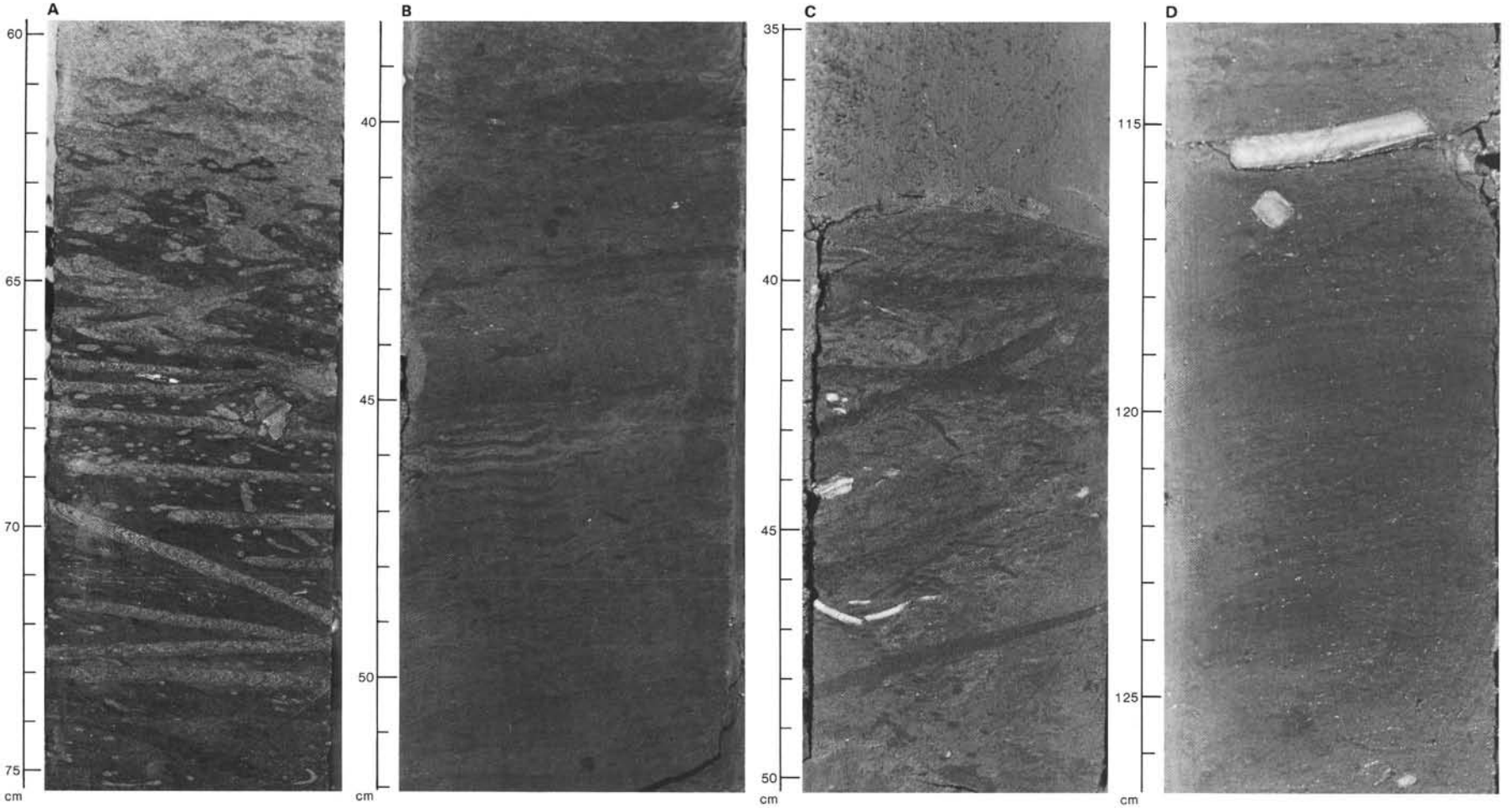

Figure 7. Lithologic Unit IV. A. 612-68-6, 60–75 cm. Elegant set of spreiten-type burrows, both horizontal and oblique in relationship to the sediment. B. 612-66-6, 38–52 cm. Cross-section of Zoophycos (45–48 cm). C. 612-66-1, 35–50 cm. Horizontal to oblique spreiten burrows plus *Inoceramus* shell fragments (white) in foraminifer–nannofossil chalk. D. 612-63-1, 113–127 cm. Burrow-mottled nannofossil chalk with large *Inoceramus* shell fragments.

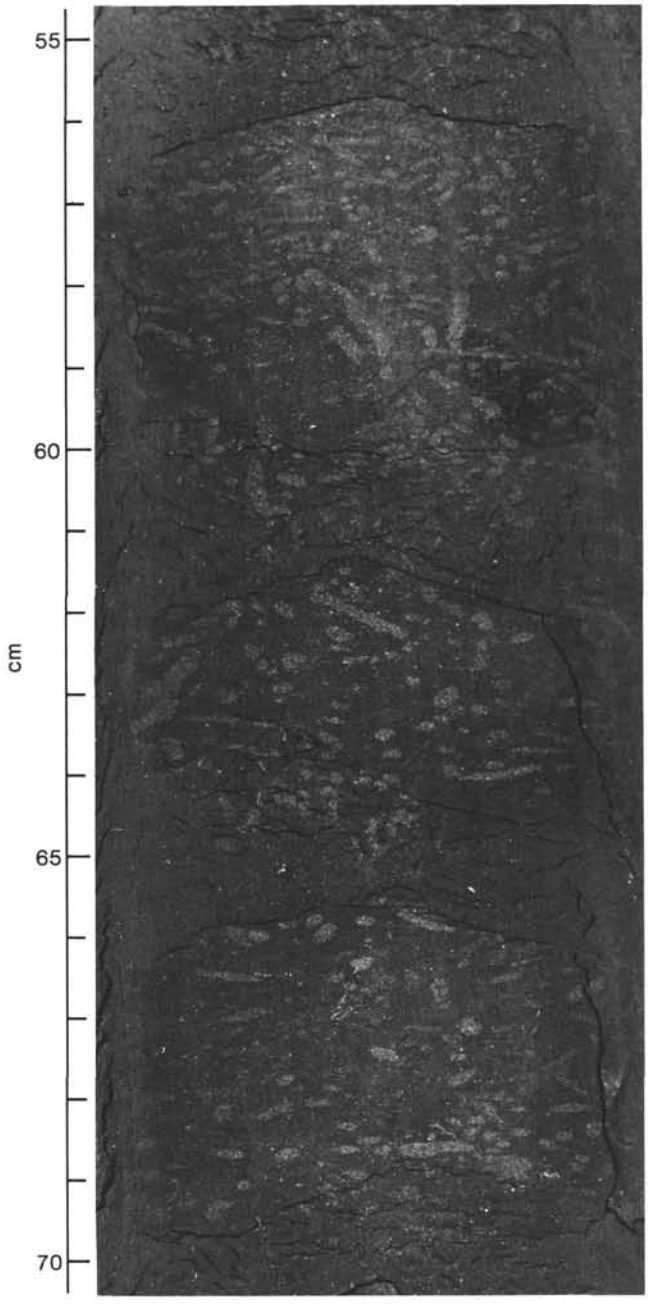

Figure 8. Lithologic Unit V (Sample 612-71-3, 55–70 cm). Chondrites in mudstone; note ooze at margins of core and surrounding core "biscuits."

leocene strata, although the presence of a thin uncored Paleocene unit cannot be ruled out.

The Eocene biostratigraphic succession (Cores 612-60 through 612-17), apart from a hiatus of 5 to 6 m.y. at the middle Eocene/upper Eocene contact, and a <2 m.y. hiatus at the lower Eocene/middle Eocene contact, appears to be almost complete. Calcareous nannofossils are abundant and preservation is moderate to good throughout, although both the radiolarians and the foraminifers are poorly to moderately preserved in the lower Eocene and lower middle Eocene.

The Eocene succession is overlain by a thin (1 m) layer of lower Oligocene sediment, which in turn is over-

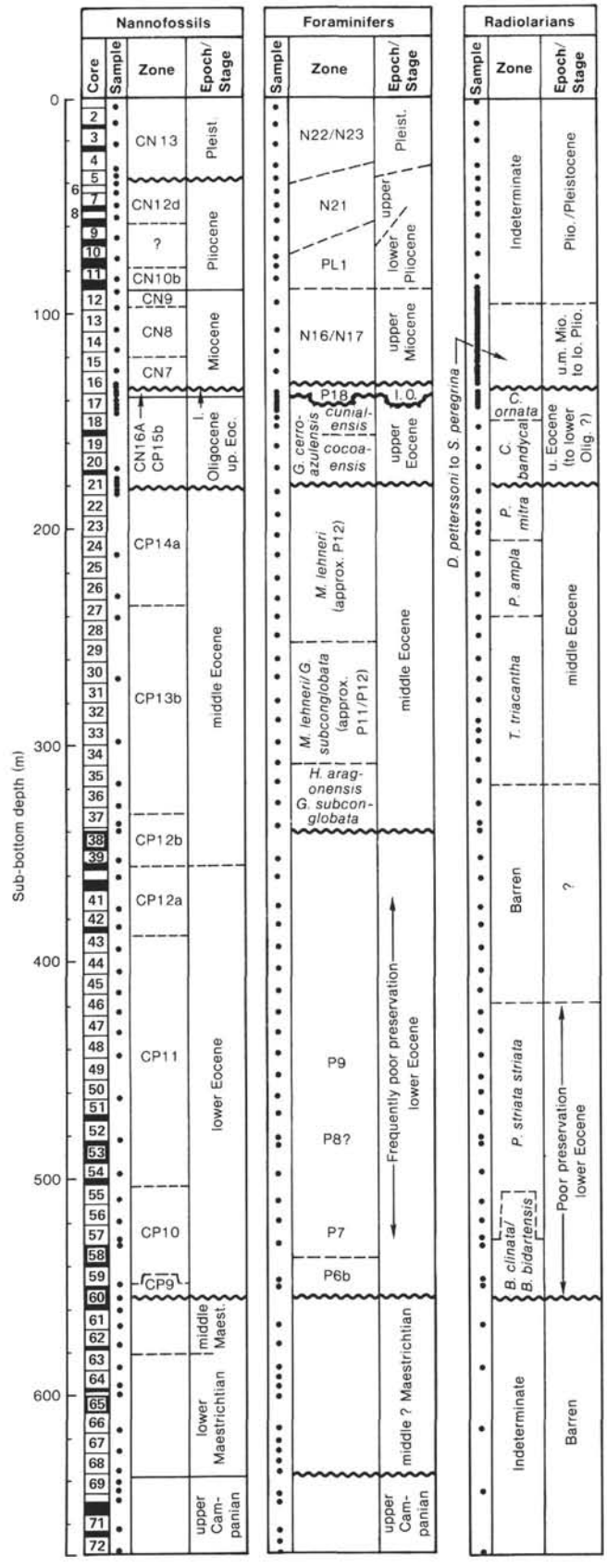

Figure 9. Biostratigraphic columns for Site 612.

lain by upper Miocene sediments. The unconformity between the Oligocene and upper Miocene represents the largest hiatus at Site 612 (~25 m.y.). The lower Oligocene/upper Miocene contact is in Core 612-16, there being general agreement on the age of the upper Miocene sediments (Cores 612-16 through 612-12). The upper Miocene/lower Pliocene contact is somewhere between Cores 612-12 and 612-11, but poor microfossil assemblages preclude precise placement of the contact (Fig. 1).

A Pliocene–Pleistocene succession extends from Cores 612-11 to 612-1. This section remains undifferentiated at the present time on the basis of the radiolarians; however, the foraminifers indicate that the Pliocene/Pleistocene contact is present in Core 612-5. Nannofossils indicate that an unconformity is present between upper Pliocene and upper Pleistocene strata in Section 612-5-3 and that the lower/upper Pliocene contact lies between Cores 612-8 and 612-11.

Foraminifers

Cretaceous: Planktonic and Benthic Foraminifers

The upper Campanian sediments are found in Cores 612-72 through 612-69-3, 8 cm (675.30–639.60 m). They comprise dark, organic-rich clays and yield a rich, varied, and diagnostic foraminiferal fauna. The greater than 250 μm size fraction of samples in this interval has planktonic:benthic ratios of approximately 3:1, with agglutinated and calcareous benthic foraminifers being equally represented. The planktonic fauna is composed largely of species such as *Globotruncana linneiana, G. arca, G. bulloides,* and *G. orientalis*, together with larger numbers of the faintly keeled species *Archaeoglobigerina cretacea. G. calcarata*, the zonal index species for upper Campanian, was not recorded. The benthic assemblage is diverse and contains many of the species used extensively in N.W. European biostratigraphy (e.g., *Reusella szajnochae szajnochae, Bolivinoides laevigatus, Neoflabellina praereticulata, Globorotalites hiltermanni, G. micheliniana,* and *Gavelinella cristata*), as documented by Hart et al. (1981) in the United Kingdom.

This benthic assemblage changes in many respects at the Campanian/Maestrichtian contact. The Maestrichtian (Cores 612-69-3, 8 cm through 612-61, 639.60–559.40 m) is characterized by related species of many of the above genera, together with other forms (e.g., *Stensioina pommerana, Gavelinella clementiana, Eponides biconvexa, Bolivina incrassata, Bolivinoides miliaris, Pullenia quaternaria*.

The planktonic foraminifers are slightly more numerous than in the Campanian; average counts of the same size fraction give planktonic:benthic ratios of approximately 9:1. The keeled globotruncanids dominate the fauna (principally *Globotruncana gansseri* s. l, *G. fornicata–G. patelliformis–G. contusa* transitional forms, *G. walfishensis, Planoglobulina multicamerata, Heterohelix* spp., *Rugoglobigerina* spp., *Pseudotextulari elegans*, and *Globotruncanella havanensis*). This fauna indicates a level in the lower part of the middle Maestrichtian, or perhaps just including a small amount of lower Maestrichtian. The uppermost samples from Core 612-61 do not contain a fauna of late Maestrichtian age (*Abathomphalus mayaroensis* was not recovered).

Cenozoic: Planktonic Foraminifers

The Cretaceous/Cenozoic contact was not recovered; Core 612-60 was empty apart from the core catcher, which contained a piece of moderately hard, pale colored, siliceous nannofossil chalk. This sample, and that from the overlying Sample 612-59,CC both contain foraminiferal assemblages that indicate a position within the lower Eocene (probably Zone P6b: *Morozovella subbotinae* Zone). The faunas are poorly preserved but contain an identifiable assemblage that includes *Globorotalia subbotinae, Muricoglobigerina soldadoensis, Subbotina linaperta, and S. triloculinoides*(?). There was no evidence for a Paleocene fauna, although one could have been present in the unrecovered section of Core 612-60.

Lower Eocene

As indicated above, there is some evidence to suggest that Samples 612-59,CC and 612-60,CC represent the lowermost Eocene biozone (Zone P6b). The succession above this level contains a foraminiferal fauna greatly affected by problems of preservation and processing. The sediments are silicified (see Lithology section) and difficult to process effectively for microfossils. The faunas obtained are therefore rather reduced in number and diversity, and those individuals encountered in the shipboard examination were coated with adherent sediment. The recognition of some of the species was difficult, and in some cases (e.g., *Morozovella*) zonal markers may have been missed. Some key species normally encountered in the lower Eocene (e.g., *M. formosa formosa* and *M. formosa gracilis*) were not found, making zonal boundaries difficult to position accurately.

In Sample 612-58,CC, *M. subbotinae* is joined by the first members of the *M. aragonensis–M. lensiformis* group, although the poor preservation makes accurate determination of individual species impossible. This would indicate the appearance of a Zone P7 assemblage. This remains almost unchanged in Sample 612-49,CC, where *Pseudohastigerina* appears together with *Globorotalia pseudotopilensis* and *G. quetra*. Sample 612-47,CC provides the next zonal boundary with the appearance of an assemblage typical of Zone P9, characterized by *M. caucasica, P. wilcoxensis,* and *G. quetra*. This assemblage then remains unchanged until the appearance of one characteristic of the middle Eocene.

Middle Eocene

Cores 612-21 through 612-37, representing approximately 160 m of section, are assigned to the middle Eocene using planktonic foraminifers.

In the lower portion of this section, planktonic foraminifers are rare and generally poorly preserved so that foraminiferal biostratigraphic resolution is limited. Thus, although the section appears to be complete paleontologically, poor resolution may have prevented shipboard

detection of a hiatus at the unconformable lower/middle Eocene contact.

Cores 612-37 through 612-35 are assigned to the undifferentiated *Hantkenina aragonensis–Globigerinatheka subconglobata* zones (Stainforth et al., 1975) which are equated with Blow's (1979) Zones P10–P11 (Berggren et al., 1985). This assignment is based upon the last appearance of *Morozovella caucasica* in Core 612-38, together with the presence of *Subbotina frontosa, M. aragonensis, Acarinina bullbrooki, A. broedermanni,* and *Pseudohastigerina wilcoxensis* in Cores 612-35 to 612-37. On the basis of the last occurrence of *in situ A. aragonensis* in Core 612-35, overlying Cores 612-34 through 612-29 are assigned to the undifferentiated *G. subconglobata/M. lehneri* Zones, which correlate with Blow's (1979) Zones P11–P12. These cores probably are part of the *G. subconglobata* Zone (Zone P11), based upon the occurrence of *A. broedermannii* (last appearance (LA) Zone P11, Blow, 1970; LA *G. subconglobata* Zone, Stainforth et al., 1975).

On the basis of the presence of *S. frontosa, Globorotalia cerroazulensis pomeroli* (FA Core 612-28), and *G. cerroazulensis possagnoensis*, Cores 612-28 through 612-21 are assigned to the *G. cerroazulensis possagnoensis* Zone of Toumarkine and Bolli (1970). The absence of *Orbulinoides beckmanni* at Site 612 precludes using the Bolli (1957) or Blow (1979) zonations directly; the correlation of the *G. cerroazulensis possagnoensis* Zone with Bolli's and Blow's zonations is ambiguous. Toumarkine and Bolli (1970) and Stainforth et al. (1975) suggested that *S. frontosa* became extinct at the top of the *M. lehneri* Zone (equivalent to Blow's Zone P12); Blow (1979) suggested that this extinction occurred even earlier (top of his Zone P11). Using the former correlations, Cores 612-28 through 612-21 are part of the *M. lehneri* Zone (=Zone P12); using Blow's correlations, these cores are part of Zone P11. However, recent magnetobiostratigraphic correlations (see Berggren et al., 1985) suggest that *S. frontosa* ranges into magnetochron C18, and thus into the *O. beckmanni* Zone and lower portions of the *Truncorotaloides rohri* Zone (equivalent to Zone P13 and lower P14 of Blow, 1979). Using these correlations, Cores 612-28 through 612-21 are part of the undifferentiated *M. lehneri/O. beckmanni*-lower *T. rohri* Zones.

In addition to the zonal marker species, *Truncorotaloides rohri, T. topilensis, Acarinina bullbrooki, Hantkenina alabamensis, Globigerinatheka index, G. kugleri, Morozovella lehneri,* and *M. spinulosa* characterize the section between Cores 612-28 and 612-21. Isolated occurrences of *A. aragonensis* in Samples 612-24,CC and 612-27,CC are interpreted as having been reworked. An alternative interpretation would extend the boundary between the *G. subconglobata* and the *M. lehneri/O. beckmanni*/lower *T. rohri* zones to between Samples 612-24,CC and 612-23,CC. However, the presence of *H. alabamensis* (Core 612-24 and above; FA P12, Blow, 1979) and *T. topilensis* (Core 612-28 and above; FA P12, Blow 1979) and the absence of *A. broedermanni* (last occurrence in Core 612-29; LA P11, Blow, 1979; LA *G. subconglobata* Zone, Stainforth et al., 1975) favor assignment of this section to the *M. lehneri* Zone.

Upper Eocene–Lowermost Oligocene

An unconformity representing a 5 m.y. hiatus in Core 612-21 separates the *Morozovella lehneri/Orbulinoides beckmanni*-lower *Truncorotaloides rohri* Zone (with abundant *Subbotina frontosa*) from an association containing *Globorotalia cerroazulensis cerroazulensis* in abundance along with rare *G. cerroazulensis cocoaensis* and *G. cerroazulensis pomeroli*. This association is indicative of the late Eocene *G. cerroazulensis cocoaensis* Zone of Toumarkine and Bolli (1970; not the *G. cerroazulensis* Zone of Bolli, 1957). The presence of *Globigerinatheka semiinvoluta* in Sample 612-19,CC indicates that Cores 612-19 and 612-20 correlate with the uppermost part of the *G. semiinvoluta* Zone, yielding a relatively precise biostratigraphic estimate of the age of the section immediately overlying the unconformity noted in Section 612-21-5. This zonal assignment is in good agreement with the nannofossil assignment to Zone CP15b and yields an estimated age of approximately 37.8 Ma using the time scale of Berggren et al. (1985). *Globorotalia cerroazulensis cunialensis* occurs in Samples 612-18,CC and 612-17,CC, yielding an assignment to the uppermost Eocene *G. cerroazulensis cunialensis* Zone of Toumarkine and Bolli (1970).

The Eocene/Oligocene boundary is recognized by the extinction of *Hantkenina* spp. and *G. cerroazulensis* ssp. This extinction occurs in the upper part of Core 612-17 or between Cores 612-17 and 612-16. These taxa are abundant in Sections 611-17-4 through 612-17-6; in Sections 612-17-1 to 612-17-3 they are less abundant and sporadic, which suggests possible reworking. Therefore, Sections 612-17-3 through 612-17-1 may be either Eocene or Oligocene. Samples 612-16,CC through 612-16-6, 117–119 cm are assigned to the lower Oligocene *Pseudohastigerina micra–Cassigerinella chipolensis* Zone (approximately = Zone P18). Thus, there are approximately 33 m of upper Eocene, 4.5 m of Eocene–Oligocene (undifferentiated), and 1 m of lowermost Oligocene section present at Site 612. Evidence of reworking indicates that a short hiatus (0.5 m.y.) may be represented at the Eocene/Oligocene contact. This is supported by the fact that the last occurrence of rosette-shaped discoasters (*Discoaster barbadiensis* and *D. saipanensis*) occurs at the top of Core 612-17, about the same level as the last appearance of *Hantkenina* and *G. cerroazulensis*. Elsewhere, the last occurrence of rosette-shaped discoasters clearly precedes the planktonic foraminiferal last appearances (e.g., Snyder et al., 1984, Berggren et al., 1985). These relationships need to be evaluated by quantitative shore-based studies. The thin Oligocene section overlying the possible unconformity may represent only ~100,000 yr. In general, preservation is good in the upper Eocene–lowermost Oligocene section, and both planktonic and benthic foraminifers, although somewhat diluted by siliceous microfossils, are abundant.

Upper Neogene

An unconformity representing a 25-m.y. hiatus separates lowermost Oligocene sediments at the base of Core 612-16 from upper Neogene sediments in Section 612-

16-6. Core 612-15 contains few planktonic foraminifers; benthic foraminifers indicate a Neogene age based upon the presence of *Bulimina striata mexicana* s.s. Sample 612-14,CC is assigned to the upper Miocene (probably Zone N16); it contains *Neogloboquadrina acostaensis, Globoquadrina dehiscens, Globorotalia merotumida/plesiotumida, N. continousa,* and *Globigerinoides parkerae.* A probable late late Miocene (Zone N17) age is indicated for Sample 612-13,CC by the presence of *Globigerina nepenthes, G. plesiotumida, Globoquadrina altispira globosa,* and *N. acostaensis.* However, it is possible that this sample may be lowermost Pliocene: (1) *G. dehiscens* is absent from this level, although it occurs in the underlying section; (2) small pin-hole secondary apertural openings were observed on the spiral side of "*Sphaerodinellopsis*," indicating that these specimens might be assigned to *Sphaerodinella dehiscens dehiscens* forma *immatura*, which apparently is limited to the early Pliocene. Sample 612-12,CC is barren, but 612-12-5, 7–9 cm yielded a poor assemblage of the *Globorotalia sphericomiozea-puncticulata* group along with *N. acostaensis* and the "*Sphaeroidinellopsis*" form described above. It is possible that this level may be Pliocene. Sample 612-11,CC contains a fauna similar to Sample 612-12-5, 7–9 cm, although it includes *N. humerosa, G. nepenthes*, and forms provisionally assigned to *G. margaritae*. On the basis of the occurrence of specimens tentatively assigned to *G. margaritae* combined with the nannofossil evidence, we place the Miocene/Pliocene boundary between Cores 612-11 and 612-12. Samples 612-10,CC and 612-9,CC are barren, whereas Sample 612-8,CC contains *Globorotalia crassiformis* and *G. inflata* indicative of the late Pliocene. Core 612-7 is assigned to upper Pliocene Zone N21; it includes *G. tosaensis tosaensis* and *G. tosaensis tenuitheca*. Thus, the lower/upper Pliocene boundary occurs between Samples 612-8,CC and 612-11,CC. A Pleistocene age is indicated for Cores 612-1 through 612-4 by the presence of *Globorotalia truncatulinoides*. Sample 612-5,CC contains *G. crassula*, while *G. truncatulinoides* is absent; it is therefore assigned to the upper Pliocene, in agreement with the nannofossil assignment.

In general, the late Neogene planktonic foraminiferal assemblages at Site 612 are dominated by cool-water, low-diversity assemblages (e.g., with abundant neogloboquadrinids). Biostratigraphic zonation is difficult to determine because of the absence of many marker species. This is in sharp contrast to the diverse assemblages noted in the lower Pliocene at slightly lower latitude Site 603. It is possible that the planktonic assemblages at Site 612 reflect colder conditions because of differences in the late Neogene hydrography of the western North Atlantic.

Cenozoic Benthic Foraminiferal Paleoecology

The Cenozoic section recovered at Site 612 was deposited at bathyal depths (viz. 200–2000 m). The poor preservation of the lower to lower middle Eocene section precludes detailed paleobathymetric estimates, although deposition probably occurred at upper (200–ca. 500 m) to middle (500–1000 m) bathyal depths. The presence of common *Nuttallides truempyi* in lower Eocene Sample 612-60,CC suggests deposition at middle bathyal depths (below ca. 500–600 m; Berggren and Aubert, in press). No *N. truempyi* were noted in Cores 612-38 through 612-59, although detailed examination may reveal its presence. The lower Eocene section, Cores 612-60 through 612-38, contain common *Lenticulina* spp. and *Osangularia mexicana. Gavelinella capitata, Gavelinella* cf. *G. micra, Cibicidoides* spp. (including *C. ungerianus*), *Bulimina tuxpamensis, Bulimina* cf. *B. macilenta, Pullenia eocenica, Hanzawaia cushmani*, and *Alabamina* cf. *A. dissonata* also are present in this section. The latter is considered to be a lower bathyal to abysssl taxon (extending to the lower bathyal only in the late Paleocene to early Eocene; Tjalsma and Lohmann, 1983). However, the specimens noted here are not typical.

The middle Eocene section (Cores 612-37 through 612-21) contains abundant *Lenticulina* spp., *Osangularia mexicana,* and *Gavelinella semicribrata* s.s. and s.1. Other common taxa include *Hanzawaia cushmani, Oridorsalis* sp., *Vulvulina spinosa, G. micra, Uvigerina rippensis,* and *Globocassidulina subglobosa. Nuttallides truempyi* and *Bulimina trinitatensis* occur sporadically throughout the section. In general, the association is quite rich in species. Associated taxa include *Gyroidinoides* spp. (including *G. girardana*), *Cibicidoides* spp. (including *C. ungerianus, C. tuxpamensis), Anomalina spissiformis, Bulimina macilenta, B. tuxpamensis, Bulimina* cf. *B. alazanensis, Pullenia eocenica, P. quinqueloba, P. bulloides, Turrilina robertsi-brevispira, Bolivinopsis cubensis, B. spectabilis, Pleurostomella* spp., *Gaudryina laevigata, Nonion havanense,* and *Karreriella subglabra* (see Tjalsma and Lohmann, 1983, and Miller, 1983, for illustrations and taxonomy).

The middle Eocene section is interpreted to have been deposited in middle bathyal (possibly upper bathyal) depths on the following criteria:

1. The low, sporadic abundance of *Nutallides truempyi* precludes a lower bathyal assignment (cf. lower bathyal sites of Tjalsma and Lohmann, 1983, and Miller et al., 1985; *N. truempyi* is typically greater than 10% in this time interval at lower bathyal locations);

2. The absence of *Clinapertina* spp., *Abyssammina* spp., *Cibicidoides grimsdalei*, and the rare occurrence of *Alabamina* cf. *A. dissonata* and *Aragonia* spp. also argue against a lower bathyal or abyssal assignment (Tjalsma and Lohmann, 1983; Miller, 1983; Miller et al. in press);

3. The presence of *Bulimina trinitatensis* and *N. truempyi* suggests deposition in the middle bathyal zone or deeper (below ca. 500–600 m; Berggren and Aubert, in press);

4. The presence of rare *Lenticulina decorata* suggests deposition may have been as shallow as upper bathyal (van Morkhoven et al. unpub. data); and

5. The absence of lenticulinids, vaginulinids, uvigerinids, trifarinids, siphoninids, and pararotaliids, which are typical of middle Eocene sediments on the emergent coastal plain of North Carolina (Jones, 1983) and New Jersey (Charletta, 1980) indicates deposition at greater than neritic depths.

A benthic foraminiferal faunal change occurs between the middle Eocene and the upper Eocene section. Although *Lenticulina* spp. and *Osangularia mexicana* continue as abundant taxa, *Planulina renzi* appears in abundance in the upper Eocene to lowermost Oligocene section (Core 612-20 through Section 612-16-6). *Bulimina alazanensis* and *Uvigerina basicordata* are also abundant taxa; the first appearance of the latter form agrees with its first appearance in the Gulf of Mexico (F.P.C. van Morkhoven, pers. comm., 1984). *Nuttallides truempyi* was not observed in this section. The faunal change may be attributed to either a shallowing to upper bathyal depths (ca. 300–400 m) or a faunal change that began in the deep sea near the end of the middle Eocene (Tjalsma and Lohmann, 1983; Miller, 1983; Miller et al., in press).

Cores 612-15 through 612-6 contain a typical late Neogene bathyal assemblage. Cores 612-15 through 612-13 (upper Miocene) contain *Bulimina striata mexicana, Melonis affine, M. "pompilioides" Hoeglundina elegans, Pullenia quinqueloba, P. bulloides, Cibicidoides bradyi, Sigmoilopsis schlumbergeri, Gyroidinoides* sp., *Cassidulina crassa, Karreriella bradyi, Ehrenbergina* sp., *Astrononion* sp., *Globobulimina* sp., *Pyrgo* sp., *Plectofrondicularia* sp., and *Martinottiella nodulosa*. Two apparently anomalous occurrences are *Buliminella elegantissima* and *Uvigerina senticosa. B. elegantissima* is generally found in neritic deposits and is quite abundant in Oligocene through Pliocene neritic deposits on the U.S. Atlantic margin (Olsson et at., 1980). *U. senticosa* is generally found at abyssal depths.

The Pliocene section (Cores 612-9 through 612-6) contains a rich uvigerinid–buliminid fauna. Bulumimids include *Bulimina marginata, B. aculeata* (only above Core 612-9), and *B. striata mexicana; Uvigerina aculeata* and *U. peregrina* dominate the uvigerinids. *Sphaeroidina bulloides, Pullenia bulloides,* and *Stilostomella* spp. also occur in abundance. The paleobathymetry of this section is difficult to interpret. *B. marginata* occurs primarily in outer neritic depths in this region today (Miller and Lohmann, 1982); however, elsewhere it has been shown to range into upper bathyal depths (ca. 400 m). *Planulina wuellerstorfi* and *Anomalinoides globulosus*, which occur in this section, apparently have their upper depth limits in the middle or lower bathyal zones. The Pliocene section is tentatively interpreted as having been deposited at middle bathyal depths.

Lower Pleistocene Core 612-5 contains large lenticulinids provisionally assigned to *L. americana;* they are interpreted as downslope contaminants. Above this (Core 612-1 through 612-4; upper Pleistocene), the benthic foraminiferal fauna is dominated by *Elphidium* and *Nonionella*, which probably represent downslope transport from the shelf. Associated taxa include rare *Bulimina striata mexicana, Bolivina* sp., and *Globobulimina* sp., and *Cassidulina* spp., which are more normal bathyal constituents.

Calcareous Nannofossils

The calcareous nannofossil assemblages at Site 612 are generally well preserved and abundant throughout a 675 m succession of calcareous and siliceous sediments that range in age from late Campanian to Pleistocene (Fig. 9). The sequence includes four major gaps in the nannofossil zonation, one between the middle Maestrichtian and the lower Eocene, another between the middle and upper Eocene, a third one between the lower Oligocene and the upper Miocene, and a fourth one between the upper Pliocene and the upper Pleistocene.

The samples studied for this preliminary report are from core catchers, except where more closely spaced samples were examined near some stratigraphic boundaries. Several biostratigraphic zones that have not been identified here may be revealed when more samples are studied. This study employs the zonations of Bukry (1973, 1975), Okada and Bukry (1980), and Gartner (1977) and the time scale of Berggren et al. (1985).

Cretaceous

Upper Campanian (675.30–640.75 m)

The oldest sediment cored at Site 612 is dark gray upper Campanian calcareous shale and mudstone that is approximately 35 m thick. The flora is diverse, and diagnostic species include *Broinsonia parca* and the last occurrence of *Eiffellithus eximius* in Sample 612-69-3, 125 cm (640.75 m).

Lower and Middle Maestrichtian (640.15–559.40 m)

A lithologic boundary is present in Section 612-69-3 and probably coincides with the Campanian/Maestrichtian stage boundary. Campanian strata are overlain by approximately 80 m of gray marly chalk of early Maestrichtian age. The lower Maestrichtian interval is recognized by the presence of *Broinsonia parca* above the last occurrence of *Eiffellithus eximius. B. parca* is present up to Sample 612-63,CC (588.3 m).

Upper Maestrichtian strata are not present, as indicated by the absence of diagnostic species such as *Lithraphidites quadratus, Micula mura,* and *Nephrolithus frequens*. Strata ranging in age from late Maestrichtian to Paleocene may be present in the stratigraphic interval spanned by Core 612-60 (559.40–549.80 m) where only 79 cm of core was recovered, but at present, there is no paleontologic evidence to support this possibility.

Tertiary

Lower Eocene (550.33–366.70 m)

Strata of early Eocene age are represented by approximately 183 m of siliceous chalk (Fig. 9). The oldest Tertiary sediment recovered is a core catcher sample presumably taken in the top 79 cm of the interval penetrated by Core 612-60 (549.80–559.40 m). A marked lithologic change from Tertiary siliceous chalk to dark gray Maestrichtian marly chalk occurs in the unrecovered part of Core 612-60.

Nannofossils in core catcher 612-60 are assigned to the *Discoaster binodosus* Subzone (CP9b) of early Eocene age. Species present include *Campylosphaera eodela, Chiasmolithus californicus, Discoaster diastypus, Ellipsolithus macellus, Helicosphaera seminulum, Neo-*

coccolithes dubius, and *Toweius eminens.* The earliest Eocene subzone (CP9a), recognized by the presence of *Tribrachiatus contortus,* was not recovered and may be missing in this section or may lie in the uncored interval.

A nannofossil flora assigned to the *T. orthostylus* Zone (CP10) is present from Samples 612-59,CC to 612-55,CC (549.80–511.50 m). The first appearance of *D. lodoensis* is at the base of this zone, and some of the associated species are *Campylosphaera dela, Chiasmolithus californicus, C. consuetus, Discoaster diastypus, D. mirus, D. multiradiatus, Discoasteroides kuepperi, Hilicosphaera seminulum, Lophodolithus nascens, Neococcolithes dubius, Toweius eminens,* and *Tribrachiatus orthostylus.*

The *Discoaster lodoensis* Zone (CP11) is present from Samples 612-54,CC to 612-43,CC (502.00–395.60 m), from the first appearance of *Coccolithus crassus* to the first appearance of *D. sublodoensis.* Nannofossil species present include, among others, *Campylosphaera dela, Chiasmolithus californicus, C. consuetus, C. grandis, Discoaster barbadiensis, D. binodosus, D. lodoensis, Discoasteroides kuepperi, Helicosphaera lophota, H. seminulum,* and *Sphenolithus radians.*

A relatively thin interval of the section representing the *Discoasteroides kuepperi* Subzone (CP12a) is present from Samples 612-42,CC to 612-40,CC (386.00–366.70 m) and completes the lower Eocene sequence. The base of this interval is placed at the first occurrence of *Discoaster sublodoensis,* and the assemblage contains species also commonly found in the underlying Zone CP11.

Middle Eocene (357.00–181.41 m)

Middle Eocene siliceous chalk is approximately 176 m thick and appears to be biostratigraphically conformable with the underlying lower Eocene. The *Rhabdosphaera inflata* Subzone (CP12b) is present from Samples 612-39,CC to 612-37,CC (357.00–337.70 m). *Rhabdosphaera inflata* is restricted to this interval and associated species include *Chiasmolithus expansus, C. grandis, C. solitus, Discoaster barbadiensis, D. sublodoensis, Hilicosphaera lophota, H. seminulum, Neococcolithes dubius,* and *Sphenolithus radians.*

The overlying strata from Samples 612-36,CC to 612-27,CC (328.10–241.40 m) are assigned to the *Chiasmolithus gigas* Subzone (CP13b) of the tripartite *Nannotetrina quadrata* Zone (CP13). Subzones CP13a and CP13c were not recognized, but they may be revealed when more closely spaced samples are studied. *Chiasmolithus gigas* is restricted to the beds assigned to Subzone CP13b. Other species present are *Campylosphaera dela, Chiasmolithus expansus, C. grandis, C. solitus, Discoaster barbadiensis, D. saipanensis, Helicosphaera lophota, H. seminulum, Neococcolithes dubius,* and *Sphenolithus furcatolithoides.*

The upper part of the middle Eocene is represented by the *Discoaster bifax* Subzone (CP14a) and extends from Samples 612-26,CC to 612-21-5, 121 cm (231.80–181.41 m). The last occurrence of *Chiasmolithus solitus* and the first occurrences of *D. bifax* and *Reticulofenestra umbilica* are in this interval, and other species in the assemblage include *Campylosphaera dela, Chiasmolithus expansus, C. grandis, Discoaster barbadiensis, D. saipanensis, Helicosphaera lophota, H. seminulum,* and *Neococcolithes dubius.*

The *Discoaster saipanensis* Subzone (CP14b) is missing from the section as is the overlying *Chiasmolithus oamaruensis* Subzone (CP15a). A hiatus of approximately 5 m.y. is represented by a disconformable contact between middle Eocene and upper Eocene strata (Fig. 9).

Upper Eocene (181.37–136.40 m)

The upper Eocene siliceous ooze is assigned to the *Isthmolithus recurvus* Subzone (CP15b) and extends for approximately 45 m from 612-21-5, 111 cm to 612-17-1, 20 cm. The base of the zone is placed at the first appearance of *I. recurvus,* and the top is at the last occurrences of *Discoaster barbadiensis* and *D. saipanensis.* Species observed in this interval include *Chiasmolithus oamaruensis, Dictyoccoccites bisectus, D. scrippsae, Discoaster nodifer, Helicosphaera bramlettei, H. compacta,* and *Reticulofenesta umbilica.*

Discoaster barbadiensis and *D. saipanensis* become increasingly rare up the section and disappear at the top of this zone. The Eocene/Oligocene contact may occur between Cores 612-17 and 612-16.

Lower Oligocene (136.20–135.37 m)

Oligocene strata at this site are only about 1.0 m thick. They are assigned to the *Coccolithus subdistichus* Subzone (CP16a), the oldest zone in the Oligocene. The base of the zone is placed provisionally at Sample 612-6,CC, just above the last occurrence of *Discoaster barbadiensis* in Sample 612-17-1, 20 cm. The nannofossil assemblage is similar to that of the underlying uppermost Eocene, except that *D. barbadiensis* and *D. saipanensis* are absent. The top of the zone is at a lithologic break between Samples 612-16-6, 105 cm and 612-16-6, 117 cm.

Upper Miocene (135.25–89.47 m)

A disconformity separates upper Eocene siliceous ooze from upper Miocene calcareous mud and glauconitic sand (Fig. 9). It represents a hiatus of approximately 24 m.y. that includes much of the early Oligocene, the late Oligocene, and the early and middle Miocene.

The oldest Miocene strata in the section are assigned to the *Discoaster hamatus* Zone (CN7). These beds are present from Samples 612-16-6, 105 cm to 612-15,CC (135.25–126.70 m). *D. hamatus* is restricted to this interval, and other members of the assemblage include *D. belli, D. bollii, D brouweri, D. challengeri, D. intercalaris, D. pentaradiatus, D. quinqueramus, D. variabilis,* and *Reticulofenestra pseudoumbilica.*

The *Discoaster neohamatus* Zone(CN8) is present in Samples 612-14,CC and in 612-13,CC (117.20–107.50 m). This zone lies above the last occurrence of *D. hamatus* and contains the first appearance of *D. loeblichii;* otherwise the flora is similar to that observed in Zone CN7.

The core catcher sample of Core 612-12 is glauconitic sand barren of nannofossils. Sample 612-12-1, 137 cm (89.47 m) is assigned to the *Discoaster quinqueramus* Zone (CN9). The flora contains *D. quinqueramus* and the first appearances of *D. berggrenii* and *D. surculus.*

Other species represented include *Ceratolithus armatus, Discoaster brouweri, D. variabilis, Sphenolithus abies,* and *Triquetrorhabdulus rugosus.*

The uppermost subzone in the Miocene (CN10a) was not recognized, but it may be revealed with closer sampling. At present, a biostratigraphic gap in the section has not been confirmed.

Lower Pliocene (88.10 m)

A lower Pliocene flora is present in a single sample from 612-11, CC. It is assigned to the *Ceratolithus acutus* Subzone (CN10b) and contains *Amaurolithus amplificus, C. acutus, Discoaster asymmetricus, D. berggrenii, D. brouweri, D. pentaradiatus, D. surculus, D. variabilis,* and *Reticulofenestra pseudoumbilica.*

Upper Pliocene (59.00–37.05 m)

The beds from Samples 612-8,CC to 612-5-3, 45 cm (59.00–37.05 m) are assigned to the *Calcidiscus macintyeri* Subzone (CN12d) of latest Pliocene age. They contain *Discoaster brouweri*, which becomes rare near the top of this interval. Other *Discoaster* species are absent except for *D. asymmetricus* in Sample 612-8,CC. The nannofossil assemblage also contains *Calcidiscus macintyeri, Ceratolithus cristatus, Crenalithus doronicoides, Cyclococcolithina leptopora, Helicosphaera carteri, Pseudoemiliania lacunosa,* and *P. ovata.*

Core catcher samples from Cores 612-9 and 612-10 from the undated interval between the lower and upper Pliocene are composed of glauconitic sand barren of nannofossils; the missing zones may be recognized upon closer sampling.

Quaternary

Upper Pleistocene (36.92–0.00 m)

A lithologic boundary is present in Section 612-5-3 where upper Pliocene calcareous mud and interbedded glauconitic sand is overlain by upper Pleistocene glauconitic, calcareous mud. Beds of early Pleistocene age are not present.

Sample 612-5-3, 32 cm (36.92 m) contains rare nannofossils and is assigned to the *Gephyrocapsa oceanica* Zone (Gartner, 1977). The flora contains *Coccolithus pelagicus, Crenalithus doronicoides, C. productellus, Cyclococcolithina leptopora, Gephyrocapsa caribbeanica, G. oceanica,* small *Gephyrocapsa* species, and *Helicosphaera carteri. Discoaster brouweri* is not present.

The remaining strata in the section from Samples 612-5-2, 110 cm to 612-1,CC (36.20–0.00 m) are assigned to the *Emiliania huxleyi* Zone (CN15) of latest Pleistocene age. The flora contains *E. huxleyi* and many members of the assemblage found in the older Pleistocene sediment with the exception of *Pseudoemiliania lacunosa* and *P. ovata.*

Radiolarians

The abundance, preservation, and diversity of the radiolarian assemblages at Site 612 varies through the section. A few poorly preserved Cretaceous radiolarians occur at the base of the section, but no detailed age assignments could be made. The middle to upper Eocene assemblage is well preserved and diverse, although many of the species used to identify the zones of Riedel and Sanfilippo (1978) are sparse or absent. Also, some intervals of the Eocene section have undergone silica diagenesis in the form of dissolution, recrystallization, and replacement of the radiolarians. The Neogene radiolarian assemblages are sparse at Site 612, particularly in the glauconitic intervals. The assemblages are dominated by biostratigraphically nondiagnostic taxa, possibly due to the influence of a deltaic system on the shelf (Poag, 1980, 1985), which created conditions inhospitable to most pelagic radiolarian faunal elements (as observed by Palmer, 1986, in deposits of comparable age in the mid-Atlantic Coastal Plain).

In this study, core catcher samples from Cores 612-1 through 612-72 were examined. Radiolarians were prepared for study according to standard procedures (Riedel and Sanfilippo, 1977). Additional samples from each section of Cores 612-12 through 612-35 were studied in order to improve biostratigraphic resolution in the Miocene through upper Eocene interval.

The Cenozoic radiolarian zones of Riedel and Sanfilippo (1978) and subsequent modifications to the upper Eocene by Riedel and Sanfilippo in Saunders et al. (1985) are used. However, some of the datums within these zones are difficult to recognize at Site 612 because of the relative sparseness of many tropical species on which the zones are based. Therefore, other taxa are used to supplement the age determinations, based on biostratigraphic data in Foreman (1973), Sanfilippo and Riedel (1973, 1982), Nigrini (1977), and Westberg and Riedel (1978).

Correlation of the radiolarian zones of Riedel and Sanfilippo (1978) with other biostratigraphic and chronostratigraphic sytems is based on the Berggren et al. (1985) time scale. This time scale changes the traditional age assignments of certain zones. For example, the *Thyrsocyrtis bromia* Zone extends only to the Eocene/Oligocene boundary according to Riedel and Sanfilippo (1978); in Saunders et al. (1985) these authors subdivide the *T. bromia* Zone into the *Cryptoprora ornata, Calocyclas bandyca,* and *Carpocanistrum azyx* zones, with the top of the *C. azyx* Zone approximating the Eocene/Oligocene boundary. According to the Berggren et al. (1985) time scale, the *C. azyx* Zone (formerly upper *T. bromia* Zone) extends into the lower Oligocene.

Other major differences are the placement of the lower/middle Eocene and middle/upper Eocene boundaries. According to Riedel and Sanfilippo (1978), these fall within the *Thyrsocyrtis triacantha* and *Podocyrtis mitra* Zones respectively. In the Berggren et al. (1985) time scale the same boundaries are placed within the *Carpocanistrum azyx* and *Theocotyle cryptocephala* zones.

Cretaceous

The only Cretaceous radiolarians observed at Site 612 are from Sample 612-61,CC (569.0 m). These include badly corroded spongodiscids and a few specimens of *Dictyomitra* sp. c.f. *D. multicostata.*

Lower Eocene

Radiolarians are not well preserved in Cores 612-60 through 612-49 (559.4–453.7 m), but sufficient diagnostic taxa are found to allow recognition of lower Eocene zones.

Sample 612-60,CC (559.4 m) is barren of radiolarians, but Samples 612-59,CC (549.0 m) and 612-58,CC (540.2 m) contain *Buryella tetradica* and *Phormocyrtis striata exquisita*, indicating the *Buryella clinata* or *Bekoma bidartensis* zones. The *Bekoma bidartensis* Zone is partly of Paleocene age, but this assignment does not conclusivley demonstrate the presence of Paleocene strata at Site 612.

Sample 612-57,CC (530.6 m) is barren of radiolarians, but Cores 612-56,CC through 612-46,CC (521.0–424.6 m) contain poorly preserved *Phormocyrtis striata striata, Periphaena delta, Theocotyle ficus, Amphicraspedum murrayanum, Buryella clinata, Calocycloma ampulla, Amphicraspedum prolixum* group, *Lithochytris archaea, Stylotrochus quadribranchiatus multibranchiatus, Podocyrtis diamesa* and *Lophocyrtis biaurita,* but not *Dictyophimus craticula, Theocotyle cryptocephala,* or *Dictyoprora mongolfieri*. This assemblage suggests the *Phormocyrtis striata striata* Zone.

Middle Eocene

The lower/middle Eocene boundary is not recognized on the basis of radiolarian zones because of the poor silica preservation in Samples 612-45,CC through 612-36-5, 110–112 cm. The *Theocotyle cryptocephala* and *Dictyoprora mongolfieri* zones are not recognized at Site 612, although they may be represented by the diagenetically altered interval in Samples 612-45,CC through 612-36-5, 110–112 cm (414.9–325.6 m).

From Samples 612-36-3, 110-112 cm through 612-21,CC (322.6–183.8 m), a diverse and well-preserved assemblage is found. Taxa that range through the interval include: *Lithapium anoectum, Spongatractus pachystylus, Lithocyclia ocellus, Periphaena tripyramis triangula, P. tripyramis tripyramis, P. decora, Ceratospyris articulata, Lophocyrtis biaurita, Calocyclas hispida, Dictyophimus craticula, Lithochytris vespertilio, Lamptonium obelix, Phormocyrtis striata striata, Theocorys anapographa, Podocyrtis papalis, Thyrsocyrtis hirsuta, T. rhizodon, Theocotylissa ficus, Dictyprora urceolus* and *D. amphora*. Other taxa with restricted ranges allow subdivision of this interval into three zones.

The *Thyrsocyrtis triacantha* Zone is identified from Samples 612-36-3, 110–112 cm through 612-27,CC (322.6–241.4 m) above the first appearance of *Eusyringium lagena* and below the last appearance of *Podocyrtis dorus*. The *P. phyxis* to *P. ampla* transition was not recognized because of the scarcity of these taxa. Other species restricted to this interval include *Lamptonium fabaeforme chaunothorax, Theocotyle cryptocephala* and rare *T. nigriniae*.

The *Podocyrtis ampla* Zone is recognized from Samples 612-27-5, 110–112 cm through 612-24-1, 110–112 cm (238.9–204.1 m) below the last occurrence of *P. dorus* to below the *P. sinuosa* to *P. mitra* evolutionary transition. The interval contains the last appearance of *Theocotyle conica, P. diamesa*, and *Thyrsocyrtis tensa* and the evolutionary transition of *Eusyringium lagena* to *E. fistuligerum*.

The *P. mitra* Zone is found from Samples 612-23,CC through 612-21,CC (203.0–183.8 m) above the *P. sinuosa* to *P. mitra* evolutionary transition, and below the first appearance of upper Eocene taxa above Sample 612-21,CC (183.8 m). This interval contains the last appearance of *P. ampla fasciolata* but not the *Lithapium anoectum* to *L. mitra* evolutionary transition, nor the last appearance of *Lophyocyrtis biaurita*, suggesting that only the lower portion of the *P. mitra* Zone is present.

Upper Eocene to (to lower Oligocene?)

Samples 612-20-3, 110–112 cm through 612-16,CC (168.8–136.2 m) contain the upper Eocene *Calocyclas bandyca* and *Cryptoprora ornata* zones (formerly the upper part of the *Thyrsocyrtis bromia* zone of Riedel and Sanfilippo, 1978). Diagnostic forms include: *Lithocyclia aristotelis, Theocyrtis tuberosa, Cryptoprora ornata, Dictyoprora armadillo, Lychnocanoma amphitrite, Lophocyrtis jacchia, Cyclampterium longiventer, Lithapium mitra, Artophormis barbadensis, Dictyoprora pirum, D. mongolfieri, Tristylospiris triceros*, and *D. ovata*.

The *Carpocanistrum azyx* Zone (formerly the lower part of the *T. bromia* Zone) appears to be absent since *Lophocyrtis jacchia* and *Lychnocanoma amphitrite* are consistently present. Likewise, the *Podocyrtis goetheana* and *P. chalara* Zones appear to be absent, suggesting a biostratigraphic gap of 5 m.y., from 42.2 to 37.2 Ma.

The upper Eocene interval can be subdivided into the *Calocyclas bandyca* Zone below the last appearance of *C. turris, C. hispida,* and *Thyrsocyrtis bromia* in Sample 612-18-3, 110–112 cm (149.8 m) and the *Cryptoprora ornata* Zone above. The *C. ornata* Zone contains the Eocene/Oligocene boundary, according to the Berggren et al. (1985) time scale, although Riedel and Sanfilippo (in Saunders et al., 1985) place the top of this zone at the Eocene/Oligocene boundary. The appearance of *Artophormis gracilis* in Sample 612-17,CC (145.7 m) and *Lithocyclia angusta* in Sample 612-17-3, 110–112 cm (140.3 m) in subordinate abundances to their respective ancestors, *A. barbadensis* and *L. aristotelis,* suggests that the top of the *C. ornata* Zone is approached but not reached through Sample 612-16,CC (136.2 m). Therefore, radiolarian results suggest that the interval is entirely of late Eocene age, but do not conclusively demonstrate the presence or absence of lower Oligocene deposits in Hole 612.

Upper Middle Miocene to Pliocene

Neogene radiolarians are much less abundant and more poorly preserved than Eocene radiolarians at Site 612. Although predominantly nondiagnostic taxa are found, Samples 612-16-5, 110–112 cm through 612-13-6, 110–112 cm (133.8–106.4 m) contain *Diartus petterssoni, Didymocyrtis antepenultima, Stichocorys delmontensis, Cyrtocapsella tetrapera, Spirocyrtis subscalaris*, and *Phormostichoartus corbula*. Forms intergradational between *Didymocyrtis laticonus* and *Diartus petterssoni*, and between *Diartus petterssoni* and *D. hughesi* were observed.

A few specimens of *Stichocorys peregrina* were found, apparently below the range attributed to this species by Riedel and Sanfilippo (1978).

Some poorly reserved and possibly reworked lower to middle Miocene taxa, such as *Didymocyrtis prismatica* and *D. violina* occur in this interval, although strata of this age were not recognized at Site 612 by foraminifer or nannofossil biostratigraphy. The ranges of many species in this interval overlap the *Diartus petterssoni* and *Didymocyrtis antepenultma* zones, although it is not possible to assign a specific zone. The base of the *Diartus petterssoni* Zone is at 13.2 Ma on the Berggren et al. (1985) time scale. The top of the *Thyrsocyrtis bromia* Zone in Sample 612-16,CC (136.2 m) is placed at 35.4 Ma by Berggren et al. (1985). These results indicate that a minimum of 22 m.y. is missing between the top of the *Thyrsocyrtis bromia* Zone in Sample 612-16,CC (136.2 m) and the *Diartus petterssoni* to *Didymocyrtis antepenultima* Zone interval beginning in Sample 612-16-5, 110-112 cm (133.8 m).

Radiolarians occur sporadically in Samples 612-13-5, 110–112 cm through 612-13-1, 110–112 cm (104.9–98.9 m) and are absent from the highly glauconitic portions of this interval. The assemblage is dominated by biotratigraphically nondiagnostic forms, including *Dictyocoryne* spp., *Eucyrtidium* spp., *Lynchnocanoma* spp., pyloniids, actinommids, porodiscids, and other circular spongodiscids. A few specimens of *Stichocorys peregrina, Didymocyrtis penultima, Spongaster berminghami, D. antepenultima,* and *Stichocorys delmontensis* suggest a *S. peregrina* Zone to *D. penultima* Zone assignment for this interval. *Diartus hughesi* is also observed in this assemblage, although this is above the range indicated for the species by Riedel and Sanfilippo (1978). Some reworked lower to middle Eocene radiolarians are found as well, including *Lithocyclia ocellus* and *Calocyclas hispida*.

Pliocene–Pleistocene

An undifferentiated Pliocene–Pleistocene interval is recognized in Samples 612-12,CC through 612-1,CC (97.8–4.8 m) on the basis of a sparse radiolarian assemblage. Most of the assemblage consists of nondiagnostic taxa such as *Dictyocoryne* spp., *Eucyrtidium* spp., porodiscids, pyloniids, and litheliids. Stratigraphically important forms are rare and include *Pterocorys zancleus, Pterocorys hertwigii, Theocalyptra davisiana, Didymocyrtis avita,* and *Lamprocyrtis heteroporos*. This assemblage is assigned an undifferentiated Pliocene–Pleistocene age rather than a specific zone, since the diagnostic taxa are extremely rare in most samples. It is not possible to determine whether a biostratigraphic gap exists between this and the underlying interval.

An unusual radiolarian assemblage is found in Sample 612-4,CC (33.6 m), containing a flood of *Theocalyptra davisiana*. Great abundances of this species have been linked with glacial epochs (Morley and Hays, 1979). Futhermore, Benson (1972) noted that this species was "ubiquitous and often dominant in Pleistocene (and glacial Pliocene?) assemblages cored in the North Atlantic on DSDP Leg 12." Its abundance in Sample 612-4,CC may record a glacial event in the Pliocene–Pleistocene of Site 612.

Neogene Paleoenvironments

A few preliminary comparisons may be drawn between the Neogene radiolarian assemblage of Site 612 and that of the mid-Atlantic Coastal Plain (Palmer, 1986; and unpub. data). Large abundances of *Dictyocoryne, Didymocyrtis*, porodiscids, and other circular spongodiscids were observed in the Neogene interval of Site 612. These forms are abundant in the neritic deposits of the Atlantic Coastal Plain. Modern representatives of these taxa have been found in abundance in the plankton of modern eutrophic shelves by Casey et al. (1982). The predominance of these taxa at Site 612 may result from the environmental effects of the prograding Neogene delta system previously recognized in this area (Poag, 1980; 1985). The brackish plume associated with large river deltas may be traced across a wide region of the surrounding shelf. It may be that terrestrial runoff supplied a brackish surface layer which extended to the Site 612 area during the Neogene. Since most radiolarians live in the surface waters (Petrushevskaya, 1971), the fauna may have become restricted to the few taxa that could tolerate these conditions. Futhermore, delicate taxa and tropical species are rare, suggesting that dissolution and the middle latitude setting of Site 612 may also have affected the Neogene assemblage.

A striking difference between the Neogene radiolarian faunas of Site 612 and those of the mid-Atlantic Coastal Plain is the occurrence in Hole 612 of the deep dwelling radiolarians, *Cornutella, Bathropyramis,* and *Peripyramis*, which were found by Casey (1977) in plankton at depths of 500 to 1000 m. In the Coastal Plain, *Cornutella* is absent, apparently excluded from the shallow shelf setting. *Bathropyramis* and *Peripyramis* only appear in the Coastal Plain (at low levels of abundance) in a single horizon where upwelling was evidently intense (as indicated by the occurrence of phosphorite; Palmer, unpubl. data).

These preliminary observations of the Neogene radiolarian fauna of Site 612 suggest deposition in waters of bathyal depth which were influenced by the brackish plume of a prograding delta landward of the site. The radiolarian fauna is similar to that of the mid-Atlantic Coastal Plain in that taxa characteristic of eutrophic shelves are abundant, but is unlike the Coastal Plain fauna in that deep-dwelling taxa are consistently present.

SEDIMENTATION RATES AND SUBSIDENCE HISTORY

The sedimentation rates for Site 612 have been calculated on the basis of the detailed faunal and floral examination (aboard ship) of core catcher samples (see sections on Foraminifer, Nannofossil, and Radiolarian Biostratigraphy). Using the Berggren et al. (1985) Cenozoic time scale and the Cretaceous time scale of van Hinte (1976), age/depth plots have been constructed for the foraminifer, nannofossil, and radiolarian data (Figs. 10–12). These are similar in most respects, but it was decid-

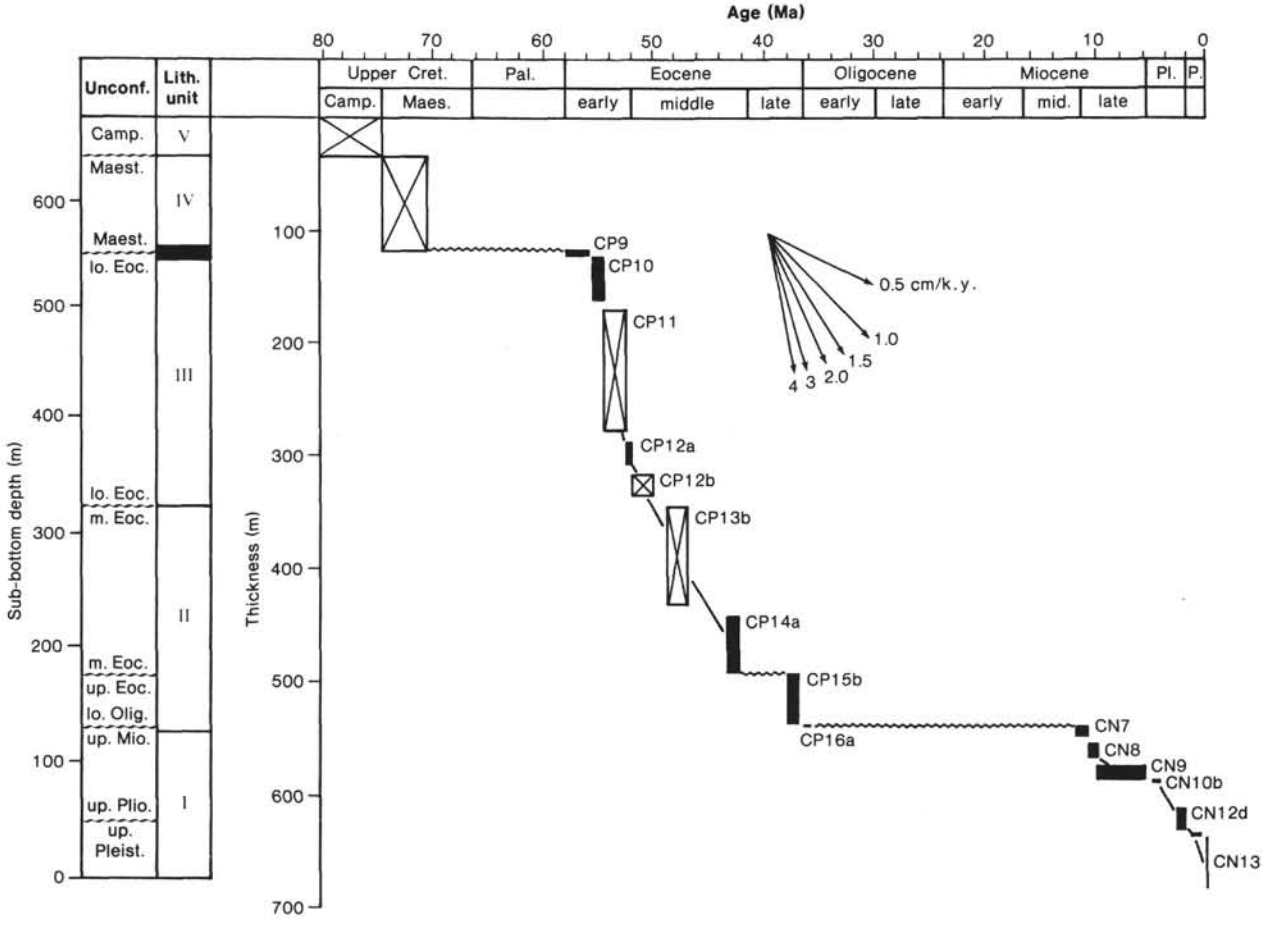

Figure 10. Sediment accumulation rates at Site 612 based on nannofossil biostratigraphy.

ed that they would be presented separately until shore-based work was completed.

The durations of the major hiatuses are similar among the three figures. A prominent feature is the ~10 m.y. hiatus at the Cretaceous/Tertiary contact. Other major hiatuses occur between the middle and late Eocene (~5 m.y.), between the early Oligocene and the late Miocene (~25 m.y.), and between the late Pliocene and late Pleistocene (~1.5 m.y.). The duration of the hiatuses associated with the unconformity noted near the lower/middle Eocene contact and the upper Miocene/Pliocene contact is evidently too short to be estimated (from shipboard data) on the basis of missing biozones.

The limited data available for the Cretaceous indicates an average sedimentation rate of 1.2 cm/k.y. (12 m/m.y.). The hiatus at the Cretaceous/Tertiary boundary (admittedly with a poor recovery record) is estimated to have been about 10 m.y.

Lower Eocene sedimentation rates are estimated to be approximately 3.5 to 4.0 cm/k.y. (35–40 m/m.y.). Middle Eocene rates are slightly lower, approximately 2.0 to 3.0 cm/k.y. (20–30 m/m.y.). Approximately 5 m.y. are represented by the hiatus at the middle/upper Eocene contact. Above this, upper Eocene to lowermost Oligocene sedimentation rates are probably similar to those estimated for the middle Eocene (approximately 30 m/m.y.), although this is tentative (i.e., rates could have been as high as 45 m/m.y. or as low as 15 m/m.y.).

The unconformity between the lower Oligocene and the upper Miocene sections represents approximately a 25-m.y. hiatus, which is the longest hiatus documented at Site 612. Above the unconformity, the sedimentation rate averaged 1.2 cm/k.y. (12 m/m.y.) up to the Pleistocene. Late Miocene sedimentation rates were lower (~5–8 m/m.y.) than Pliocene rates (~15–20 m/m.y.). Upper Pleistocene rates were quite high (~80 m/m.y.).

The sedimentation rates for Hole 612 were analyzed using the "backstripping" technique of Watts and Ryan (1976) and Steckler and Watts (1978). Backstripping involves two procedures. First, the stratigraphy at a well site is reconstructed for different periods of geological time taking into account compaction (mechanical), long-term changes in sea level, and changes in water depth. Second, the stratigraphy is unloaded from the well site using the Airy or flexural model of isostasy. The resulting tectonic subsidence at the well site provides information on the origin of vertical movements (uplift and subsidence) in the vicinity of the well site. A somewhat similar approach was taken by van Hinte (1978) in his "geohistory analysis" technique.

The general equation for backstripping can be written:

$$Y = S^* \frac{(\rho_m - \bar{\rho}_s)}{(\rho_m - \rho_w)} + W_d - \Delta_{SL} \frac{\rho_m}{(\rho_m - \rho_w)} \qquad (1)$$

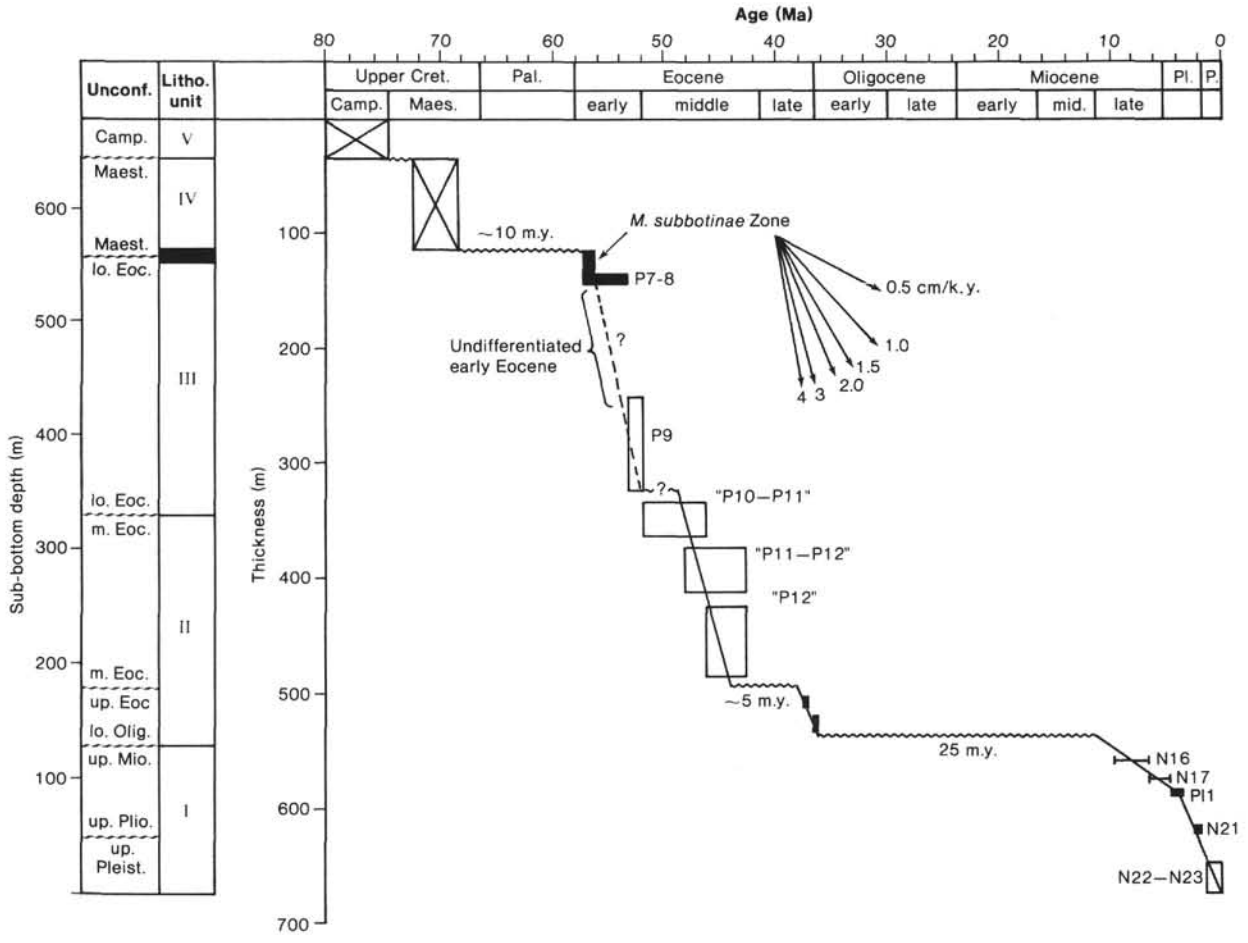

Figure 11. Sediment accumulation rates at Site 612 based on foraminifer biostratigraphy.

where ρ_m is the average mantle density, ρ_s is the average density of sediments, ρ_w is the average density of seawater, Δ_{SL} is the elevation of long-term sea level (positive for a sea level rise), S^* is the sediment thickness corrected for compaction, Y is the tectonic subsidence, and W_d is the water depth.

To correct for the effect of compaction (Eq. 1), we used shipboard measurements of sonic velocity to determine the variation of porosity with depth (Physical Properties section). By assuming the porosity–depth curve had remained constant, the thickness and density of each layer were calculated as they appeared during geological time. We assumed a constant grain density of 2.50 g/cm^3 for the sediments at Site 612. The sea level correction was made using the long-term sea level curve of Watts and Steckler (1979). We did not apply a correction for water depths. Equation 1 can then be rewritten:

$$Y' = Y - W_d \qquad (2)$$

where Y' is the depth to the basement through time corrected for sediment and water loading, but still contains both tectonic and water depth effects.

Figure 13 shows the sediment accumulation (S) and Y' for Hole 612. The region between the curves labeled S and Y' represents that part of the subsidence caused by sediment and water loading. The region above the curve labeled Y' represents that part due to tectonic and water depth effects. The relative smoothness of Y' compared to S shows that backstripping successfully removes variation in sedimentation rates that result from variations in sediment supply and local seafloor processes. For example, during the late Miocene to Holocene the sedimentation rate ranges from 0.1 to 2 cm/k.y. (1–20 m/m.y.). Backstripping reduces the variations to a smooth curve of average slope of about 0.3 cm/k.y. (3 m/m.y.).

Site 612 is located seaward of the East Coast Magnetic Anomaly and hence is believed to overlie oceanic crust (e.g., Grow and Klitgord, 1980). If this is the case, then following rifting the basement at Site 612 should have subsided like oceanic crust.

Figure 14 compares Y' at Site 612 to the predictions of the cooling plate model, which Parsons and Sclater (1977) have shown explains the subsidence of mid-oceanic ridge crests. We assumed that the crust underlying Site 612 is 175 m.y. old. The solid line in Figure 14 is predicted thermal subsidence at Site 612 for 97.5 to 175 m.y. following rifting. Figure 14 shows there is general agreement between backstripped and predicted curves. The main difference is in amplitude; the backstripping curve suggests 370 m of tectonic subsidence while the predicted curve implies 475 m. The difference could be explained by uncertainties in the initial age of rifting. Alternatively, water depth changes and/or sedimentary

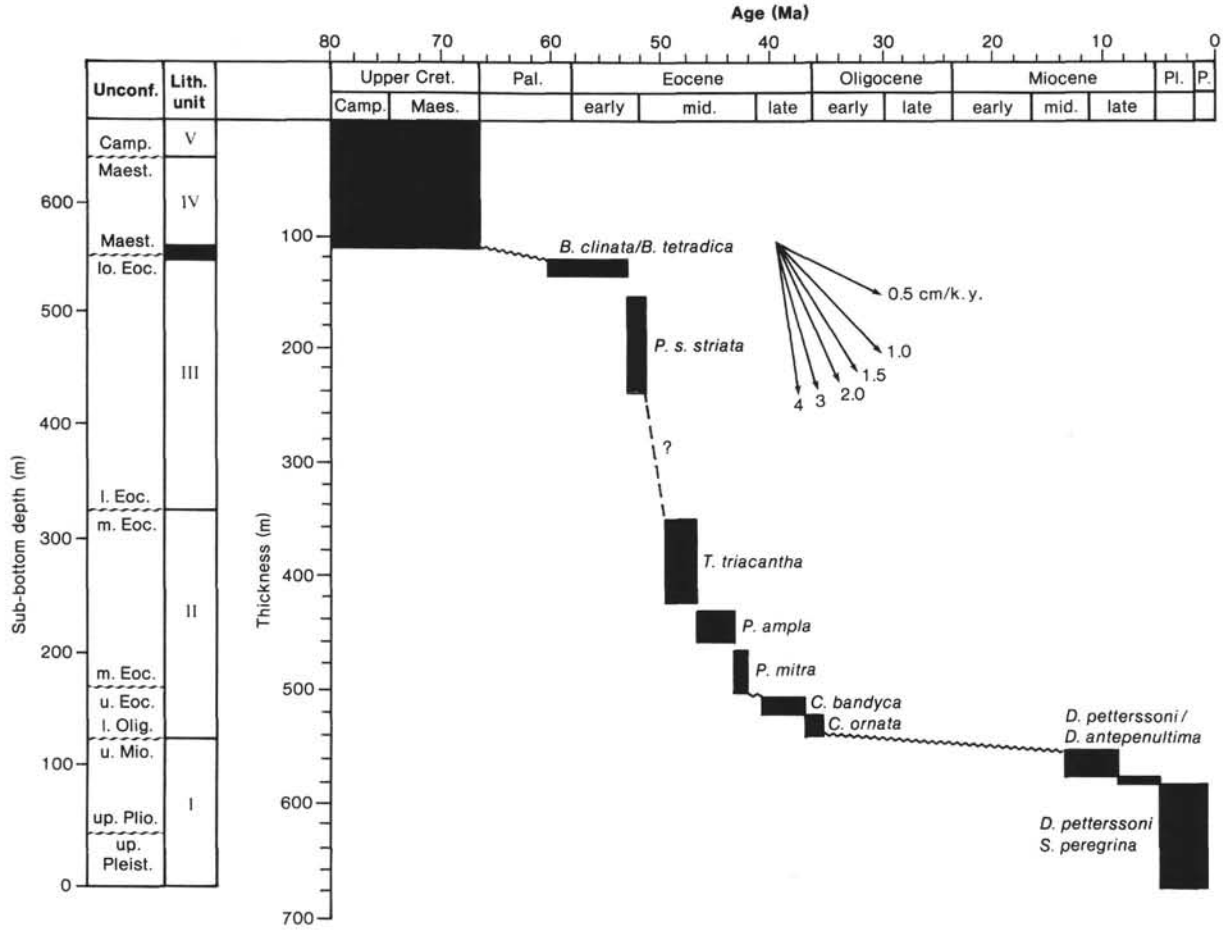

Figure 12. Sediment accumulation rates at Site 612 based on radiolarian biostratigraphy.

loading during major hiatuses could account for the difference (Fig. 14).

Backstripping suggests that thermal contraction of the lithosphere following rifting is a major contributor to the subsidence history at Site 612. In general, sedimentation rates exceeded subsidence rates due to thermal contraction, suggesting that sedimentary supply was more than sufficient to keep up with the steady subsidence of the margin. The differences between sedimentation and subsidence rates were greatest during the early to middle Eocene and late Miocene to Pliocene and late Pleistocene, suggesting significant upbuilding and/or outbuilding of the margin during these periods.

GEOCHEMISTRY

Inorganic Geochemistry

Interstitial Water

Interstitial water was squeezed from 13 core samples spaced approximately every 50 m. Interstitial water samples were analyzed for the standard DSDP suite of components: pH, salinity, alkalinity, chlorinity, calcium, and magnesium. pH and alkalinity were measured with a Corning Model 130 pH meter. Salinity was measured by a salinity refractometer (American Optical Company) and chloride concentrations were measured by titration with silver nitrate. Calcium and magnesium were measured by the method of Tsunogai et al. (1968).

The results are listed in Table 2 and shown graphically in Figure 15. The most characteristic features of the interstitial water from Site 612 are the elevated salinity and chlorinity profiles. Salinity increased from a minimum value of 34.5‰ (surface sea water is 33.8 ‰) at the shallowest depth sampled (~25.0 m) to 53‰ at 583.05 m. Chlorinity showed a very similar profile to salinity: below 196 m sub-bottom depth the two profiles are virtually parallel.

Manheim and Hall (1976) reported interstitial water salinities as high as 55‰ at about 207 m sub-bottom depth in Hole ASP 15 (7 km to the southwest of Hole 612). They suggested that this unusually high salinity may be explained by the presence of underlying salt layers. At Hole 612, the movement of saline fluids coming from below could cause the increase in salinity and chlorinity concentrations found with depth throughout this hole.

Alkalinity, on the other hand, decreases with depth (Fig. 15). Alkalinities almost 10 times as high as those generally found in seawater (surface seawater is 2.32 mEq/1) occur in the top 313.25 m of this hole. These high alkalinities may result from sulfate reduction by bacteria in

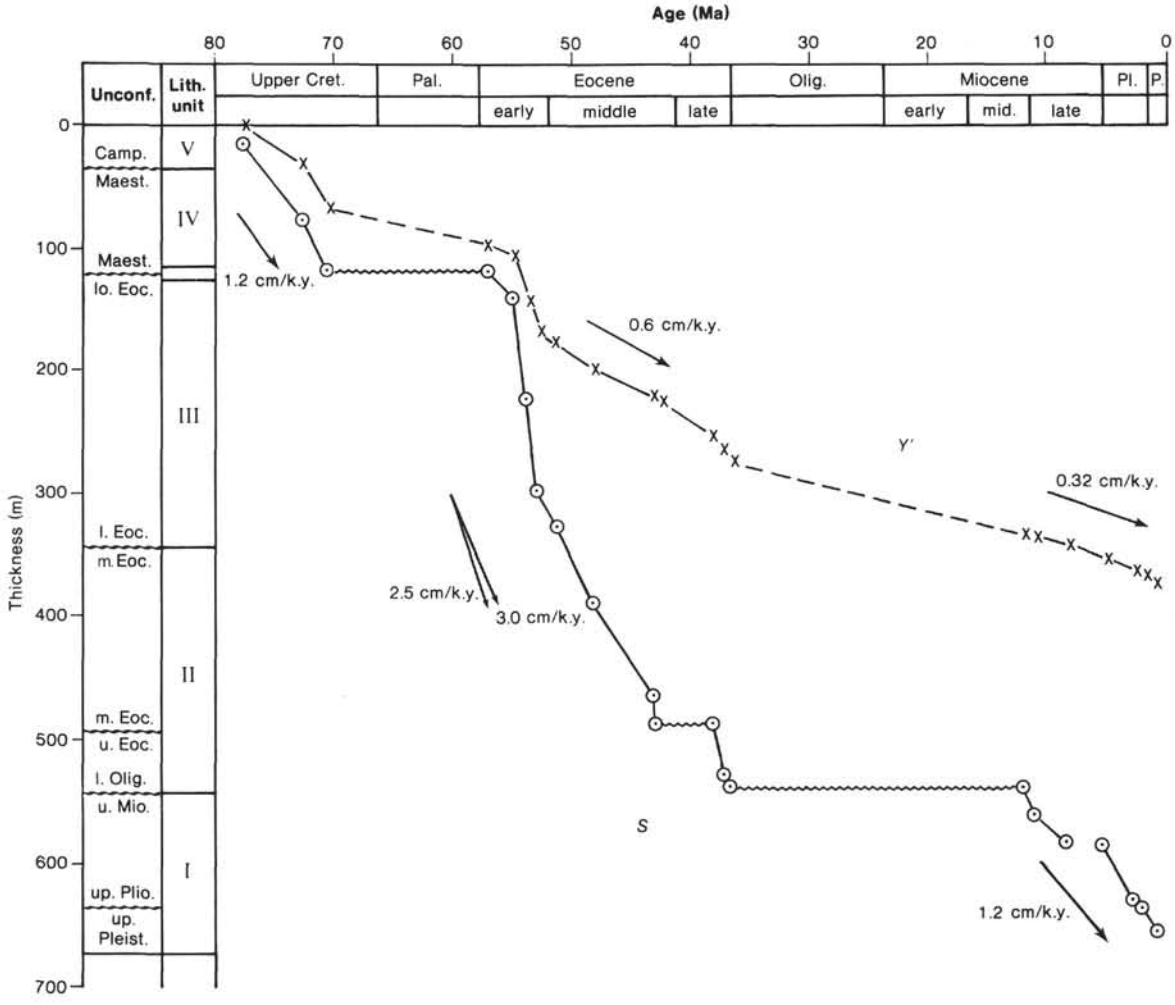

Figure 13. Sedimentation rate and tectonic subsidence at Site 612, based on nannofossil biostratigraphy in Figure 10.

these uppermost sediments recovered at Hole 612. Between 350.25 m and 583.05 m, alkalinity ranges between 8.09 and 12.29 mEq/1.

The alkalinity profile does not follow any of the other profiles except at 350 m sub-bottom depth, where there are parallel decreases in salinity, chlorinity, calcium concentration, and alkalinity, and an increase in organic carbon (Fig. 15). The decrease in these concentrations and small increase in pH coincide with the middle Eocene diagenetic boundary (324 m) and the presence of procellanite. This boundary is 8 m above the middle/lower Eocene stratigraphic boundary. The depletion of these inorganic components may be related to the formation of opal C-T.

Magnesium values throughout Hole 612 are depleted relative to seawater (See Table 2 and Fig. 15). The depletion of magnesium above 100 m sub-bottom depth may be related to the formation of glauconite. Glauconite is abundant in lithologic Unit I (0–136 m sub-bottom depth) at Hole 612. However, magnesium concentrations below 100 m sub-bottom depth increase slightly with depth even though they remain depleted relative to seawater.

Calcium increases with depth (Table 2 and Fig. 15). Calcium depletion relative to seawater is found at depths shallower than 100 m sub-bottom, indicative of calcium carbonate precipitation. Calcium carbonate precipitation may result from the high alkalinities (approximately 10 times higher than surface seawater) found in the uppermost sediments in this hole (Gieskes, 1981).

Calcium values approach the concentration of seawater between 103 and 150 m sub-bottom depth. Below 150 m sub-bottom depth, calcium concentrations in the pore waters increase above the concentration of calcium in seawater.

Calcium enrichment and magnesium depletion relative to seawater is commonly observed in most calcareous and calcareous-siliceous sediments deposited at rapid sedimentation rates (few cm/k.y.). This is attributed to the substitution of magnesium in the pore waters for calcium in the sediments (Sayles and Manheim, 1975).

Changes in magnesium (Mg) and Calcium (Ca) concentrations relative to seawater can be plotted as ΔCa and ΔMg where ΔCa = [Ca concentration in the pore water − Ca concentration in surface seawater] and ΔMg = [Mg concentration in the pore water − Mg concentration in surface seawater]. Negative values (i.e., $-\Delta$Mg) reflect depletion relative to seawater. At other DSDP sites (e.g., Sites 28, 29, and 62) Sayles and Manheim (1975)

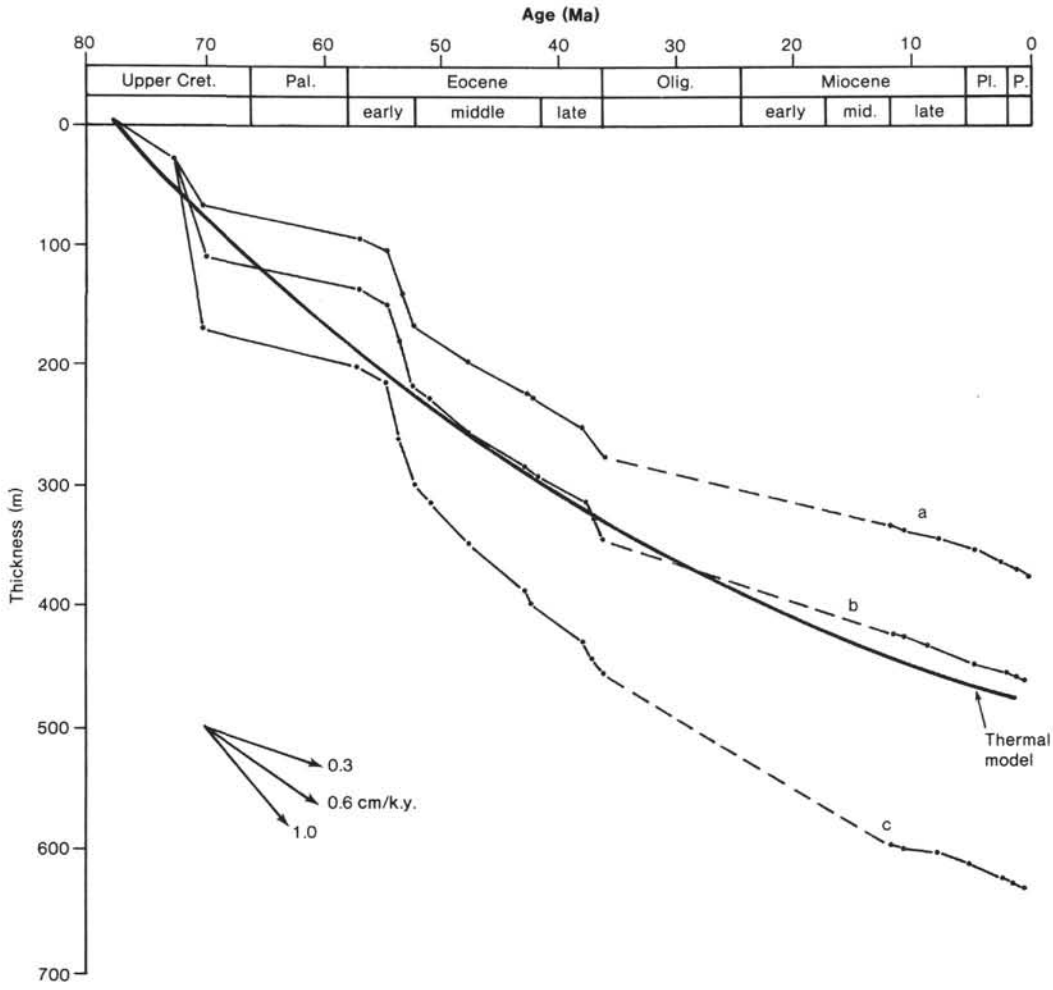

Figure 14. Comparison of the observed (dotted lines) tectonic subsidence (Y') and predicted (solid line) subsidence based on a cooling plate model at Site 612: (a) with no sediment loaded during the 10 m.y. hiatus at the Cretaceous/Tertiary contact or the 25 m.y. hiatus at the early Oligocene/late Miocene contact; (b) with 75 and 100 m of sediments; and (c) with 200 and 300 m.

Table 2. Summary of shipboard inorganic geochemical data for Hole 612.

Core-Section (interval in cm)	Sub-bottom depth (m)	pH	Alkalinity (mEq/1)	Salinity (‰)	Calcium (m*M*)	Magnesium (m*M*)	Chlorinity (‰)
IAPSO		8.05	2.35	34.8	10.55	64.54	19.375
SSW	-0-	8.23	2.32	33.8	10.37	52.39	18.75
4-4, 145–150	25.48	7.5	28.7	34.5	4.41	47.59	19.90
8-2, 140–150	55.05	7.31	17.14	35.5	8.15	45.93	18.65
13-4, 140–150	103.75	7.14	25.27	39.0	10.25	40.92	19.18
18-3, 145–150	150.18	6.70	21.02	40.5	10.23	42.07	24.32
22-3, 145–150	188.27	6.67	20.96	43.0	12.22	42.46	23.46
28-3, 140–150	245.85	6.50	20.17	47.5	16.22	42.14	25.47
35-3, 140–150	313.25	6.53	19.41	49.8	17.97	42.95	28.40
39-2, 140–150	350.25	7.01	12.29	46.3	15.04	43.68	27.74
43-3, 140–150	390.45	6.85	14.38	50.0	18.18	43.57	29.79
48-3, 140–150	438.75	No water recovery					
52-3, 140–150	477.55	6.93	13.68	51.7	19.35	45.31	30.41
59-3, 140–150	544.65	7.01	8.09	51.0	22.08	44.60	30.31
63-3, 140–150	583.05	6.81	11.01	53.0	27.29	46.46	31.63
68-4, 140–150	632.85	NES[a]	NES[a]	51.8	29.07	42.01	30.78

[a] NES = not enough sample.

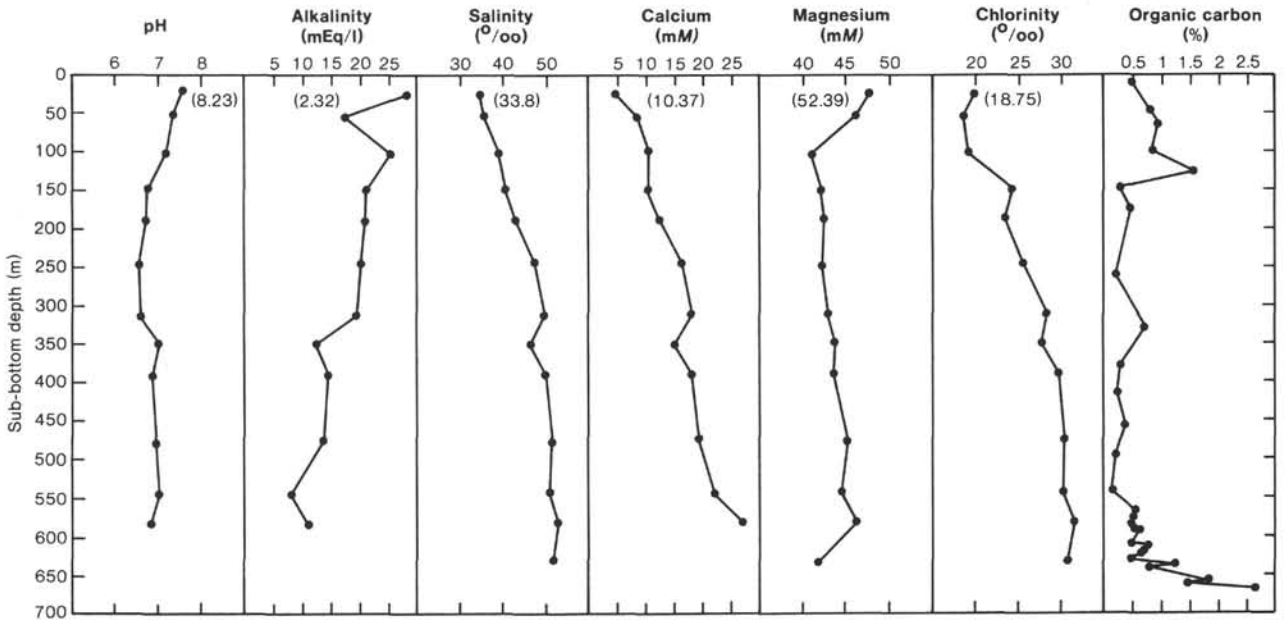

Figure 15. Shipboard interstitial water profiles and percentage organic carbon for Hole 612. Values in parentheses are concentrations in surface seawater.

showed a good linear correlation between ΔCa and −ΔMg except for small deviations due to the effects of losses or gains of sulfate and alkalinity.

In Figure 16, ΔMg and ΔCa are shown graphically for Hole 612. The line drawn through Figure 16 represents the "expected" correlation between magnesium and calcium (Sayles and Manheim, 1975). As discussed above, and unlike Sayles and Manheim (1975), the calcium values reported above 100 m sub-bottom depth for Hole 612 are below the concentration of seawater. It is also evident from these data that below 100 m sub-bottom depth, −ΔMg values are less than the "expected" values resulting from magnesium and calcium exchanges. This deviation from the "expected" at Hole 612 may be attributed to movement of fluids from below as implied by the salinity and chlorinity profiles.

The pH values decrease linearly with depth to 150 m sub-bottom depth (SBD). Below 150 m SBD, the interstitial water levels remain fairly constant at slightly acidic pH (<7.0), although a slight increase coinciding with the middle Eocene diagenetic boundary (324 m) was observed.

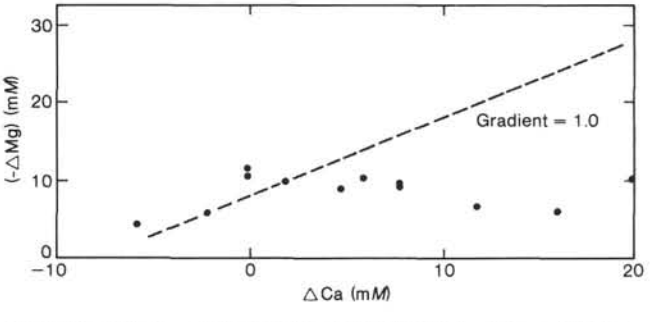

Figure 16. Plot of −ΔMg and ΔCa for Hole 612 (−ΔMg = Mg concentration in pore water − Mg concentration in surface seawater; ΔCa = Ca concentration in pore water − Ca concentration in surface seawater). −ΔMg reflects negative values due to Mg depletion relative to surface seawater.

Organic Geochemistry

Interstitial Gas

No visible evidence of gas was observed in any of the 72 cores from Site 612. Neither bubbling of gases from the sediment nor gas cracks needed for gas sampling were observed in any of the cores.

Rock-Eval Pyrolysis

In order (1) to check for the presence of heavier nonvolatile hydrocarbons and (2) to test if these sediments have a potential for hydrocarbon generation, the Girdel Rock-Eval apparatus was used to analyze 50 samples from cores recovered at Site 612. In addition, percentage organic carbon was determined on samples from this hole using the shipboard Hewlett-Packard 185B carbon analyzer.

The Girdel Rock-Eval instrument uses the technique of pyrolysis–FID (flame ionization detection) described by Espitalié et al. (1977). Basically, this technique consists of heating an 80 to 100 mg dry sediment sample in a stream of helium for 5 min. After 5 min., the sample is heated at 25.0°C/min. from 250° to 550°C. During this heating the gases generated are split into two parts: one part is sent to a flame ionization detector (FID) which is specific for hydrocarbon detection and the other part to a carbon dioxide (CO_2) trap.

Heating the sample to 250°C releases hydrocarbons which are monitored by the FID, and a peak (S_1) is produced on a chart recorder. The area of this peak is proportional to the amount of free hydrocarbons in the sediment or rock. The second peak (S_2) is produced by the hydrocarbons cracked from the organic matter during

pyrolysis (250–550°C). The area of this peak is proportional to the amount of hydrocarbon that can be generated from the sediment or rock with increasing time and temperature. Carbon dioxide (CO_2) produced during the pyrolysis is released from the trap and monitored by a thermal conductivity detector to produce a third peak (S_3).

In theory, the area of the S_3 peak is proportional to the amount of CO_2 generated from the pyrolysis of the organic material in the sediment. The temperature at which this peak is trapped (390°C) is presumably below the temperatures required for carbonate decomposition. The number of milligrams of CO_2 evolved per gram of organic carbon is referred to as the oxygen index of the sediment. The number of milligrams of hydrocarbon per gram of organic carbon is the hydrogen index of the sediment. Both these parameters are used in the classification of kerogen (Hunt, 1977).

Girdel Rock-Eval analysis of Site 612 sediments did not show S_1 or S_2 peaks, with the exception of a very small S_2 peak from a sample at 670.8 m sub-bottom depth. S_3 peaks are generally significant: Figure 17 is a plot of mg of CO_2/g of sediment for some of the samples from Hole 612.

Figure 18 is a plot of percent organic carbon as a function of sub-bottom depth for Hole 612. Most of the values are below 1.0% except for samples from 129 m SBD and samples between 638.71 and 670.81 m SBD. Below 638.7 m SBD, in lithologic Unit V, percentage organic carbon ranges between 0.80% (Core 69) and 2.68% (Core 72). This change parallels a change in lithology. Lithology Unit IV is a glauconitic marly limestone. Unit V, in which these higher values in percent organic matter are observed, is a black, glauconitic marly shale. The peak in percentage organic carbon at 129 m SBD coincides with the lower Oligocene/upper Miocene contact. This peak may reflect higher biological productivity in overlying waters as observed by an increase in fossil assemblages.

Organic carbon values are lowest in the lower Eocene (lithologic Unit III, Cores 612-39 to 612-60, 347.3–559.4 m SBD). Intense burrowing observed in lithologic Unit III may have resulted in the low organic carbon values because of reworking of organic matter by bottom dwelling organisms.

No strong correlation exists between percentage organic carbon and CO_2 generated from pyrolysis. Inorganic CO_2 produced from carbonate decomposition could be contributing to the results observed.

Nevertheless, a depth plot of CO_2 generated from pyrolysis (Fig. 17) resembles the trends observed in a depth plot of percentage organic carbon (Figure 18) except at 330 m sub-bottom depth. Parallel changes in percentage organic carbon and CO_2 generated from pyrolysis and back of a significant S_2 peak (hydrocarbons generated from cracking of organic matter) suggest that most of the organic carbon at Hole 612 may be available as oxygenated organic matter.

From these results, it can be concluded that the organic matter in the sediments at Hole 612 is potentially a poor source for hydrocarbon generation. This is in

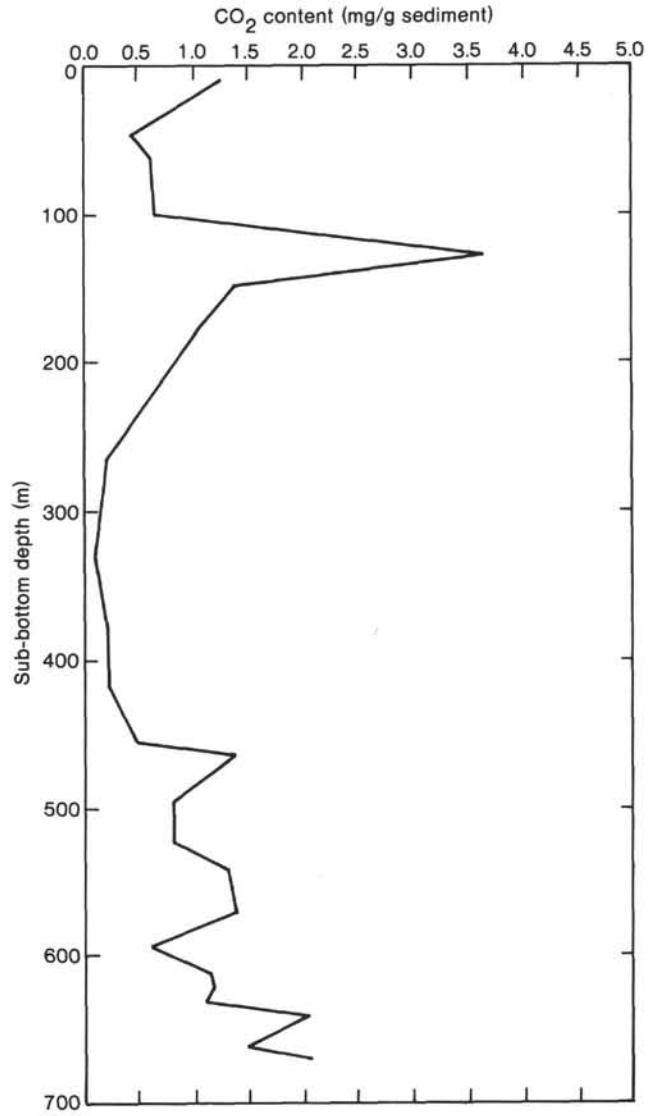

Figure 17. Content of CO_2 (in mg/g of sediment) calculated from S_3 peak, plotted versus depth for Hole 612.

agreement with the fact that neither free hydrocarbons (no S_1 peak) nor core gas were observed at this site. It can be inferred that the depositional environments for most of the sediments in Hole 612 were well oxygenated, with bottom dwelling organisms preventing significant accumulation of organic matter suitable for generation of petroleum hydrocarbons.

Microbiological Experiments

Microbiological experiments with sediments from Hole 612 were carried out using radiolabeled bacterial substrates as described elsewhere (Tarafa et al., this volume). Bacterial oxidation of acetate to CO_2 was experimentally significant at 3 m (Core 612-1), 19 m (Core 612-3,), 35 m (Core 612-5), and 46 m (Core 612-7) SBD. Organic carbon in Core 612-2 is 0.47% and 0.78% in Core 7, suggesting that there is enough organic carbon in these uppermost sediments to support bacterial growth. Acetate levels are also high enough to support bacterial

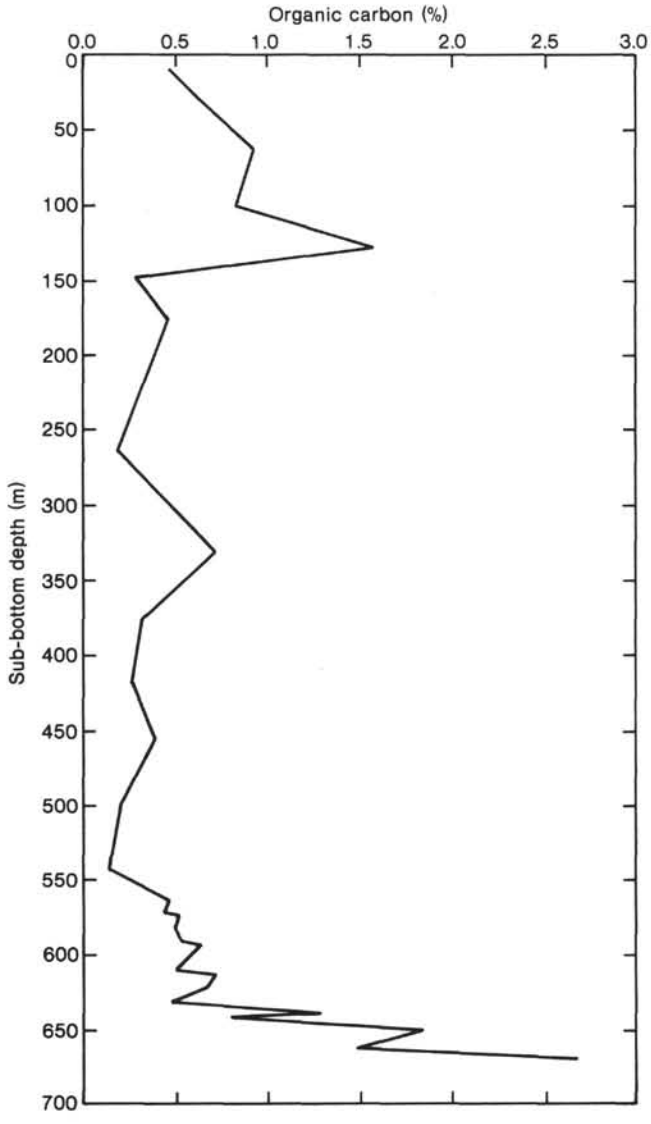

Figure 18. Organic carbon (%) versus sub-bottom depth for Hole 612.

growth. Whether sulfate reduction by microorganisms occurred in the same cores is still under investigation. Possible experimental problems resulting from reaction of reduced sulfur with iron could have prevented accurate measurement of the ^{35}S label (Howarth and Jørgensen, in press). Production of methane from acetate is significant in microbiological experiments from sediments at 46 m SBD (Core 612-7). Methane generation from methylamine is evident in microbiological experiments with sediments from 42 m SBD (Core 612-6). Microbiological gas production may be occurring at Hole 612, but rates are low and do not produce the positive gas pressures required for visual detection of core gas.

PHYSICAL PROPERTIES

Shipboard measurements of sediment wet-bulk density, porosity, water content, grain density, and sonic velocity were performed at Site 612. The procedures were those of Boyce (1976). The results of these measurements are plotted versus depth below the seafloor in Figure 19 and summarized in relation to the lithostratigraphy in Table 3. Tables 4 and 5 contain complete listings of the data.

Perhaps the most striking characteristic of the cores recovered at both Sites 612 and 613 is the variability of the sediments at almost any scale considered. This variability presents problems in the interpretation of physical properties data since our sampling interval is generally on the order of meters. While differences in the properties of the samples are real, the depth plots do not reveal the true spacing of property fluctuations. This problem becomes more apparent when considering the plots of the geophysical well logs (see Fig. 20). A comparison of well log and laboratory measurements is presented in Goldberg et al. (this volume).

The most general division of the physical properties differences observed at Site 612 is between the upper unlithified Units (I and II) and the lower lithified Units (III, IV, and V) of the stratigraphic column. This distinction is seen in values of bulk density, porosity, and sonic velocity, with velocity and density increasing while porosity decreases with the onset of lithification. Lithostratigraphic Units I and II exhibit behavior typical of marine oozes and chalks undergoing mechanical compaction. The values within each individual unit are governed by composition and grain morphology. Unit I consists of muds and glauconitic sands. The average grain density is high because of the presence of glauconite and detrital quartz ($\rho > 2.6$ g/cm^3) and the relatively minor contribution of low density biogenic silica (ρ = 2.2–2.4 g/cm^3). This is seen in contrast with Unit II, which is predominately composed of microfossil tests and test fragments. Not only does the presence of the biogenic silica tests lower the average grain density, but both siliceous and calcareous tests remain open, creating voids in the sediment which increase porosity and lower density.

Although Units I and II can be readily distinguished on the basis of porosity and density, there is very little difference in sonic velocity. Velocity measurements from Unit I show some fluctuations that correlate with density differences, but in general the behavior is that of a nonrigid mixture of sediment and water. Unit II velocity values show a small increase with depth which may be attributed to a slight stiffening of the sediment matrix owing to mechanical compaction.

The Unit II/Unit III boundary marks the true onset of lithification in the sediment column and is identified with substantial changes in bulk density, porosity, and sonic velocity. The difference is directly attributable to the dissolution of siliceous microfossils and precipitation of siliceous lepispheres in the matrix and pore spaces remaining in the sediment (see Wilkens et al., this volume). This process decreases porosity in two ways; first by dissolving siliceous tests that had been keeping the sediment framework open and second by precipitating silica inside the areas of the sediment kept open by calcareous tests. The combination of a reduction in porosity and an increase in grain density due to the denser form of silica in Unit III versus Unit II results in a large increase in bulk density. At the same time, the sonic velocity increases due to both the density increase and to a

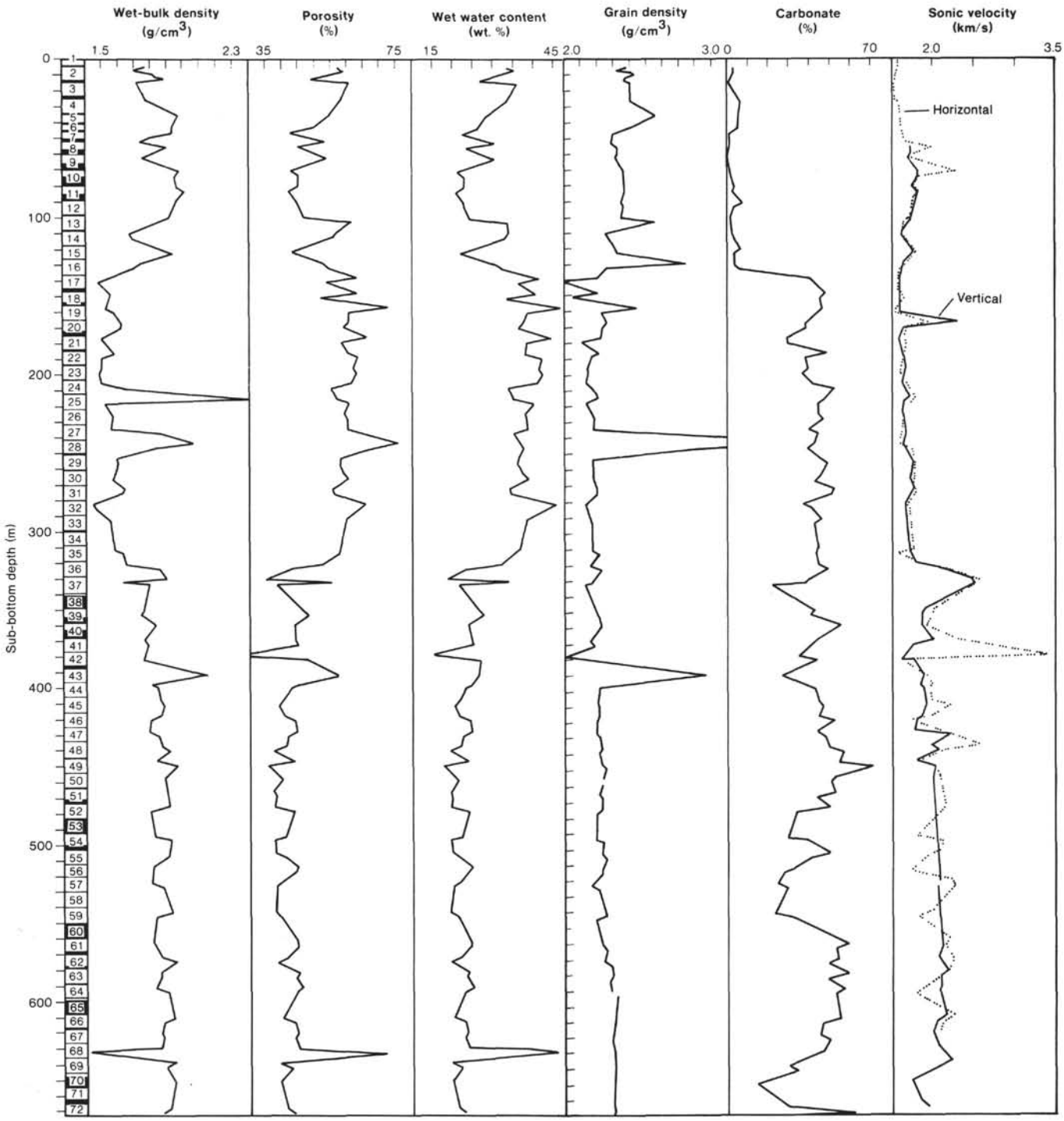

Figure 19. Physical properties values from Hole 612.

stiffening of the sediments which is attributable to the precipitated silica acting as a matrix cement.

Units IV and V are not markedly different from Unit III in physical properties even though they are compositionally distinct. The properties of all three units are typical of lithified sediments of similar composition. Velocities vary over a wide range and seem to correlate roughly with local variations in density and porosity.

DOWNHOLE LOGGING

Introduction

In order to facilitate the correlation of borehole stratigraphy with seismic reflection profiles, a suite of Schlumberger logs were recorded at DSDP Site 612. The following logs were acquired on two wireline trips from near the bottom of the hole (670 m sub-bottom) to the bot-

Table 3. Summary of physical properties measurements, Site 612.

Litho. unit	Wet-bulk density (gm/cm^3)	Porosity (%)	Grain density (gm/cm^3)	Sonic velocity (km/s)
I	1.6–2.0	40–60	2.5–2.8	1.5–1.8
II	1.5–1.6	55–65	2.2–2.4	1.5–1.8
III	1.75–1.95	35–45	2.4–2.5	1.6–2.3
IV	1.8–2.0	40–45	2.5–2.6	2.0–2.3
V[a]	1.90–1.95	40–45	2.6	1.6–2.2

[a] Only 6 samples analyzed.

Table 4. Physical properties data, Hole 612.

Sub-bottom depth (m)	Grain density (g/cm^3)	Water content (wt. %)	Porosity (vol. %)	Wet-bulk density (g/cm3)
5.56	2.77	33.20	57.3	1.77
7.06	2.64	35.4	58.5	1.69
8.56	2.81	33.4	57.8	1.78
10.06	2.85	31.5	56.1	1.82
11.56	2.76	30.0	53.6	1.83
13.06	2.73	26.8	49.4	1.89
15.14	2.80	36.2	60.8	1.72
26.22	2.80	33.7	58.1	1.77
35.86	3.12	28.4	54.7	1.97
43.21	2.81	26.4	49.6	1.93
46.86	2.59	22.6	42.5	1.93
52.81	2.58	30.84	53.51	1.73
55.81	2.65	23.54	44.92	1.91
62.71	2.64	30.78	54.02	1.75
70.91	2.72	21.50	42.67	1.98
73.91	2.73	23.02	44.94	1.95
80.61	2.74	22.99	45.01	1.96
83.61	2.74	20.94	42.07	2.01
90.32	2.70	22.88	44.52	1.95
93.32	2.72	23.21	45.12	1.94
100.01	2.70	24.38	46.54	1.91
103.01	3.11	33.64	61.22	1.82
109.71	2.50	33.80	56.80	1.66
112.71	2.53	33.27	55.78	1.68
119.41	2.61	25.26	46.88	1.86
122.41	2.64	22.10	42.80	1.94
128.92	3.51	30.13	52.00	1.73
131.92	2.51	31.94	54.08	1.69
138.42	2.40	41.47	63.00	1.52
141.42	1.99	36.19	53.03	1.47
147.92	2.44	40.66	62.59	1.54
150.92	2.10	33.40	51.31	1.54
157.42	2.88	47.79	72.53	1.52
160.44	2.46	38.41	60.49	1.57
166.94	2.52	37.28	59.97	1.61
169.94	2.47	36.24	58.44	1.61
176.44	2.45	44.46	66.19	1.49
179.44	2.22	38.23	57.84	1.51
186.04	2.42	37.96	59.69	1.57
189.04	2.33	42.12	62.93	1.49
196.08	2.29	41.32	61.67	1.49
199.06	2.30	42.30	62.72	1.48
205.28	2.28	40.96	61.23	1.49
208.28	2.35	33.86	54.63	1.61
214.88	2.42	34.95	56.55	2.42
217.88	2.28	40.10	60.45	1.51
224.48	2.34	37.91	58.82	1.55
227.44	2.38	38.26	59.59	1.56
234.06	2.36	38.46	59.57	1.55
237.08	3.40	35.08	64.78	1.85
243.46	5.34	36.81	75.69	2.06
246.66	3.61	37.68	68.55	1.82
253.21	2.37	36.31	57.44	1.58
256.22	2.37	36.21	57.40	1.59
262.82	2.37	37.45	58.70	1.57
265.82	2.37	38.81	60.08	1.55
272.46	2.40	34.02	55.34	1.63
275.42	2.41	34.30	55.69	1.62
282.02	2.27	45.49	65.48	1.44

Table 4 (continued).

Sub-bottom depth (m)	Grain density (g/cm^3)	Water content (wt. %)	Porosity (vol. %)	Wet-bulk density (g/cm3)
285.04	2.28	43.49	63.66	1.46
291.62	2.33	38.40	59.23	1.54
294.62	2.35	38.05	59.09	1.55
311.08	2.35	36.50	57.48	1.57
314.02	2.44	35.16	56.97	1.62
320.72	2.33	31.98	52.29	1.64
323.72	2.47	23.29	42.81	1.84
330.32	2.36	18.36	34.69	1.89
331.86	2.35	34.19	54.99	1.61
333.38	2.26	21.31	37.94	1.78
349.52	2.39	26.40	46.11	1.75
352.62	2.42	27.91	48.33	1.73
359.22	2.46	23.98	43.71	1.82
369.00	2.33	25.03	43.75	1.75
372.11	2.38	25.15	44.41	1.77
378.64	2.03	15.32	26.83	1.75
381.66	2.43	27.28	47.67	1.75
391.26	3.70	26.77	57.51	2.15
397.81	2.44	24.90	44.72	1.80
399.31	2.44	23.36	42.69	1.83
407.46	2.42	21.75	40.25	1.85
410.46	2.43	20.67	38.74	1.87
417.16	2.43	21.83	40.47	1.85
420.16	2.41	24.67	44.07	1.79
427.11	2.40	25.06	44.56	1.78
430.11	2.44	22.80	41.86	1.84
436.52	2.47	22.23	41.40	1.86
439.50	2.44	19.55	37.26	1.91
446.22	2.46	24.15	43.90	1.82
449.22	2.50	18.13	35.60	1.96
455.92	2.47	20.78	39.33	1.89
458.58	2.47	21.54	40.41	1.88
465.62	2.43	19.75	37.42	1.89
468.62	2.46	20.10	38.19	1.90
475.32	2.46	19.83	37.79	1.91
478.32	2.40	24.41	43.68	1.79
494.72	2.39	22.69	41.24	1.82
496.22	2.48	19.68	37.79	1.92
504.22	2.47	19.97	38.14	1.91
507.22	2.52	21.70	41.13	1.90
513.71	2.47	24.96	45.06	1.81
516.71	2.46	24.50	44.39	1.81
523.41	2.34	22.12	39.91	1.80
526.31	2.42	20.49	38.39	1.87
542.51	2.51	19.78	38.22	1.93
545.61	2.38	21.64	39.67	1.83
561.71	2.47	24.81	44.91	1.81
564.71	2.52	24.74	45.27	1.83
571.31	2.49	22.57	42.04	1.86
574.31	2.57	19.86	38.94	1.96
580.91	2.59	24.48	45.63	1.86
583.91	2.55	23.80	44.39	1.86
590.52	2.57	25.53	46.81	1.83
593.52	2.64	23.44	44.66	1.91
609.91	2.61	20.77	40.59	1.95
612.91	2.59	23.64	44.48	1.88
619.52	2.58	24.22	45.20	1.87
622.52	2.57	23.61	44.32	1.88
629.11	2.60	24.41	45.59	1.87
632.11	2.60	51.12	73.09	1.43
638.71	2.61	20.01	39.49	1.97
641.71	2.60	22.88	43.51	1.90
649.91	2.59	20.59	40.22	1.95
662.61	2.59	21.64	41.72	1.93
667.81	2.61	22.09	42.51	1.92
670.81	2.58	23.62	44.40	1.88

Table 5. Shipboard sonic velocity measurements, Hole 612.

Sub-bottom depth (m)	Sonic velocity (km/s)	H/V[a]	Liner (Yes/No)
.75	1.563	H	Y
5.55	1.564	H	Y
15.15	1.513	H	Y
26.25	1.532	H	Y
26.70	1.576	H	Y
46.85	1.620	H	Y
52.83	1.657	H	N
55.83	1.972	H	N
55.83	1.721	V	N
59.73	1.769	H	N
59.73	1.731	V	N
62.73	1.736	H	N
62.73	1.704	V	N
70.93	2.277	H	N
70.93	1.814	V	N
73.93	1.820	H	N
73.93	1.809	V	N
80.63	1.739	H	N
80.63	1.736	V	N
83.63	1.816	H	N
83.63	1.824	V	N
90.33	1.752	H	N
90.33	1.775	V	N
93.33	1.758	H	N
93.33	1.764	V	N
100.03	1.728	H	N
100.03	1.733	V	N
103.03	1.639	H	N
103.03	1.713	V	N
109.73	1.614	H	N
109.73	1.610	V	N
112.73	1.626	H	N
112.73	1.613	V	N
119.43	1.704	H	N
119.43	1.720	V	N
122.43	1.783	H	N
122.43	1.754	V	N
128.93	1.671	H	N
128.93	1.625	V	N
131.93	1.585	H	N
131.93	1.615	V	N
138.43	1.588	V	N
141.43	1.569	H	N
147.93	1.606	H	N
147.93	1.583	V	N
150.93	1.639	H	N
160.43	1.526	H	N
160.43	1.591	V	N
166.95	1.944	H	N
166.95	2.312	V	N
169.93	1.676	H	N
169.93	1.626	V	N
176.43	1.637	H	N
176.43	1.574	V	N
179.43	1.656	H	N
179.43	1.572	V	N
186.03	1.648	H	N
186.03	1.608	V	N
189.03	1.427	H	N
189.03	1.630	V	N
196.05	1.651	V	N
199.05	1.591	H	N
199.05	1.451	V	N
205.23	1.144	H	N
205.23	1.614	V	N
214.83	1.785	H	N
214.83	1.710	V	N
217.83	1.630	V	N
224.43	1.624	H	N
224.43	1.612	V	N
227.43	1.615	H	N
227.43	1.636	V	N
237.03	1.608	H	N
237.03	1.662	V	N
243.63	1.568	H	N

Table 5 (continued).

Sub-bottom depth (m)	Sonic velocity (km/s)	H/V[a]	Liner (Yes/No)
243.63	1.625	V	N
246.63	1.724	H	N
253.23	1.438	H	N
253.23	1.715	V	N
256.23	1.767	H	N
256.23	1.753	V	N
264.33	1.759	H	N
264.33	1.716	V	N
267.33	1.744	H	N
267.33	1.711	V	N
272.43	1.761	H	N
272.43	1.748	V	N
275.43	1.767	H	N
275.43	1.725	V	N
282.03	1.673	H	N
282.03	1.643	V	N
285.03	1.701	H	N
285.03	1.661	V	N
311.03	1.745	H	N
311.03	1.702	V	N
314.03	1.566	H	N
314.03	1.709	V	N
320.73	1.811	H	N
320.73	1.789	V	N
323.73	2.110	H	N
323.73	2.068	V	N
330.33	2.513	H	N
330.33	2.468	V	N
333.33	2.536	H	N
333.33	2.509	V	N
349.53	2.000	H	N
349.53	1.876	V	N
352.53	1.993	H	N
352.53	1.847	V	N
359.23	1.876	H	N
359.23	1.840	V	N
368.93	2.266	H	N
368.93	1.982	V	N
372.10	1.734	V	N
378.65	3.292	H	N
378.65	1.639	V	N
381.63	1.595	H	N
381.63	1.595	V	N
381.65	1.750	V	N
391.23	1.906	H	N
391.23	1.859	V	N
397.83	1.990	H	N
397.83	1.821	V	N
399.33	1.960	H	N
399.33	1.870	V	N
407.43	1.968	H	N
407.43	1.898	V	N
410.43	2.200	H	N
410.43	1.899	V	N
417.13	2.013	H	N
417.13	1.861	V	N
420.13	1.703	H	N
420.13	1.781	V	N
426.83	1.747	V	N
429.83	2.205	V	N
436.53	2.561	H	N
436.53	1.971	V	N
439.53	2.126	H	N
439.53	2.052	V	N
446.23	1.819	H	N
446.23	1.765	V	N
449.23	1.986	H	N
449.23	1.987	V	N
455.93	2.066	H	N
455.93	1.973	V	N
475.33	2.137	H	N
494.73	1.788	H	N
497.73	2.100	H	N
504.23	2.056	H	N
507.23	1.903	H	N

Table 5 (continued).

Sub-bottom depth (m)	Sonic velocity (km/s)	H/V[a]	Liner (Yes/No)
516.73	1.692	H	N
523.40	2.232	H	N
523.40	2.052	V	N
526.40	2.266	H	N
526.40	2.032	V	N
542.50	1.938	H	N
545.50	1.791	H	N
561.70	2.188	H	N
564.70	2.113	H	N
564.70	2.081	V	N
571.30	2.042	V	N
574.30	2.227	H	N
574.30	2.075	V	N
580.90	2.152	H	N
580.90	2.149	V	N
583.83	2.056	V	N
583.90	2.060	H	N
590.60	2.056	V	N
593.60	1.717	H	N
593.60	2.048	V	N
609.93	2.261	H	N
609.93	2.128	V	N
612.93	2.092	H	N
612.93	2.008	V	N
619.53	2.047	H	N
619.53	1.961	V	N
622.53	2.075	H	N
629.13	2.146	H	N
629.13	2.024	V	N
638.73	2.278	H	N
638.73	2.184	V	N
641.73	2.432	H	N
649.93	2.037	H	N
649.93	1.692	V	N
662.63	2.087	H	N
662.63	1.794	V	N
667.83	2.031	H	N
667.83	1.917	V	N

[a] H = horizontal propagation direction, V = vertical propagation direction.

tom of the casing (100 m sub-bottom): caliper, centralized and compensated gamma ray, spherically focused resistivity, medium- and deep-investigation induction, long-spaced sonic traveltime, bulk density, and neutron porosity (Fig. 20). Based on these measurements, five "log-lithologic" units have been identified by sharp responses in the logs and correlated to the cored section. These units are generally coincident with lithostratigraphic boundaries and are subsequently referred to by the lithologic units (see Lithology section). In this preliminary analysis, we have also defined some subunits that reflect particular log features.

Thin bed resolution is approximately 60 cm for all of the logs, with the exception of 120- to 150-cm resolution for the neutron and deep induction tools. The depth of investigation from the borehole wall is dependent on the characteristics of each tool. The depth of investigation is about 1 cm for the gamma ray, neutron, and density tools, 20 cm for the sonic and spherically focused tools, and 100 cm for the deep-induction tool (personal communication, K. King, 1983). The penetration of mud into the wallrock is apparent by the separation of the deep- and shallow-investigation resistivity logs. Only the deep investigation resistivity log is shown in Figure 20. Other variations of the logs in Figure 20 imply relative lithologic, physical property, or borehole condition changes. Following is a discussion of the log responses in each lithologic unit with emphasis on Subunit IIIA, shaded in Figure 20.

Log-Lithology Response

The sidewall gamma ray responds to natural gamma radiation in the formation, usually indicating the presence of potash clays in shale. The natural radiation measured by the gamma ray log decreases dramatically at the Unit I/II boundary, about 135 m BSF, and again, although less dramatically, at Subunit IIA/IIB boundary, about 180 m BSF. At the Unit IIIA/IIIB boundary, gamma ray values increase sharply and then decrease 10 m below Unit IIIA. There is a gradual increase and more erratic character of the log in Units III and IV and then a sharp increase at the top of Unit V.

The spherically focused resistivity and induction logs measure resistivity across an induced potential difference, dependent on the conductivity of the formation and the pore fluids. These electrical logs show slight variation between Units I and II, with a small but constant offset between shallow- and deep-investigation tool responses. Unit III and IV show a continuous increase in resistivity. A 10 m thick, high-resistivity log response at the top and bottom of Subunit IIIA, about 325 m BSF, suggests a dramatic change in lithology or pore water geochemistry. This may be due to a diagenetic boundary of reprecipitated biogenic silica (see Geochemistry section). Also, associated with this interval is an increase in pore water resistivity implied by a drop in the pore water salinity (see Geochemistry section). Unit V shows a sharp decrease in resistivity at the upper boundary and approximately constant resistivity to 670 m BSF. The separation between shallow- and deep-investigation tools increases threefold at the top of Unit III and remains constant to 670 m BSF, probably indicating an increase in mud invasion and permeability.

Sonic traveltime is a formation physical property, measured by differencing the first arrival of compressional energy recorded at two receivers on the sonic tool. The traveltime varies with lithology but is strongly dependent on porosity. The traveltime of sonic waves is an average measurement of the travel path from source to receiver. Nevertheless, sharp changes in traveltime can occur across lithologic boundaries, although the actual range of response is smoothed. The average formation velocity, the inverse of traveltime, generally increases with depth due to compaction, although anomalous high average velocities are observed in Subunit IIIA and some intervals in Units IIIB and IV.

Independent calculations of porosity from neutron, density, and sonic measurements typically differ. Neutron logs respond primarily to hydrogen content of pore fluids in the formation, a direct measure of water content. The bulk-density and traveltime logs also respond to formation porosity, but the porosity calculations require accurate grain density estimations best obtained by laboratory experiments. The neutron porosity log tends to vary rapidly and measure between the other two porosity calculations. Relative changes in average porosity

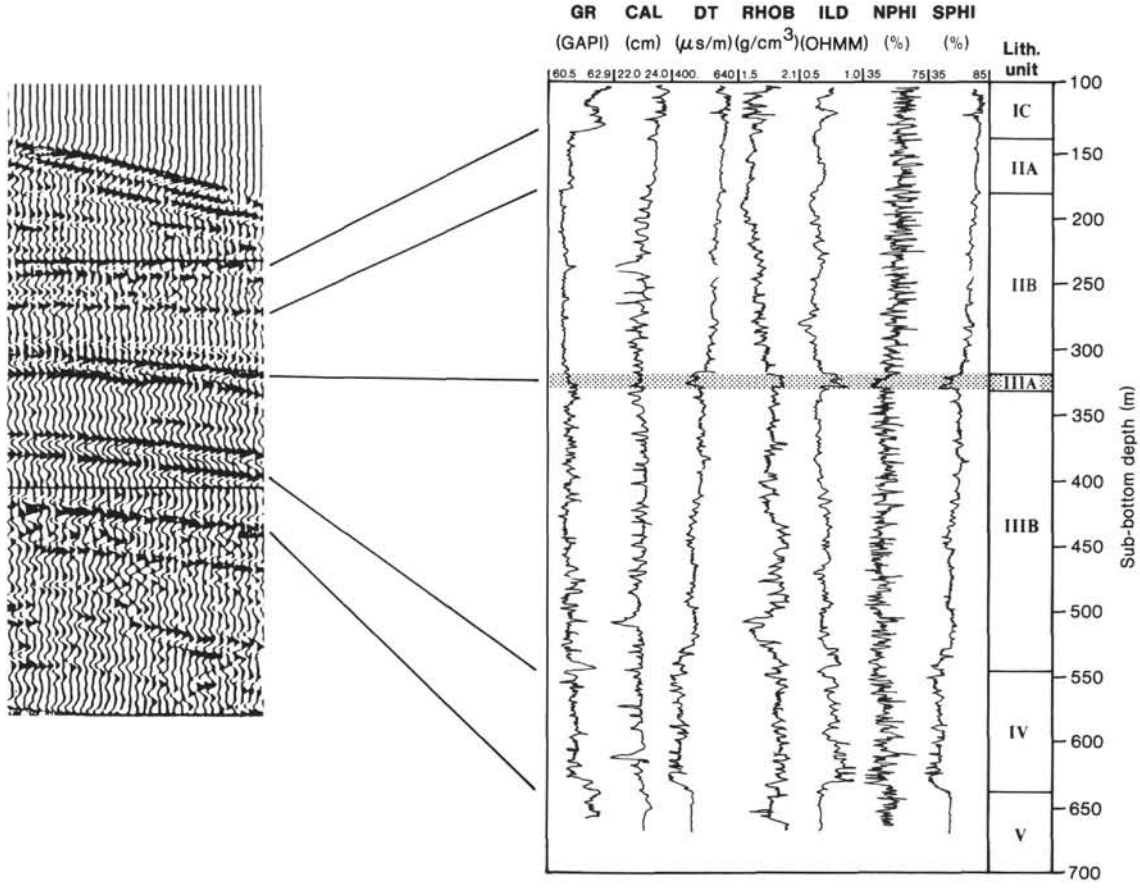

Figure 20. Geophysical logs recorded in Hole 612 and correlation to U.S.G.S. Line 25. GR = gamma ray, CAL = caliper, DT = interval transit time, RHOB = bulk density, ILD = deep induction log, NPHI = neutron porosity, SPHI = spherically focused resistivity.

between lithologic units can be described by observing common responses of the three measurements: a continuous decrease in average porosity is observed in successive and more compacted units. There is anomalous, low porosity in Subunit IIIA, clearly distinguished in all of the logs. The bulk density and neutron porosity logs show a slightly low porosity interval from about 420 to 450 m BSF and a slightly high porosity interval from 500 to 530 m BSF, within Subunit IIIB.

Seismic/Lithologic Correlation

The following analysis approximates the seismic two-way traveltime to each log-lithologic boundary. Table 6 shows the average interval velocity (V_p) and the approximate depth of each lithostratigraphic unit. Also shown in Table 6 are the average bulk density (ρ), the approximate interval thickness (Z), interval two-way traveltime, and cumulative sub-bottom two-way traveltime. The average velocity and bulk density are measured within each subunit from logs unless otherwise noted in the table. Several values have been extrapolated to the unlogged upper units from nearby Site 613 or inferred from laboratory measurements.

The seismic reflectors observed in the section of U.S.G.S. Line 25 (transect across continental slope) in Figure 20 are caused by impedance changes in the sediments below the seafloor. The seismic impedance is defined by

$$\xi = \rho V_p$$

where ρ is the bulk density, and V_p is the formation compressional velocity. Impedance contrasts can be calculated at the lithologic boundaries, and synthetic seismograms can be generated for comparison to the section. A simple approximation of synthetic seismogram

Table 6. Approximate two-way traveltimes below seafloor of lithologic boundaries at Site 612 (see Fig. 20).

Sub-bottom depth (m)	V_p (km/s)	ρ	Z (km)	Traveltime (s)	Cumulative Traveltime (s)	Lith. boundary
0	1.64[a]	1.85[b]	0.00	0.00	0.000	SF/IA
40	1.75[a]	1.85[b]	0.04	0.024	0.024	IA/IB
70	1.75[a]	1.85[b]	0.03	0.034	0.058	IB/IB
110	1.70[a]	1.65[b]	0.04	0.046	0.104	IB/IC
130	1.67	1.65	0.02	0.024	0.128	IC/IIA
180	1.74	1.70	0.05	0.060	0.188	IIA/IIB
320	2.00	1.95	0.14	0.161	0.349	IIB/IIIA
330	2.00	1.87	0.01	0.010	0.359	IIIA/IIIB
550	2.22	1.95	0.22	0.220	0.579	IIIB/IV
640	2.00	1.90	0.09	0.081	0.660	IV/V

[a] From sonic log in well Site 612.
[b] From laboratory density measurements.

is calculable by twice the interval thickness divided by the interval velocity, explicitly

$$\Delta TT = 2\Delta / V_p.$$

Table 6 shows the values of cumulative traveltime (TT) summed below the seafloor arrival. TT values reflect the seismic two-way time associated with the impedence contrasts across lithologic boundaries. The approximate location of the reflectors in U.S.G.S. Line 25 in Figure 20 are correlated by the two-way times calculated to the corresponding depth intervals in the logs.

Although the correlation is preliminary, we are able to constrain the approximate depths of several reflectors by the integrated log response. The boundaries between all of the cored units correspond to unique, high-amplitude reflectors in the section. Of particular interest for further study is complex reflector and associated log responses of Subunit IIIA.

Conclusions

Five log-lithologic units have been identified between sharp features on the logs and, within the depth resolution achievable, are coincident with the lithostratigraphic units identified in the cored section. Seismic two-way traveltimes have been calculated by the interval velocities from the sonic log and the lithostratigraphic boundaries and correlated to U.S.G.S. seismic Line 25. The much-simplified, preliminary correlation reasonably constrains the seismic reflectors with depth in well Site 612. Further analysis using synthetic seismograms will improve the constraints of seismic reflectors with depth.

SEISMOSTRATIGRAPHY

Introduction

Site 612 is located approximately 0.2 km northeast of shot point 3045 on U.S.G.S. multichannel seismic reflection profile Leg 25, which is approximately 0.7 km northwest of the intersection of Line 25 and U.S.G.S. Line 34 (Figs. 21, 22, and 23). Poag (1980, 1985) has presented a seismostratigraphic interpretation of this segment of the New Jersey margin, assisted by geologic data from the COST B-3, ASP-14, ASP-15, and DSDP 108 boreholes, whose stratigraphic sections were projected onto Line 25. The new data from DSDP Sites 604, 605, and 612, coupled with new high-resolution seismic lines gathered by *Glomar Challenger*, confirm the general stratigraphic framework presented by Poag, while providing additional details and some important modifications.

Line 25 (depth section; Fig. 23) shows that the Cenozoic section of the New Jersey slope is built upon a gently arched erosion surface of Upper Cretaceous sedimentary rocks. The Paleogene sequence (chiefly Eocene) thickens significantly between the B-3 and 612 sites. Middle Eocene strata crop out downdip from Site 612 and form a broad seafloor exposure (12 km across) between shot points 3080 and 3320 (Line 25; Figs. 22 and 23; also see Fig. 7 of Background and Objectives chapter, this volume), before plunging beneath the wedge of upper rise deposits.

Above the Paleogene section, Neogene strata form a thick, seaward tapering wedge that constitutes the upper continental slope. Some of the individual depositional sequences in this Neogene wedge are deeply eroded or pinch out at their seaward termini. Others crop out near Site 612. Neogene strata are generally absent over the Eocene outcrop belt but appear again downslope to form a large portion of the upper rise wedge.

A wedge of Quaternary sediment blankets the upper slope but thins significantly across the lower slope, forming scattered patches across the Eocene outcrop belt before thickening seaward on the upper rise. Robb et al. (1981) and Hampson and Robb (1984) have shown that the Neogene and Quaternary strata form elongate fingers, in map view, that extend down the slope (Fig. 7 of Background and Objectives chapter, this volume) and are separated by erosional channels and submarine canyons, which expose the underlying, more resistant, Tertiary and Upper Cretaceous beds.

Correlation of Seismic Reflections with Downhole Geophysical Logs

The use of acoustic velocity measurements and integrated transit time derived from the downhole sonic logs at Site 612 allows an assessment of the relationships between the prominent seismic reflections on Leg 25 and geologic boundaries in the borehole section. The reflections of highest amplitude at Site 612 coincide with the greatest changes in velocity displayed by the sonic log. The deepest high-amplitude reflector at Site 612 is at 2.57 (based on interval velocity of 2.180 m/s from Line 25; 2.189 m/s from sonic log; Fig. 24). This reflector coincides with the unconformable lower Maestrichtian/upper Campanian contact at 640.5 m below the seafloor (BSF) (Figs. 22 and 23). This reflector diminishes in amplitude updip and downdip from Site 612 and becomes discontinuous. It is obscure where it crosses the B-3 well projection. Another strong reflector is present at 2.49 s (two-way traveltime) at Site 612 (Fig. 25) and is coincident with the lower Eocene/possibly Paleocene (or lower Eocene/middle Maestrichtian) unconformity at approximately 551 m (BSF) (Figs. 22 and 23). The reflection loses amplitude and continuity within a few kilometers updip from Site 612. It is truncated as it onlaps a strong reflector that forms the Cretaceous/Tertiary contact at the COST B-3 projection. Downdip, this reflector can be traced beneath the continental rise.

A third high-amplitude reflector is present at 2.25 s at Site 612 (Fig. 26) and is associated with a 10-m-thick zone of porcellanite (diagenetic front) at the base of the middle Eocene section (323–333 m BSF; Figs. 22 and 23). The unconformable contact between the middle and lower Eocene sections is present at 331.9 m BSF and cannot be distinguished as a separate reflector on Line 25. This middle–lower Eocene reflector is the strongest and most continuous one crossing Site 612, but like the previously discussed reflector, it changes character rapidly up- and downdip. It can be easily traced 7 km updip from Site 612, and appears to maintain its position at the middle/lower Eocene contact. It loses amplitude updip before reaching the COST B-3 projection on Line

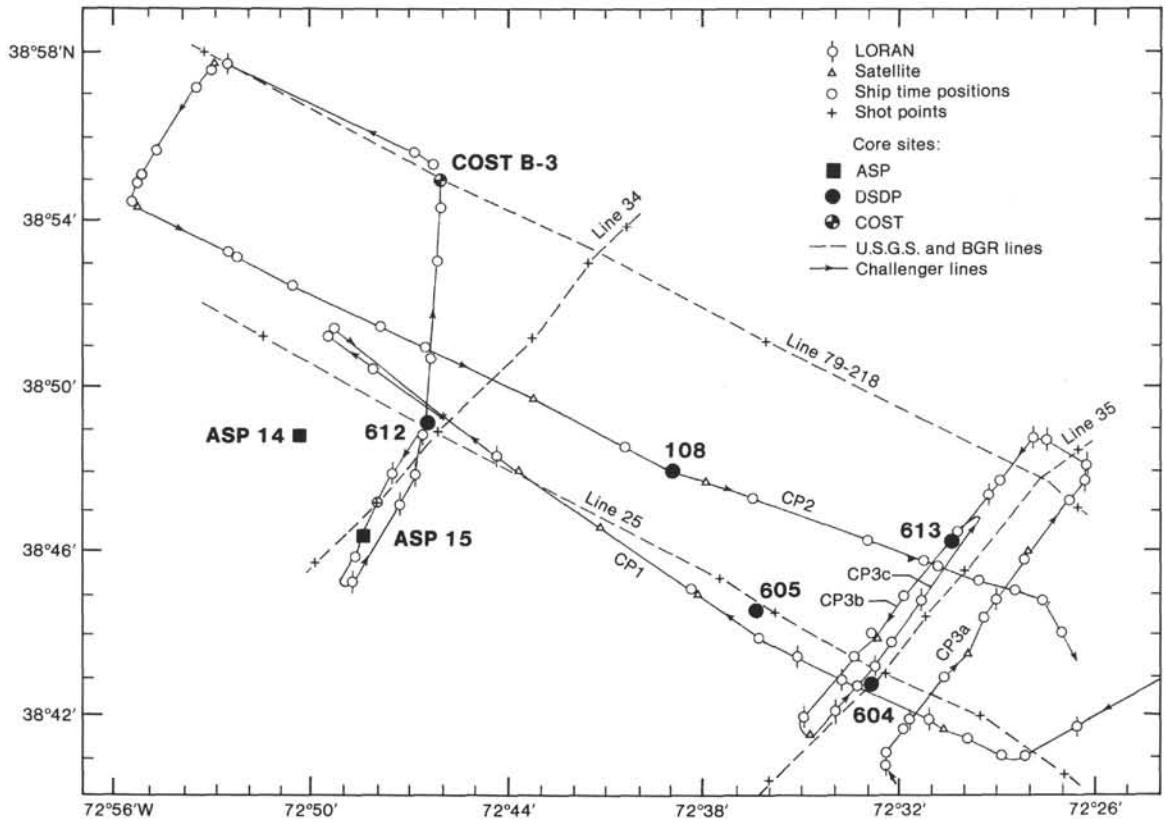

Figure 21. Location of boreholes and seismic reflection profiles in the vicinity of Site 612. ASP = Atlantic Slope Project (Poag, 1978). COST = Continental Offshore Stratigraphic Test (Poag, 1978). The CP lines are single-channel water gun profiles surveyed by *Glomar Challenger* during Leg 95. Other lines are multichannel common-depth-point profiles surveyed by the U.S.G.S. and BGR.

25, but on Line 79-218, which actually crosses the B-3 well site (Figs. 21 and 27), this reflector retains its high amplitude across the well site. This strong reflector becomes discontinuous and loses strength as it crosses the fault system 2 km downdip from Site 612 (Figs. 22 and 23; on Line 25). Along Line 34, which crosses slightly oblique to depositional strike, 0.7 km downdip from Site 612, this high-amplitude reflector is continuous in typical expression (usually accompanied by one or two closely-spaced parallel reflectors) for about 25 km to the southwest and about 30 km to the northeast of Site 612, before weakening and becoming intermittent.

The unconformable middle/upper Eocene contact appears as a strong reflector at 2.09 s at Site 612 (Figs. 22 and 28), but it is weak updip where it crosses the COST B-3 well projection. The Eocene/Oligocene contact and Oligocene/Miocene unconformity are so close together (~1 m apart) that they show up as a single moderately strong, but intermittent, reflector across Site 612 (2.03 s; Figs. 22 and 28). However, both the Eocene/Oligocene and Oligocene/Miocene contacts are quite strong separate reflectors at the B-3 projection.

Another significant reflector is present at 1.99 s at Site 612 (Figs. 22 and 28) (top of the upper Miocene section). It is an irregular, high-amplitude reflector, which forms a channeled surface in the vicinity of Site 612. This stratigraphic contact is just below the end of the drill pipe as positioned during logging, thus the velocity contrast was not recorded.

The other major stratigraphic boundaries at Site 612 display low velocity contrasts, and likewise appear as low-amplitude reflections as they cross Site 612 on Line 25.

Seismic and Depositional Sequences

Seismic sequences bounded by onlapping or truncated reflections can be easily identified on Line 25. The upper contact of the oldest unit drilled at Site 612 (upper Campanian stage) is expressed as a high-amplitude reflector at Site 612 (2.57 s) and is unconformable in Core 612-69 (Fig. 22). The upper Campanian surface is irregularly eroded between Site 612 and the COST B-3 projection on Line 25 (Fig. 22). Onlapping reflections at the base of the Campanian section indicate a period of nondeposition between the Campanian and Santonian sequences.

Forty-five meters of middle Maestrichtian sediments were penetrated in the B-3 well, but the upper Maestrichtian section is missing there. A couplet of high-amplitude reflections bounding the Maestrichtian interval can be traced along Line 79-218 to Line 34 to Line 25. The Maestrichtian section is too thin to display internal reflections (Fig. 22) at the B-3 well projection. The upper Maestrichtian reflections are truncated between the B-3 projection and Site 612. The absence of upper Maes-

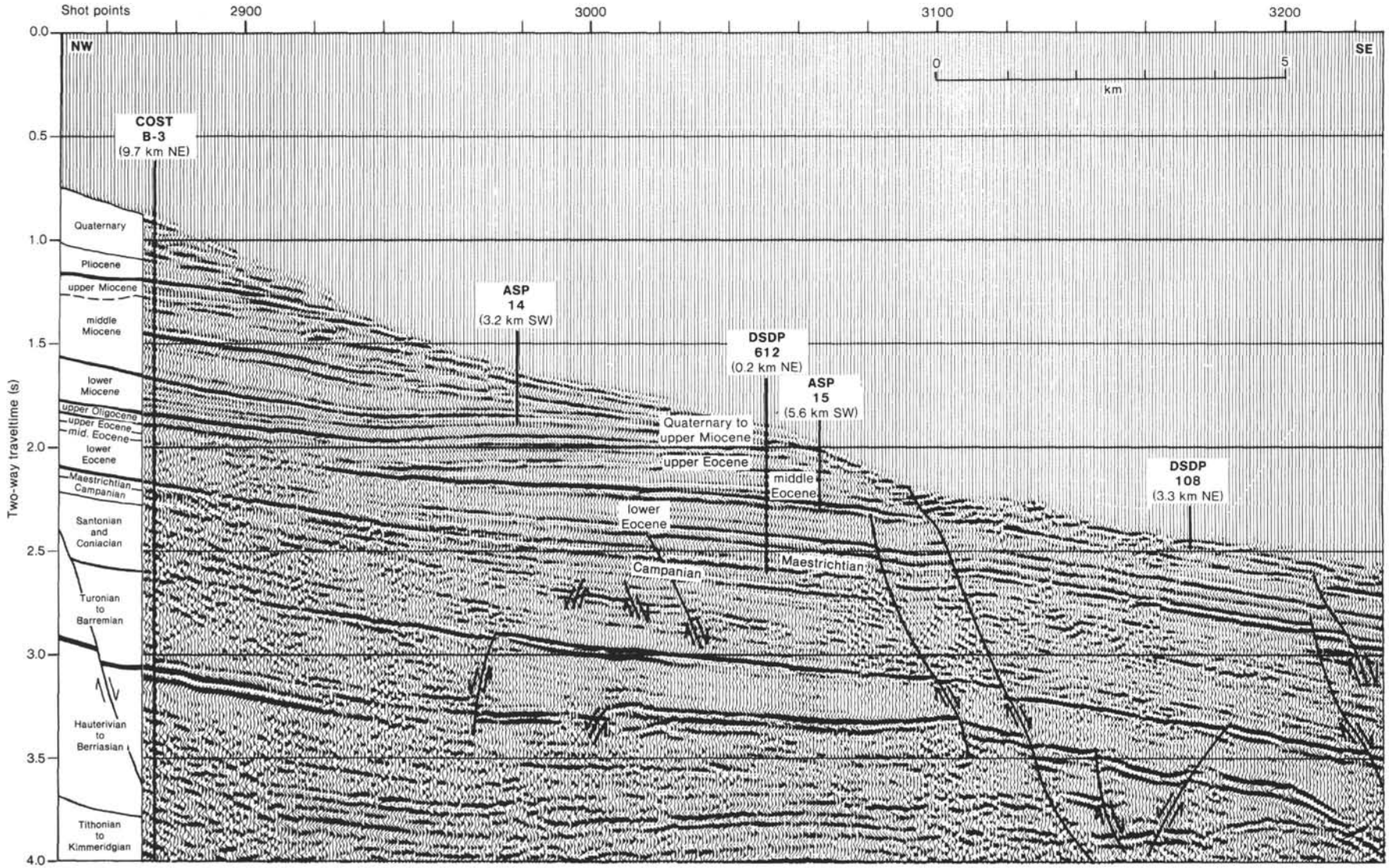

Figure 22. Multichannel seismic reflection profile (Line 25) crossing the continental slope in a dip direction near Site 612. Numbers in parentheses below site labels indicate distance and direction of actual sites from Line 25. Vertical heavy lines show the stratigraphic section penetrated by each corehole and well. Several normal faults are indicated.

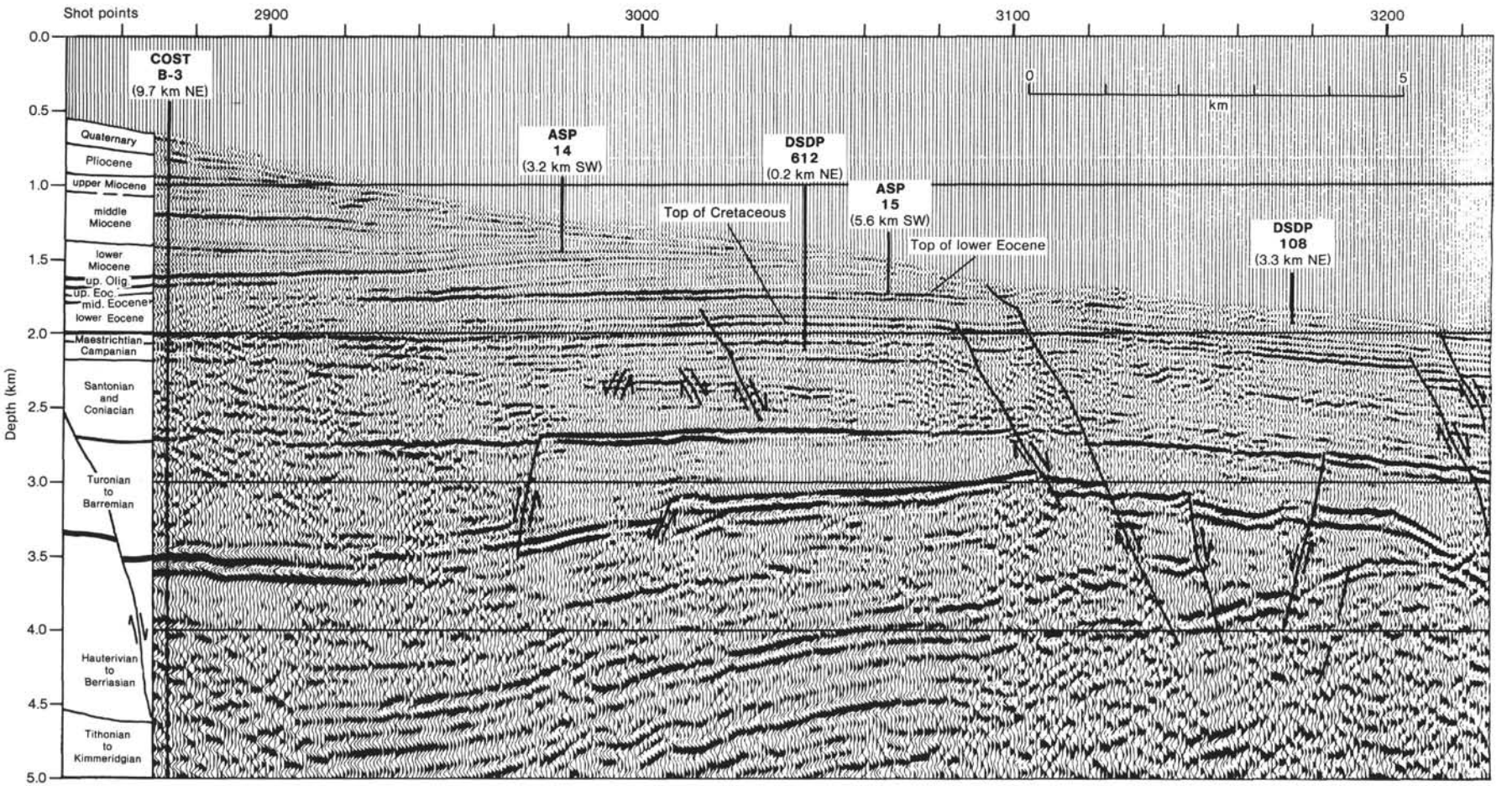

Figure 23. Multichannel seismic reflection profile (Line 25) as in Figure 22, except that depth is measured in kilometers to show cross-sectional geometry more accurately.

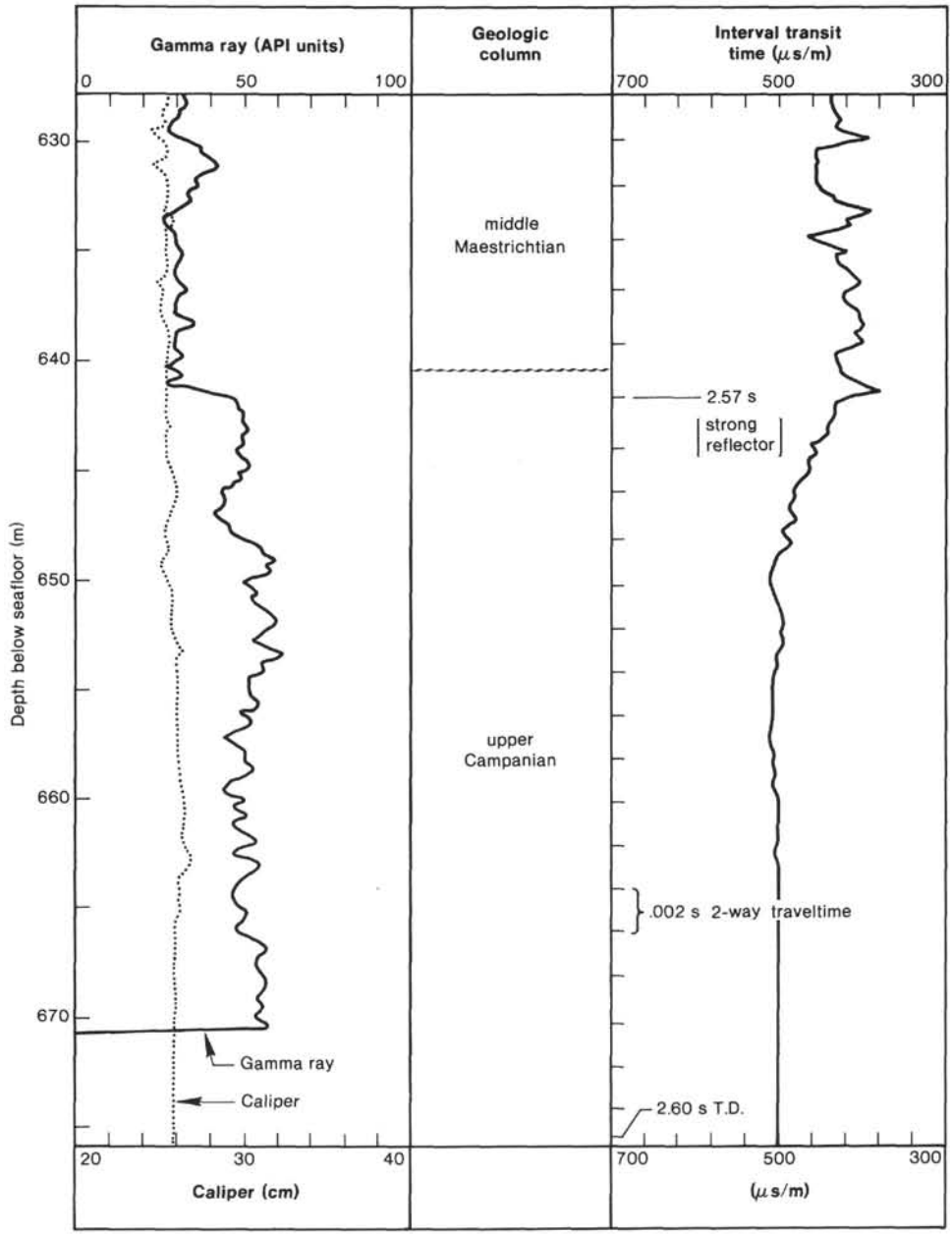

Figure 24. Segment of downhole geophysical log at Site 612. Note that sonic velocity is the reciprocal of interval transit time, and increases from left to right (sonic scale is in microseconds per meter).

trichtian and Paleocene strata in the shelf and slope sections suggests widespread erosion during this time period (Poag, 1985).

No Paleocene sediments were noted at the B-3 well or at Site 612, although a thick Paleocene sequence is present within the upper rise wedge at Site 605. However, the interval in which a thin Paleocene unit could have been present at Site 612 was poorly recovered (Core 612-60). Evidence for the possible presence of a 4-m-thick Paleocene section is present on the downhole gamma ray log, where a distinct increase of 25 gamma units at 552 to 556 m (2.49 s) indicates a significantly clay-enriched zone (Fig. 25). The presence of clay-rich Paleocene strata at Site 605 supports the inference that this gamma ray spike may represent Paleocene beds at Site 612.

Lower Eocene strata are bounded by the two strongest reflectors seen on Line 25 (Figs. 22 and 23). The upper reflector truncates underlying ones at the B-3 well projection, indicating that erosion has removed some of the upper strata. An erosion surface was also observed at Site 612 at this contact and can be widely extrapolated on the seismic grid. Onlapping middle Eocene reflections indicate that a period of nondeposition followed the erosion.

Middle Eocene sediments are thick at Site 612 (Figs. 22 and 23), but thin markedly updip to the B-3 projection. Identical geometry of the middle Eocene sequence is seen on Line 79-218, which crosses the B-3 site (Fig. 27). The updip thinning is the result of severe erosion, as evidenced by the truncation of underlying reflections

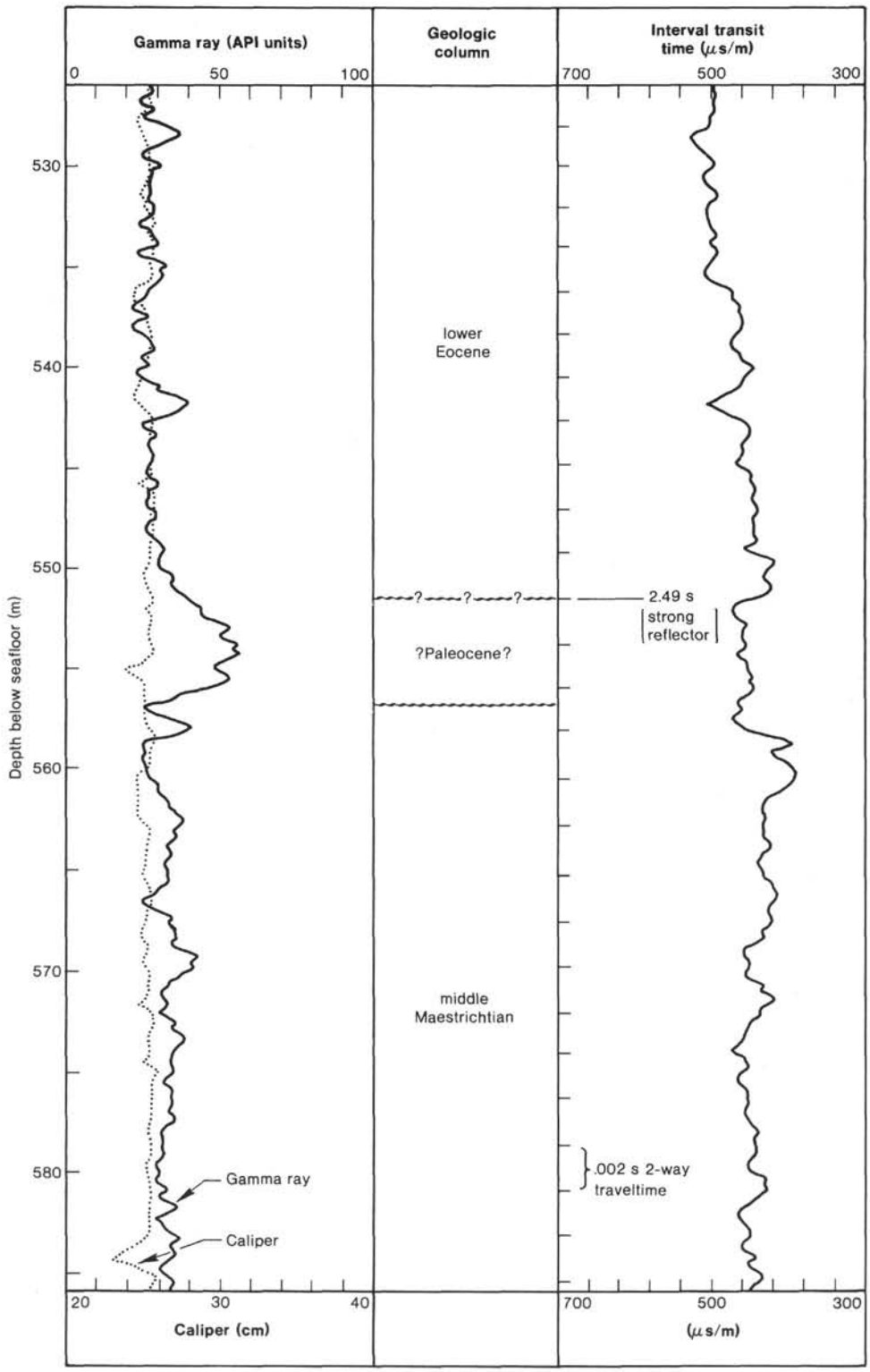

Figure 25. Segment of downhole geophysical log at Site 612. See note for Figure 24.

against the highest middle Eocene reflector. Downdip, truncated reflections also record erosion across the middle Eocene surface on all the nearby seismic lines.

The upper Eocene sequence is thickest between the B-3 projection and Site 612 (Figs. 22 and 23). A few faint reflections are truncated at the upper sequence boundary, giving evidence of the erosion recorded at the B-3 well. However, the upper contact appears not to have been recovered at Site 612 and cannot be evaluated.

Ninety-one meters of upper Oligocene section rest on the upper Eocene erosion surface at the B-3 well (Fig. 27), and its bounding reflectors can be clearly traced to

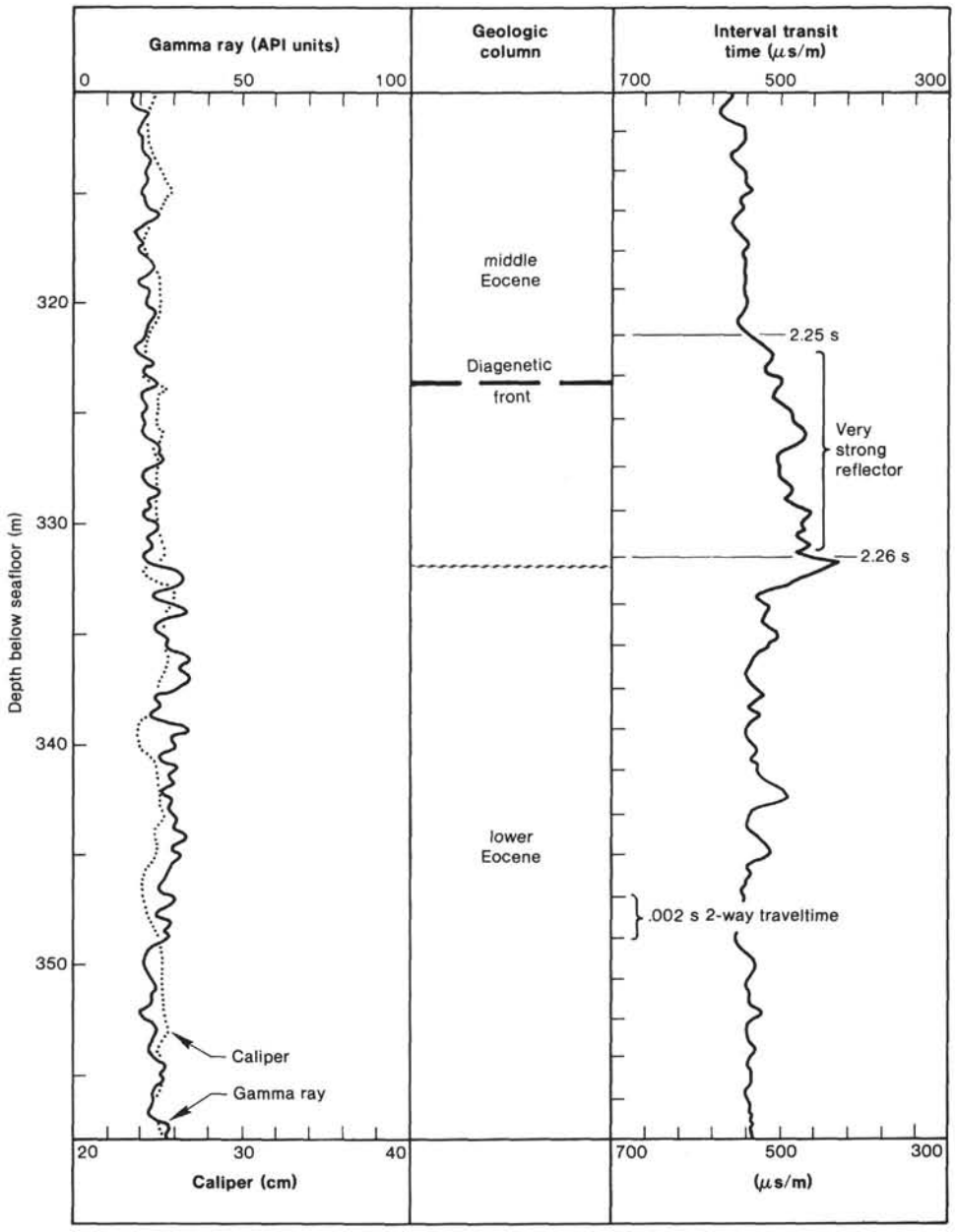

Figure 26. Segment of downhole geophysical log at Site 612. See note for Figure 24.

Line 25 (Figs. 22 and 23). However, toward Site 612, the reflections diminish and finally disappear. Lower Oligocene strata are present at Site 612 and ASP 15 (although the latter was incompletely cored; Poag, 1985). The Oligocene unit at Site 612 is only 1 m thick (Fig. 28), which is too thin to be resolved by seismic reflection profiling.

The lower Miocene strata appear to drape conformably across the upper Oligocene surface at the COST B-3 well and at its projection on Line 25 (Figs. 22, 23, and 27). This sequence then thins to a feather edge between ASP 14 and Site 612. No lower Miocene sediments were recovered at Site 612, but 2 m of lower Miocene sediments were penetrated by the nearby ASP 15 corehole (Fig. 21; Poag, 1985). The lower Miocene sequence apparently is distributed irregularly near its downdip termination on the middle slope. The upper surface of the lower Miocene sequence has been eroded, as evidenced by truncated reflections; the upper part of the lower Miocene section is missing at the COST B-3 well.

Middle Miocene beds on the upper slope form the seaward terminus of a 1000-m-thick shelf sequence of prograding, clinoform, deltaic strata (Poag, 1980, 1985). The upper surface of the middle Miocene beds has been severely eroded between the COST B-3 well and Site 612 (as shown by numerous truncated reflections across the top of the sequence) and forms a rugged buried topography (Figs. 22 and 23). Like the lower Miocene, this sequence is represented at ASP 15, but not at Site 612; this is a result of its irregular seaward termination.

Upper Miocene strata were encountered at Site 612, but not at ASP 14 and 15; discontinuous coring in the ASP coreholes may have prevented recovery there (Poag,

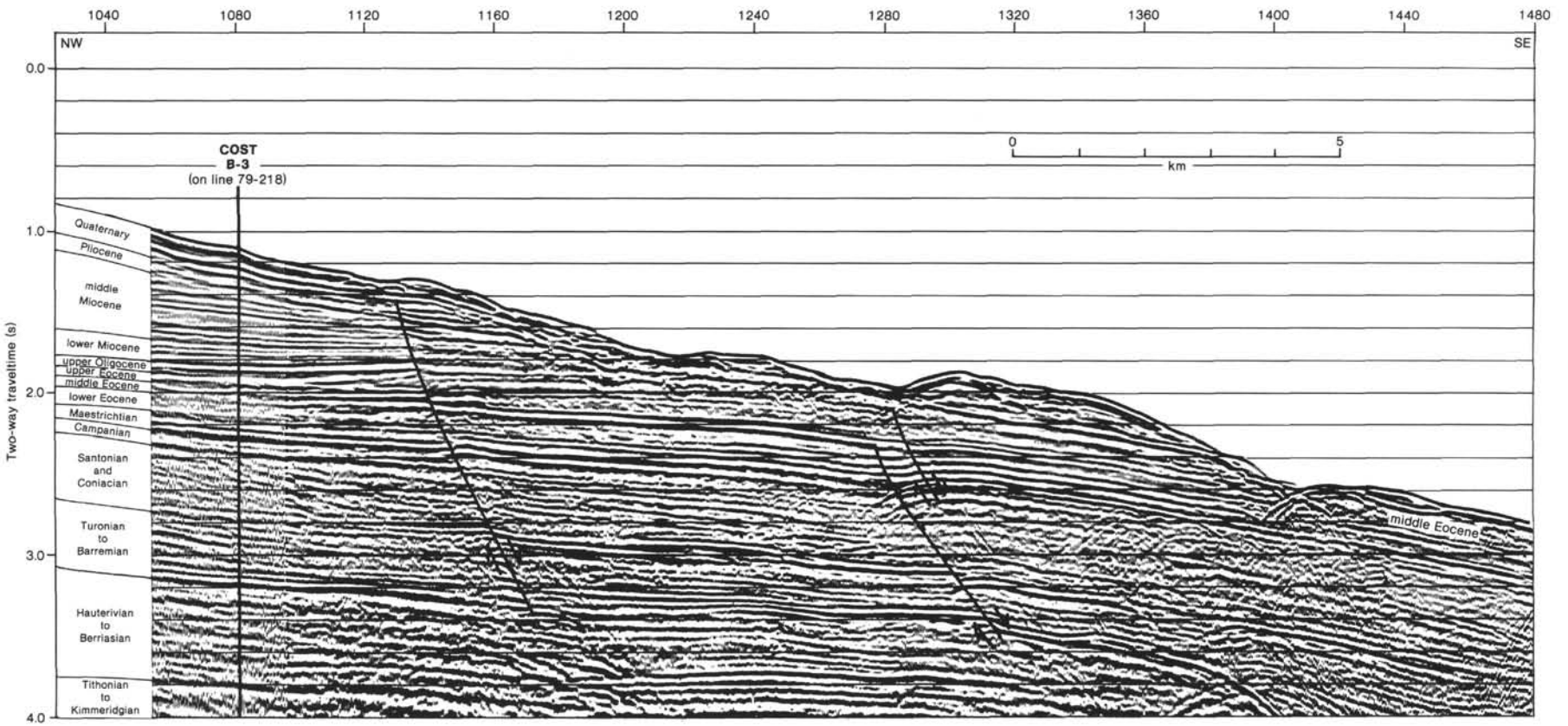

Figure 27. Multichannel seismic reflection profile (Line 79-218) crossing the continental slope and the COST B-3 well site. Depth is measured in 2-way traveltime. Several large normal faults are noted. Stratigraphic data are from Poag (1980, 1985).

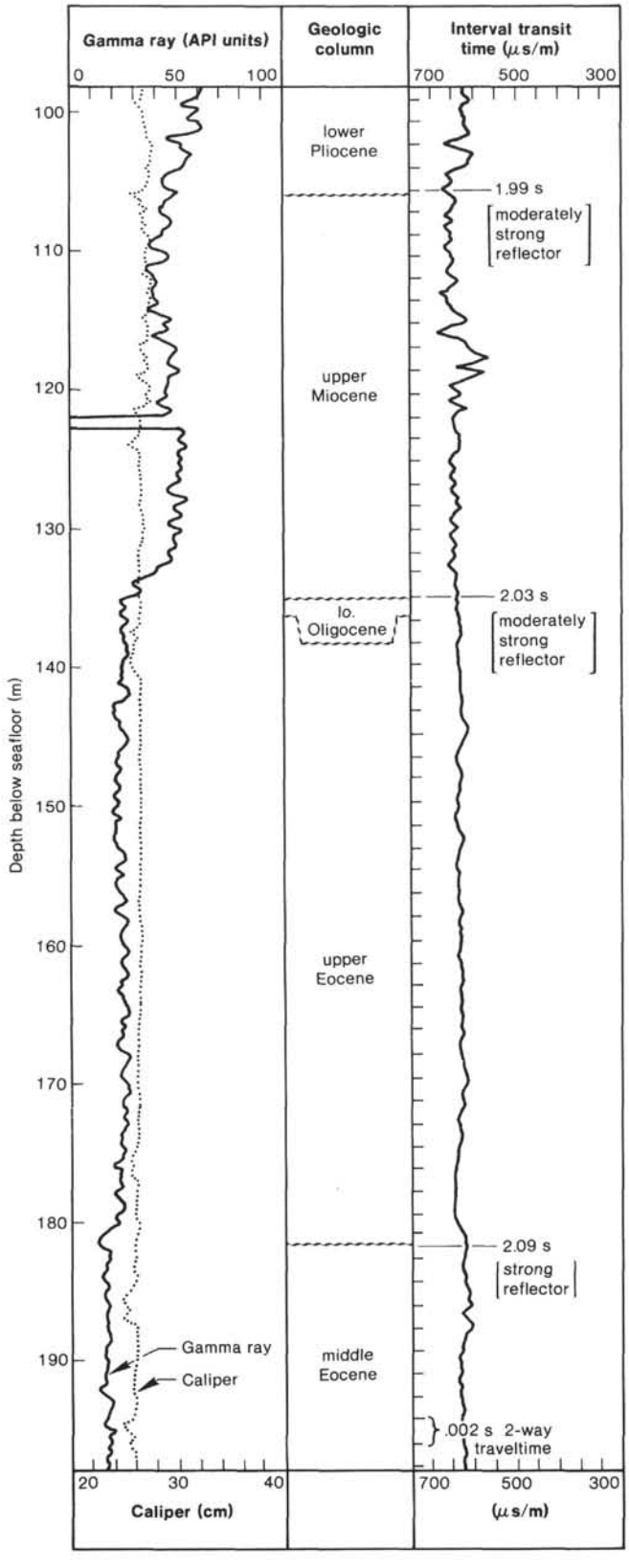

Figure 28. Segment of downhole geophysical log at Site 612. See note for Figure 24.

1985). At any rate, it is difficult to trace an upper Miocene sequence updip toward the COST B-3 projection. Some irregular reflections appear to drape across the channeled middle Miocene surface, filling in the channels (Figs. 22 and 23), and these presumably are of late Miocene age. The COST B-3 section was not sampled above the middle Miocene because of the lack of return mud circulation to the drill floor at shallow penetration depths.

Pliocene strata were not recovered at the ASP sites. However, the thickness of the Pliocene unit at Site 612 (~60 m) suggests that it is widespread. A presumed Pliocene unit was recognized at B-3 on the basis of downward displaced foraminifers (cavings) and seismostratigraphy by Poag (1980, 1985). The relatively thick Pliocene sequence at Site 612 appears to confirm Poag's interpretation. The upper boundary of this preserved Pliocene sequence truncates underlying reflections and is downlapped by reflections of the Pleistocene sequence (Figs. 22 and 23), indicating that erosion and nondeposition were responsible for the unconformity.

The Quaternary sequence forms a 200-m-thick downlapping wedge across the B-3 projection and then drapes across the lower slope in a layer not more than about 40 m thick (Figs. 22 and 23). Its surface is irregular, appearing to have been eroded in places and comprising slumps or sediment mounds in others.

Seismic Facies Analysis

The geometry of seismic sequences and the characteristic patterns of the internal seismic reflections allow one to draw preliminary conclusions regarding lithofacies relationships and paleoenvironments of the continental slope along Line 25 (see Vail et al., 1977, for further explanation of seismic facies analysis).

The Campanian seismic sequence thickens rapidly downdip from the COST B-3 well projection to Site 612 and reaches a maximum thickness near shot point 3120 (Line 25) where it crosses a suite of normal faults (Figs. 22 and 23). This geometric pattern suggests that the Campanian shelf edge lay near shot point 3120. The reflections within the Campanian outer-shelf sequence (COST B-3 well to Site 612) are discontinuous, of variable amplitude, and subparallel, as is typical of marine clastic sequences deposited in a regime of varying energy (Fig. 22). However, at the fault system and downslope from it, the reflections on Line 25 become erratic and somewhat chaotic. On Line 79-218, a series of rapidly varying high- to low-amplitude, nonparallel to parallel, sometimes anastomosing reflections suggests the chaotic depositional style of debris flows (Fig. 27).

The general position of the Campanian shelf edge appears to have been maintained in the Maestrichtian (Fig. 23). Facies relationships suggest that terrigenous debris was reaching the slope as reported at Site 605, although turbidites rather than debris flows may have been the distributing agents, as the reflections are somewhat more regular than those of the Campanian. The upper-slope Maestrichtian deposits are considerably thicker than those of the shelf, and by the end of the Maestrichtian

the sharpness of the shelf break was diminished by upper slope infill.

In the Eocene section, seismic facies characteristics change considerably from those of the underlying sections (Fig. 22). Between Site 612 and shot point 2920 (Line 25), the entire Eocene section is characterized by broad, acoustically transparent bands separated by occasional high- to moderate-amplitude reflections that are continuous across the interval. These characteristics are typical of marine carbonate or shale facies of uniform lithology, such as were encountered at Site 612. Updip at the COST B-3 projection, the internal reflections of the Eocene section become intermittent and of variable amplitude, suggesting less uniform conditions and some influence from terrigenous sedimentation. This more variable facies was sampled at the COST B-3 well where calcareous claystone, biomicritic limestone, and chalk constitute the Eocene section.

Seaward of the fault system that is located downdip from Site 612 (Fig. 22), numerous, subcontinuous, high- to low-amplitude reflections may be observed in the lower Eocene section, indicating more variable lithologies. The reflections also become somewhat sinuous, suggesting a more vigorous depositional regime than that present landward. At Site 605, a monotonous, sometimes cyclic sequence of clay-rich, nannofossil limestone containing thin foraminiferal turbidites was recovered.

By early Eocene time, the physiographic expression of the shelf edge appears to have been quite subtle, giving the Eocene margin the geometry of a gently sloping carbonate ramp (Fig. 23). However, the present crest of the anticlinal structure may have been the principal change in slope during the time, as suggested by the changing depositional styles between Sites 612 and 605 and by the general thinning of the section downdip from Site 612.

The middle Eocene margin appears to have retained its ramplike physiography, although the upper surface of the middle Eocene section is too severely eroded to allow confident estimation of its original geometry (Figs. 22 and 23). The facies downslope from Site 612 does not appear to change until about 3 km farther southeast from Site 605, where more numerous internal reflections appear. Site 605 recovered biosiliceous nannofossil chalk, with negligible clay content in the middle Eocene section. Upper Eocene seismic facies and lithofacies are similar to those of the middle Eocene.

The Oligocene section is too thin to display seismic facies characteristics, and its limited distribution provides little information regarding the position of the Oligocene shelf edge (Figs. 22 and 23). During the Miocene, however, the shelf edge appears to have been prominent again, having shifted landward, as indicated by the rapid thinning of prograding sequences seaward from shot point 2600 (12 km landward of the COST B-3 well projection). This point of rapid thinning appears to have been the shelf break at the end of the Miocene.

The lower Miocene section contains evenly spaced, uniformly converging, subcontinuous, variable-amplitude reflections typical of terrigenous marine facies (Fig. 22). Such sediments are present in the COST B-3 well and ASP 14 corehole. The prograded, clinoform, variable amplitude reflections of the middle Miocene section in the COST B-3 well are typical of deltaic deposition. The upper Miocene section is not well represented on Line 25 but appears to be similar to the lower Miocene in thickness and geometry (Figs. 22 and 23).

The Pliocene shelf edge appears to have been at the same location as that of the upper Miocene, but the intra-Pliocene reflections are weaker, suggesting more uniform conditions of deposition (Figs. 22 and 23). However, on Line 79-218, several strong, continuous reflections are present within the Pliocene section, suggesting a variable depositional regime (Fig. 27). The Pliocene glauconitic sands and muds of Site 612 were deposited under the more varied conditions.

Reflections in the Quaternary section near the COST B-3 projection (Line 25) are clinoform, variable-amplitude, sinuous reflections typical of deltaic sequences (Fig. 22). Farther down slope, between the projections of the ASP 14 and ASP 15 coreholes, the Quaternary section is much thinner, but appears to encompass a few subcontinuous, parallel reflections. A variety of lithologies (quartzose and glauconitic sands, silts, silty clays, debris flow deposits, displaced blocks of Paleogene strata) attest to a variable, high energy depositional regime on this part of the continental slope.

Even farther downdip, near Site 605, the Quaternary section contains a central, high-amplitude, continuous reflector. Above and below it are low-amplitude, discontinuous reflections, some of which are arched and truncated. Such indications of a variable and often chaotic depositional regime are borne out by the presence of debris flow deposits and other coarse-grained terrigenous strata in the Quaternary section at Site 605.

Summary and Conclusions

The seismostratigraphic interpretations are generally consistent with the borehole data and provide an extrapolation of the known stratigraphy along the chief control lines in the vicinity of the COST B-3 well and Site 612. The erosion surfaces at Site 612 correspond to truncating and often onlapped reflectors on the profiles, providing evidence of widespread erosional events usually followed by periods of nondeposition before the onset of the next depositional sequence.

The seismostratigraphic results provide reason to suspect that a thin Paleocene interval may have been present in poorly recovered Core 612-60. Furthermore, although no significant biostratigraphic break was seen at the Pliocene/upper Miocene contact, truncated reflections at that level indicate that an erosional regime was present on the slope during the time interval. Site 612 was generally too far below the sea surface to have been affected directly by relative changes in post-Campanian sea levels, nonetheless the depositional sequences cored there accumulated in harmony with the shelf sequences described by Poag (1985), and most of the boundary unconformities correlate well with major unconformities of the Vail depositional model (Fig. 29; Vail et al., 1977). However, at this stage of analysis, our investigations provide no new data concerning the cause of the relative sea-level changes inferred.

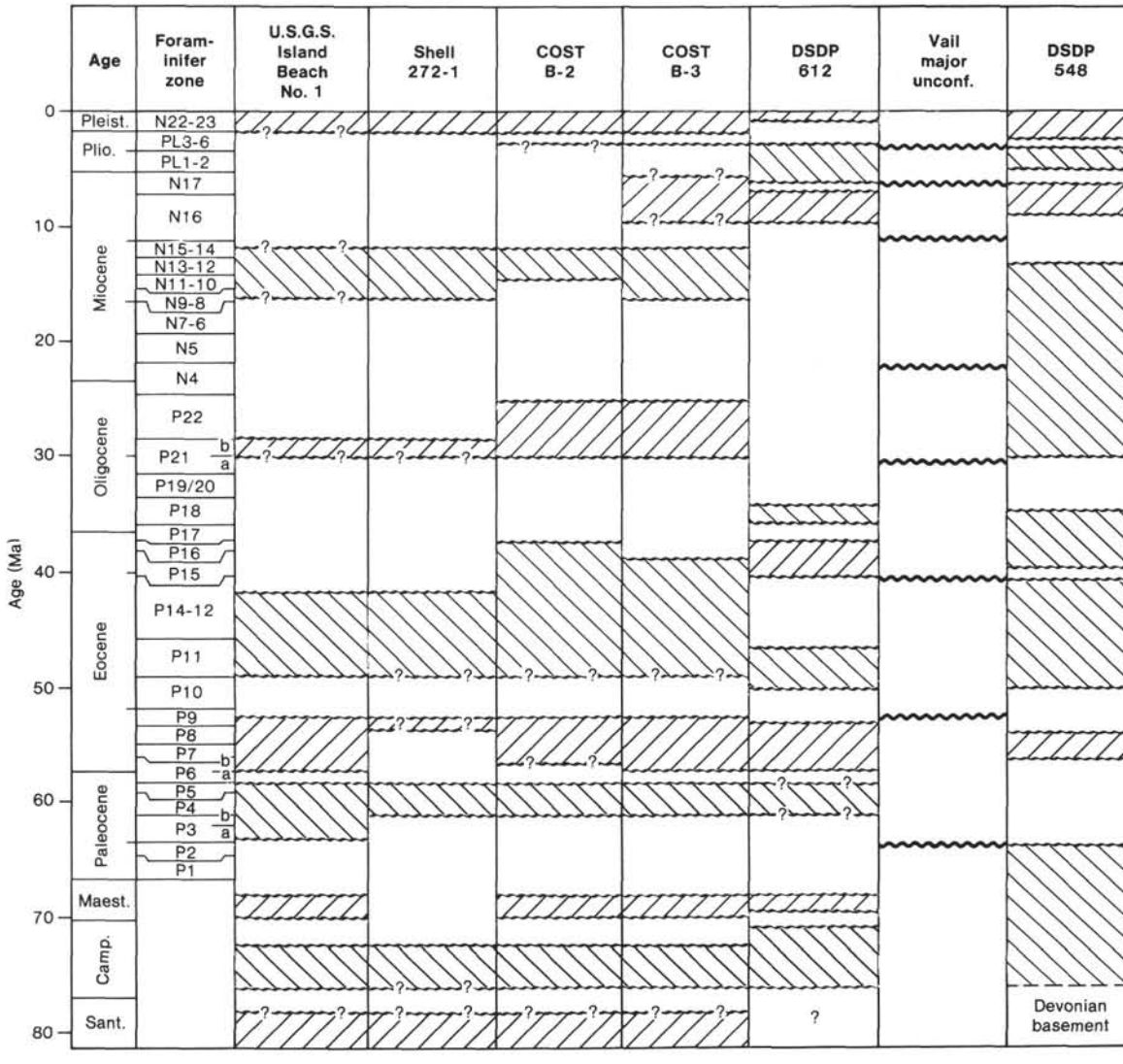

Figure 29. Summary stratigraphic chart for the New Jersey Transect and Goban Spur Transect (Irish continental margin). Blanks in the stratigraphic columns indicate hiatuses. Positions of hiatuses are compared with positions of major unconformities of the Vail depositional model (Vail et al., 1977). Vertical scale in Ma (mega-annums, or millions of years). Scale after Vail and Mitchum (1979). Data for Island Beach, Shell, and COST B wells are from Poag (1985). Data for DSDP Site 548 (Goban Spur) from Graciansky, Poag, et al., (1985).

SUMMARY AND CONCLUSIONS

Introduction

Site 612 was selected to provide a midslope stratigraphic section along the New Jersey Transect. Its position at the intersection of U.S.G.S. multichannel seismic Lines 25 and 34 affords excellent correlation of the sedimentary sequences here with seismic sequences recorded on the dense grid of seismic lines crossing this part of the New Jersey margin. The site is located just updip of the broad submarine outcrop of middle Eocene biosiliceous carbonate-rich strata that were sampled by DSDP Leg 11 at Site 108 (Hollister, Ewing, et al., 1972). It serves as the stratigraphic link between the COST B-3 well on the upper slope 10 km to the north and Site 605 on the upper rise, 17 km to the southeast. Chief operational objectives were to continuously core the section to approximately 800 m and to obtain a suite of downhole geophysical logs.

In terms of scientific goals, this site was selected to provide the most complete Cenozoic and Upper Cretaceous section possible for this part of the margin, given the limitations of open-hole drilling. The principal specific objectives were

1. To establish the composition, stratigraphic framework and depositional environments of sediments constituting the middle continental slope.

2. To establish a detailed biozonation and to accurately date the unconformities and major seismic reflections in the section.

3. To document the lateral variability of lithofacies and biofacies between the COST B-3 well and Site 605.

4. To identify depositional sequences and evaluate their relationships to seismic sequences, relative sea level

changes, oceanic current patterns, water-mass composition, sediment provenance and accumulation rates, and basin subsidence history.

Results

Five distinct lithologic units were documented at Site 612. The lowermost (Unit V) comprises 35.7 m of thin black, foraminifer or nannofossil chalks alternating with mudstone and shale of late Campanian age. The major component is fine grained terrigenous detritus (chiefly clay with subordinate amounts of quartz sand or silt and mica). The clay enrichment relative to overlying Maestrichtian beds is clearly reflected in the consistently higher values recorded on the gamma ray log (20–30 API units higher). The dark color is in part attributable to an abundance of organic matter and pyrite. The TOC value of 2.68% is the highest and only significant amount recorded at Site 612.

Rich, varied, diagnostic foraminifers and calcareous nannofossils are present in the upper Campanian unit, but radiolarians were not observed. A low planktonic: benthic foraminiferal ratio of 3:1 (in the >250-μm size fraction) and the general nature of the benthic assemblage are suggestive of shelf deposition. Sedimentation rate cannot be determined because of the incomplete penetration of the Campanian.

The upper boundary of this Campanian unit is an erosional contact with middle Maestrichtian strata that coincides with a distinct upward increase in sonic velocity and a major upward decrease in the abundance of benthic foraminifers. The acoustic impedance contrast at the contact produces a weak, undulating reflection at 2.57 s on Line 25 that can be traced across truncated underlying reflections.

The geometry of this Campanian unit in depth section (Line 25), in conjunction with the paleoecological inferences drawn from foraminiferal assemblages and lithology, suggests that Site 612 was in an outer shelf position during the late Campanian.

Lithologic Unit IV comprises ca. 80.2 m of dark gray, marly, intensely burrowed foraminifer–nannofossil and nannofossil–foraminifer chalks, including some lithified limestone layers. Terrigenous components are present throughout, but decrease significantly toward the top (e.g., clay ranges from 30 to 50%). Average sedimentation rate was 2.1 cm/k.y. Sedimentation rates in this summary are based upon averaging over the total estimated time represented by a given depositional sequence [in the case of lithologic Unit IV, the time interval is the middle Maestrichtian]. This method contrasts with that used earlier in this chapter, in which sedimentation rates were calculated for single biozones and then either averaged or given a range of values.

Calcareous microfossil groups are well represented in these strata and indicate an age of middle Maestrichtian. Radiolarians are rare and poorly preserved (only observed in Core 612-61, at the top of the section).

The top of the Maestrichtian unit is placed within an interval of poor core recovery (612-60). Because the distance between the lower Eocene beds above and the middle Maestrichtian below is less than 9 m, it is presumed that the contact is unconformable. This inference is supported by the fact that a similar stratigraphic interval is missing in updip wells. A high-amplitude reflection found at 24.9 s on Line 25 represents the top of the middle Maestrichtian section and can be widely traced.

The depth-section geometry of the Maestrichtian sequence suggests that the shelf edge was still southeastward of Site 612, but paleontologic data suggest that the water deepened relative to late Campanian depths.

A significant increase in gamma ray values between 556 and 552 m (increase of 25 API units) indicates a clay-enriched zone, which also yields lower sonic velocity values. Clay enrichment is a characteristic of the Paleogene strata that are present at Site 605. Tracing the Paleocene seismic sequence from Site 605 toward 612 suggests that a very thin section could be present there. Thus a 4-m Paleocene(?) section is tentatively recognized at Site 612.

The early Eocene brought a major change in depositional regime to Site 612, as it did to the adjacent shelf and upper slope. Light gray, carbonate-enriched, biosiliceous oozes and chalks dominated deposition until the early Oligocene, although interrupted by two significant erosional events. A total of 415 m of these deposits is present at Site 612. Diagenetic characteristics have been used to recognize two distinctive lithologic units within this sequence. The upper part, assigned to lithologic Unit II (188.1-m thick) contains well-developed microfossil assemblages that indicate an early Oligocene to middle Eocene age. The abundance of siliceous microfossils (radiolarians and diatoms) is especially notable in Unit II and distinguishes it from Unit III. A zone of progressive, downward intensifying silica diagenesis begins around 245 m BSF and culminates in an 8-m zone of porcellanite at the base of the middle Eocene. Sonic velocities reach peak values for the site in this interval (2.28 km/s on sonic log; 2.52 km/s horizontal measurement from shipboard velocimeter). The top of the porcellanite at 323.4 m is taken as the top of lithologic Unit III (ca. 226.9 m thick), below which variably intense diagenesis has converted most of the biosiliceous components to silica cements. The top of a zone of high salinities in interstitial waters is nearly coincident with the top of the porcellanite (ca. 300 m).

Both Units II and III contain bathyal microfossil assemblages, as would be expected from evidence of a major Cenozoic marine transgression noted in the shelf and coastal plain borings. The seafloor must have been well oxygenated as indicated by the pervasive, intense burrowing, light colored sediments, and sparsity of organic carbon. The gently seaward-sloping geometry seen on the depth section of Line 25 suggests that no distinctive shelf edge was developed. Rather, a wide carbonate ramp formed the continental margin during the Paleogene.

Rates of deposition increased from about 2.1 cm/k.y. in the middle Maestrichtian to about 3.9 cm/k.y. in the early Eocene, but decreased again to about 2.5 cm/k.y. in the middle Eocene.

The Paleogene section is bounded at the top and bottom by erosional unconformities, and contains two additional ones that form the lower Eocene/middle Eo-

cene and middle Eocene/upper Eocene contacts. Each contact is marked by identifiable seismic reflections, permitting regional extrapolation of each depositional sequence. The extrapolations show that the middle Eocene sequence thins significantly updip toward the B-3 well projection on Line 25, and crops out downdip just southeastward of Site 612. The upper Eocene sequence is thickest between the B-3 well and Site 612, and does not appear to be present beneath the slope southeastward from 612. However, an upper Eocene section may be present beneath the upper rise (see Site 613).

Upper Oligocene strata seen in the B-3 well appear to be absent southeastward of shot point 2960 on Line 25. The Oligocene/Eocene contact appears to be biostratigraphically unconformable, and presumably was crossed between Cores 612-16 and 612-17, thus not having been recovered. The depositional rate of the Oligocene interval is difficult to estimate because of the thinness of the section (~1 m) and the unknown length of the time represented.

A depositional regime characterized by increased terrigenous detritus and low carbonate contents (carbonate bomb analysis) encompassed Site 612 sometime between the early Oligocene and late Miocene and has been maintained to the present. The sediments resulting from this terrigenous phase are placed in lithologic Unit I (135.3 m thick), which is subdivided into three parts.

The lower contact of Subunit IC (28.4 m thick) is an unconformity representing a hiatus of ca. 25 m.y. Therefore, the precise beginning of terrigenous influence must be based on evidence from updip wells, which indicate a change in the late Oligocene (Poag, 1985). Subunit IC is composed of chiefly dark gray to olive gray muds, containing light brown, irregularly-dispersed barite concretions, and abundant diatoms (as much as 40%).

The calcareous and siliceous microfossils are moderately well represented and well preserved in this subunit, and date it as late Miocene. A distinct upward increase in gamma ray values on the geophysical log marks the lower unconformable contact and reflects the increased clay content. This subunit accumulated at the lowest rate of any unit cored at Site 612 (0.5 cm/k.y.).

Lithologic Subunit IB (69.65 m) is separated from Subunit IC by an erosional contact separating Tortonian beds from the Messinian section. The chief lithologic characteristic of Subunit IB is the presence of alternating mud and glauconite sand sequences. The muddy sediments are interrupted repeatedly by glauconite-quartz sand beds, which commonly have sharp, eroded basal contacts. Some beds contain as much as 50% glauconite grains, which are fresh, irregular, and unoxidized, indicating very little, if any, transport. The glauconite enrichment indicates a high original organic content, but TOC values are low. The rate of sedimentation also was low (1.8 cm/k.y.).

Lithologic Subunit IA (uppermost Pleistocene) is much like Subunit IC, lacking the plethora of glauconite sand layers within the terrigenous muds, although containing glauconite-filled burrows. It is separated from Subunit IB by a basal unconformity, and its microfossils indicate that the lower Pleistocene is missing here. In fact the total Pleistocene section (36.95 m thick) accumulated in no more than 0.44 m.y., making it by far the most rapidly accumulated unit at greater than 80 cm/k.y.

Lithologic Unit I is too thin at Site 612 to be easily separated into subunits on seismic profiles and is too near the seafloor to have been logged. However, similar sequences recorded at the ASP 15 corehole suggest that its lithologic characteristics are representative of the middle slope depositional setting.

Conclusions

In a regional sense, the depositional sequences documented at Site 612 fit very well into the framework previously established on the coastal plain, shelf, and upper slope, as expected. Eight unconformable sequence boundaries were penetrated at Site 613, and six of the contacts were recovered undisturbed in our cores. Equivalent unconformities bound the depositional sequences of the contiguous coastal plain, continental shelf, and upper slope (Poag, and Schlee, 1984; Poag, 1985). Poag (1985) concluded that this framework of depositional sequences punctuated by periods of widespread erosion and encompassing cyclical fluctuations in paleobathymetry closely resembles the pattern of relative sea level changes described by P. R. Vail and his colleagues. The fact that bathyal water depths generally prevailed at Site 612 prevents shipboard recognition of microfaunal paleobathymetric cycles there, but the arrangement of depositional sequences separated by regional episodes of erosion is complementary to that of the shelf and upper slope.

Perhaps one of the biggest surprises at Site 612 is the sparsity of obviously displaced sedimentary strata (such as debris flow deposits and turbidites) other than those at the principal unconformities. The only period of frequent activity of this kind was the Pliocene, and then it appears to have been only of local extent.

Another notable divergence from expected relationships is the apparent deepening of Maestrichtian paleoenvironments as compared to the Campanian, whereas wells on the coastal plain and shelf indicate the reverse (Poag, 1985). More detailed comparisons are needed to document these relationships more thoroughly.

Additionally, the thick middle Miocene sequence that dominated early Neogene deposition on the shelf and upper slope (Poag, 1985) is not represented at Site 612, apparently having been stripped away by subsequent submarine erosion.

The backstripping method of subsidence analysis shows that tectonic subsidence (thermal contraction of the lithosphere) was the dominant cause of subsidence in the Cenozoic at Site 612 (located above oceanic basement), but that sediment loading continued to play an important role. Three periods of notably accelerated loading subsidence seem to be indicated by the Site 612 data. These three pulses (Eocene, late Miocene, and late Pleistocene) have also been noted on the New Jersey shelf and upper slope in the COST B-2 and B-3 wells (Watts and Steckler, 1979; Heller et al., 1982; Poag, 1985). A fourth acceleration pulse, noted in the middle Miocene at the B wells, is not represented by deposition at Site 612.

REFERENCES

Benson, R. N., 1972. Radiolarians—Site 114. *In* Laughton, A. S., Berggren, W. A., et al., *Init. Repts. DSDP*, 12: Washington (U.S. Govt. Printing Office), 324-325.

Berggren, W. A., and Aubert, J., in press. Paleogene benthonic foraminiferal biostratigraphy and bathymetry of the Central Coast Ranges of California. *U.S. Geol. Surv. Prof. Paper.*

Berggren, W. A., Kent, D. V., Flynn, J. J., and Van Couvering, J., 1985. Cenozoic geochronology. *Geol. Soc. Am. Bull.*, 96:1407-1418.

Blow, W. H., 1979. *The Cainozoic Globigerinida:* Leiden (E. J. Brill).

Bolli, H. M., 1957. Planktonic foraminifera from the Eocene Navet and San Fernando Formations of Trinidad, B.W.I. *U.S. Natl. Mus. Bull.*, 215:155-172.

Boyce, R. E., 1976. I. Definitions and laboratory techniques of compressional sound velocity parameters and wet-water content, wet-bulk density, and porosity parameters by gravimetric and gamma ray attentuation techniques. *In* Schlanger, S. O., Jackson, E. D., *Init. Repts. DSDP*, 33: Washington (U.S. Govt. Printing Office), 931-958.

Bukry, D., 1973. Low-latitude coccolith biostratigraphic zonation. *In* Edgar, N. T., Saunders, J. B., et al., *Init. Repts. DSDP*, 15: Washington (U.S. Govt. Printing Office), 685-703.

———, 1975. Coccolith and silicoflagellate stratigraphy, northwestern Pacific Ocean. *In* Larson, R. L., Moberly, R., et al., *Init. Repts. DSDP*, 32: Washington (U.S. Govt. Printing Office), 677-701.

Casey, R. E., 1977. The ecology and distribution of recent radiolaria. *In* Ramsay, A. T. S. (Ed.), *Oceanic Micropaleontology,* (Vol. 2): London (Academic Press), 809-845.

Casey, R. E., Spaw, J. M., and Kunze, F. R., 1982. Polycystine radiolarian distribution and enhancement related to oceanographic conditions in a hypothetical ocean. *Trans. Gulf Coast Assoc. Geol. Soc.*, 32:319-333.

Charletta, A. C., 1980. Eocene benthic foraminiferal paleoecology and paleobathymetry of the New Jersey continental margin [Ph.D. dissert.]. Rutgers, The State University of New Jersey, New Brunswick, N.J.

Espitalié, J., Laporte, J. L., Madec, M., Marquis, F., Leplat, P., et al., 1977. Méthode rapide de caractérisation des roches mères, de leur potentiel pétrolier et de leur degré dévolution. *Rev. Inst. Fr. Pet.*, 32:23-47.

Foreman, H. P., 1973. Radiolaria of Leg 10 with systematics and ranges for the families Amphipyndacidae, Artostrobiidae, and Theoperidae. *In* Worzel, J. L., Bryant, W., et al., *Init. Repts. DSDP*, 10: Washington (U.S. Govt. Printing Office), 407-474.

Gartner, S., 1977. Calcareous nannofossil biostratigraphy and revised zonation of the Pleistocene. *Mar. Micropaleontol.*, 2:1-25.

Gieskes, J. M., 1981. Deep-sea drilling interstitial water studies: implications for chemical alteration of the oceanic crust, Layers I and II. *Spec. Publ. Soc. Econ. Paleontol. Mineral.*, 32:149-167.

Graciansky, P. C. de, Poag, C. W., et al., 1985. *Init. Repts. DSDP*, 80: Washington (U.S. Govt. Printing Office).

Grow, J., and Kiltgord, K., 1980. Structural framework. Structural Framework, Stratigraphy, and Petroleum Geology of the area of Oil and Gas Lease Sale No. 49 on the U.S. Atlantic Continental Shelf and Slope. *U.S.G.S. Circular*, 812:8-35.

Hampson, J. C., Jr., and Robb, J. M., 1984. Geologic map of the Continental Slope between Lindenkohl and South Toms Canyons, offshore New Jersey. U.S. Geological Survey Misc. Invest., 1:50,000, 1 sheet.

Hart, M. B., Bailey, H. W., Fletcher, B. N., Price, R., and Swiecicki, A., 1981. Cretaceous. *In* Jenkins, D. G., and Murray, J. W. (Eds.), *Stratigraphical Atlas of Fossil Foraminifera:* Chichester (Horwood), pp. 149-227.

Heller, P. L., Wentworth, C. M., and Poag, C. W., 1982. Episodic post-rift subsidence of the U.S. Atlantic continental margin. *Geol. Soc. Am. Bull.*, 93:379-390.

Hollister, C. D., Ewing, J. I., et al., 1972. Site 108—Continental slope. *In* Hollister, C. D., Ewing, J. I., et al., *Init. Repts. DSDP*, 11: Washington (U.S. Govt. Printing Office), 357-364.

Howarth, R. W., and Jørgensen, B. B., in press. Formulation of ^{35}S-labelled elemental sulfur and pyrite in costal marine sediments (Limfjorden and Kysing Fjord, Denmark) during short-term $^{35}SO_4^{2-}$ reduction measurements. *Geochim. Cosmochim. Acta.*

Hunt, J., 1977. *Petroleum Geochemistry and Geology:* San Francisco (Freeman).

Jansa, L. F., Enoc, P., Tucholke, B. E., Gradstein, F. M., and Sheridan, R. E., 1979. Mesozoic-Cenozoic sedimentary formations of the North American Basin; western North Atlantic. *In* Talwani, M., Hay, W., and Ryan, W. B. F. (Eds.), *Deep Sea Drilling Results in the Atlantic Ocean: Continental Margins and Paleoenvironment:* Washington, D.C. (Am. Geophys. Union), Maurice Ewing Series, 3:1-57.

Jones, G. D., 1983. Foraminiferal biostratigraphy and depositional history of the middle Eocene rocks of the coastal plain of North Carolina. *Geol. Surv. N. Carolina, Spec. Publ.*, 8:1-80.

Lancelot, Y., Seibold, E., et al., 1978. *Init. Repts. DSDP*, 41: Washington (U.S. Govt. Printing Office).

Manheim, F. T., and Hall, R. E., 1976. Deep evaporitic strata off New York and New Jersey—evidence from interstitial water chemistry of drill holes. *J. Res. U.S.G.S.*, 4:697-702.

Miller, K. G., 1983. Eocene-Oligocene paleoceanography of the deep Bay of Biscay: benthic foraminiferal evidence. *Mar. Micropaleontol.*, 7:403-440.

Miller, K. G., Curry, W. B., and Ostermann, D. R., 1985. Late Paleogene (Eocene to Oligocene) benthic foraminiferal paleoceanography of the Goban Spur region, DSDP Leg 80. *In* Graciansky, P. C. de, Poag, C. W., et al., *Init. Repts. DSDP*, 80: Washington (U.S. Govt. Printing Office), 508-538.

Miller, K. G., and Lohmann, G. P., 1982. Environmental distribution of recent benthic foraminifera on the northeast U.S. continental slope. *Geol. Soc. Am. Bull.*, 93:200-206.

Morley, J. J., and Hays, J. D., 1979. *Cycladophora davisiana:* a stratigraphic tool for Pleistocene North Atlantic and interhemispherical correlation. *Earth Planet. Sci. Lett.*, 44:383-389.

Nigrini, C., 1977. Tropical Cenozoic Artostrobiidae (Radiolaria). *Micropaleontology*, 23:241-269.

Okada, H., and Bukry, D., 1980. Supplementary modification and introduction of code numbers to the low-latitude coccolith biostratigraphic zonation (Bukry, 1973, 1975). *Mar. Micropaleontol.*, 5:321-325.

Olsson, R. K., Miller, K. G., and Ungrady, T. E., 1980. Late Oligocene transgression of middle Atlantic Coastal Plain. *Geology*, 8: 549-554.

Palmer, A. A., 1986. Miocene radiolarian biostratigraphy, U.S. mid-Atlantic Coastal Plain. *Micropaleontology*, 32:19-31.

Parsons, B., and Sclater, J., 1977. An analysis of the variation of ocean floor bathymetry and heat flow with age. *J. Geophys. Res.*, 82: 803-827.

Petrushevskaya, M. G., 1971. Spumellarian and nasselaarian radiolaria in the plankton and sediments of the Central Pacific. *In* Funnell, B. M., and Riedel, W. R. (Eds.), *The Micropaleontology of Oceans:* London (Cambridge University Press), pp. 309-318.

Poag, C. W., 1978. Stratigraphy of the Atlantic continental shelf and slope of the United States. *Ann. Rev. Earth Planet. Sci.*, 6:251-280.

———, 1980. Foraminiferal biostratigraphy, paleoenvironments, and depositional cycles in the Baltimore Canyon trough. *In* Scholle, P. A. (Ed.), *Geological Studies of the COST B-3 Well, United States Mid-Atlantic Continental Slope Area.* U.S. Geol. Surv. Circular, 833:44-65.

———, 1985. Depositional history and stratigraphic reference section for central Baltimore Canyon trough. *In* Poag, C. W. (Ed.), *Geological Evolution of the U.S. Atlantic Margin:* New York (Van Nostrand Reinhold), pp. 217-263.

Poag, C. W., and Schlee, J. S., 1984. Depositional sequences and stratigraphic gaps on submerged United States Atlantic margin. *In* Schlee, J. S. (Ed.), *Interregional Unconformities and Hydrocarbon Accumulation*. Am. Assoc. Pet. Geol. Mem., 36:165-182.

Riedel, W. R., and Sanfilippo, A., 1977. Cainozoic Radiolaria. *In* Ramsay, A. T. S. (Ed.), *Oceanic Micropaleontology:* New York (Academic Press), pp. 847-912.

———, 1978. Stratigraphy and evolution of tropical Cenozoic radiolarians. *Micropaleontology*, 23:61-96.

Robb, J. M., Hampson, J. C., Jr., Kirby, J. R., and Twichell, D. C., 1981. Gomorphology and sediment stability of a segment of the U.S. continental slope off New Jersey. *Science*, 211:935-937.

Sanfilippo, A., and Riedel, W. R., 1973. Cenozoic radiolaria (exclusive of theoperids artostrobiids, and amphipyndacids) from the Gulf of Mexico, Deep Sea Drilling Project Leg 10. *In* Worzel, J. L., Bryant, W., et al., *Init. Repts. DSDP*, 10: Washington (U.S. Govt. Printing Office), 475–607.

———, 1982. Revision of the radiolarian genera *Theocotyle, Theocotylissa* and *Thycsocyctis. Micropaleontology*, 28:170–188.

Saunders, J. B., Bernoulli, D., Muller-Merz, E., Oberhansli, H., Perch-Nielsen, K., Riedel, W. R., Sanfilippo, A., and Torrini, R., Jr., 1985. The stratigraphy of the late Eocene to early Oligocene in the Bath Cliff Section, Barbados, West Indies. *Micropaleontology*, 30:390–425.

Sayles, F. L., and Manheim, F. T., 1975. Interstitial solutions and diagenesis in deeply buried sediments: results from the Deep Sea Drilling Project. *Geochim. Cosmochim. Acta*, 39:103–127.

Scholle, P. A. (Ed.), 1980. Geological studies of the COST No. B-3 well, United States Mid-Atlantic Continental Slope area. *U.S. Geol. Surv. Circ.*, 833.

Snyder, S. W., Müller, C., and Miller, K. G., 1984. Eocene–Oligocene boundary: biostratigraphic recognition and gradual paleoceanographic change at DSDP Site 549. *Geology*, 12:112–115.

Stainforth, R. M., Lamb, J. L., Luterbacher, H., Beard, J. H., and Jeffords, R. M., 1975. Cenozoic planktonic foraminiferal zonation and characteristics of index fossils. *Univ. Kansas Paleontol. Contrib.*, 62:1–425.

Steckler, M. S., and Watts, A. B. 1978. Subsidence of the Atlantic-type continental margin off New York. *Earth Planet. Sci. Lett.*, 41:1–13.

Tjalsma, R. C., and Lohmann, G. P., 1983. Paleocene–Eocene bathyal benthic foraminifera from the Atlantic Ocean. *Micropaleontol., Spec. Publ.*, 4:1–90.

Toumarkine, M., and Bolli, H. M., 1970. Evolution de *Globorotalia cerroazulensis* (Cole dans l'Eocene moyen et superieur de Possagno). *Rev. Micropaleontol.*, 13:131–145.

Tsunogai, S., Nishimura, M., and Nakaya, S. 1978. Complexometric titration of calcium in the presence of large amounts of magnesium. *Talahta*, 15:385–390.

Tucholke, B. E., 1979. Relationship between acoustic stratigraphy and lithostratigraphy in the western North Atlantic Basin. *In* Tucholke, B. E., Vogt, P. R., et al., *Init. Repts. DSDP*, 43: Washington (U.S. Govt. Printing Office), 827–846.

Vail, P. R., and Mitchum, R. M., Jr., 1979. Global cycles of relative changes of sea level from seismic stratigraphy. *In* Watkins, J. S., Montadert, L., and Dickerson, P. W. (Eds.), *Geological and Geophysical Investigations of Continental Margins*. Am. Assoc. Pet. Geol. Mem., 29:469–472.

Vail, P. R., Mitchum, R. M., Jr., and Thompson, S., III, 1977. Seismic stratigraphy and global changes of sea level: Part IV: Global cycles of relative changes of sea level. *In* Payton, C. E. (Ed.), *Seismic Stratigraphy—Applications to Hydrocarbon Exploration*. Am. Assoc. Pet. Geol. Mem., 26:83–98.

van Hinte, J. E., 1976. A Cretaceous time scale. *Am. Assoc. Pet. Geol. Bull.*, 60:498–516.

———, 1978. Geohistory analysis—application of micropaleontology in exploration geology. *Am. Assoc. Pet. Geol. Bull.*, 62(2): 201–222.

Watts, A. B., and Ryan, W. B. F., 1976. Flexure of the lithosphere and continental margin basins. *Tectonophysics*, 36:24–44.

Watts, A. B., and Steckler, M. S., 1979. Subsidence and eustasy at the continental margin of eastern North America. *In* Talwani, M., Hay, W. W., and Ryan, W. B. F. (Eds.), *The Continental Margin of Eastern North America: Continental Margins and Paleoenvironments*. Deep Drilling Results in the Atlantic Ocean, American Geophysical Union. Maurice Ewing Symposium, Ser. 3, pp. 273–310.

Westberg, M. J. and Riedel, W. R., 1978. Accuracy of radiolarian correlations in the Pacific Miocene. *Micropaleontology*, 24:1–23.

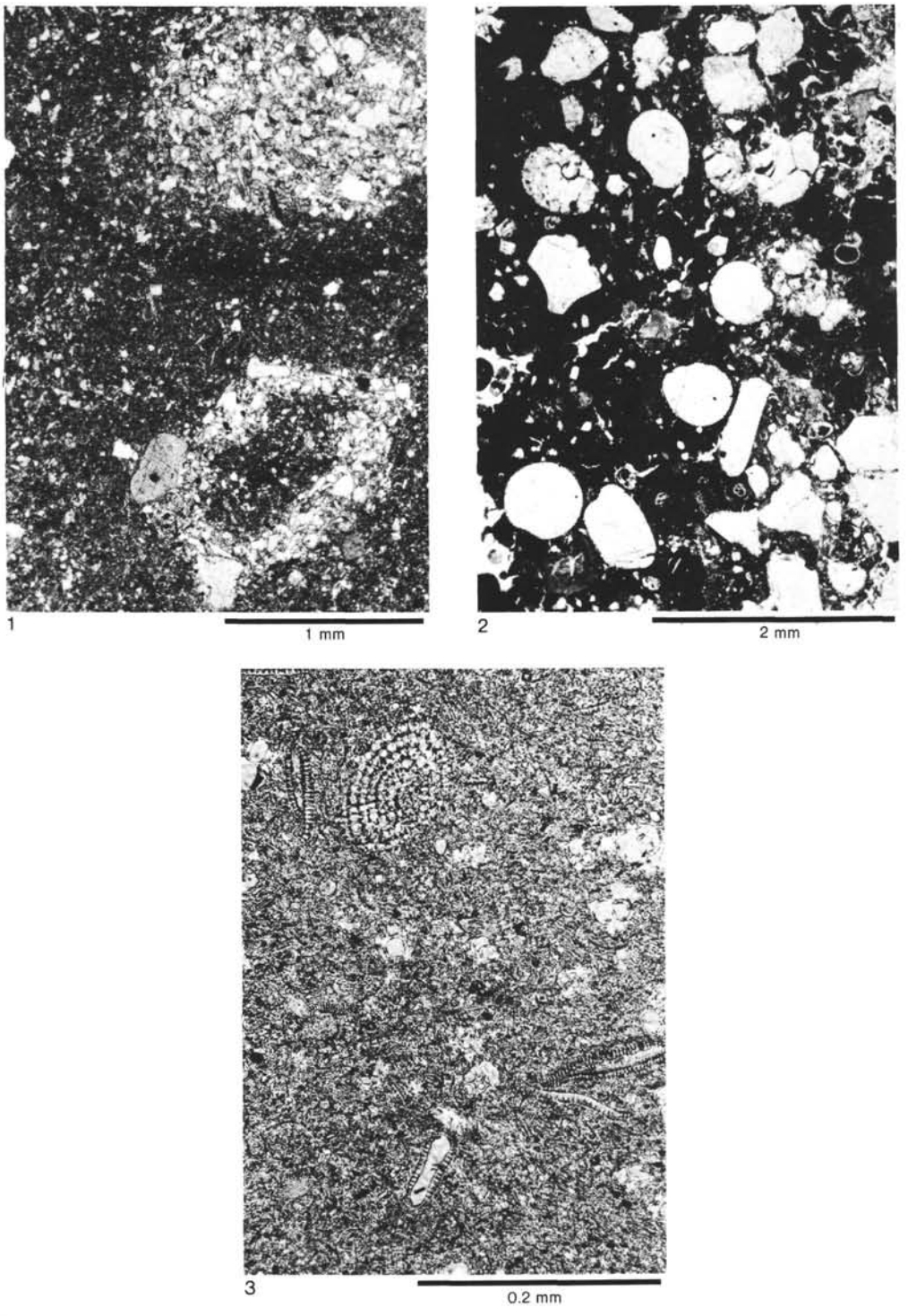

Plate 1. **1.** Silt and sand-mottled micaceous mud, Unit I (Sample 612-3-2, 10–14 cm). Angular to subangular quartz and feldspar grains fill small burrows or coat the walls of agglutinating foraminifers. Sulfide micronodules and crystals are authigenic. Sulfidic halo around upper sand mottle is due to local anaerobic conditions. Partially crossed nicols. **2.** Layer of microtektites in siliceous nannofossil ooze at the middle/upper Eocene contact, Unit II (Sample 612-21-5, 111–114 cm). The tektites consist of clear silica glass (they are rarely vesicular) and are spherical, tear shaped, or dumbbell shaped in form. Large irregular fragments are broken tektites or impact glass. **3.** Siliceous nannofossil chalk showing little to no diagenetic alteration, Unit II (Sample 612-35-5, 10–14 cm). Opaline radiolarian tests, diatom frustules, and delicate planktonic foraminifers are preserved, and the pore spaces are open.

SITE 612 HOLE CORE 1H CORED INTERVAL 0.0–4.8 m

TIME–ROCK UNIT	BIOSTRATIGRAPHIC ZONE	FOSSIL CHARACTER: FORAMINIFERS	NANNOFOSSILS	RADIOLARIANS	DIATOMS	SECTION	METERS	GRAPHIC LITHOLOGY	DRILLING DISTURBANCE	SEDIMENTARY STRUCTURES	SAMPLES	LITHOLOGIC DESCRIPTION
Pleistocene	N22/N23 *Emiliania huxleyi* Zone (CN15) Indeterminate Pliocene–Pleistocene	CG	CG	RM		1, 2, 3, 4, CC	0.5, 1.0	Void			*	Unbedded homogeneous dark gray MUD. Numerous pyritic black mottles (bioturbation). Homogeneous dark gray color.

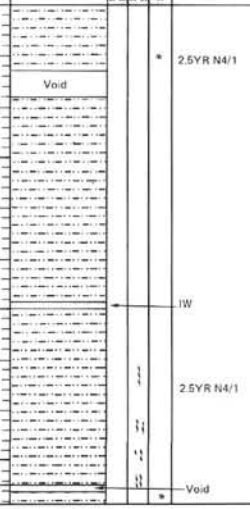

2.5YR N4/1

IW

2.5YR N4/1

Void

SMEAR SLIDE SUMMARY (%):

	1, 50 D	CC, 15 D
Sand	5	25
Silt	20	35
Clay	75	40
Composition:		
Quartz	30	58
Feldspar	TR	2
Mica	2	TR
Heavy minerals	TR	5
Clay	64	30
Volcanic glass	TR	TR
Glauconite	TR	2
Pyrite	2	–
Micronodules	–	1
Carbonate unspec.	2	2
Foraminifers	TR	TR
Diatoms	–	TR

Information on core description sheets, for ALL sites, represents field notes taken aboard ship under time pressure. Some of this information has been refined in accord with post-cruise findings, but production schedules prohibit definitive correlation of these sheets with subsequent findings. Thus the reader should be alerted to the occasional ambiguity or discrepancy.

SITE 612 HOLE CORE 2H CORED INTERVAL 4.8–14.4 m

TIME–ROCK UNIT	BIOSTRATIGRAPHIC ZONE	FOSSIL CHARACTER: FORAMINIFERS	NANNOFOSSILS	RADIOLARIANS	DIATOMS	SECTION	METERS	GRAPHIC LITHOLOGY	DRILLING DISTURBANCE	SEDIMENTARY STRUCTURES	SAMPLES	LITHOLOGIC DESCRIPTION
Pleistocene	N22/N23 *Emiliania huxleyi* Zone (CN15) Indeterminate Pliocene–Pleistocene	CG	CG	RM		1, 2, 3, 4, 5, 6, CC	0.5, 1.0					Unbedded (Section 1, 2) to irregularly thin to medium bedding (Section 3–6). Homogeneous dark gray MUD (exceptionally sand mud in Core Catcher). Numerous pyritic black burrow-mottles filled by medium to coarse quartz sand well rounded with graded bedding and containing large quantity of disseminated organic matter. Numerous minor erosion? surfaces (Section 3–6) → irregularly thin to medium bedded.

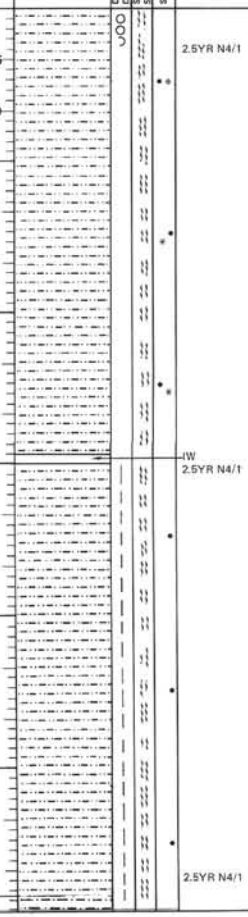

2.5YR N4/1

IW

2.5YR N4/1

2.5YR N4/1

SMEAR SLIDE SUMMARY (%):

	2, 83 M	3, 80 D
Texture:		
Sand	100	100
Composition:		
Quartz	60	80
Feldspar	20	2
Heavy minerals	14	12
Glauconite	2	5
Pyrite	2	1
Foraminifers	2	–

ORGANIC CARBON AND CARBONATE (%):

	1, 76	2, 76	3, 76	4, 76
Organic carbon	–	–	–	0.47
Carbonate	3	3	3	2

	5, 76	6, 76
Organic carbon	–	–
Carbonate	2	1

SITE 612 HOLE CORE 3H CORED INTERVAL 14.4–24.0 m

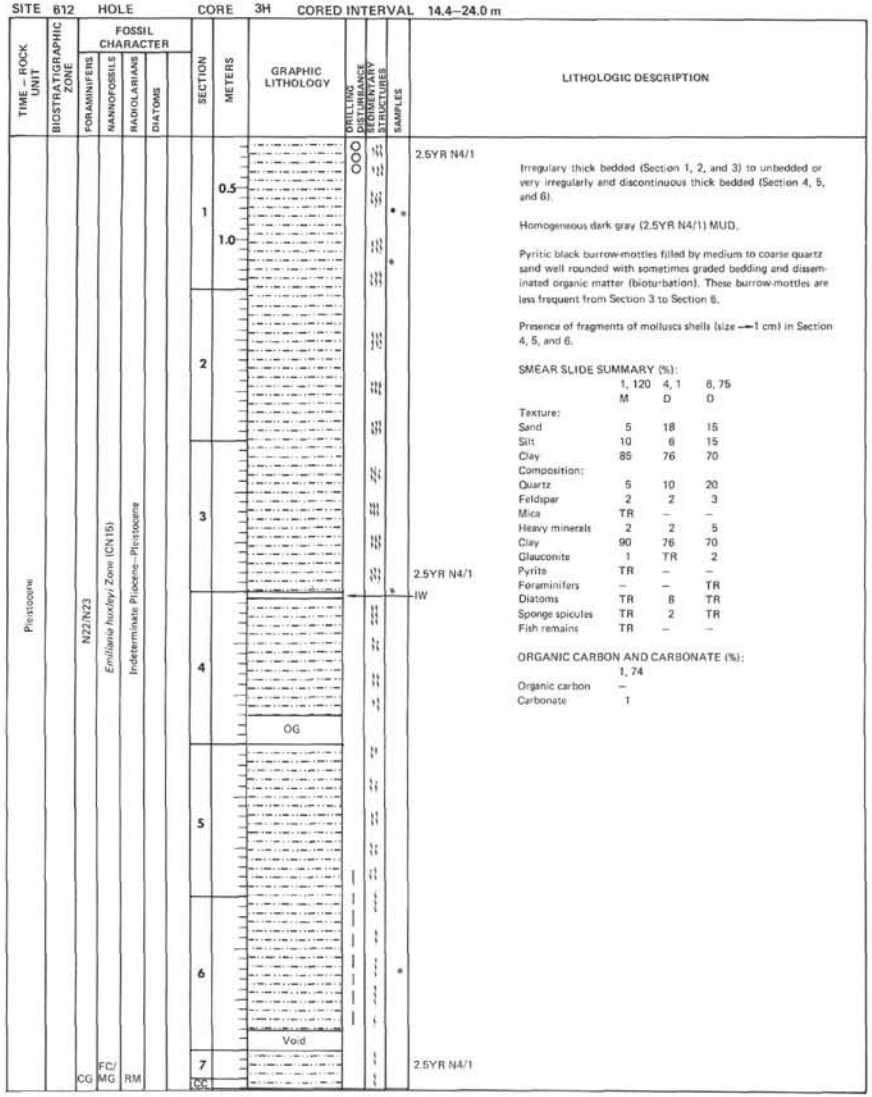

LITHOLOGIC DESCRIPTION

Irregulary thick bedded (Section 1, 2, and 3) to unbedded or very irregularly and discontinuous thick bedded (Section 4, 5, and 6).

Homogeneous dark gray (2.5YR N4/1) MUD.

Pyritic black burrow-mottles filled by medium to coarse quartz sand well rounded with sometimes graded bedding and disseminated organic matter (bioturbation). These burrow-mottles are less frequent from Section 3 to Section 6.

Presence of fragments of molluscs shells (size —1 cm) in Section 4, 5, and 6.

SMEAR SLIDE SUMMARY (%):

	1, 120 M	4, 1 D	6, 75 D
Texture:			
Sand	5	18	15
Silt	10	6	15
Clay	85	76	70
Composition:			
Quartz	5	10	20
Feldspar	2	2	3
Mica	TR	–	–
Heavy minerals	2	2	5
Clay	90	76	70
Glauconite	1	TR	2
Pyrite	TR	–	–
Foraminifers	–	–	TR
Diatoms	TR	8	TR
Sponge spicules	TR	2	TR
Fish remains	TR	–	–

ORGANIC CARBON AND CARBONATE (%):

	1, 74
Organic carbon	–
Carbonate	1

SITE 612 HOLE CORE 4H CORED INTERVAL 24.0–33.6 m

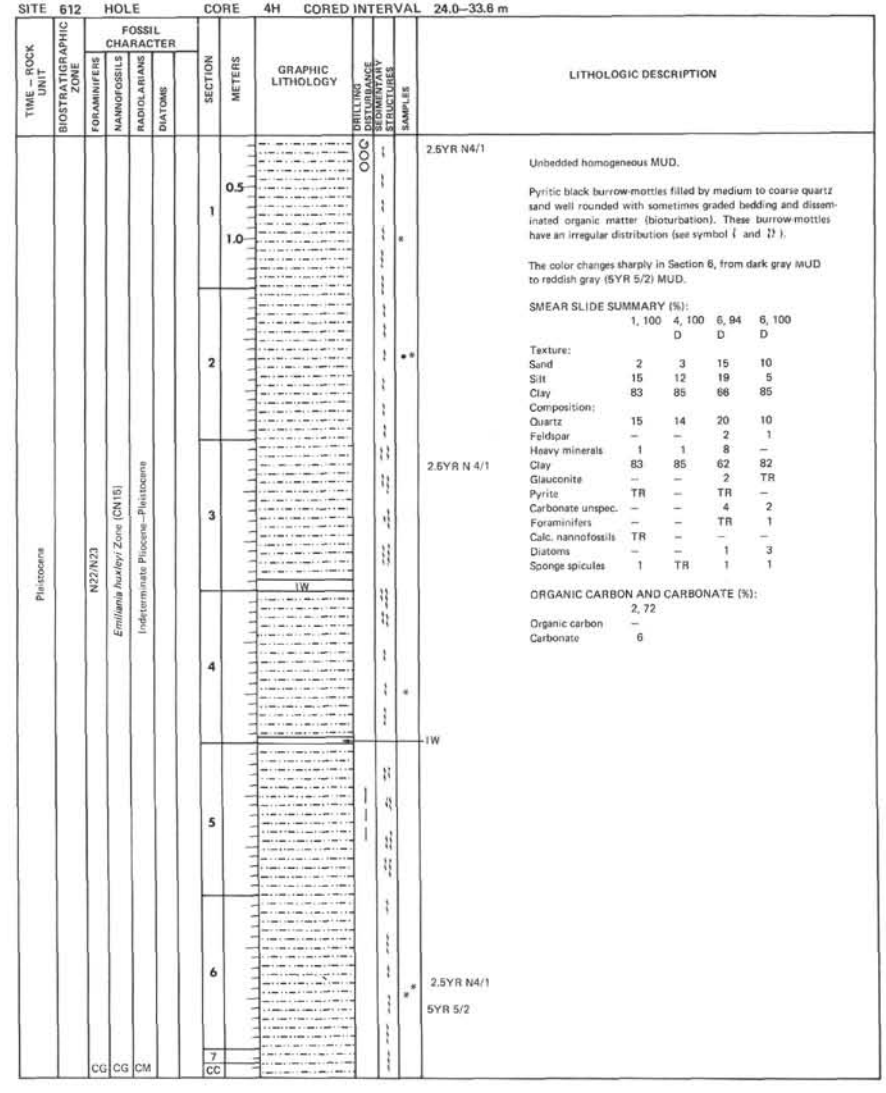

LITHOLOGIC DESCRIPTION

Unbedded homogeneous MUD.

Pyritic black burrow-mottles filled by medium to coarse quartz sand well rounded with sometimes graded bedding and disseminated organic matter (bioturbation). These burrow-mottles have an irregular distribution (see symbol (and ⇶).

The color changes sharply in Section 6, from dark gray MUD to reddish gray (5YR 5/2) MUD.

SMEAR SLIDE SUMMARY (%):

	1, 100	4, 100 D	6, 94 D	6, 100 D
Texture:				
Sand	2	3	15	10
Silt	15	12	19	5
Clay	83	85	66	85
Composition:				
Quartz	15	14	20	10
Feldspar	–	–	2	1
Heavy minerals	1	1	8	–
Clay	83	85	62	82
Glauconite	–	–	2	TR
Pyrite	TR	–	TR	–
Carbonate unspec.	–	–	4	2
Foraminifers	–	–	TR	1
Calc. nannofossils	TR	–	–	–
Diatoms	–	–	1	3
Sponge spicules	1	TR	1	1

ORGANIC CARBON AND CARBONATE (%):

	2, 72
Organic carbon	–
Carbonate	6

SITE 612 HOLE CORE 5H CORED INTERVAL 33.6–40.6 m

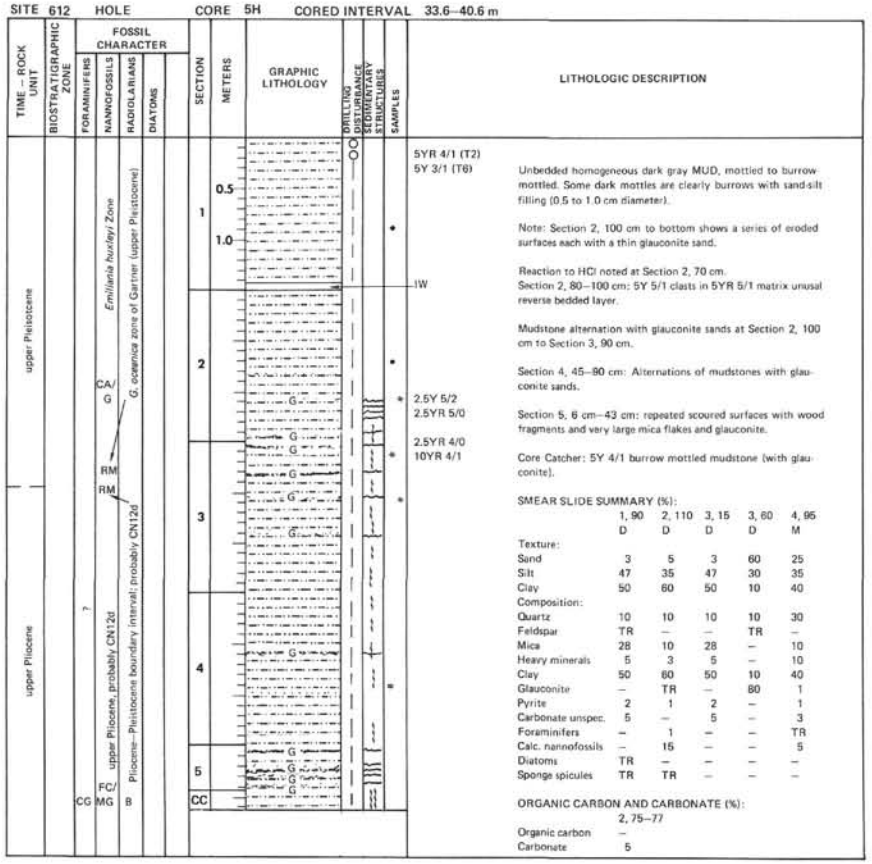

Unbedded homogeneous dark gray MUD, mottled to burrow-mottled. Some dark mottles are clearly burrows with sand-silt filling (0.5 to 1.0 cm diameter).

Note: Section 2, 100 cm to bottom shows a series of eroded surfaces each with a thin glauconite sand.

Reaction to HCl noted at Section 2, 70 cm.
Section 2, 80–100 cm: 5Y 5/1 clasts in 5YR 5/1 matrix unusal reverse bedded layer.

Mudstone alternation with glauconite sands at Section 2, 100 cm to Section 3, 90 cm.

Section 4, 45–80 cm: Alternations of mudstones with glauconite sands.

Section 5, 6 cm–43 cm: repeated scoured surfaces with wood fragments and very large mica flakes and glauconite.

Core Catcher: 5Y 4/1 burrow mottled mudstone (with glauconite).

SMEAR SLIDE SUMMARY (%):

	1, 90	2, 110	3, 15	3, 60	4, 95
	D	D	D	D	M
Texture:					
Sand	3	5	3	60	25
Silt	47	35	47	30	35
Clay	50	60	50	10	40
Composition:					
Quartz	10	10	10	10	30
Feldspar	TR	–	–	TR	–
Mica	28	10	28	–	10
Heavy minerals	5	3	5	–	10
Clay	50	60	50	10	40
Glauconite	–	TR	–	80	1
Pyrite	2	1	2	–	1
Carbonate unspec.	5	–	5	–	3
Foraminifers	–	1	–	–	TR
Calc. nannofossils	–	15	–	–	5
Diatoms	TR	–	–	–	–
Sponge spicules	TR	TR	–	–	–

ORGANIC CARBON AND CARBONATE (%):

	2, 75–77
Organic carbon	–
Carbonate	5

SITE 612 HOLE CORE 6H CORED INTERVAL 40.6–44.6 m

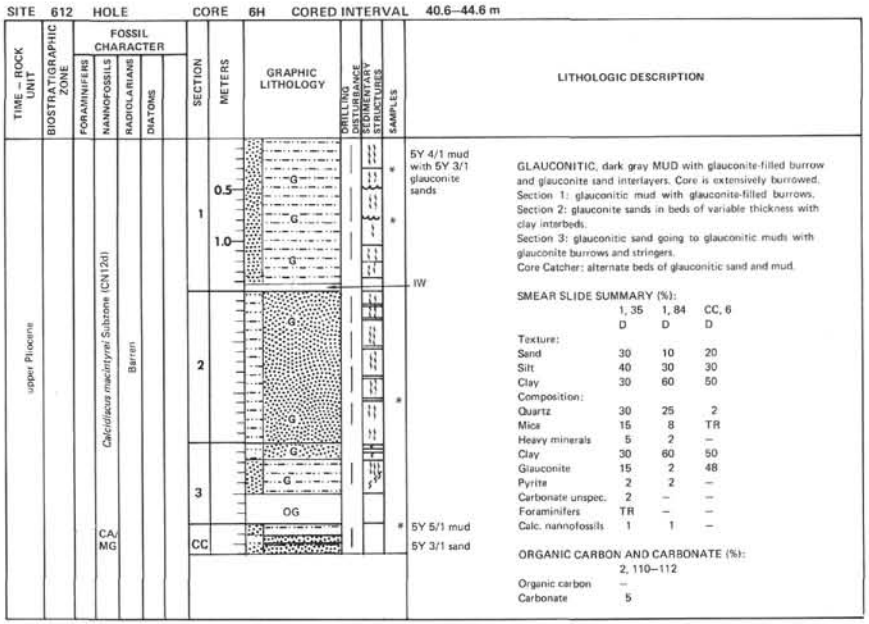

GLAUCONITIC, dark gray MUD with glauconite-filled burrow and glauconite sand interlayers. Core is extensively burrowed.
Section 1: glauconitic mud with glauconite-filled burrows.
Section 2: glauconite sands in beds of variable thickness with clay interbeds.
Section 3: glauconitic sand going to glauconitic muds with glauconite burrows and stringers.
Core Catcher: alternate beds of glauconitic sand and mud.

SMEAR SLIDE SUMMARY (%):

	1, 35	1, 84	CC, 6
	D	D	D
Texture:			
Sand	30	10	20
Silt	40	30	30
Clay	30	60	50
Composition:			
Quartz	30	25	2
Mica	15	8	TR
Heavy minerals	5	2	–
Clay	30	60	50
Glauconite	15	2	48
Pyrite	2	2	–
Carbonate unspec.	2	–	–
Foraminifers	TR	–	–
Calc. nannofossils	1	1	–

ORGANIC CARBON AND CARBONATE (%):

	2, 110–112
Organic carbon	–
Carbonate	5

SITE 612 HOLE CORE 7H CORED INTERVAL 44.6–52.1 m

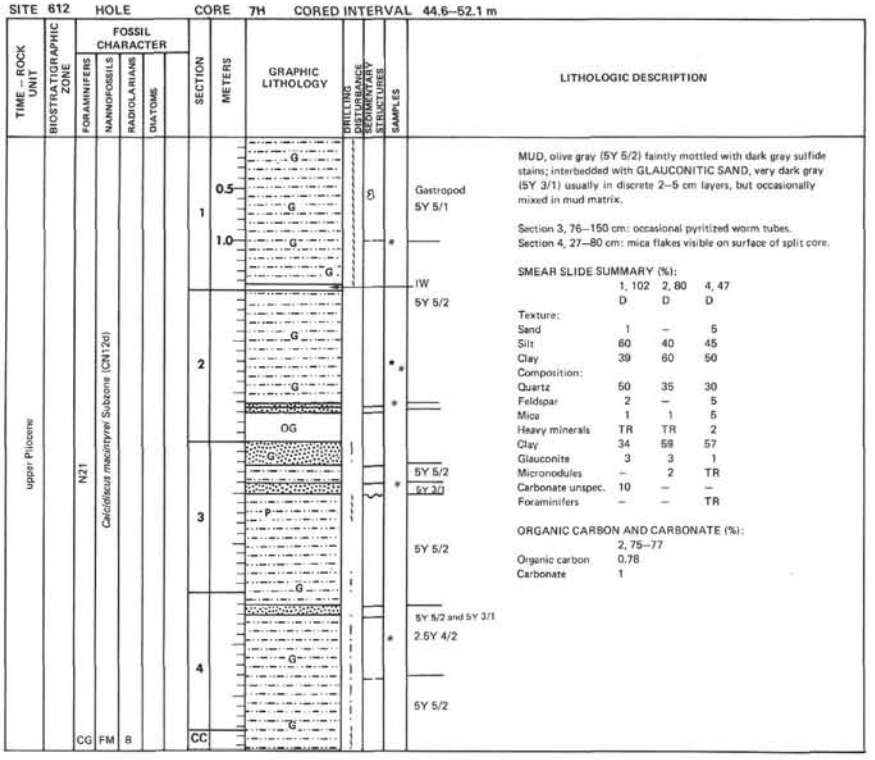

MUD, olive gray (5Y 5/2) faintly mottled with dark gray sulfide stains; interbedded with GLAUCONITIC SAND, very dark gray (5Y 3/1) usually in discrete 2–5 cm layers, but occasionally mixed in mud matrix.

Section 3, 76–150 cm: occasional pyritized worm tubes.
Section 4, 27–80 cm: mica flakes visible on surface of split core.

SMEAR SLIDE SUMMARY (%):

	1, 102	2, 80	4, 47
	D	D	D
Texture:			
Sand	1	–	5
Silt	60	40	45
Clay	39	60	50
Composition:			
Quartz	50	35	30
Feldspar	2	–	5
Mica	1	1	5
Heavy minerals	TR	TR	2
Clay	34	59	57
Glauconite	3	3	1
Micronodules	–	2	TR
Carbonate unspec.	10	–	–
Foraminifers	–	–	TR

ORGANIC CARBON AND CARBONATE (%):

	2, 75–77
Organic carbon	0.78
Carbonate	1

SITE 612 HOLE CORE 8X CORED INTERVAL 52.1–59.0 m

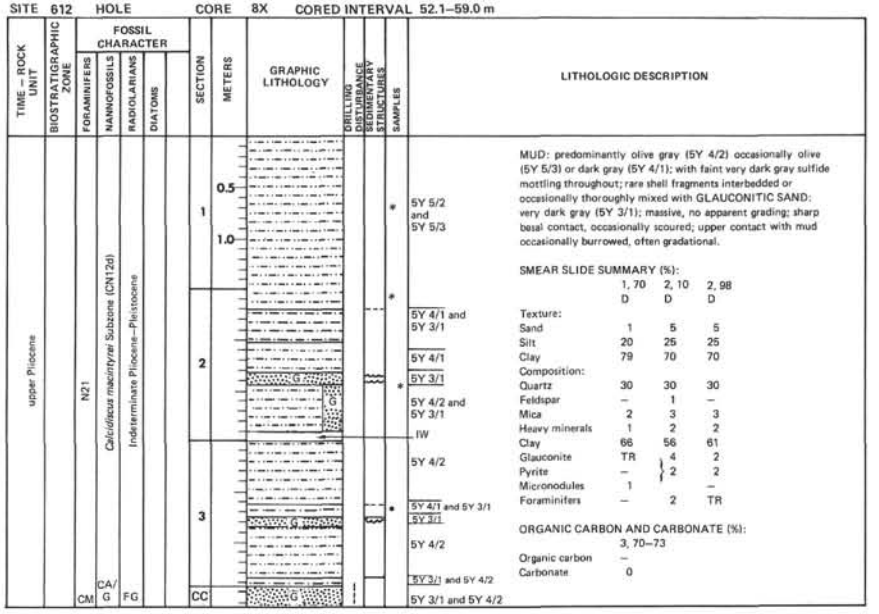

MUD: predominantly olive gray (5Y 4/2) occasionally olive (5Y 5/3) or dark gray (5Y 4/1); with faint very dark gray sulfide mottling throughout; rare shell fragments interbedded or occasionally thoroughly mixed with GLAUCONITIC SAND: very dark gray (5Y 3/1); massive, no apparent grading; sharp basal contact, occasionally scoured; upper contact with mud occasionally burrowed, often gradational.

SMEAR SLIDE SUMMARY (%):

	1, 70	2, 10	2, 98
	D	D	D
Texture:			
Sand	1	5	5
Silt	20	25	25
Clay	79	70	70
Composition:			
Quartz	30	30	30
Feldspar	–	1	–
Mica	2	3	3
Heavy minerals	1	2	2
Clay	66	56	61
Glauconite	TR	4	2
Pyrite	–	2	2
Micronodules	1		–
Foraminifers	–	2	TR

ORGANIC CARBON AND CARBONATE (%):

	3, 70–73
Organic carbon	–
Carbonate	0

SITE 612 HOLE CORE 9X CORED INTERVAL 59.0–68.7 m

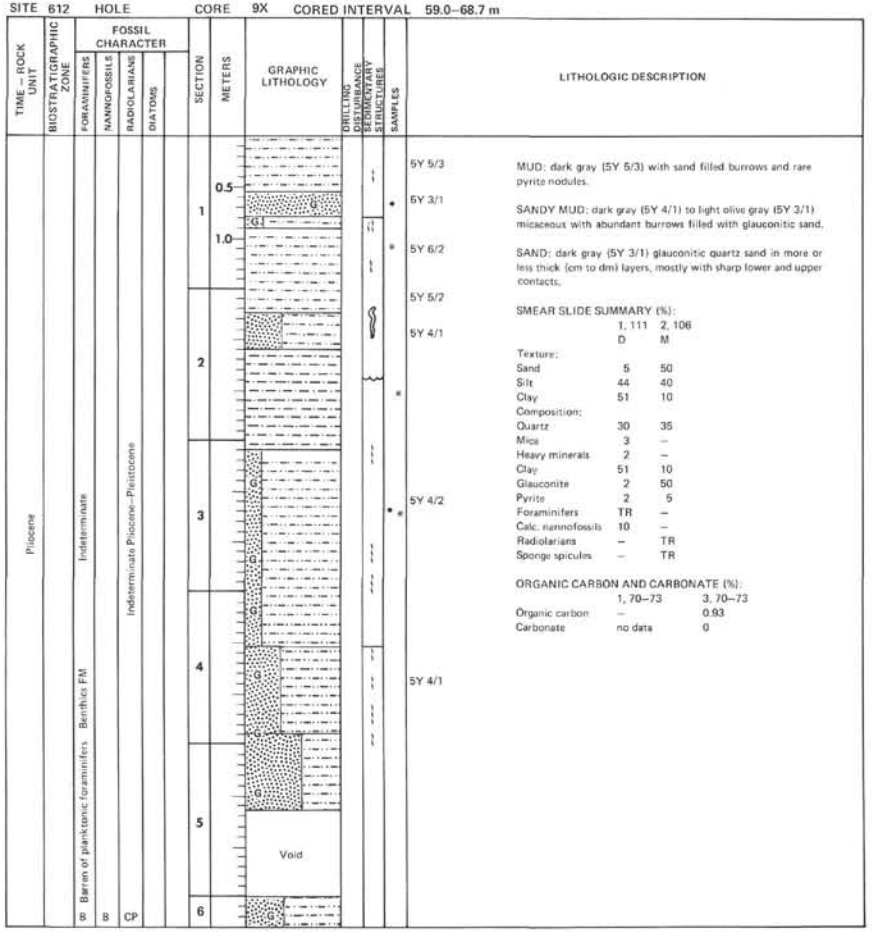

SITE 612 HOLE CORE 10X CORED INTERVAL 68.7–78.4 m

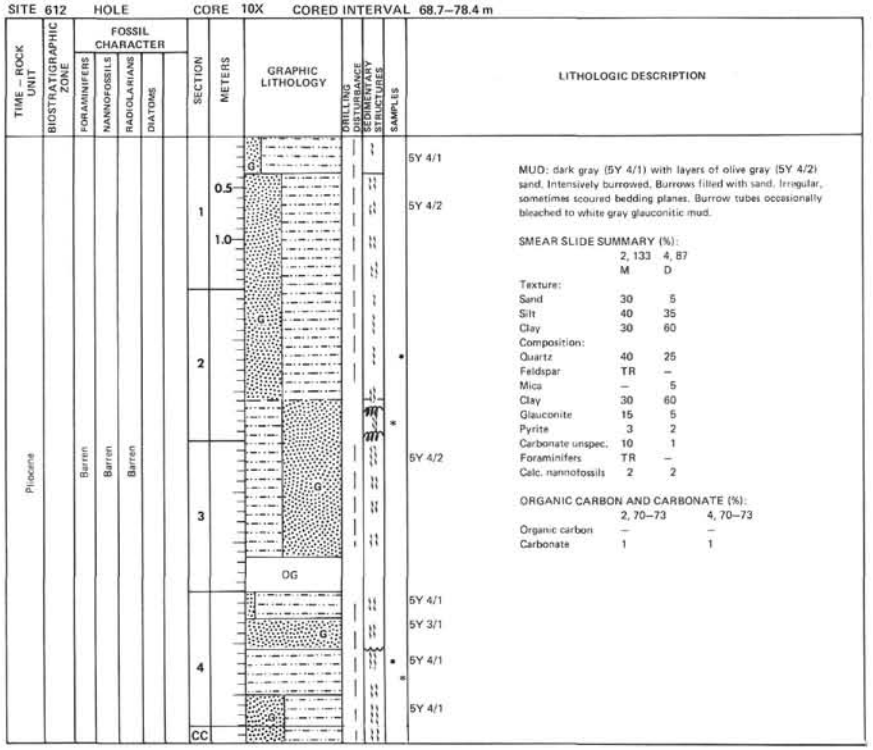

SITE 612 HOLE CORE 11X CORED INTERVAL 78.4–88.1 m

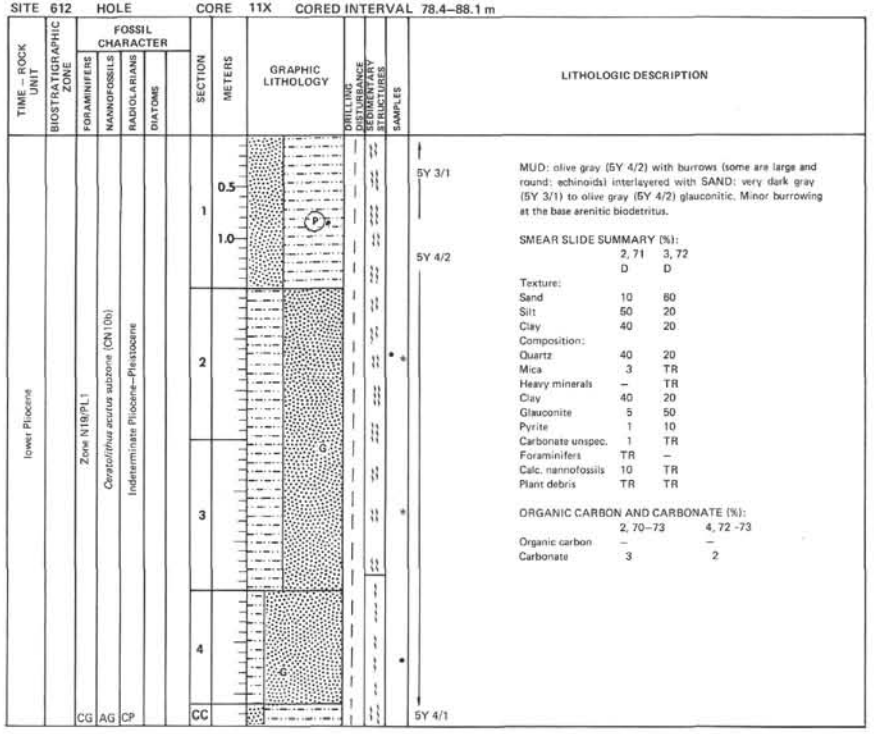

MUD: olive gray (5Y 4/2) with burrows (some are large and round: echinoids) interlayered with SAND: very dark gray (5Y 3/1) to olive gray (5Y 4/2) glauconitic. Minor burrowing at the base arenitic biodetritus.

SMEAR SLIDE SUMMARY (%):

	2, 71	3, 72
	D	D
Texture:		
Sand	10	60
Silt	50	20
Clay	40	20
Composition:		
Quartz	40	20
Mica	3	TR
Heavy minerals	–	TR
Clay	40	20
Glauconite	5	50
Pyrite	1	10
Carbonate unspec.	1	TR
Foraminifers	TR	–
Calc. nannofossils	10	TR
Plant debris	TR	TR

ORGANIC CARBON AND CARBONATE (%):

	2, 70–73	4, 72 -73
Organic carbon	–	–
Carbonate	3	2

SITE 612 HOLE CORE 12X CORED INTERVAL 88.1–97.8 m

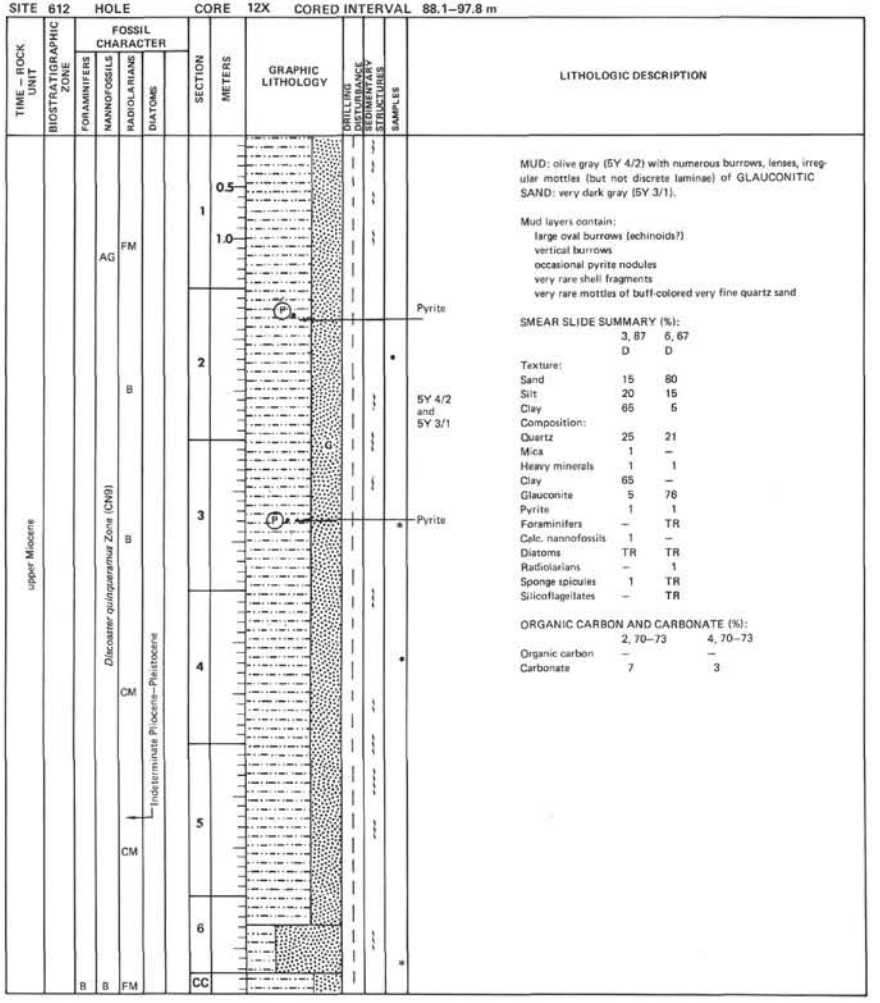

MUD: olive gray (5Y 4/2) with numerous burrows, lenses, irregular mottles (but not discrete laminae) of GLAUCONITIC SAND: very dark gray (5Y 3/1).

Mud layers contain:
- large oval burrows (echinoids?)
- vertical burrows
- occasional pyrite nodules
- very rare shell fragments
- very rare mottles of buff-colored very fine quartz sand

SMEAR SLIDE SUMMARY (%):

	3, 87	6, 67
	D	D
Texture:		
Sand	15	80
Silt	20	15
Clay	65	5
Composition:		
Quartz	25	21
Mica	1	–
Heavy minerals	1	1
Clay	65	–
Glauconite	5	76
Pyrite	1	1
Foraminifers	–	TR
Calc. nannofossils	1	–
Diatoms	TR	TR
Radiolarians	–	1
Sponge spicules	1	TR
Silicoflagellates	–	TR

ORGANIC CARBON AND CARBONATE (%):

	2, 70–73	4, 70–73
Organic carbon	–	–
Carbonate	7	3

SITE 612 HOLE CORE 13X CORED INTERVAL 97.8–107.5 m

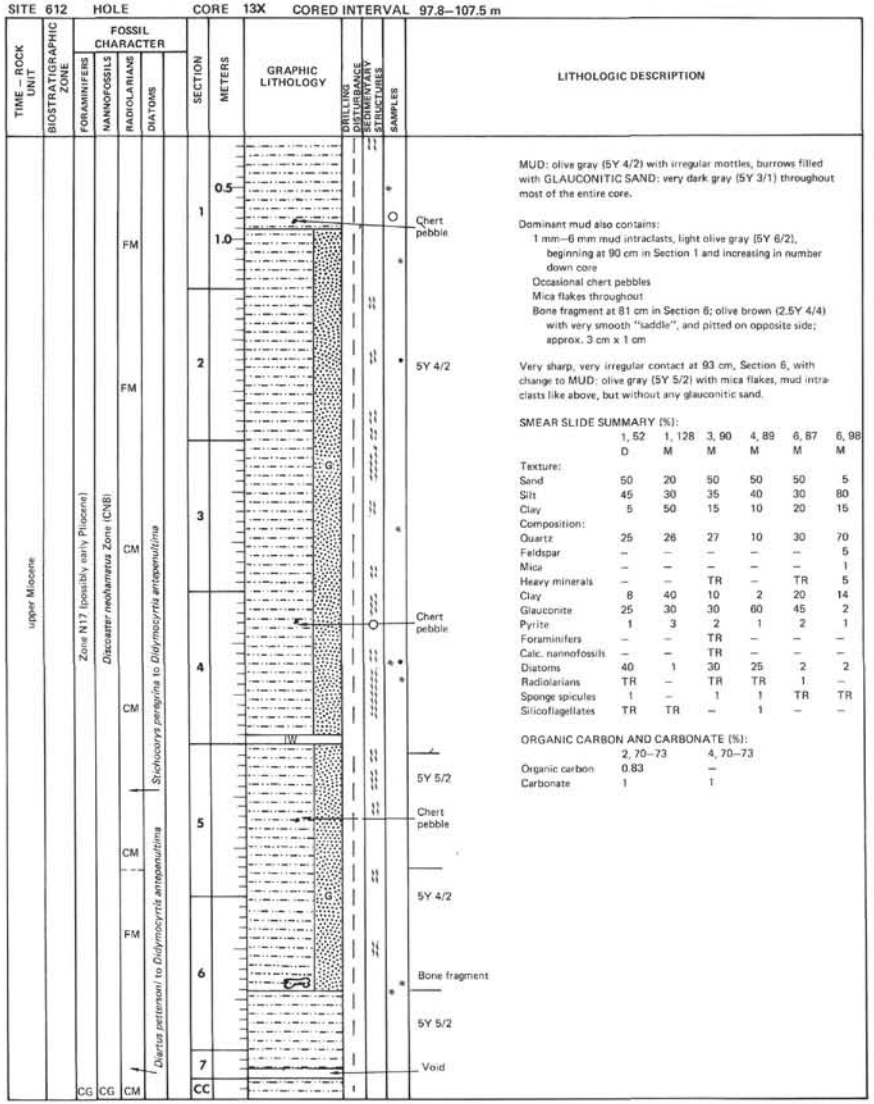

MUD: olive gray (5Y 4/2) with irregular mottles, burrows filled with GLAUCONITIC SAND: very dark gray (5Y 3/1) throughout most of the entire core.

Dominant mud also contains:
- 1 mm–6 mm mud intraclasts, light olive gray (5Y 6/2), beginning at 90 cm in Section 1 and increasing in number down core
- Occasional chert pebbles
- Mica flakes throughout
- Bone fragment at 81 cm in Section 6; olive brown (2.5Y 4/4) with very smooth "saddle", and pitted on opposite side; approx. 3 cm x 1 cm

Very sharp, very irregular contact at 93 cm, Section 6, with change to MUD: olive gray (5Y 5/2) with mica flakes, mud intraclasts like above, but without any glauconitic sand.

SMEAR SLIDE SUMMARY (%):

	1, 52 D	1, 128 M	3, 90 M	4, 89 M	6, 87 M	6, 98 M
Texture:						
Sand	50	20	50	50	50	5
Silt	45	30	35	40	30	80
Clay	5	50	15	10	20	15
Composition:						
Quartz	25	26	27	10	30	70
Feldspar	–	–	–	–	–	5
Mica	–	–	–	–	–	1
Heavy minerals	–	–	TR	–	TR	5
Clay	8	40	10	2	20	14
Glauconite	25	30	30	60	45	2
Pyrite	1	3	2	1	2	1
Foraminifers	–	–	TR	–	–	–
Calc. nannofossils	–	–	TR	–	–	–
Diatoms	40	1	30	25	2	2
Radiolarians	TR	–	TR	TR	1	–
Sponge spicules	1	–	1	1	TR	TR
Silicoflagellates	TR	TR	–	1	–	–

ORGANIC CARBON AND CARBONATE (%):

	2, 70–73	4, 70–73
Organic carbon	0.83	–
Carbonate	1	1

SITE 612 HOLE CORE 14X CORED INTERVAL 107.5–117.2 m

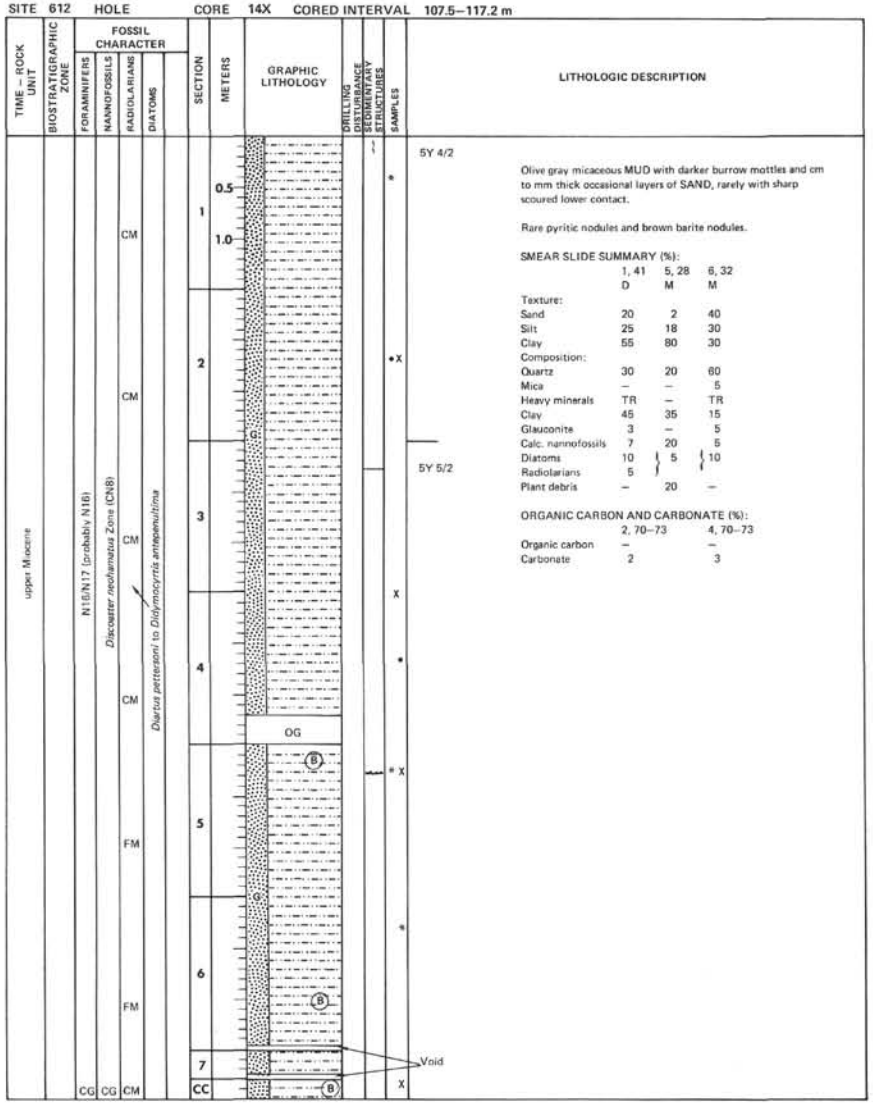

Olive gray micaceous MUD with darker burrow mottles and cm to mm thick occasional layers of SAND, rarely with sharp scoured lower contact.

Rare pyritic nodules and brown barite nodules.

SMEAR SLIDE SUMMARY (%):

	1, 41 D	5, 28 M	6, 32 M
Texture:			
Sand	20	2	40
Silt	25	18	30
Clay	55	80	30
Composition:			
Quartz	30	20	60
Mica	–	–	5
Heavy minerals	TR	–	TR
Clay	45	35	15
Glauconite	3	–	5
Calc. nannofossils	7	20	5
Diatoms	10	5	10
Radiolarians	5		
Plant debris	–	20	–

ORGANIC CARBON AND CARBONATE (%):

	2, 70–73	4, 70–73
Organic carbon	–	–
Carbonate	2	3

SITE 612 HOLE CORE 15X CORED INTERVAL 117.2–126.7 m

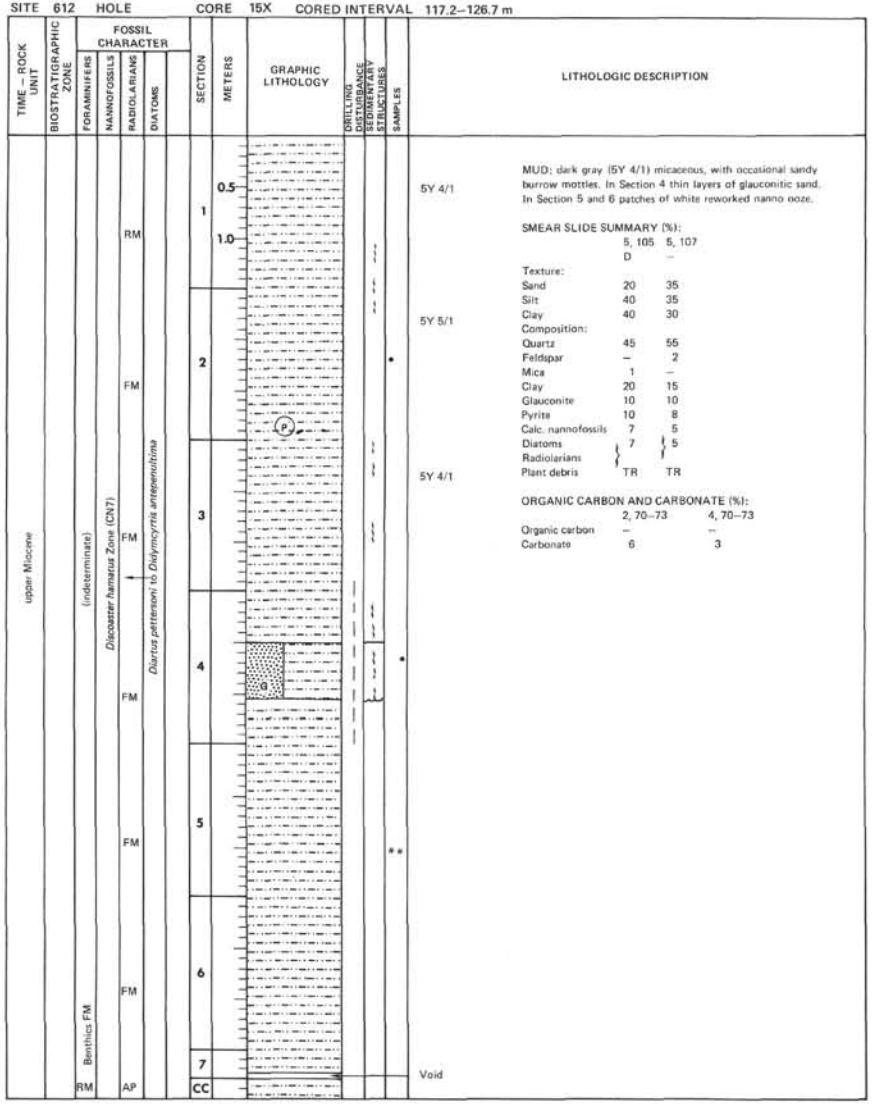

LITHOLOGIC DESCRIPTION

MUD: dark gray (5Y 4/1) micaceous, with occasional sandy burrow mottles. In Section 4 thin layers of glauconitic sand. In Section 5 and 6 patches of white reworked nanno ooze.

SMEAR SLIDE SUMMARY (%):

	5, 105	5, 107
	D	–
Texture:		
Sand	20	35
Silt	40	35
Clay	40	30
Composition:		
Quartz	45	55
Feldspar	–	2
Mica	1	–
Clay	20	15
Glauconite	10	10
Pyrite	10	8
Calc. nannofossils	7	5
Diatoms	7	5
Radiolarians		
Plant debris	TR	TR

ORGANIC CARBON AND CARBONATE (%):

	2, 70–73	4, 70–73
Organic carbon	–	–
Carbonate	6	3

SITE 612 HOLE CORE 16X CORED INTERVAL 126.7–136.2 m

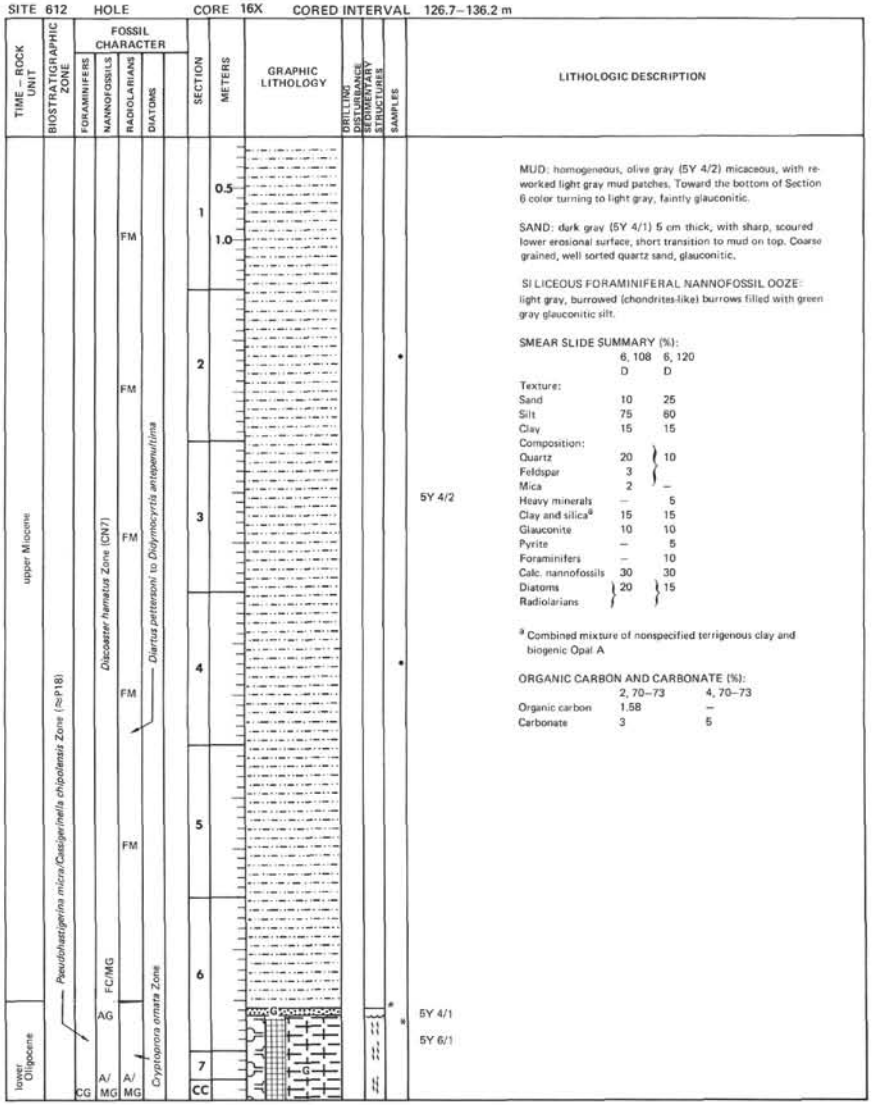

LITHOLOGIC DESCRIPTION

MUD: homogeneous, olive gray (5Y 4/2) micaceous, with reworked light gray mud patches. Toward the bottom of Section 6 color turning to light gray, faintly glauconitic.

SAND: dark gray (5Y 4/1) 5 cm thick, with sharp, scoured lower erosional surface, short transition to mud on top. Coarse grained, well sorted quartz sand, glauconitic.

SILICEOUS FORAMINIFERAL NANNOFOSSIL OOZE: light gray, burrowed (chondrites-like) burrows filled with green gray glauconitic silt.

SMEAR SLIDE SUMMARY (%):

	6, 108	6, 120
	D	D
Texture:		
Sand	10	25
Silt	75	60
Clay	15	15
Composition:		
Quartz	20	10
Feldspar	3	
Mica	2	–
Heavy minerals	–	5
Clay and silica[a]	15	15
Glauconite	10	10
Pyrite	–	5
Foraminifers	–	10
Calc. nannofossils	30	30
Diatoms	20	15
Radiolarians		

[a] Combined mixture of nonspecified terrigenous clay and biogenic Opal A

ORGANIC CARBON AND CARBONATE (%):

	2, 70–73	4, 70–73
Organic carbon	1.58	–
Carbonate	3	5

SITE 612 HOLE CORE 17X CORED INTERVAL 136.2–145.7 m

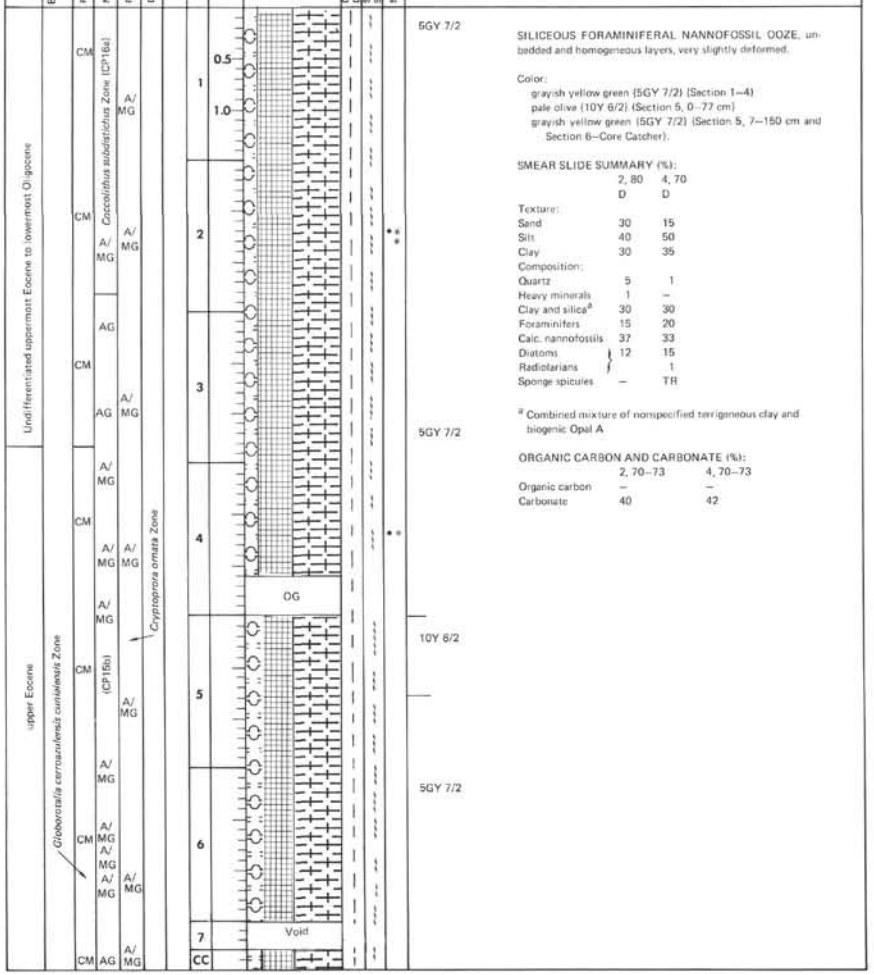

SILICEOUS FORAMINIFERAL NANNOFOSSIL OOZE, unbedded and homogeneous layers, very slightly deformed.

Color:
grayish yellow green (5GY 7/2) (Section 1–4)
pale olive (10Y 6/2) (Section 5, 0–77 cm)
grayish yellow green (5GY 7/2) (Section 5, 7–150 cm and Section 6–Core Catcher).

SMEAR SLIDE SUMMARY (%):

	2, 80	4, 70
	D	D
Texture:		
Sand	30	15
Silt	40	50
Clay	30	35
Composition:		
Quartz	5	1
Heavy minerals	1	–
Clay and silica[a]	30	30
Foraminifers	15	20
Calc. nannofossils	37	33
Diatoms / Radiolarians	12	15 / 1
Sponge spicules	–	TR

[a] Combined mixture of nonspecified terrigeneous clay and biogenic Opal A

ORGANIC CARBON AND CARBONATE (%):

	2, 70–73	4, 70–73
Organic carbon	–	–
Carbonate	40	42

SITE 612 HOLE CORE 18X CORED INTERVAL 145.7–155.2 m

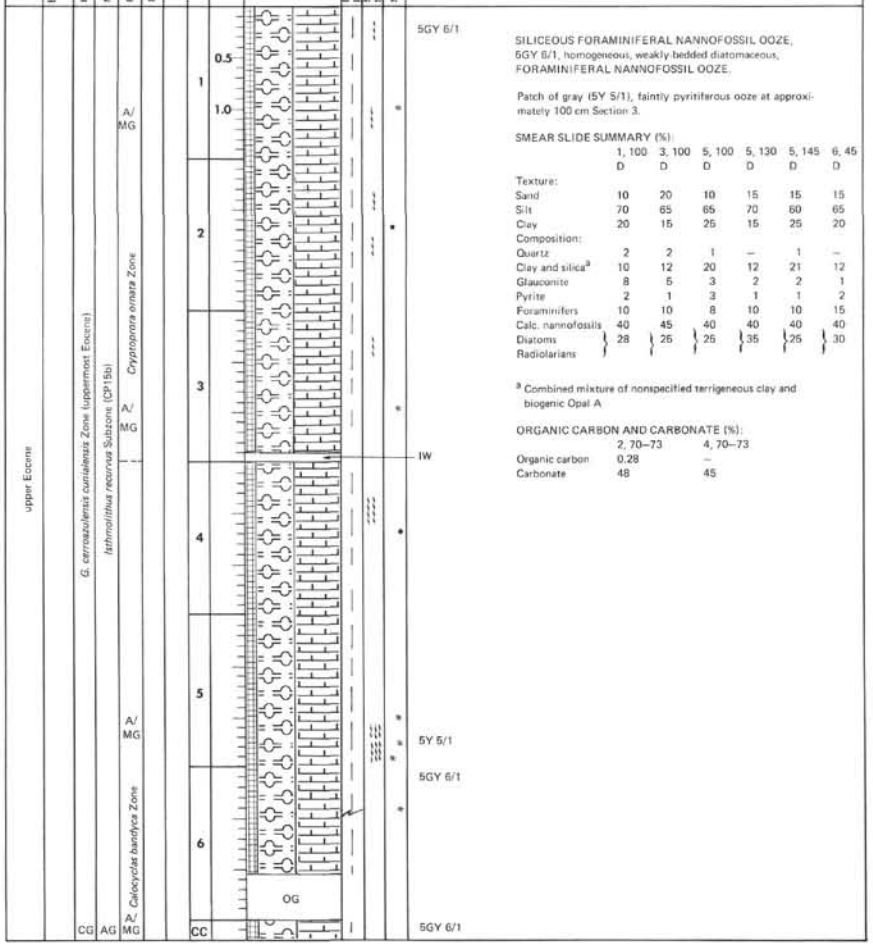

SILICEOUS FORAMINIFERAL NANNOFOSSIL OOZE, 5GY 6/1, homogeneous, weakly bedded diatomaceous, FORAMINIFERAL NANNOFOSSIL OOZE.

Patch of gray (5Y 5/1), faintly pyritiferous ooze at approximately 100 cm Section 3.

SMEAR SLIDE SUMMARY (%):

	1, 100	3, 100	5, 100	5, 130	5, 145	6, 45
	D	D	D	D	D	D
Texture:						
Sand	10	20	10	15	15	15
Silt	70	65	65	70	60	65
Clay	20	15	25	15	25	20
Composition:						
Quartz	2	2	1	–	1	–
Clay and silica[a]	10	12	20	12	21	12
Glauconite	8	5	3	2	2	1
Pyrite	2	1	3	1	1	2
Foraminifers	10	10	8	10	10	15
Calc. nannofossils	40	45	40	40	40	40
Diatoms / Radiolarians	28	25	25	35	25	30

[a] Combined mixture of nonspecified terrigeneous clay and biogenic Opal A

ORGANIC CARBON AND CARBONATE (%):

	2, 70–73	4, 70–73
Organic carbon	0.28	–
Carbonate	48	45

SITE 612 HOLE CORE 19X CORED INTERVAL 155.2–164.7 m

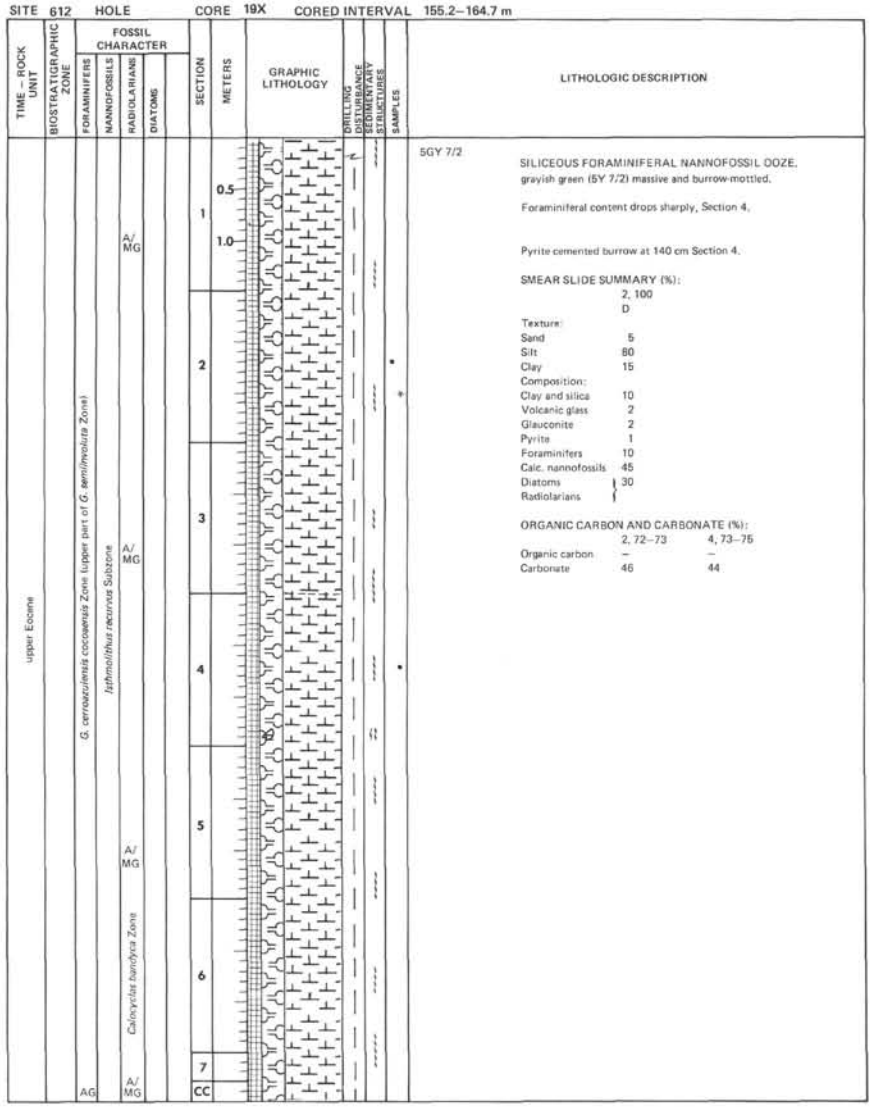

SITE 612 HOLE CORE 20X CORED INTERVAL 164.7–174.2 m

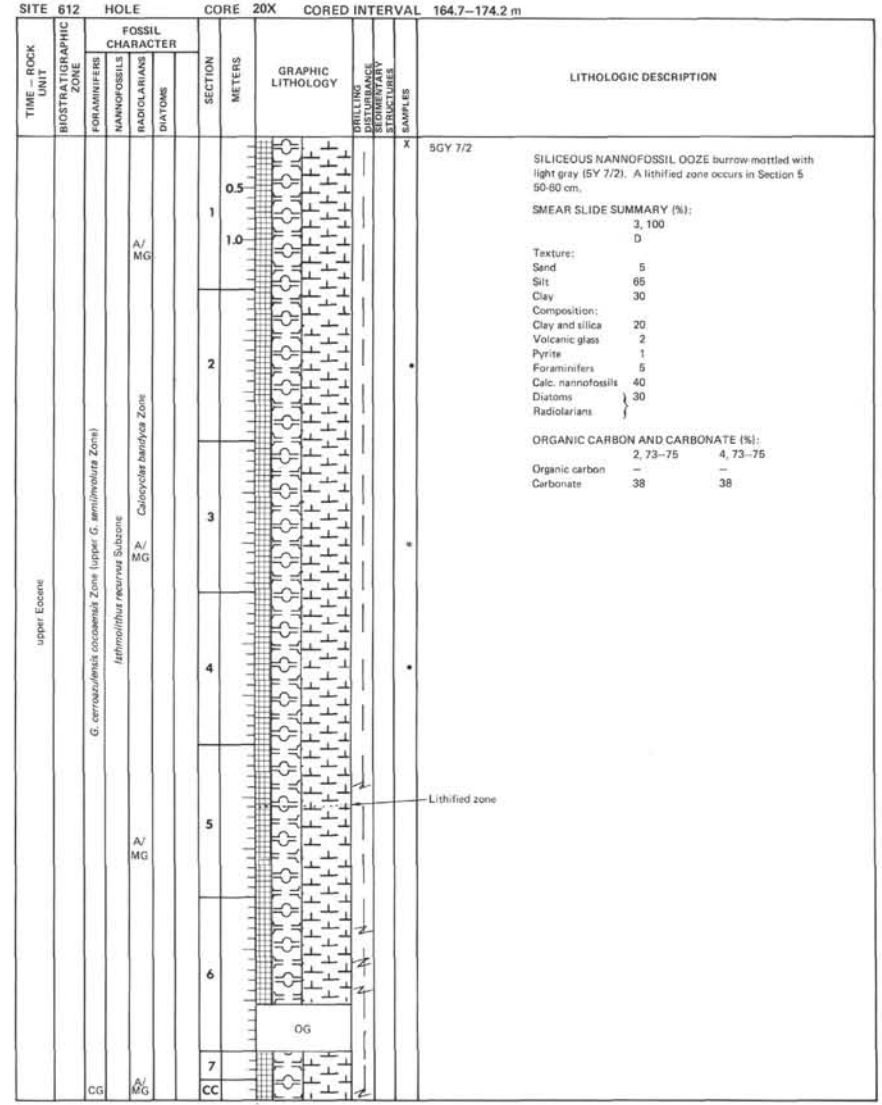

SITE 612 HOLE CORE 21X CORED INTERVAL 174.2–183.8 m

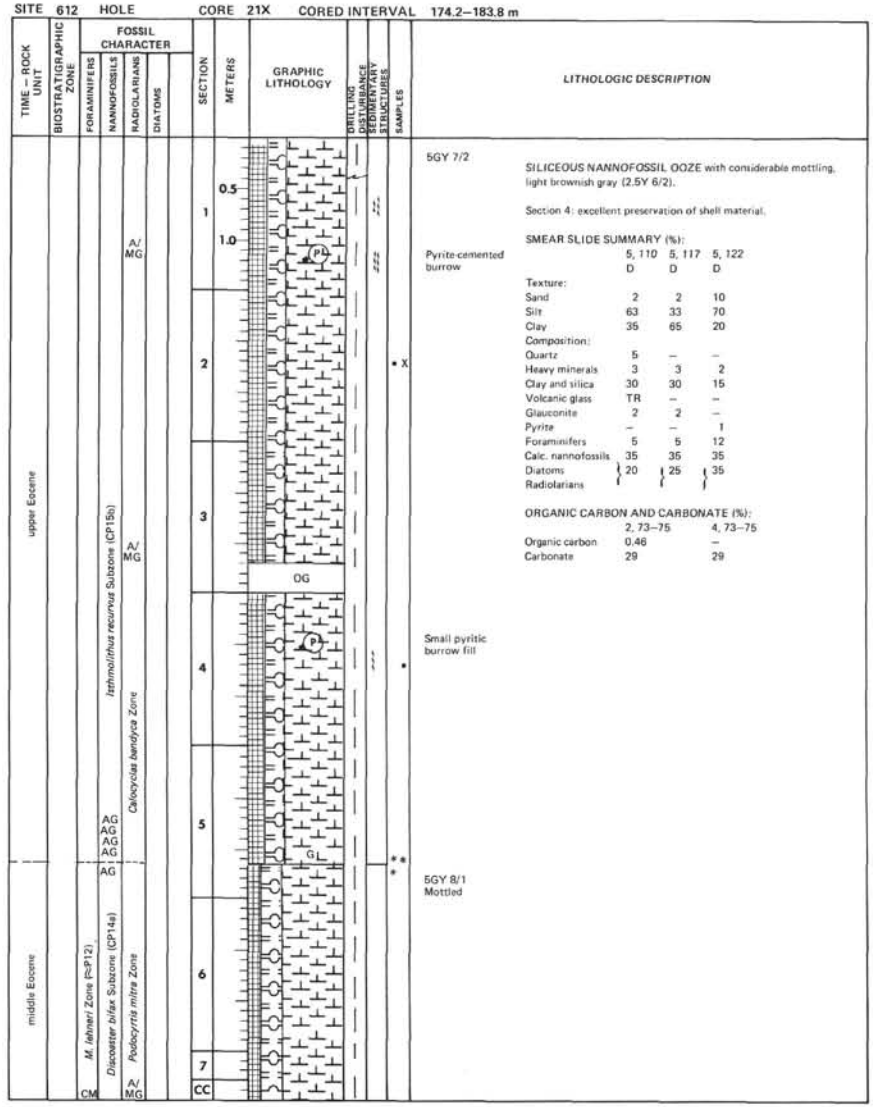

LITHOLOGIC DESCRIPTION

5GY 7/2

SILICEOUS NANNOFOSSIL OOZE with considerable mottling, light brownish gray (2.5Y 6/2).

Section 4: excellent preservation of shell material.

Pyrite-cemented burrow

SMEAR SLIDE SUMMARY (%):

	5, 110 D	5, 117 D	5, 122 D
Texture:			
Sand	2	2	10
Silt	63	33	70
Clay	35	65	20
Composition:			
Quartz	5	–	–
Heavy minerals	3	3	2
Clay and silica	30	30	15
Volcanic glass	TR	–	–
Glauconite	2	2	–
Pyrite	–	–	1
Foraminifers	5	5	12
Calc. nannofossils	35	35	35
Diatoms	20	25	35
Radiolarians			

ORGANIC CARBON AND CARBONATE (%):

	2, 73–75	4, 73–75
Organic carbon	0.46	–
Carbonate	29	29

Small pyritic burrow fill

5GY 8/1 Mottled

SITE 612 HOLE CORE 22X CORED INTERVAL 183.8–193.4 m

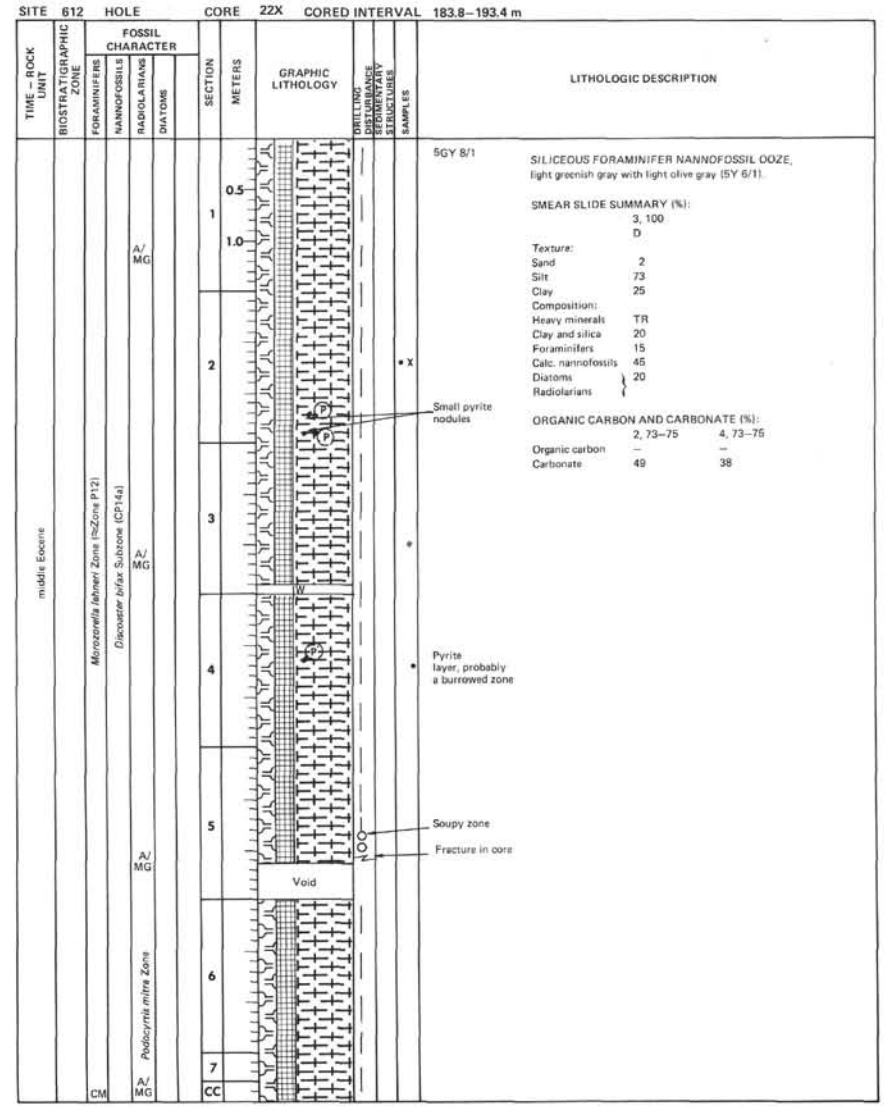

LITHOLOGIC DESCRIPTION

5GY 8/1

SILICEOUS FORAMINIFER NANNOFOSSIL OOZE, light greenish gray with light olive gray (5Y 6/1).

SMEAR SLIDE SUMMARY (%):

	3, 100 D
Texture:	
Sand	2
Silt	73
Clay	25
Composition:	
Heavy minerals	TR
Clay and silica	20
Foraminifers	15
Calc. nannofossils	45
Diatoms	20
Radiolarians	

ORGANIC CARBON AND CARBONATE (%):

	2, 73–75	4, 73–75
Organic carbon	–	–
Carbonate	49	38

Small pyrite nodules

Pyrite layer, probably a burrowed zone

Soupy zone

Fracture in core

SITE 612 HOLE CORE 23X CORED INTERVAL 193.4–203.0 m

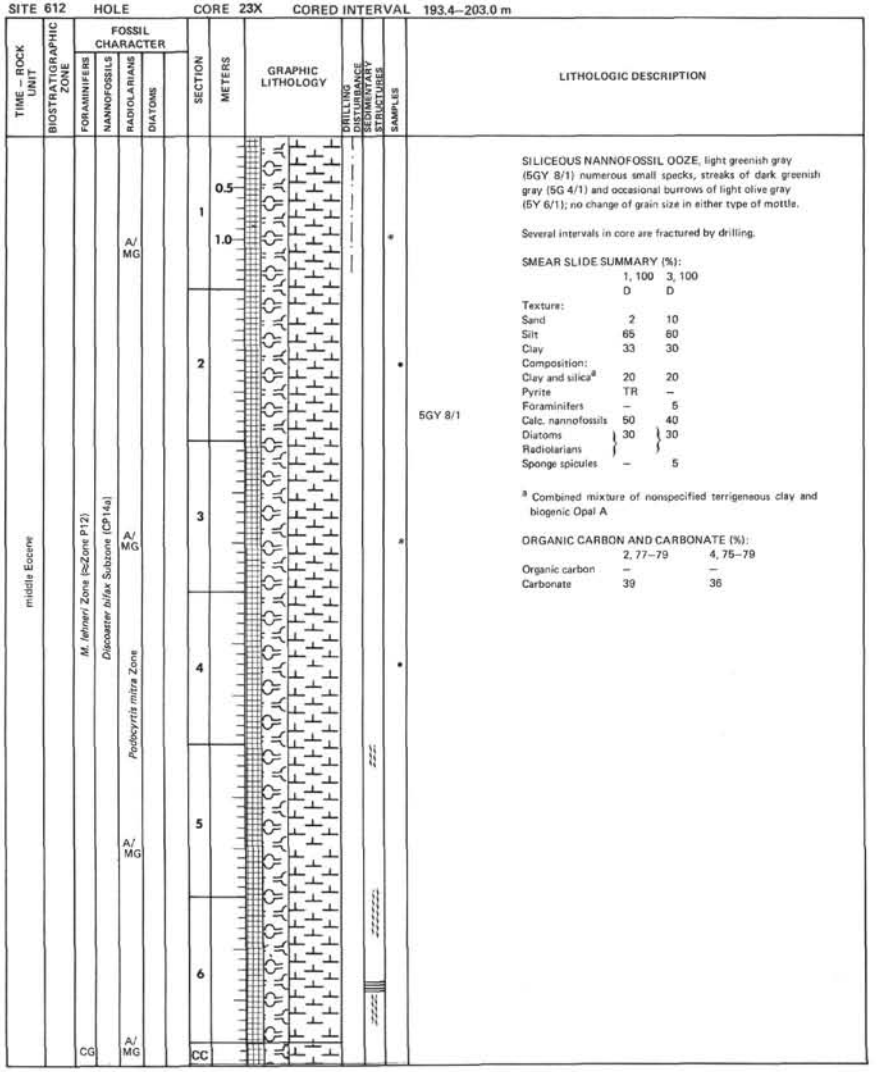

LITHOLOGIC DESCRIPTION

SILICEOUS NANNOFOSSIL OOZE, light greenish gray (5GY 8/1) numerous small specks, streaks of dark greenish gray (5G 4/1) and occasional burrows of light olive gray (5Y 6/1); no change of grain size in either type of mottle.

Several intervals in core are fractured by drilling.

SMEAR SLIDE SUMMARY (%):

	1, 100 D	3, 100 D
Texture:		
Sand	2	10
Silt	65	60
Clay	33	30
Composition:		
Clay and silica[a]	20	20
Pyrite	TR	–
Foraminifers	–	5
Calc. nannofossils	50	40
Diatoms	30	30
Radiolarians		
Sponge spicules	–	5

[a] Combined mixture of nonspecified terrigeneous clay and biogenic Opal A

ORGANIC CARBON AND CARBONATE (%):

	2, 77–79	4, 75–79
Organic carbon	–	–
Carbonate	39	36

SITE 612 HOLE CORE 24X CORED INTERVAL 203.0–212.6 m

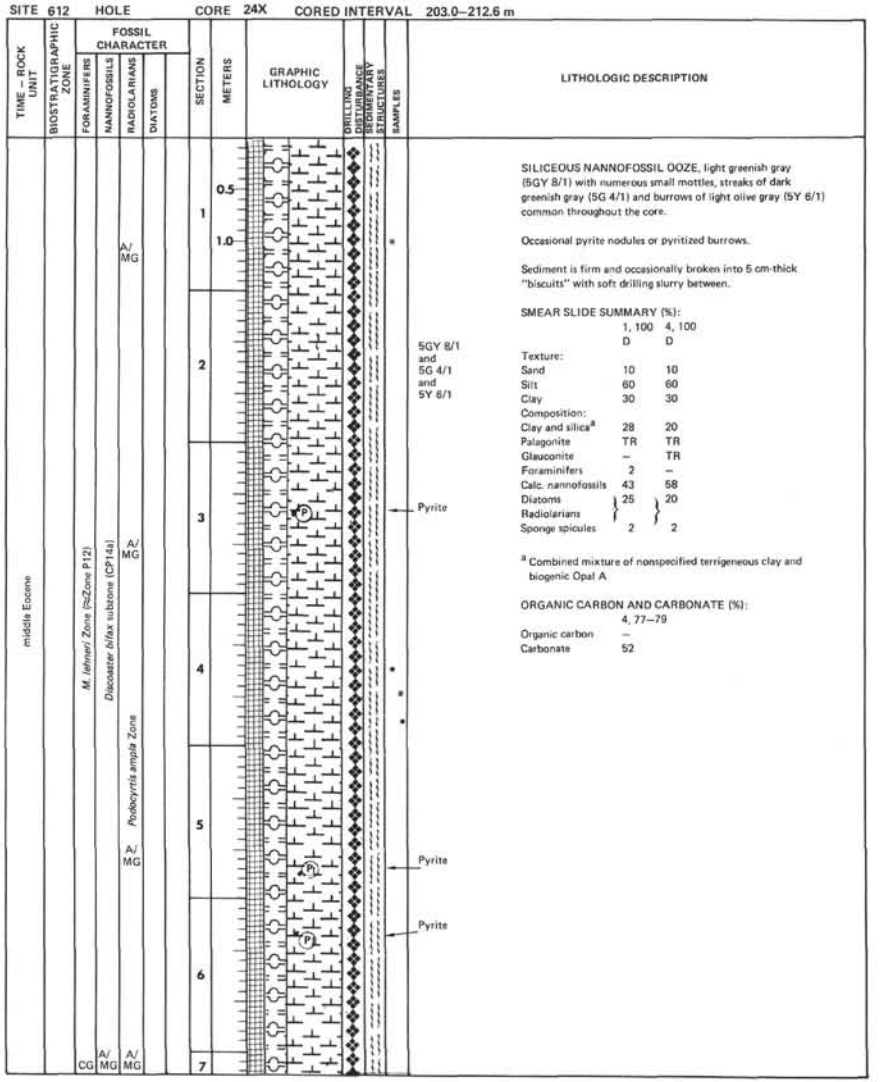

LITHOLOGIC DESCRIPTION

SILICEOUS NANNOFOSSIL OOZE, light greenish gray (5GY 8/1) with numerous small mottles, streaks of dark greenish gray (5G 4/1) and burrows of light olive gray (5Y 6/1) common throughout the core.

Occasional pyrite nodules or pyritized burrows.

Sediment is firm and occasionally broken into 5 cm-thick "biscuits" with soft drilling slurry between.

SMEAR SLIDE SUMMARY (%):

	1, 100 D	4, 100 D
Texture:		
Sand	10	10
Silt	60	60
Clay	30	30
Composition:		
Clay and silica[a]	28	20
Palagonite	TR	TR
Glauconite	–	TR
Foraminifers	2	–
Calc. nannofossils	43	58
Diatoms	25	20
Radiolarians		
Sponge spicules	2	2

[a] Combined mixture of nonspecified terrigeneous clay and biogenic Opal A

ORGANIC CARBON AND CARBONATE (%):

	4, 77–79
Organic carbon	–
Carbonate	52

SITE 612 HOLE CORE 25X CORED INTERVAL 212.6–222.2 m

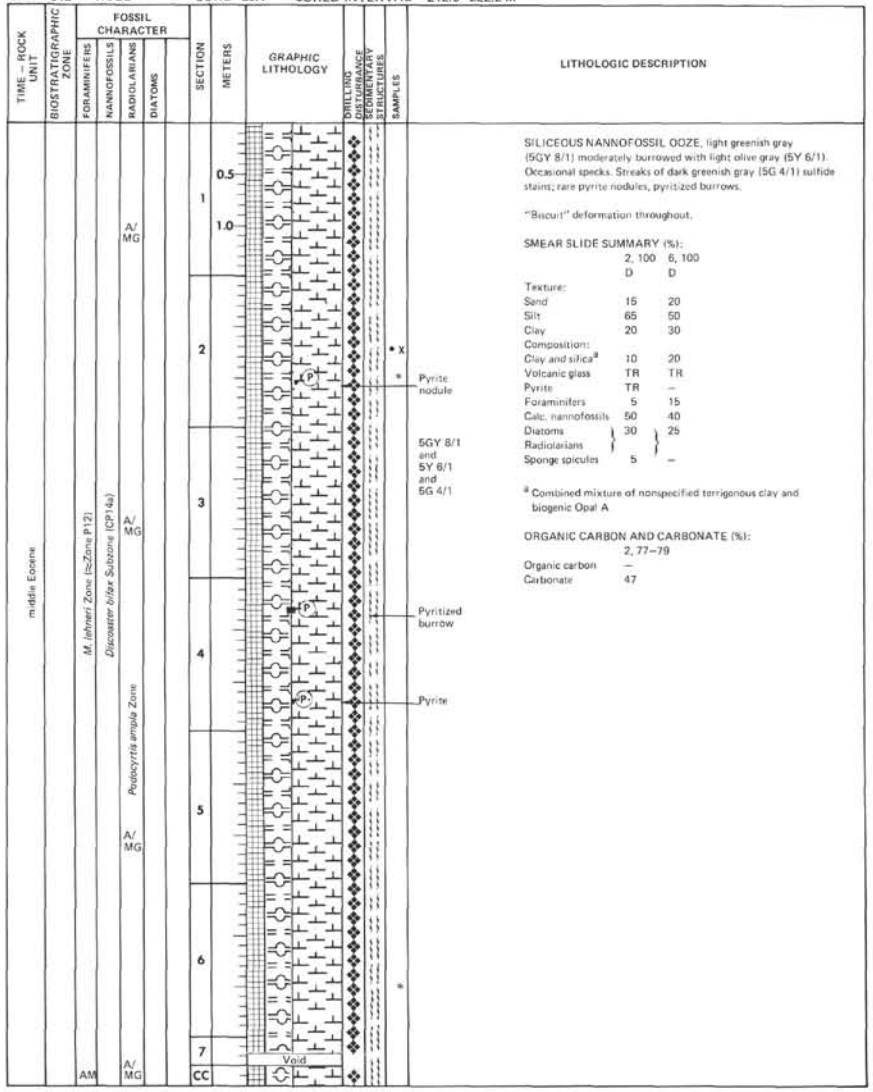

LITHOLOGIC DESCRIPTION

SILICEOUS NANNOFOSSIL OOZE, light greenish gray (5GY 8/1) moderately burrowed with light olive gray (5Y 6/1). Occasional specks. Streaks of dark greenish gray (5G 4/1) sulfide stains; rare pyrite nodules, pyritized burrows.

"Biscuit" deformation throughout.

SMEAR SLIDE SUMMARY (%):

	2, 100 D	6, 100 D
Texture:		
Sand	15	20
Silt	65	50
Clay	20	30
Composition:		
Clay and silica[a]	10	20
Volcanic glass	TR	TR
Pyrite	TR	–
Foraminifers	5	15
Calc. nannofossils	50	40
Diatoms	30	25
Radiolarians		
Sponge spicules	5	–

[a] Combined mixture of nonspecified terrigenous clay and biogenic Opal A

ORGANIC CARBON AND CARBONATE (%):

	2, 77–79
Organic carbon	–
Carbonate	47

SITE 612 HOLE CORE 26X CORED INTERVAL 222.2–231.8 m

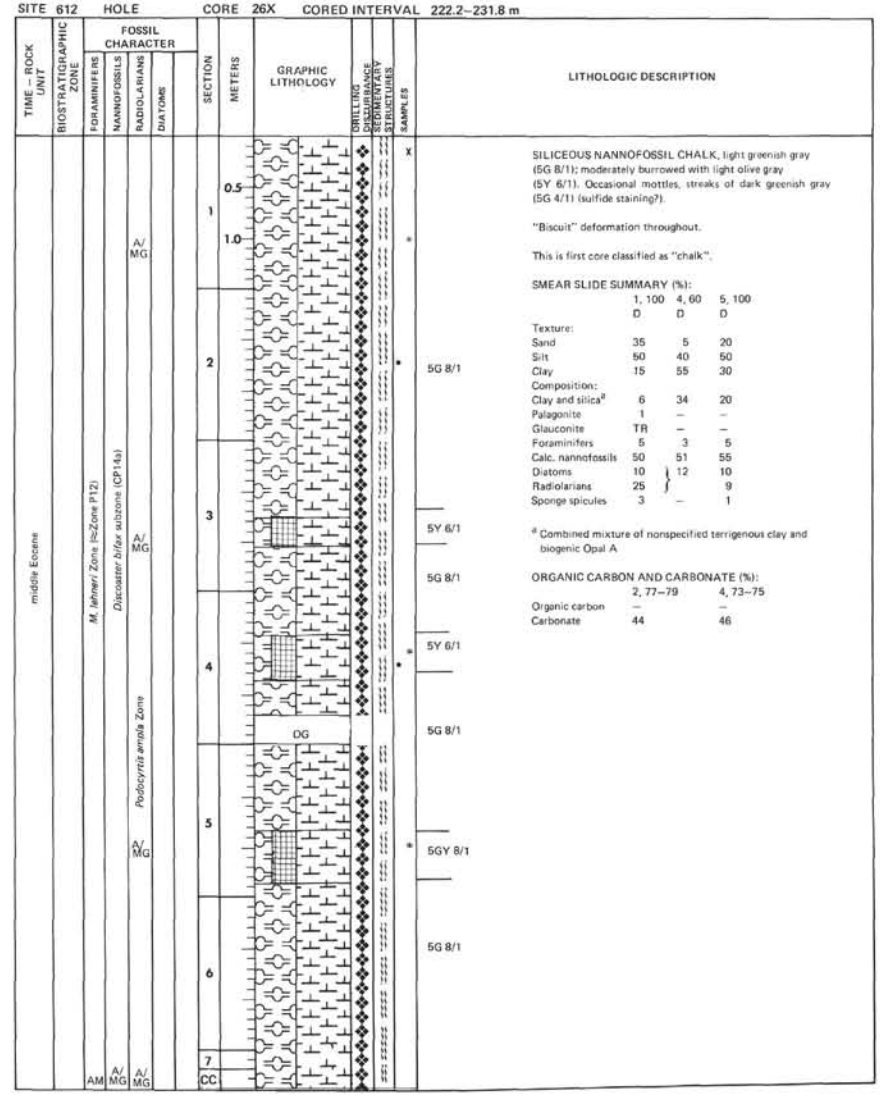

LITHOLOGIC DESCRIPTION

SILICEOUS NANNOFOSSIL CHALK, light greenish gray (5G 8/1); moderately burrowed with light olive gray (5Y 6/1). Occasional mottles, streaks of dark greenish gray (5G 4/1) (sulfide staining?).

"Biscuit" deformation throughout.

This is first core classified as "chalk".

SMEAR SLIDE SUMMARY (%):

	1, 100 D	4, 60 D	5, 100 D
Texture:			
Sand	35	5	20
Silt	50	40	50
Clay	15	55	30
Composition:			
Clay and silica[a]	6	34	20
Palagonite	1	–	–
Glauconite	TR	–	–
Foraminifers	5	3	5
Calc. nannofossils	50	51	55
Diatoms	10	12	10
Radiolarians	25		9
Sponge spicules	3	–	1

[a] Combined mixture of nonspecified terrigenous clay and biogenic Opal A

ORGANIC CARBON AND CARBONATE (%):

	2, 77–79	4, 73–75
Organic carbon	–	–
Carbonate	44	46

SITE 612 HOLE CORE 27X CORED INTERVAL 231.8–241.4 m

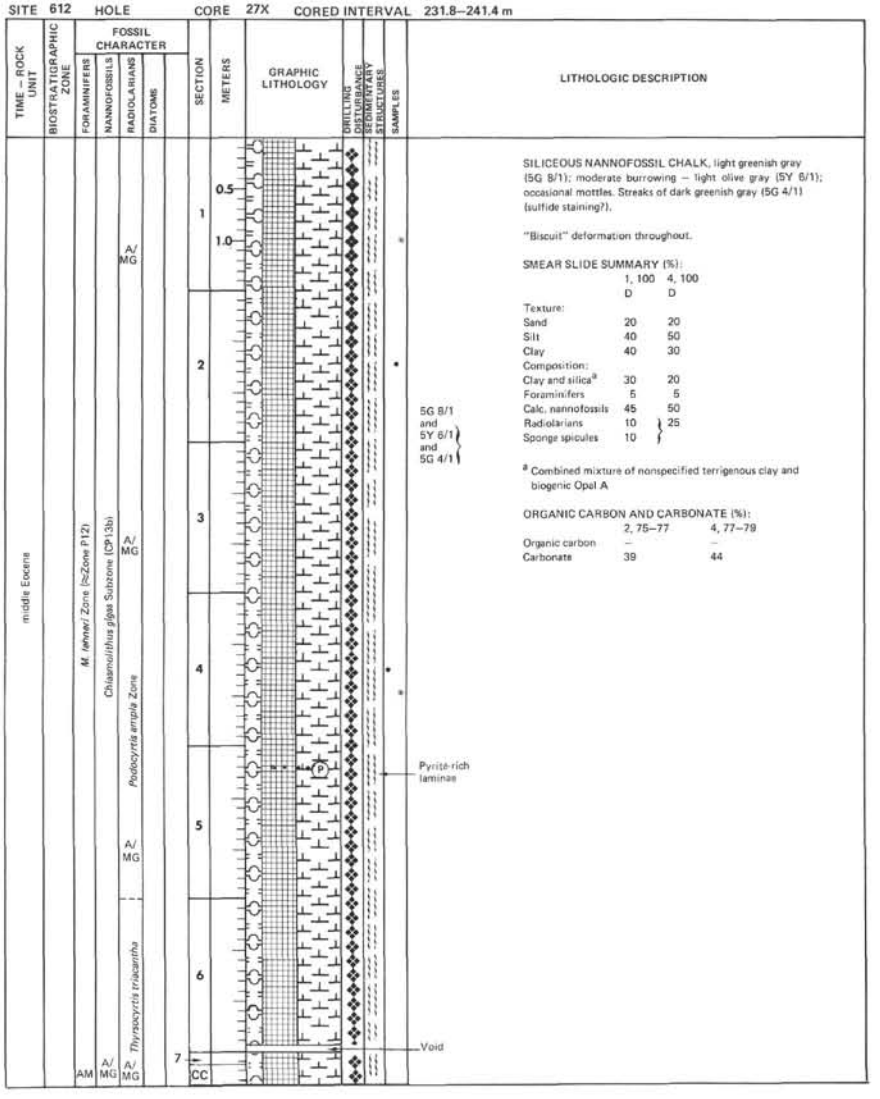

SILICEOUS NANNOFOSSIL CHALK, light greenish gray (5G 8/1); moderate burrowing – light olive gray (5Y 6/1); occasional mottles. Streaks of dark greenish gray (5G 4/1) (sulfide staining?).

"Biscuit" deformation throughout.

SMEAR SLIDE SUMMARY (%):

	1, 100 D	4, 100 D
Texture:		
Sand	20	20
Silt	40	50
Clay	40	30
Composition:		
Clay and silica[a]	30	20
Foraminifers	5	5
Calc. nannofossils	45	50
Radiolarians	10	25
Sponge spicules	10	

[a] Combined mixture of nonspecified terrigenous clay and biogenic Opal A

ORGANIC CARBON AND CARBONATE (%):

	2, 75–77	4, 77–79
Organic carbon	–	–
Carbonate	39	44

SITE 612 HOLE CORE 28X CORED INTERVAL 241.4–251.0 m

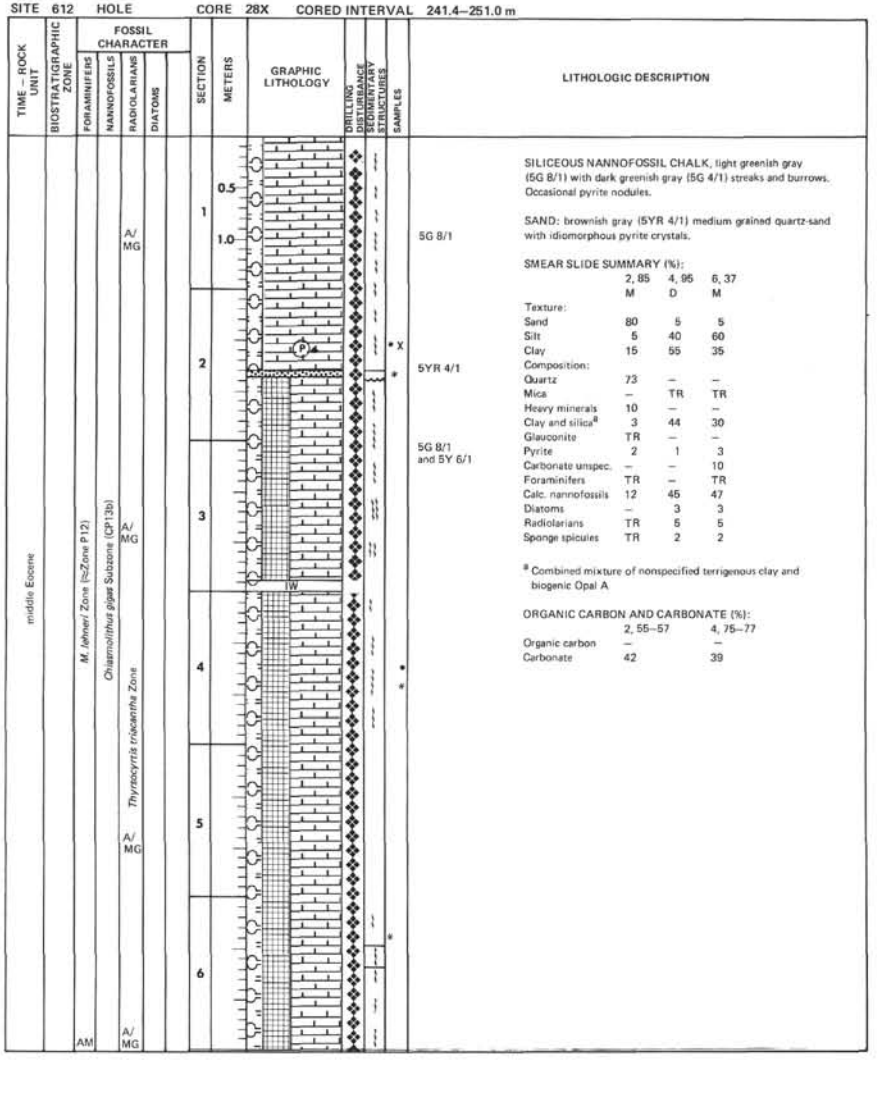

SILICEOUS NANNOFOSSIL CHALK, light greenish gray (5G 8/1) with dark greenish gray (5G 4/1) streaks and burrows. Occasional pyrite nodules.

SAND: brownish gray (5YR 4/1) medium grained quartz-sand with idiomorphous pyrite crystals.

SMEAR SLIDE SUMMARY (%):

	2, 85 M	4, 95 D	6, 37 M
Texture:			
Sand	80	5	5
Silt	5	40	60
Clay	15	55	35
Composition:			
Quartz	73	–	–
Mica	–	TR	TR
Heavy minerals	10	–	–
Clay and silica[a]	3	44	30
Glauconite	TR	–	–
Pyrite	2	1	3
Carbonate unspec.	–	–	10
Foraminifers	TR	–	TR
Calc. nannofossils	12	45	47
Diatoms	–	3	3
Radiolarians	TR	5	5
Sponge spicules	TR	2	2

[a] Combined mixture of nonspecified terrigenous clay and biogenic Opal A

ORGANIC CARBON AND CARBONATE (%):

	2, 55–57	4, 75–77
Organic carbon	–	–
Carbonate	42	39

SITE 612 HOLE CORE 29X CORED INTERVAL 251.0–260.6 m

TIME – ROCK UNIT	BIOSTRATIGRAPHIC ZONE	FOSSIL CHARACTER: FORAMINIFERS	NANNOFOSSILS	RADIOLARIANS	DIATOMS	SECTION	METERS	GRAPHIC LITHOLOGY	DRILLING DISTURBANCE	SEDIMENTARY STRUCTURES	SAMPLES
middle Eocene	*Globigerinatheka subconglobata/Morozovella lehneri* Zone (≈Zones P11/P12)	CM	*Chiasmolithus gigas* Subzone (CP13b)	A/MG		1	0.5, 1.0				•
middle Eocene	*Globigerinatheka subconglobata/Morozovella lehneri* Zone (≈Zones P11/P12)	CM	*Chiasmolithus gigas* Subzone (CP13b)	A/MG		2					• •
middle Eocene	*Globigerinatheka subconglobata/Morozovella lehneri* Zone (≈Zones P11/P12)	CM	*Chiasmolithus gigas* Subzone (CP13b)	A/MG		3					
middle Eocene	*Globigerinatheka subconglobata/Morozovella lehneri* Zone (≈Zones P11/P12)	CM	*Chiasmolithus gigas* Subzone (CP13b)	A/MG		4					•
middle Eocene	*Globigerinatheka subconglobata/Morozovella lehneri* Zone (≈Zones P11/P12)	CM	*Chiasmolithus gigas* Subzone (CP13b)	A/MG		5					
middle Eocene	*Globigerinatheka subconglobata/Morozovella lehneri* Zone (≈Zones P11/P12)	CM	*Chiasmolithus gigas* Subzone (CP13b)	A/MG		6					
middle Eocene	*Globigerinatheka subconglobata/Morozovella lehneri* Zone (≈Zones P11/P12)	CM	*Chiasmolithus gigas* Subzone (CP13b)	A/MG		7					
middle Eocene	*Globigerinatheka subconglobata/Morozovella lehneri* Zone (≈Zones P11/P12)	CM	*Chiasmolithus gigas* Subzone (CP13b)	A/MG		CC					

LITHOLOGIC DESCRIPTION

SILICEOUS NANNOFOSSIL CHALK, light greenish gray (5G 8/1) with numerous light olive gray (5Y 6/1) layers and burrows.

Biscuit deformation.

5G 8/1 and 5Y 8/1

SMEAR SLIDE SUMMARY (%):

	2, 62	4, 88
	D	D
Texture:		
Sand	5	10
Silt	55	55
Clay	40	35
Composition:		
Mica	–	TR
Clay and silica[a]	40	30
Glauconite	TR	TR
Pyrite	TR	TR
Carbonate unspec.	9	10
Foraminifers	1	TR
Calc. nannofossils	40	45
Diatoms	1	5
Radiolarians	5	5
Sponge spicules	4	5

[a] Combined mixture of nonspecified terrigenous clay and biogenic Opal A

ORGANIC CARBON AND CARBONATE (%):

	2, 70–73	4, 70–73
Organic carbon	–	–
Carbonate	45	49

SITE 612 HOLE CORE 30X CORED INTERVAL 260.6–270.2 m

TIME – ROCK UNIT	BIOSTRATIGRAPHIC ZONE	FOSSIL CHARACTER: FORAMINIFERS	NANNOFOSSILS	RADIOLARIANS	DIATOMS	SECTION	METERS	GRAPHIC LITHOLOGY	DRILLING DISTURBANCE	SEDIMENTARY STRUCTURES	SAMPLES
middle Eocene	*G. subconglobata/M. lehneri* Zone (≈Zones P11/P12)	CM	AM	A/MG		1	0.5, 1.0				•
middle Eocene	*G. subconglobata/M. lehneri* Zone (≈Zones P11/P12)	CM	AM	A/MG		2					• x
middle Eocene	*G. subconglobata/M. lehneri* Zone (≈Zones P11/P12)	CM	AM	A/MG		3					
middle Eocene	*G. subconglobata/M. lehneri* Zone (≈Zones P11/P12)	CM	AM	A/MG		4					•
middle Eocene	*G. subconglobata/M. lehneri* Zone (≈Zones P11/P12)	CM	AM	A/MG		5					
middle Eocene	*G. subconglobata/M. lehneri* Zone (≈Zones P11/P12)	CM	AM	A/MG		6					•
middle Eocene	*G. subconglobata/M. lehneri* Zone (≈Zones P11/P12)	CM	AM	A/MG		7					
middle Eocene	*G. subconglobata/M. lehneri* Zone (≈Zones P11/P12)	CM	AM	A/MG		CC					

LITHOLOGIC DESCRIPTION

SILICEOUS NANNOFOSSIL CHALK, light greenish gray (5G 8/1) with abundant yellowish gray (5Y 8/1) (chondrites-like) burrows.

Biscuit deformation.

Core in parts strongly deformed.

5G 8/1 and 5Y 8/1

SMEAR SLIDE SUMMARY (%):

	1, 77	6, 75
	D	D
Texture:		
Sand	5	10
Silt	50	50
Clay	45	40
Composition:		
Quartz	TR	–
Mica	–	TR
Clay and silica[a]	40	35
Pyrite	TR	TR
Carbonate unspec.	10	15
Foraminifers	TR	TR
Calc. nannofossils	40	35
Diatoms	2	5
Radiolarians	3	5
Sponge spicules	5	5

[a] Combined mixture of nonspecified terrigenous clay and biogenic Opal A

ORGANIC CARBON AND CARBONATE (%):

	2, 70–73	4, 70–73
Organic carbon	0.19	–
Carbonate	45	42

SITE 612 HOLE CORE 31X CORED INTERVAL 270.2–279.8 m

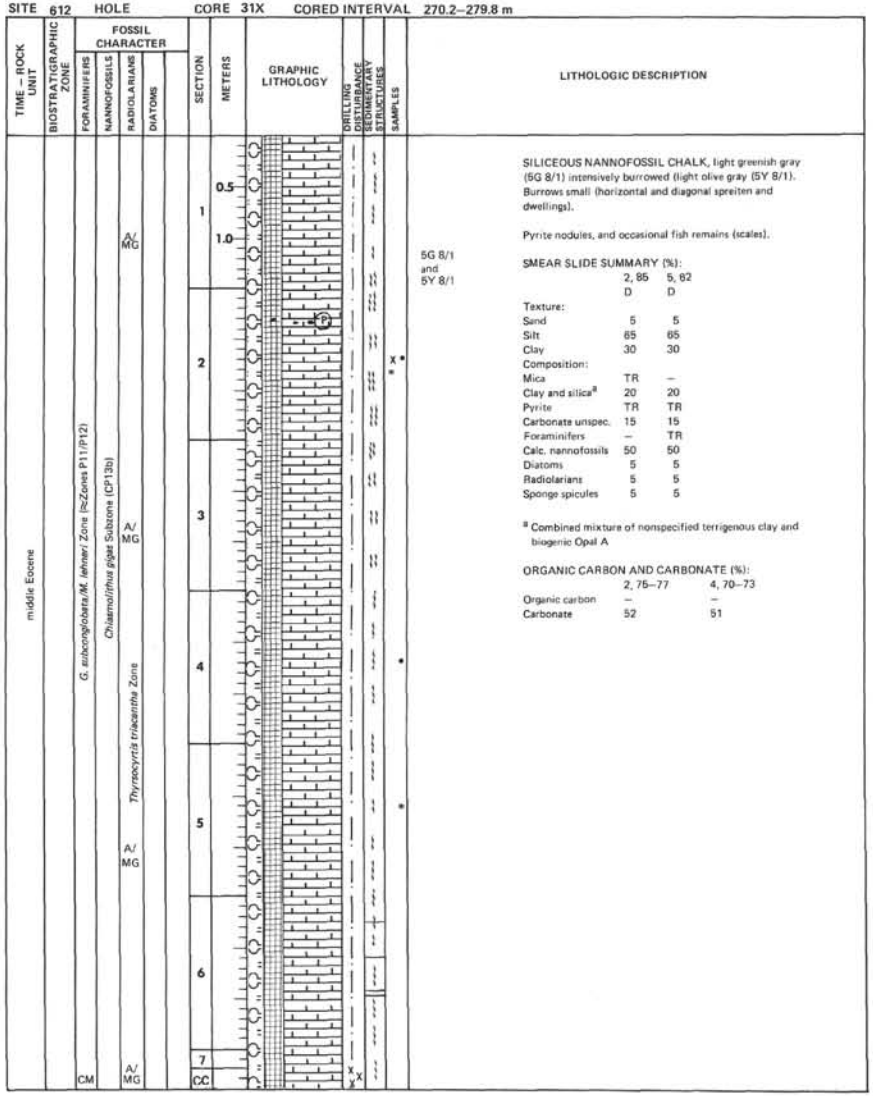

SILICEOUS NANNOFOSSIL CHALK, light greenish gray (5G 8/1) intensively burrowed (light olive gray (5Y 8/1). Burrows small (horizontal and diagonal spreiten and dwellings).

Pyrite nodules, and occasional fish remains (scales).

SMEAR SLIDE SUMMARY (%):

	2, 85	5, 62
	D	D
Texture:		
Sand	5	5
Silt	65	65
Clay	30	30
Composition:		
Mica	TR	–
Clay and silica[a]	20	20
Pyrite	TR	TR
Carbonate unspec.	15	15
Foraminifers	–	TR
Calc. nannofossils	50	50
Diatoms	5	5
Radiolarians	5	5
Sponge spicules	5	5

[a] Combined mixture of nonspecified terrigenous clay and biogenic Opal A

ORGANIC CARBON AND CARBONATE (%):

	2, 75–77	4, 70–73
Organic carbon	–	–
Carbonate	52	51

SITE 612 HOLE CORE 32X CORED INTERVAL 279.8–289.4 m

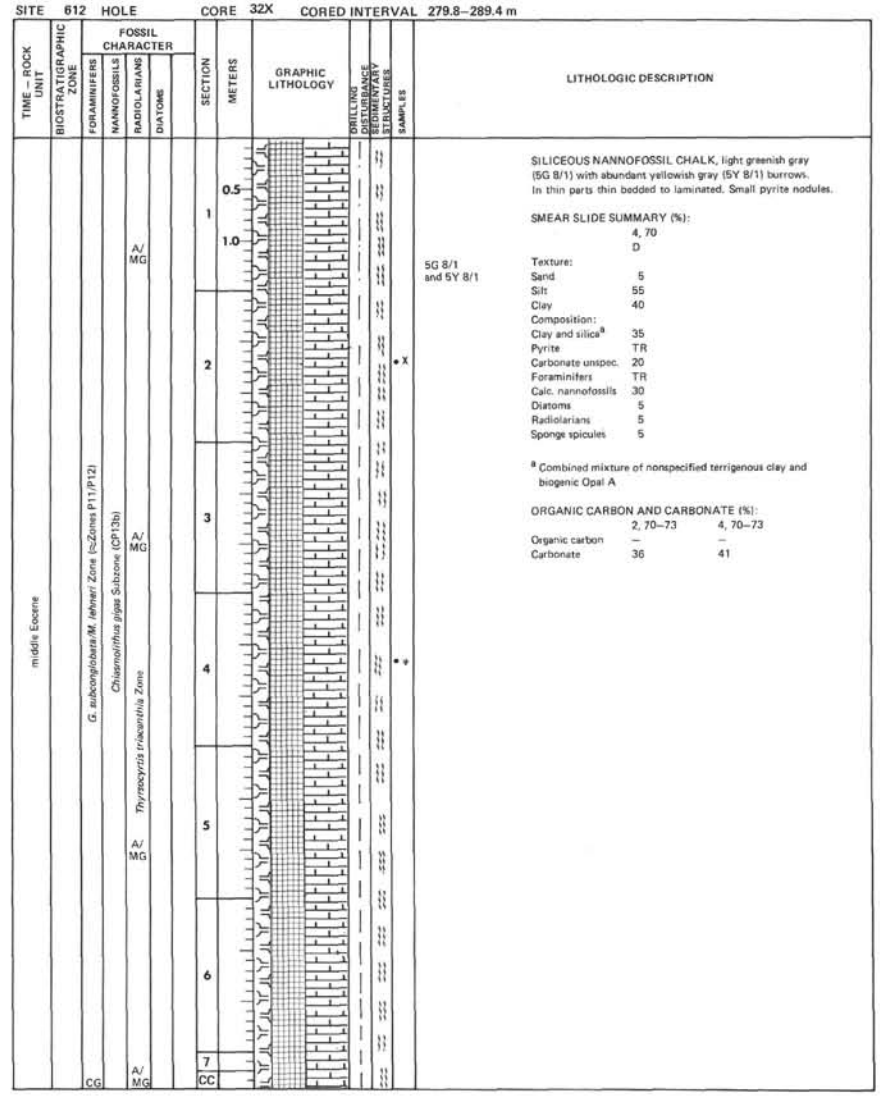

SILICEOUS NANNOFOSSIL CHALK, light greenish gray (5G 8/1) with abundant yellowish gray (5Y 8/1) burrows. In thin parts thin bedded to laminated. Small pyrite nodules.

SMEAR SLIDE SUMMARY (%):

	4, 70
	D
Texture:	
Sand	5
Silt	55
Clay	40
Composition:	
Clay and silica[a]	35
Pyrite	TR
Carbonate unspec.	20
Foraminifers	TR
Calc. nannofossils	30
Diatoms	5
Radiolarians	5
Sponge spicules	5

[a] Combined mixture of nonspecified terrigenous clay and biogenic Opal A

ORGANIC CARBON AND CARBONATE (%):

	2, 70–73	4, 70–73
Organic carbon	–	–
Carbonate	36	41

SITE 612 HOLE CORE 33X CORED INTERVAL 289.4–299.1 m

TIME – ROCK UNIT	BIOSTRATIGRAPHIC ZONE	FOSSIL CHARACTER: FORAMINIFERS	NANNOFOSSILS	RADIOLARIANS	DIATOMS	SECTION	METERS	GRAPHIC LITHOLOGY	DRILLING DISTURBANCE	SEDIMENTARY STRUCTURES	SAMPLES
middle Eocene	*G. subconglobata/M. lehneri* Zones (≈Zones P11/P12)	CM	*Chiasmolithus gigas* Subzone (CP13b) A/MG	*Thyrsocyrtis triacantha* Zone A/MG	A/MG	1	0.5, 1.0				x
						2					x *
						3					
						4					*
						5					
						6					
			A/MG	A/MG		7					
						CC			x		

5G 8/1 and 5Y 8/1

LITHOLOGIC DESCRIPTION

SILICEOUS NANNOFOSSIL CHALK, light greenish gray (5G 8/1) with abundant yellowish gray (5Y 8/1) burrow- and dwelling-structures. Small pyrite nodules and randomly distributed fine grained pyrite. Fish bones and scales (small).

SMEAR SLIDE SUMMARY (%):

	4, 90
	D
Texture:	
Sand	5
Silt	55
Clay	40
Composition:	
Clay and silica[a]	35
Carbonate unspec.	13
Foraminifers	TR
Calc. nannofossils	40
Diatoms	5
Radiolarians	2
Sponge spicules	5

[a] Combined mixture of nonspecified terrigenous clay and biogenic Opal A

ORGANIC CARBON AND CARBONATE (%):

	2, 70–73	4, 70–73
Organic carbon	–	–
Carbonate	46	42

SITE 612 HOLE CORE 34X CORED INTERVAL 299.1–308.8 m

TIME – ROCK UNIT	BIOSTRATIGRAPHIC ZONE	FOSSIL CHARACTER: FORAMINIFERS	NANNOFOSSILS	RADIOLARIANS	DIATOMS	SECTION	METERS	GRAPHIC LITHOLOGY	DRILLING DISTURBANCE	SEDIMENTARY STRUCTURES	SAMPLES
middle Eocene	*Hantkenina aragonensis/G. subconglobata* Zones (≈Zones P10/P11)	RM	*Chiasmolithus gigas* Subzone (CP13b) A/MG	*Thyrsocyrtis triacantha* Zone A/MG		1	0.5, 1.0				*
						2					
						CC					

5Y 8/1

5G 8/1

5Y 8/1 and 5Y 6/1

LITHOLOGIC DESCRIPTION

SILICEOUS NANNOFOSSIL CHALK, yellowish gray (5Y 8/1) with abundant light olive gray (5Y 6/1) burrows. From 90–120 cm light greenish gray (5G 8/1) small pyrite nodules and sand-sized fish remains (mainly scales).

SMEAR SLIDE SUMMARY (%):

	1, 92
	D
Texture:	
Sand	5
Silt	55
Clay	40
Composition:	
Clay and silica[a]	30
Glauconite	TR
Pyrite	TR
Carbonate unspec.	15
Foraminifers	TR
Calc. nannofossils	40
Diatoms	5
Radiolarians	5
Sponge spicules	5

[a] Combined mixture of nonspecified terrigenous clay and biogenic Opal A

SITE 612 HOLE CORE 35X CORED INTERVAL 308.8–318.5 m

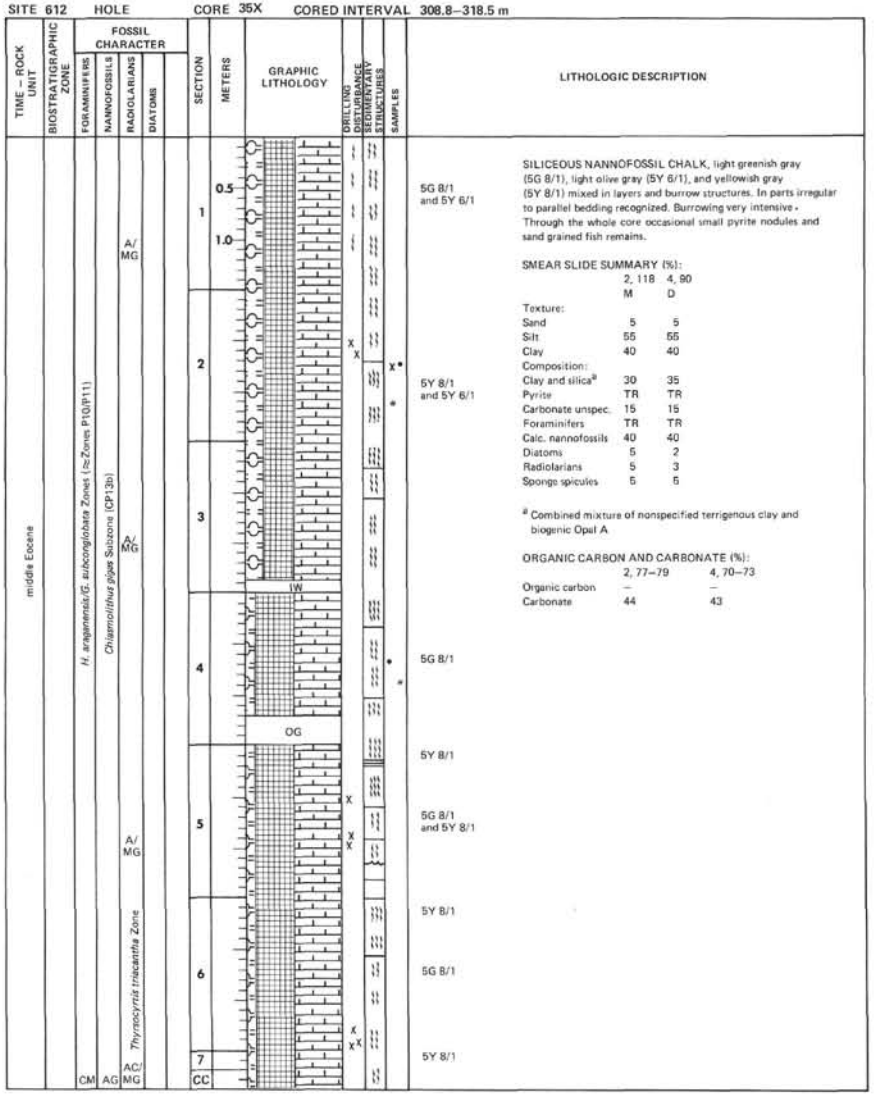

LITHOLOGIC DESCRIPTION

SILICEOUS NANNOFOSSIL CHALK, light greenish gray (5G 8/1), light olive gray (5Y 6/1), and yellowish gray (5Y 8/1) mixed in layers and burrow structures. In parts irregular to parallel bedding recognized. Burrowing very intensive. Through the whole core occasional small pyrite nodules and sand grained fish remains.

SMEAR SLIDE SUMMARY (%):

	2, 118 M	4, 90 D
Texture:		
Sand	5	5
Silt	55	55
Clay	40	40
Composition:		
Clay and silica[a]	30	35
Pyrite	TR	TR
Carbonate unspec.	15	15
Foraminifers	TR	TR
Calc. nannofossils	40	40
Diatoms	5	2
Radiolarians	5	3
Sponge spicules	5	5

[a] Combined mixture of nonspecified terrigenous clay and biogenic Opal A

ORGANIC CARBON AND CARBONATE (%):

	2, 77–79	4, 70–73
Organic carbon	–	–
Carbonate	44	43

SITE 612 HOLE CORE 36X CORED INTERVAL 318.5–328.1 m

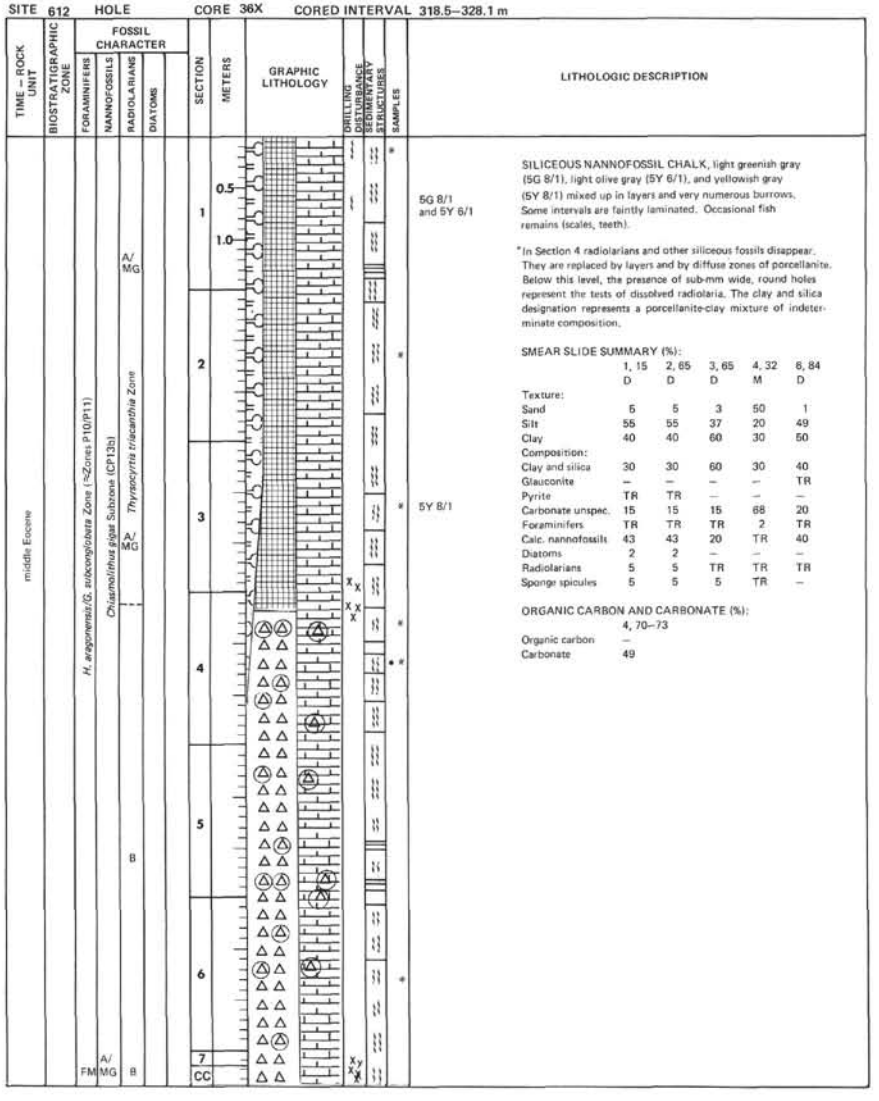

LITHOLOGIC DESCRIPTION

SILICEOUS NANNOFOSSIL CHALK, light greenish gray (5G 8/1), light olive gray (5Y 6/1), and yellowish gray (5Y 8/1) mixed up in layers and very numerous burrows. Some intervals are faintly laminated. Occasional fish remains (scales, teeth).

*In Section 4 radiolarians and other siliceous fossils disappear. They are replaced by layers and by diffuse zones of porcellanite. Below this level, the presence of sub-mm wide, round holes represent the tests of dissolved radiolaria. The clay and silica designation represents a porcellanite-clay mixture of indeterminate composition.

SMEAR SLIDE SUMMARY (%):

	1, 15 D	2, 65 D	3, 65 D	4, 32 M	6, 84 D
Texture:					
Sand	5	5	3	50	1
Silt	55	55	37	20	49
Clay	40	40	60	30	50
Composition:					
Clay and silica	30	30	60	30	40
Glauconite	–	–	–	–	TR
Pyrite	TR	TR	–	–	–
Carbonate unspec.	15	15	15	68	20
Foraminifers	TR	TR	TR	2	TR
Calc. nannofossils	43	43	20	TR	40
Diatoms	2	2	–	–	–
Radiolarians	5	5	TR	TR	TR
Sponge spicules	5	5	5	TR	–

ORGANIC CARBON AND CARBONATE (%):

	4, 70–73
Organic carbon	–
Carbonate	49

SITE 612 HOLE CORE 37X CORED INTERVAL 328.1–337.7 m

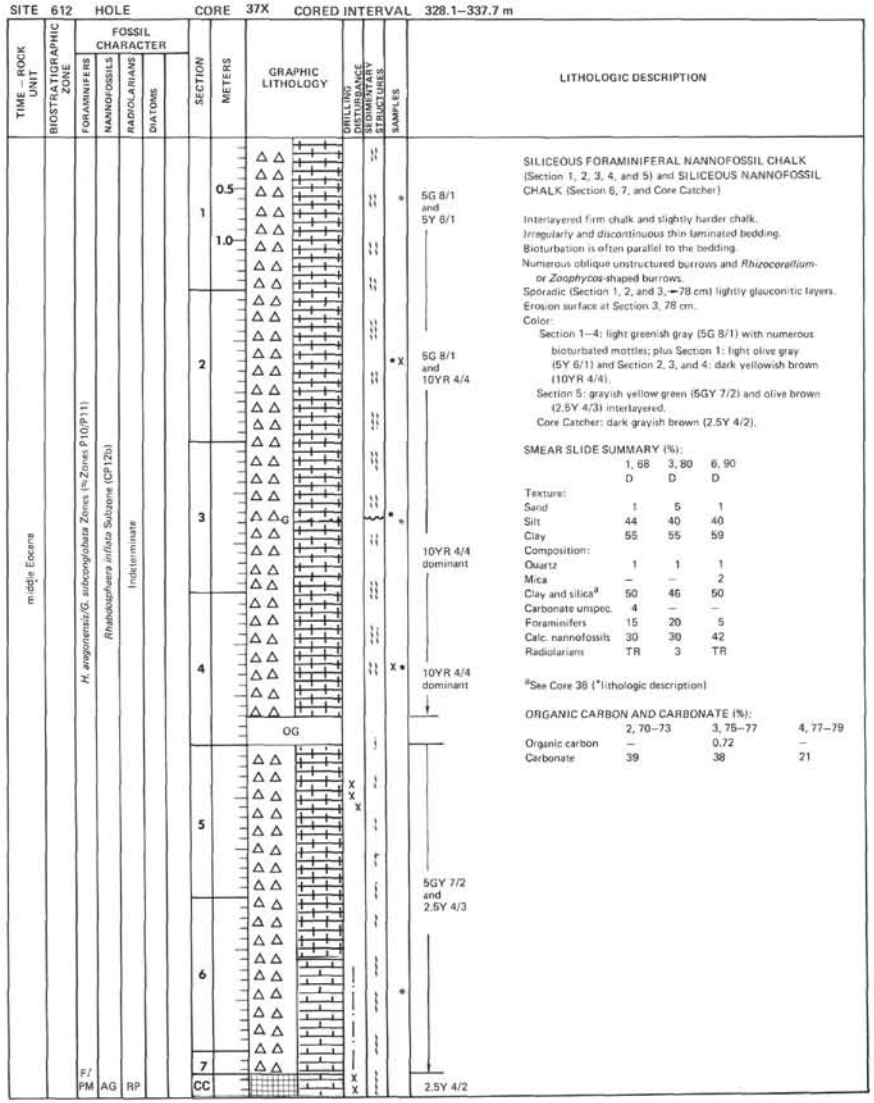

SILICEOUS FORAMINIFERAL NANNOFOSSIL CHALK (Section 1, 2, 3, 4, and 5) and SILICEOUS NANNOFOSSIL CHALK (Section 6, 7, and Core Catcher)

Interlayered firm chalk and slightly harder chalk.
Irregularly and *discontinuous* thin laminated bedding.
Bioturbation is often parallel to the bedding.
Numerous oblique unstructured burrows and *Rhizocorallium*- or *Zoophycos*-shaped burrows.
Sporadic (Section 1, 2, and 3, ~78 cm) lightly glauconitic layers.
Erosion surface at Section 3, 78 cm.
Color:
Section 1–4: light greenish gray (5G 8/1) with numerous bioturbated mottles; plus Section 1: light olive gray (5Y 6/1) and Section 2, 3, and 4: dark yellowish brown (10YR 4/4).
Section 5: grayish yellow green (5GY 7/2) and olive brown (2.5Y 4/3) interlayered.
Core Catcher: dark grayish brown (2.5Y 4/2).

SMEAR SLIDE SUMMARY (%):

	1, 68	3, 80	6, 90
	D	D	D
Texture:			
Sand	1	5	1
Silt	44	40	40
Clay	55	55	59
Composition:			
Quartz	1	1	1
Mica	–	–	2
Clay and silica[a]	50	46	50
Carbonate unspec.	4	–	–
Foraminifers	15	20	5
Calc. nannofossils	30	30	42
Radiolarians	TR	3	TR

[a]See Core 36 (*lithologic description)

ORGANIC CARBON AND CARBONATE (%):

	2, 70–73	3, 75–77	4, 77–79
Organic carbon	–	0.72	–
Carbonate	39	38	21

SITE 612 HOLE CORE 38X CORED INTERVAL 337.7–347.3 m

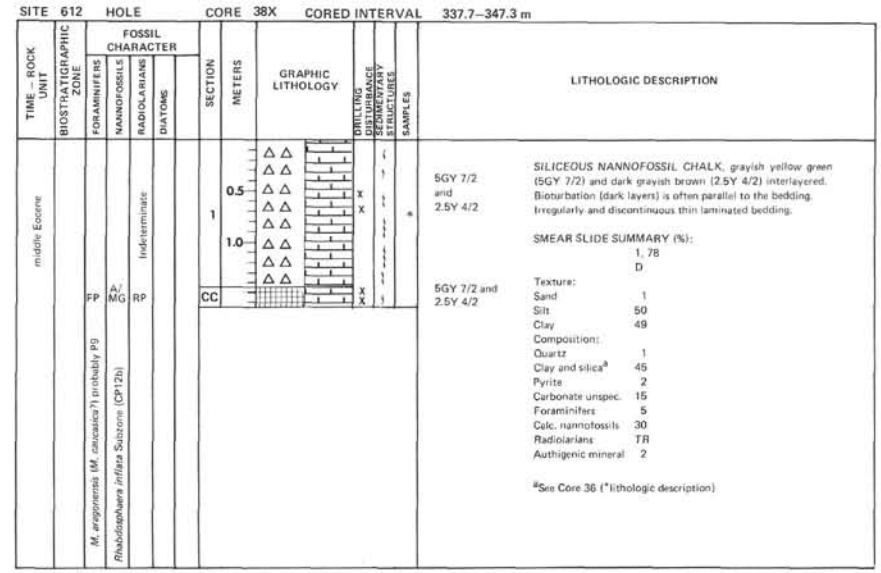

SILICEOUS NANNOFOSSIL CHALK, grayish yellow green (5GY 7/2) and dark grayish brown (2.5Y 4/2) interlayered.
Bioturbation (dark layers) is often parallel to the bedding.
Irregularly and discontinuous thin laminated bedding.

SMEAR SLIDE SUMMARY (%):

	1, 78
	D
Texture:	
Sand	1
Silt	50
Clay	49
Composition:	
Quartz	1
Clay and silica[a]	45
Pyrite	2
Carbonate unspec.	15
Foraminifers	5
Calc. nannofossils	30
Radiolarians	TR
Authigenic mineral	2

[a]See Core 36 (*lithologic description)

SITE 612 HOLE CORE 39X CORED INTERVAL 347.3–357.0 m

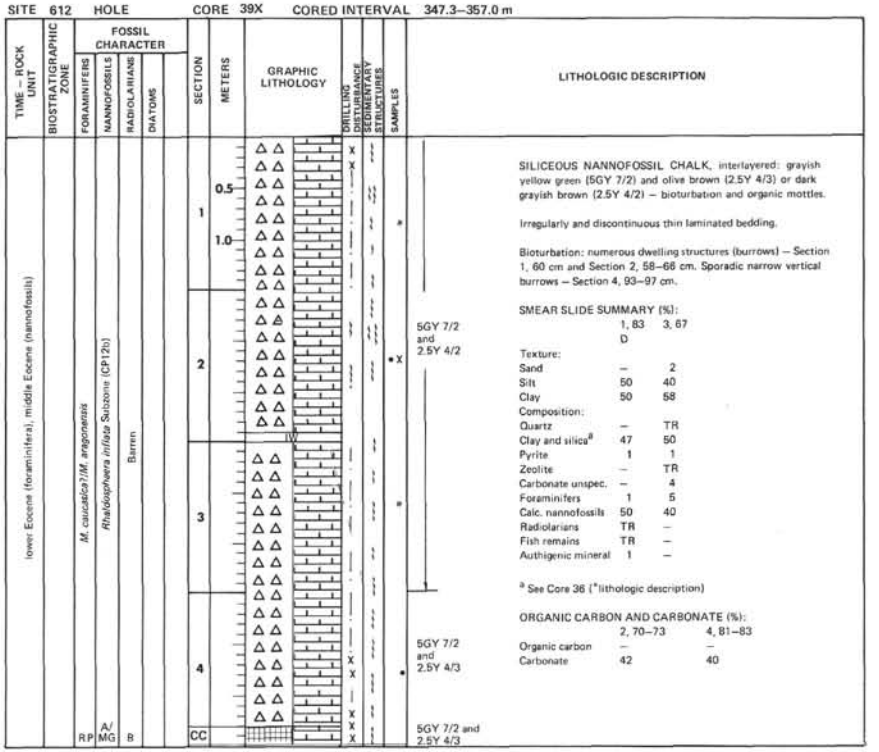

LITHOLOGIC DESCRIPTION

SILICEOUS NANNOFOSSIL CHALK, interlayered: grayish yellow green (5GY 7/2) and olive brown (2.5Y 4/3) or dark grayish brown (2.5Y 4/2) – bioturbation and organic mottles.

Irregularly and discontinuous thin laminated bedding.

Bioturbation: numerous dwelling structures (burrows) – Section 1, 60 cm and Section 2, 58–66 cm. Sporadic narrow vertical burrows – Section 4, 93–97 cm.

SMEAR SLIDE SUMMARY (%):

	1, 83 D	3, 67 D
Texture:		
Sand	–	2
Silt	50	40
Clay	50	58
Composition:		
Quartz	–	TR
Clay and silica[a]	47	50
Pyrite	1	1
Zeolite	–	TR
Carbonate unspec.	–	4
Foraminifers	1	5
Calc. nannofossils	50	40
Radiolarians	TR	–
Fish remains	TR	–
Authigenic mineral	1	–

[a] See Core 36 (*lithologic description)

ORGANIC CARBON AND CARBONATE (%):

	2, 70–73	4, 81–83
Organic carbon	–	–
Carbonate	42	40

SITE 612 HOLE CORE 40X CORED INTERVAL 357.0–366.7 m

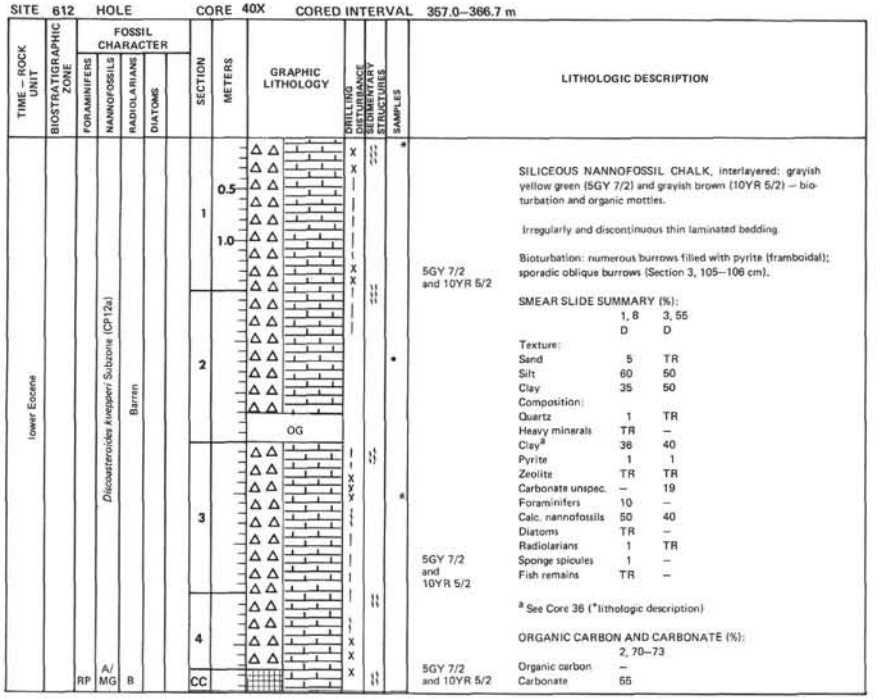

LITHOLOGIC DESCRIPTION

SILICEOUS NANNOFOSSIL CHALK, interlayered: grayish yellow green (5GY 7/2) and grayish brown (10YR 5/2) – bioturbation and organic mottles.

Irregularly and discontinuous thin laminated bedding.

Bioturbation: numerous burrows filled with pyrite (framboidal); sporadic oblique burrows (Section 3, 105–106 cm).

SMEAR SLIDE SUMMARY (%):

	1, 8 D	3, 55 D
Texture:		
Sand	5	TR
Silt	60	50
Clay	35	50
Composition:		
Quartz	1	TR
Heavy minerals	TR	–
Clay[a]	38	40
Pyrite	1	1
Zeolite	TR	TR
Carbonate unspec.	–	19
Foraminifers	10	–
Calc. nannofossils	50	40
Diatoms	TR	–
Radiolarians	1	TR
Sponge spicules	1	–
Fish remains	TR	–

[a] See Core 36 (*lithologic description)

ORGANIC CARBON AND CARBONATE (%):

	2, 70–73
Organic carbon	–
Carbonate	55

SITE 612 HOLE CORE 41X CORED INTERVAL 366.7–376.4 m

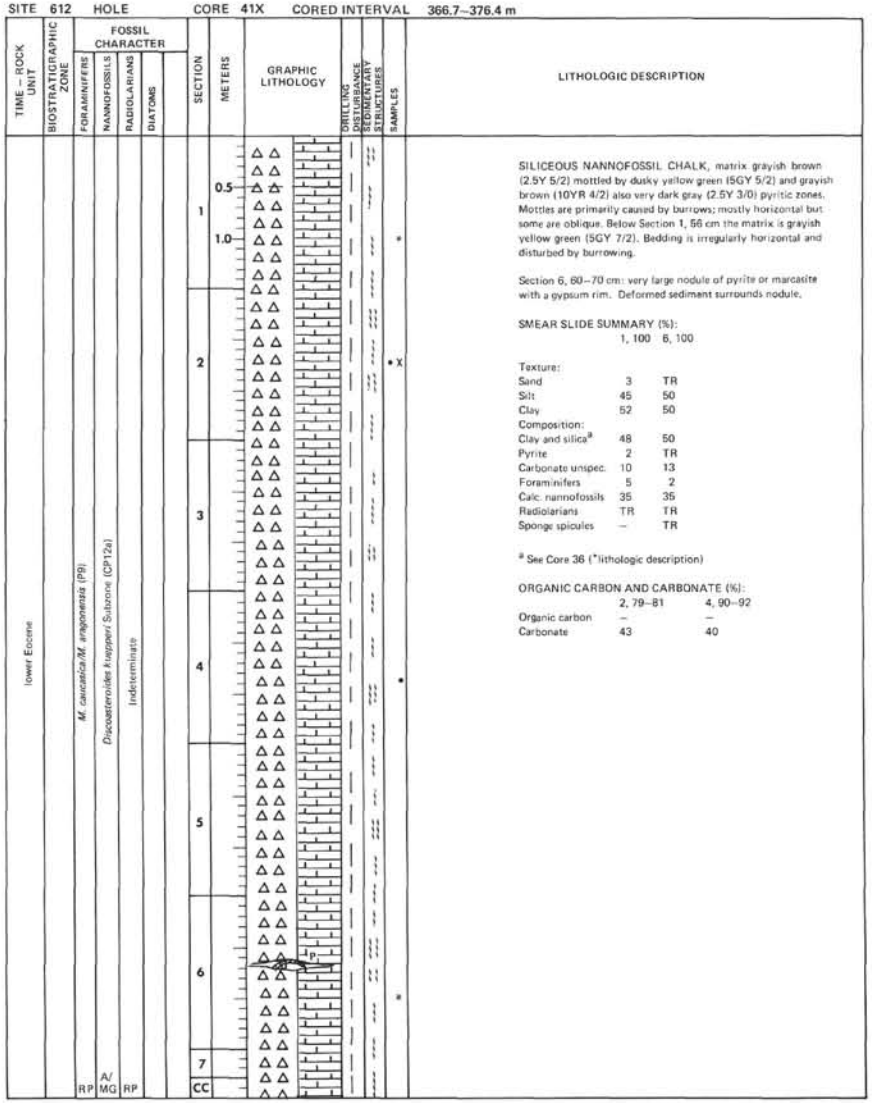

LITHOLOGIC DESCRIPTION

SILICEOUS NANNOFOSSIL CHALK, matrix grayish brown (2.5Y 5/2) mottled by dusky yellow green (5GY 5/2) and grayish brown (10YR 4/2) also very dark gray (2.5Y 3/0) pyritic zones. Mottles are primarily caused by burrows; mostly horizontal but some are oblique. Below Section 1, 56 cm the matrix is grayish yellow green (5GY 7/2). Bedding is irregularly horizontal and disturbed by burrowing.

Section 6, 60–70 cm: very large nodule of pyrite or marcasite with a gypsum rim. Deformed sediment surrounds nodule.

SMEAR SLIDE SUMMARY (%):

	1, 100	6, 100
Texture:		
Sand	3	TR
Silt	45	50
Clay	52	50
Composition:		
Clay and silica[a]	48	50
Pyrite	2	TR
Carbonate unspec.	10	13
Foraminifers	5	2
Calc. nannofossils	35	35
Radiolarians	TR	TR
Sponge spicules	–	TR

[a] See Core 36 (*lithologic description)

ORGANIC CARBON AND CARBONATE (%):

	2, 79–81	4, 90–92
Organic carbon	–	–
Carbonate	43	40

SITE 612 HOLE CORE 42X CORED INTERVAL 376.4–386.0 m

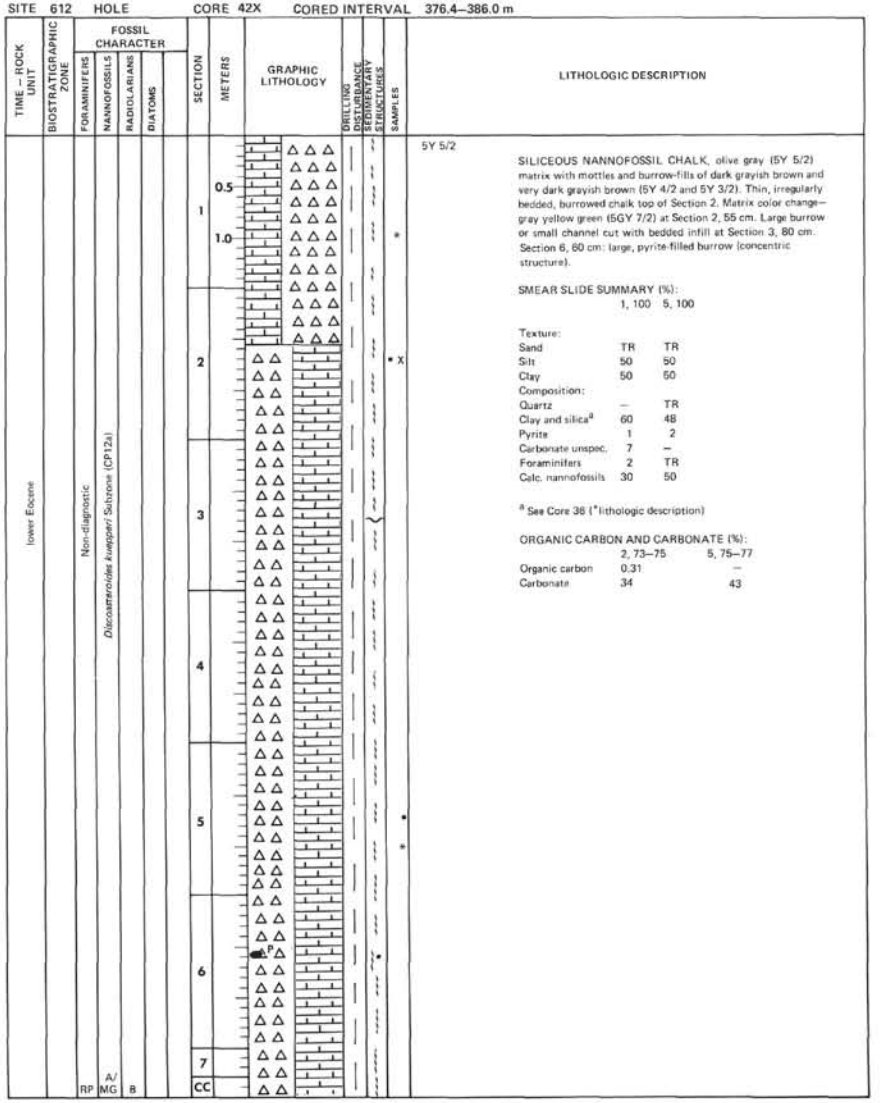

5Y 5/2

LITHOLOGIC DESCRIPTION

SILICEOUS NANNOFOSSIL CHALK, olive gray (5Y 5/2) matrix with mottles and burrow-fills of dark grayish brown and very dark grayish brown (5Y 4/2 and 5Y 3/2). Thin, irregularly bedded, burrowed chalk top of Section 2. Matrix color change—gray yellow green (5GY 7/2) at Section 2, 55 cm. Large burrow or small channel cut with bedded infill at Section 3, 80 cm. Section 6, 60 cm: large, pyrite-filled burrow (concentric structure).

SMEAR SLIDE SUMMARY (%):

	1, 100	5, 100
Texture:		
Sand	TR	TR
Silt	50	50
Clay	50	50
Composition:		
Quartz	–	TR
Clay and silica[a]	60	48
Pyrite	1	2
Carbonate unspec.	7	–
Foraminifers	2	TR
Calc. nannofossils	30	50

[a] See Core 36 (*lithologic description)

ORGANIC CARBON AND CARBONATE (%):

	2, 73–75	5, 75–77
Organic carbon	0.31	–
Carbonate	34	43

SITE 612 HOLE CORE 43X CORED INTERVAL 386.0–395.6 m

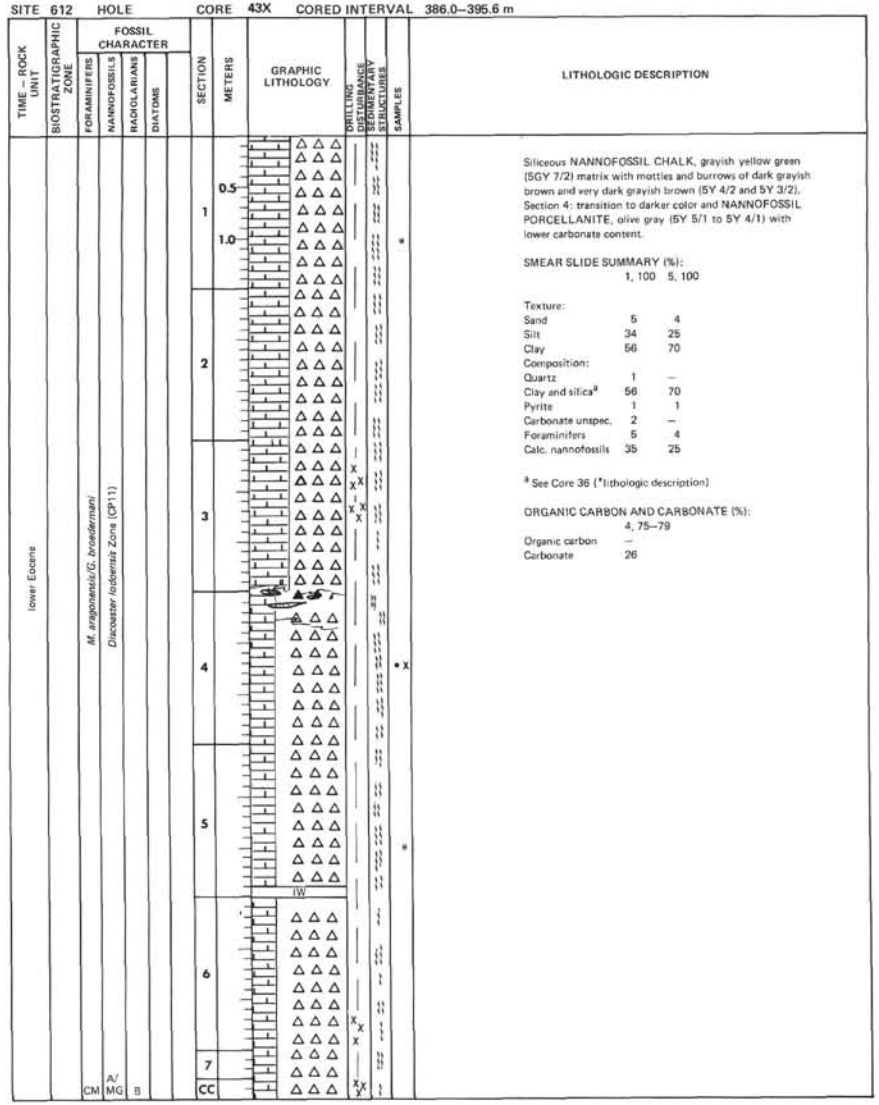

LITHOLOGIC DESCRIPTION

Siliceous NANNOFOSSIL CHALK, grayish yellow green (5GY 7/2) matrix with mottles and burrows of dark grayish brown and very dark grayish brown (5Y 4/2 and 5Y 3/2). Section 4: transition to darker color and NANNOFOSSIL PORCELLANITE, olive gray (5Y 5/1 to 5Y 4/1) with lower carbonate content.

SMEAR SLIDE SUMMARY (%):

	1, 100	5, 100
Texture:		
Sand	5	4
Silt	34	25
Clay	56	70
Composition:		
Quartz	1	—
Clay and silica[a]	56	70
Pyrite	1	1
Carbonate unspec.	2	—
Foraminifers	5	4
Calc. nannofossils	35	25

[a] See Core 36 (*lithologic description)

ORGANIC CARBON AND CARBONATE (%):

	4, 75–79
Organic carbon	—
Carbonate	26

SITE 612 HOLE CORE 44X CORED INTERVAL 395.6–405.2 m

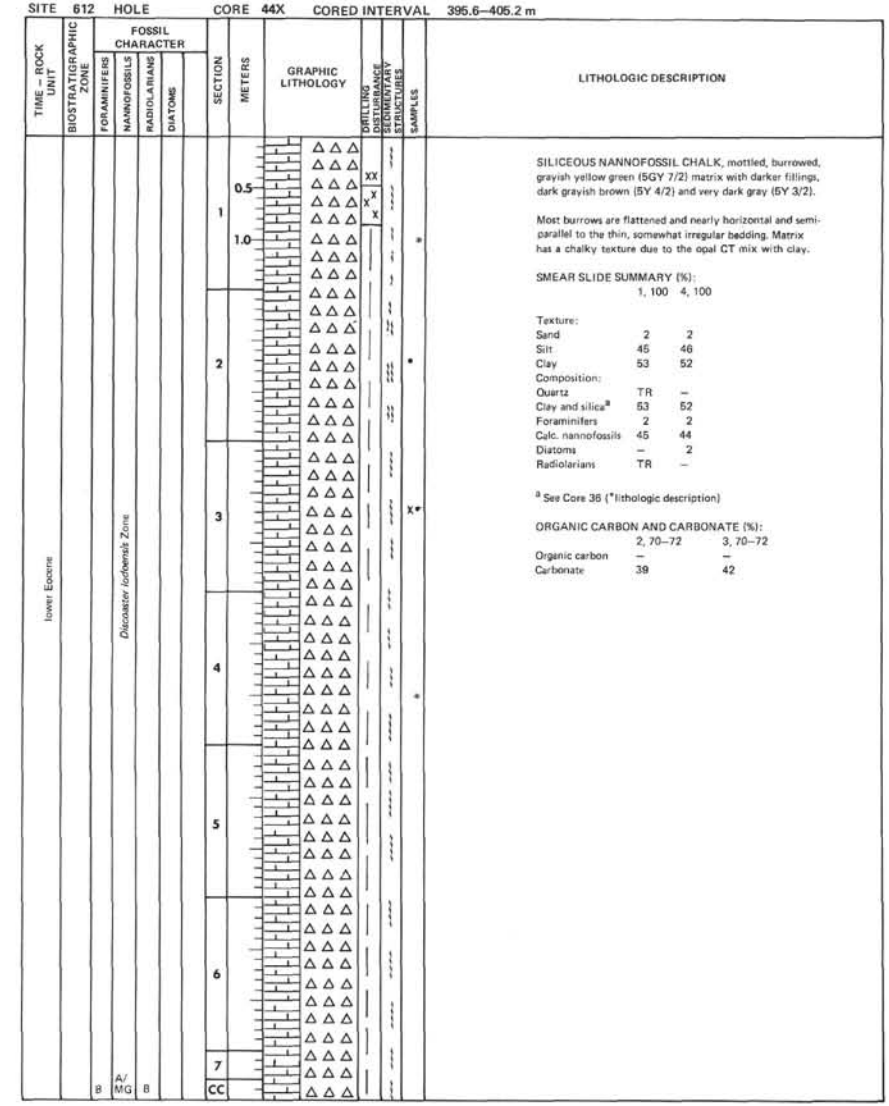

LITHOLOGIC DESCRIPTION

SILICEOUS NANNOFOSSIL CHALK, mottled, burrowed, grayish yellow green (5GY 7/2) matrix with darker fillings, dark grayish brown (5Y 4/2) and very dark gray (5Y 3/2).

Most burrows are flattened and nearly horizontal and semi-parallel to the thin, somewhat irregular bedding. Matrix has a chalky texture due to the opal CT mix with clay.

SMEAR SLIDE SUMMARY (%):

	1, 100	4, 100
Texture:		
Sand	2	2
Silt	45	46
Clay	53	52
Composition:		
Quartz	TR	—
Clay and silica[a]	53	52
Foraminifers	2	2
Calc. nannofossils	45	44
Diatoms	—	2
Radiolarians	TR	—

[a] See Core 36 (*lithologic description)

ORGANIC CARBON AND CARBONATE (%):

	2, 70–72	3, 70–72
Organic carbon	—	—
Carbonate	39	42

SITE 612 HOLE CORE 45X CORED INTERVAL 405.2–414.9 m

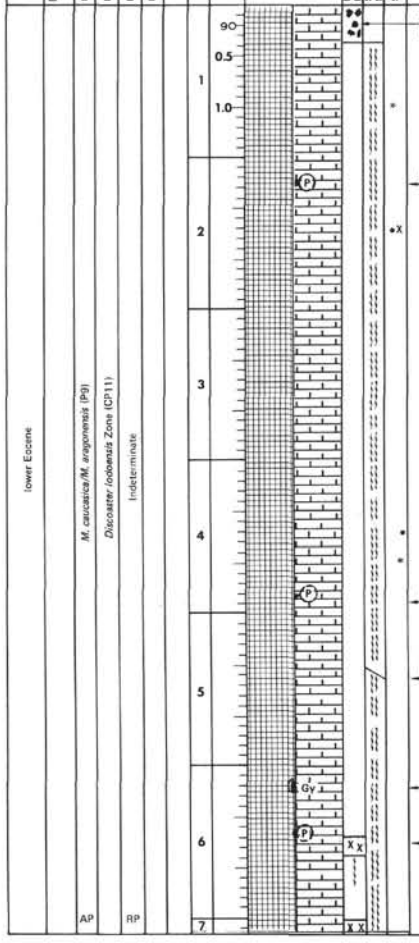

LITHOLOGIC DESCRIPTION

Marcasite/pyrite breccia

SILICEOUS NANNOFOSSIL CHALK, background color is grayish yellow green (5GY 7/2), but moderate burrowing of dark grayish brown (5Y 4/2) and very dark grayish brown (5Y 3/2) gives core an overall darker value; all mottles, burrows are flattened and lens-shaped; very fine sand-sized white specks are visible on split core (forams?); marcasite/pyrite nodules, granules scattered throughout core, and are concentrated in breccia at top of Section 1.

Core is less than 1/2 round, but intact.

Pyrite

Core expands 1 to 4 cm/section within 1/2 hr. after splitting and develops shaley partings.

SMEAR SLIDE SUMMARY (%):

	1, 100	4, 100
	D	D
Texture:		
Sand	8	5
Silt	42	43
Clay	50	52
Composition:		
Quartz	3	1
Clay and silica[a]	45	50
Pyrite	–	TR
Carbonate unspec.	5	4
Foraminifers	5	1
Calc. nannofossils	42	44

[a] See Core 36 (*lithologic description)

ORGANIC CARBON AND CARBONATE (%):

	2, 75–77	4, 75–77
Organic carbon	–	–
Carbonate	44	46

Pyrite

Fault? no indication of throw

Gypsum (?)-filled vein

Pyrite

SITE 612 HOLE CORE 46X CORED INTERVAL 414.9–424.6 m

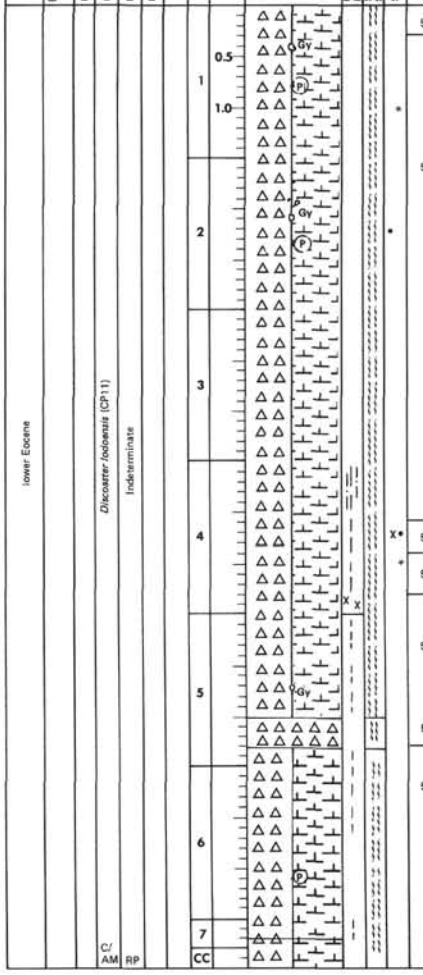

LITHOLOGIC DESCRIPTION

5GY 5/2

SILICEOUS NANNOFOSSIL CHALK, generally grayish yellow green (5GY 7/2), although the top of Section 1 is darker dusky yellow green (5GY 5/2); moderately burrowed with dark grayish brown (5Y 4/2) and very dark grayish brown (5Y 3/2); burrows are flattened, elongated and lens-shaped; similar to Core 45, this one includes:

- very fine sand-size white specks – foraminifers?
- marcasite/pyrite-filled burrows and nodules
- gypsum-filled veins
- expands after splitting

Truncated vertical burrows or dewatering veins suggest bottom currents.

5GY 7/2

PORCELLANITE: Section 5, 100–130 cm light greenish gray (5GY 8/1); hard; burrows are much less flattened and are very well preserved.

SMEAR SLIDE SUMMARY (%):

	1, 100	4, 100
	D	D
Texture:		
Sand	3	10
Silt	45	45
Clay	52	45
Composition:		
Quartz	TR	1
Clay and silica[a]	52	42
Palagonite	–	TR
Pyrite	TR	–
Carbonate unspec.	–	4
Foraminifers	3	6
Calc. nannofossils	45	47
Fish remains	–	TR

[a] See Core 36 (*lithologic description)

5GY 8/1

5GY 5/2

ORGANIC CARBON AND CARBONATE (%):

	2, 75–77	4, 75–77
Organic carbon	0.26	–
Carbonate	44	52

5GY 7/2

5GY 8/1

5GY 7/2

SITE 612 HOLE CORE 47X CORED INTERVAL 424.6–434.3 m

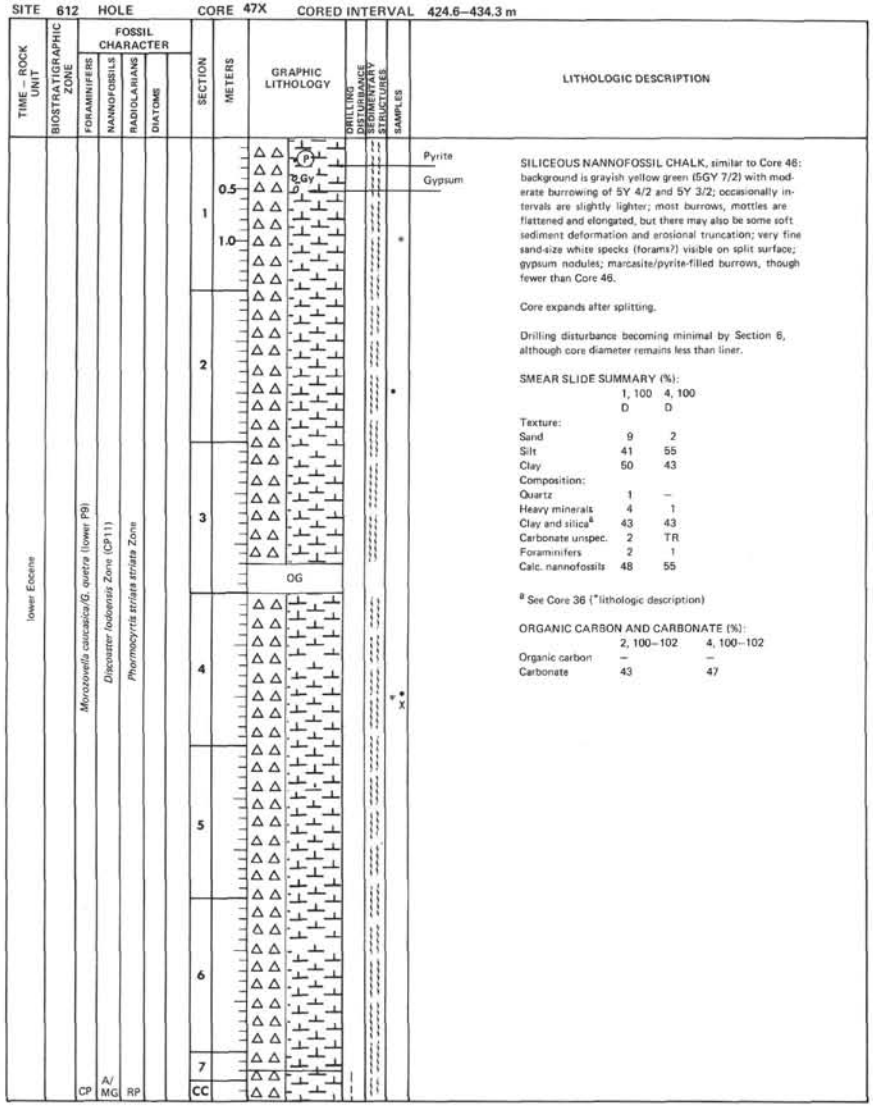

SILICEOUS NANNOFOSSIL CHALK, similar to Core 46: background is grayish yellow green (5GY 7/2) with moderate burrowing of 5Y 4/2 and 5Y 3/2; occasionally intervals are slightly lighter; most burrows, mottles are flattened and elongated, but there may also be some soft sediment deformation and erosional truncation; very fine sand-size white specks (forams?) visible on split surface; gypsum nodules; marcasite/pyrite-filled burrows, though fewer than Core 46.

Core expands after splitting.

Drilling disturbance becoming minimal by Section 6, although core diameter remains less than liner.

SMEAR SLIDE SUMMARY (%):

	1, 100	4, 100
	D	D
Texture:		
Sand	9	2
Silt	41	55
Clay	50	43
Composition:		
Quartz	1	–
Heavy minerals	4	1
Clay and silica[a]	43	43
Carbonate unspec.	2	TR
Foraminifers	2	1
Calc. nannofossils	48	55

[a] See Core 36 (*lithologic description)

ORGANIC CARBON AND CARBONATE (%):

	2, 100–102	4, 100–102
Organic carbon	–	–
Carbonate	43	47

SITE 612 HOLE CORE 48X CORED INTERVAL 434.3–444.0 m

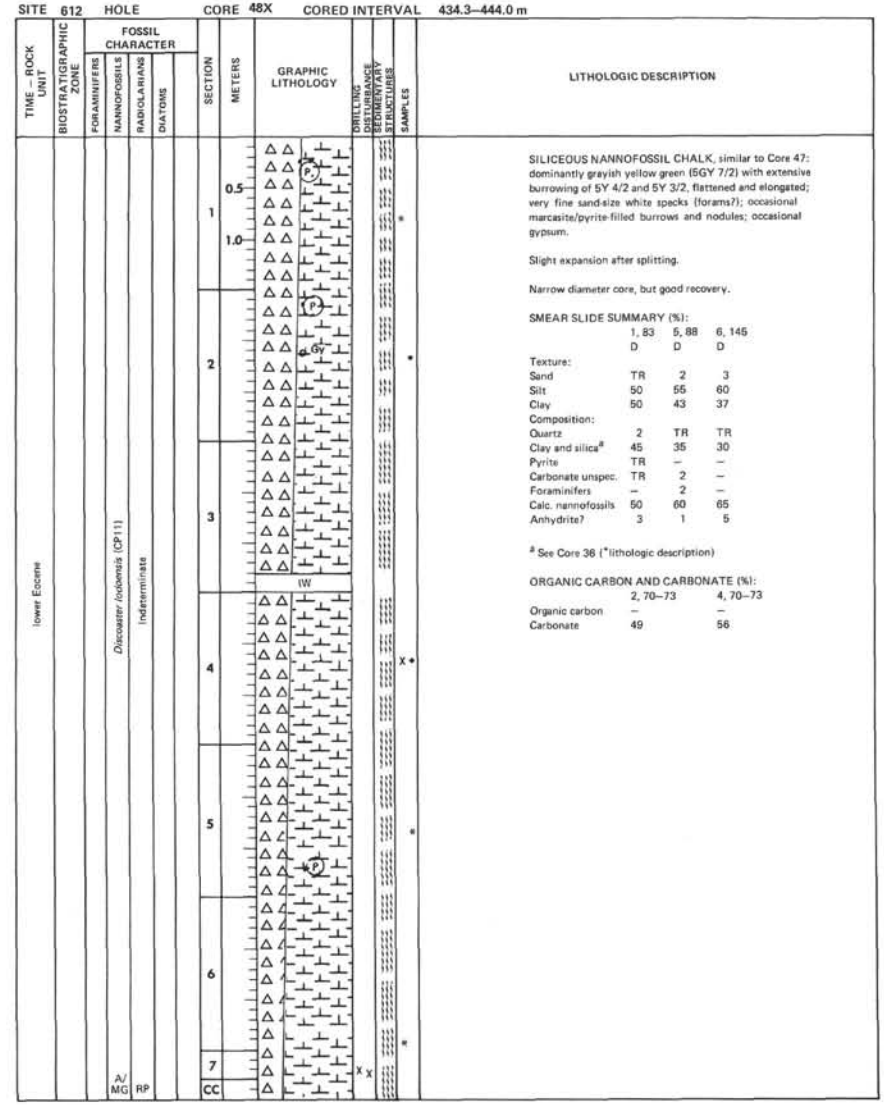

SILICEOUS NANNOFOSSIL CHALK, similar to Core 47: dominantly grayish yellow green (5GY 7/2) with extensive burrowing of 5Y 4/2 and 5Y 3/2, flattened and elongated; very fine sand-size white specks (forams?); occasional marcasite/pyrite-filled burrows and nodules; occasional gypsum.

Slight expansion after splitting.

Narrow diameter core, but good recovery.

SMEAR SLIDE SUMMARY (%):

	1, 83	5, 88	6, 145
	D	D	D
Texture:			
Sand	TR	2	3
Silt	50	55	60
Clay	50	43	37
Composition:			
Quartz	2	TR	TR
Clay and silica[a]	45	35	30
Pyrite	TR	–	–
Carbonate unspec.	TR	2	–
Foraminifers	–	2	–
Calc. nannofossils	50	60	65
Anhydrite?	3	1	5

[a] See Core 36 (*lithologic description)

ORGANIC CARBON AND CARBONATE (%):

	2, 70–73	4, 70–73
Organic carbon	–	–
Carbonate	49	56

SITE 612 HOLE CORE 49X CORED INTERVAL 444.0–453.7 m

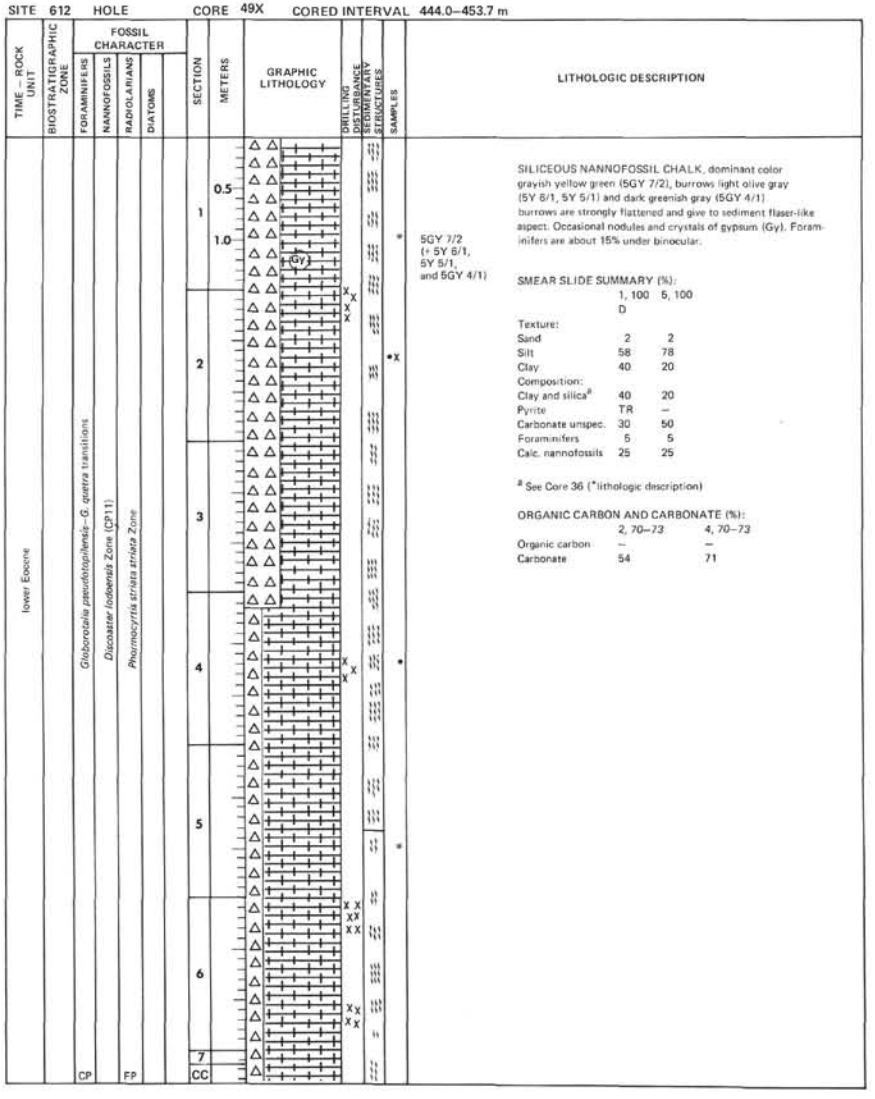

SITE 612 HOLE CORE 50X CORED INTERVAL 453.7–463.4 m

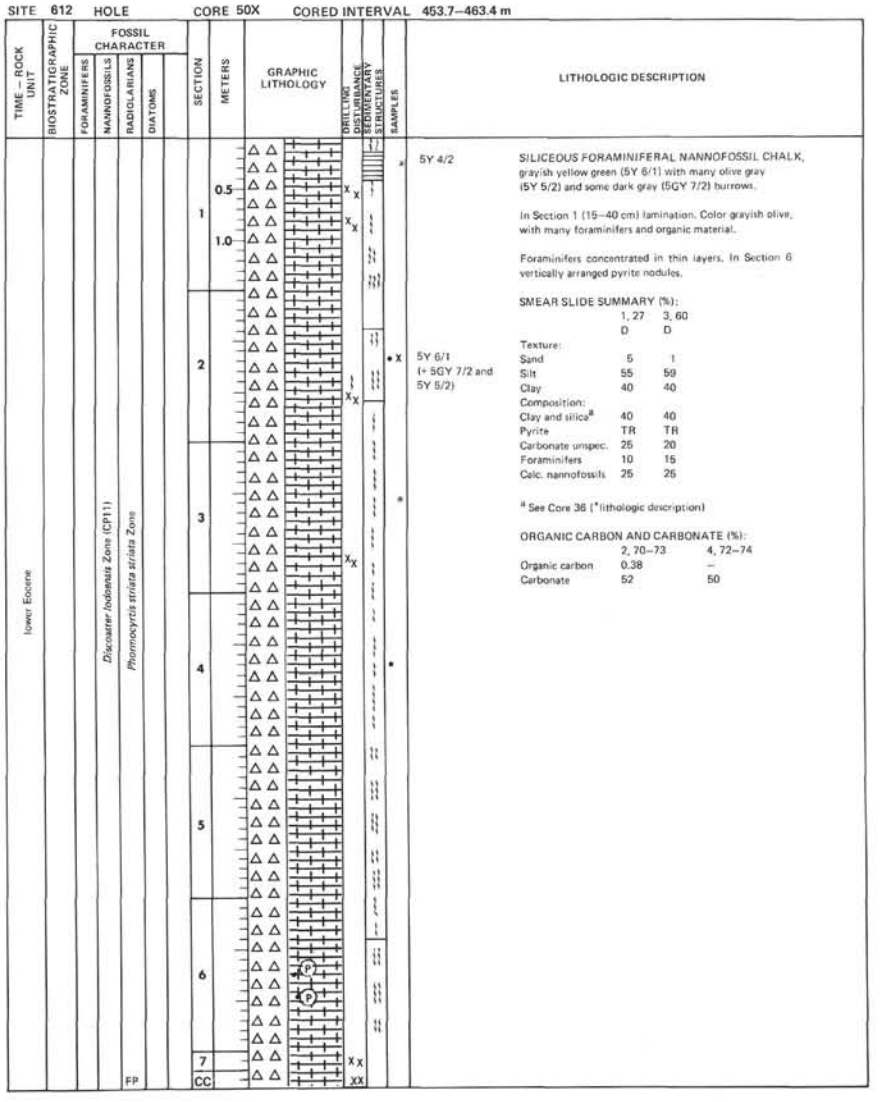

SITE 612 HOLE CORE 51X CORED INTERVAL 463.4–473.1 m

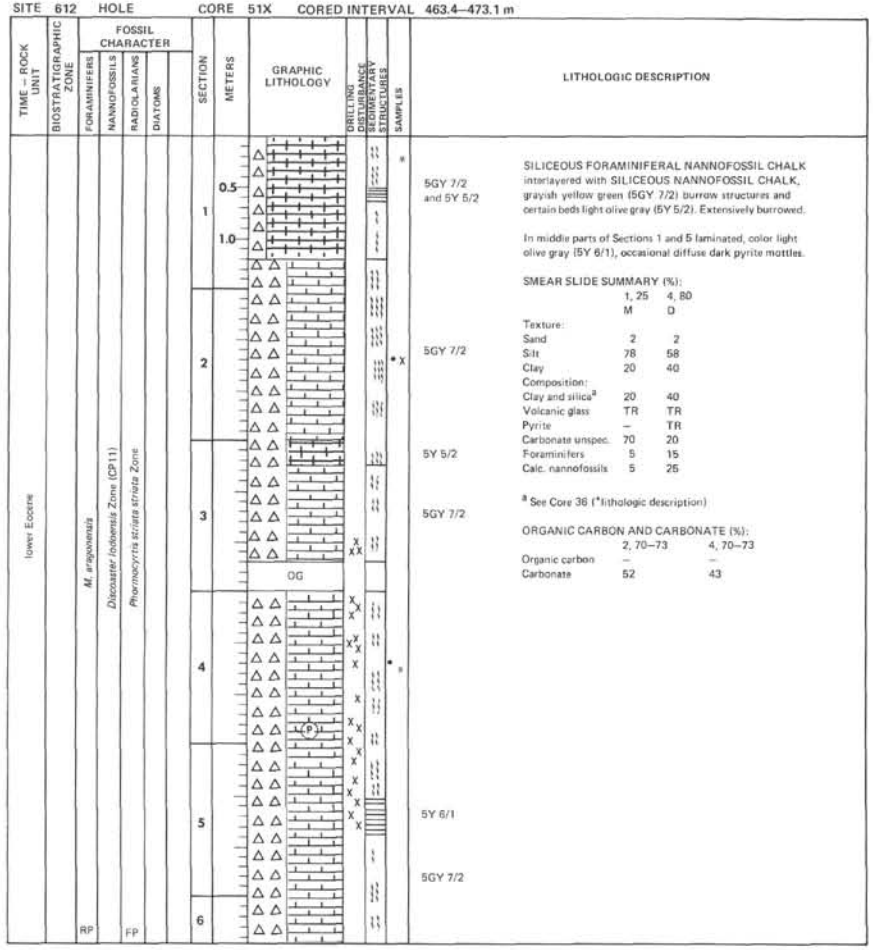

LITHOLOGIC DESCRIPTION

SILICEOUS FORAMINIFERAL NANNOFOSSIL CHALK interlayered with SILICEOUS NANNOFOSSIL CHALK, grayish yellow green (5GY 7/2) burrow structures and certain beds light olive gray (5Y 5/2). Extensively burrowed.

In middle parts of Sections 1 and 5 laminated, color light olive gray (5Y 6/1), occasional diffuse dark pyrite mottles.

SMEAR SLIDE SUMMARY (%):

	1, 25	4, 80
	M	D
Texture:		
Sand	2	2
Silt	78	58
Clay	20	40
Composition:		
Clay and silica[a]	20	40
Volcanic glass	TR	TR
Pyrite	–	TR
Carbonate unspec.	70	20
Foraminifers	5	15
Calc. nannofossils	5	25

[a] See Core 36 (*lithologic description)

ORGANIC CARBON AND CARBONATE (%):

	2, 70–73	4, 70–73
Organic carbon	–	–
Carbonate	52	43

SITE 612 HOLE CORE 52X CORED INTERVAL 473.1–482.8 m

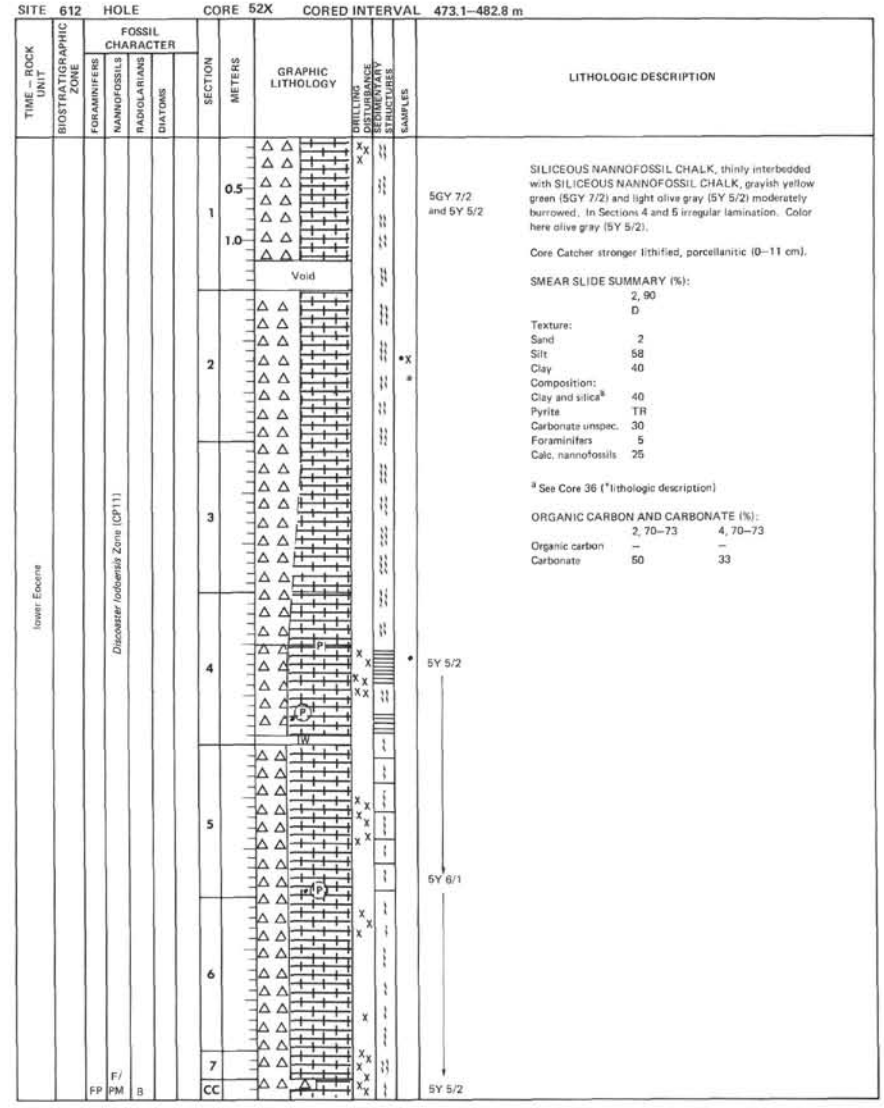

LITHOLOGIC DESCRIPTION

SILICEOUS NANNOFOSSIL CHALK, thinly interbedded with SILICEOUS NANNOFOSSIL CHALK, grayish yellow green (5GY 7/2) and light olive gray (5Y 5/2) moderately burrowed. In Sections 4 and 5 irregular lamination. Color here olive gray (5Y 5/2).

Core Catcher stronger lithified, porcellanitic (0–11 cm).

SMEAR SLIDE SUMMARY (%):

	2, 90
	D
Texture:	
Sand	2
Silt	58
Clay	40
Composition:	
Clay and silica[a]	40
Pyrite	TR
Carbonate unspec.	30
Foraminifers	5
Calc. nannofossils	25

[a] See Core 36 (*lithologic description)

ORGANIC CARBON AND CARBONATE (%):

	2, 70–73	4, 70–73
Organic carbon	–	–
Carbonate	50	33

SITE 612 HOLE CORE 53X CORED INTERVAL 482.8–492.5 m

TIME – ROCK UNIT	BIOSTRATIGRAPHIC ZONE	FOSSIL CHARACTER: FORAMINIFERS	NANNOFOSSILS	RADIOLARIANS	DIATOMS	SECTION	METERS	GRAPHIC LITHOLOGY	DRILLING DISTURBANCE	SEDIMENTARY STRUCTURES	SAMPLES	LITHOLOGIC DESCRIPTION
lower Eocene	*M. angoniensis*	FP	*Discoaster lodoensis* Zone (CP11)	FP Indeterminate		1, CC			X X X		*	5GY 7/2 and 5Y 5/2

SILICEOUS NANNOFOSSIL CHALK, grayish yellow green (5GY 7/2) with flattened olive gray (5Y 5/2) burrows. Irregularly laminated.

SMEAR SLIDE SUMMARY (%):

	1, 20 D
Texture:	
Sand	2
Silt	58
Clay	40
Composition:	
Quartz	5
Clay and silica[a]	30
Pyrite	1
Carbonate unspec.	12
Foraminifers	2
Calc. nannofossils	50

[a] See Core 36 (*lithologic description)

SITE 612 HOLE CORE 54X CORED INTERVAL 492.5–502.0 m

TIME – ROCK UNIT	BIOSTRATIGRAPHIC ZONE	FOSSIL CHARACTER: FORAMINIFERS	NANNOFOSSILS	RADIOLARIANS	DIATOMS	SECTION	METERS	GRAPHIC LITHOLOGY	DRILLING DISTURBANCE	SEDIMENTARY STRUCTURES	SAMPLES	LITHOLOGIC DESCRIPTION
lower Eocene	*M. angoniensis*	RP	*Discoaster lodoensis* Zone (CP11) CM	*Phormocyrtis striata striata* Zone RP		1	0.5, 1.0				*	5GY 7/2 and 5Y 5/2
						2					• X *	5Y 5/2 only
						3					•	5GY 7/2 and 5Y 5/2
						4						
						5					*	5GY 5/2
						CC			X X X			5GY 5/2

SILICEOUS FORAMINIFERAL NANNOFOSSIL CHALK, Section 1, 2, 3, 4 and 5, → 38 cm) and SILICEOUS NANNOFOSSIL CHALK (Section 5, 38–110 cm and Core Catcher).

Irregular and discontinuous thin bedding. At Section 3, 5, and Core Catcher, parallel, thin laminated bedding.

Interlayered (Section 1 → Section 5, 38 cm):
grayish yellow green (5GY 7/2)
light olive gray (5Y 5/2).

Dusky yellow green (5GY 5/2) at Section 5, 38 cm → Core Catcher).

Bioturbation:
many flattened burrows early horizontal (subparallel to bedding)
sporadic oblique or vertical burrows
some burrows are filled with pyrite

SMEAR SLIDE SUMMARY (%):

	1, 110 D	2, 80 D	5, 85 D
Texture:			
Sand	5	20	1
Silt	30	30	40
Clay	65	50	59
Composition:			
Quartz	TR	–	–
Heavy minerals	–	TR	–
Clay and silica[a]	60	50	55
Zeolite	–	3	–
Carbonate unspec.	5	–	–
Foraminifers	10	15	1
Calc. nannofossils	25	29	44
Radiolarians	TR	3	TR

[a] See Core 36 (*lithologic description)

ORGANIC CARBON AND CARBONATE (%):

	2, 70–73	3, 70–73
Organic carbon	–	0.22
Carbonate	29	39

SITE 612 HOLE CORE 55X CORED INTERVAL 502.0–511.5 m

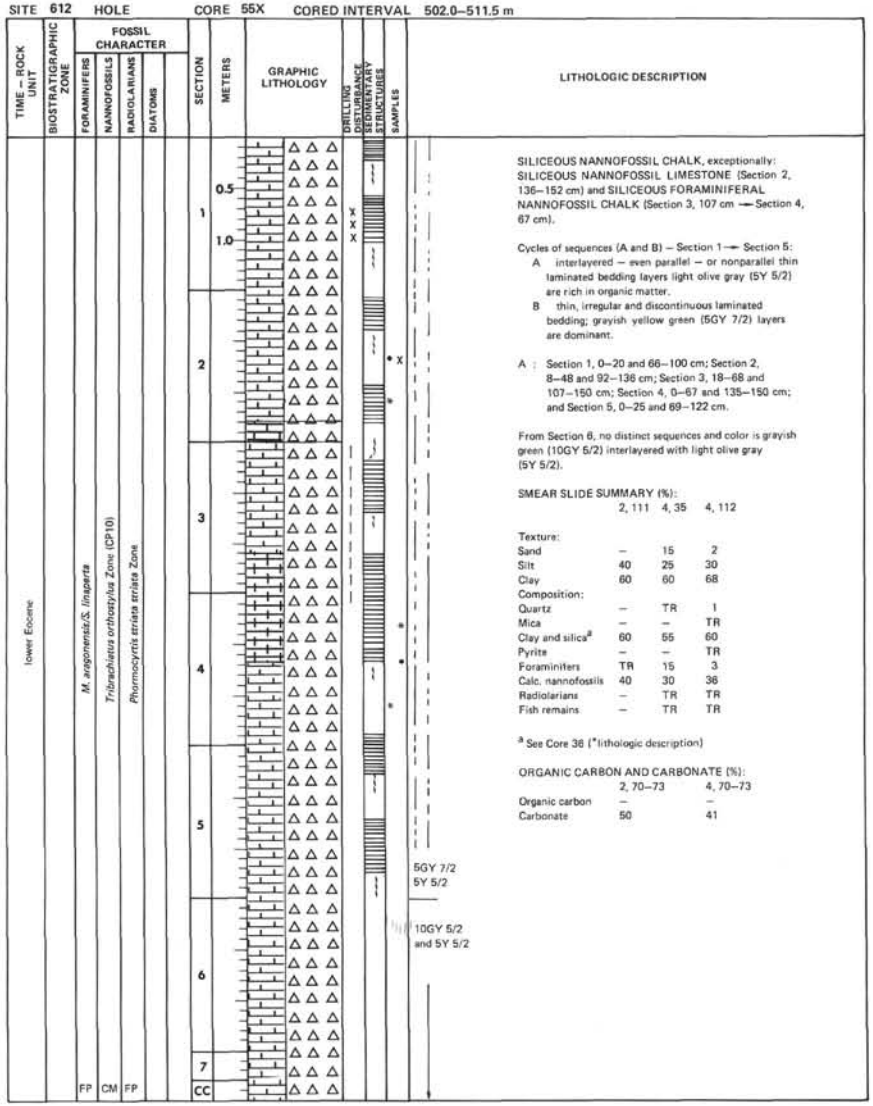

LITHOLOGIC DESCRIPTION

SILICEOUS NANNOFOSSIL CHALK, exceptionally: SILICEOUS NANNOFOSSIL LIMESTONE (Section 2, 136–152 cm) and SILICEOUS FORAMINIFERAL NANNOFOSSIL CHALK (Section 3, 107 cm — Section 4, 67 cm).

Cycles of sequences (A and B) – Section 1 → Section 5:

A interlayered – even parallel – or nonparallel thin laminated bedding layers light olive gray (5Y 5/2) are rich in organic matter.

B thin, irregular and discontinuous laminated bedding; grayish yellow green (5GY 7/2) layers are dominant.

A : Section 1, 0–20 and 66–100 cm; Section 2, 8–48 and 92–136 cm; Section 3, 18–68 and 107–150 cm; Section 4, 0–67 and 135–150 cm; and Section 5, 0–25 and 69–122 cm.

From Section 6, no distinct sequences and color is grayish green (10GY 5/2) interlayered with light olive gray (5Y 5/2).

SMEAR SLIDE SUMMARY (%):

	2, 111	4, 35	4, 112
Texture:			
Sand	–	15	2
Silt	40	25	30
Clay	60	60	68
Composition:			
Quartz	–	TR	1
Mica	–	–	TR
Clay and silica[a]	60	55	60
Pyrite	–	–	TR
Foraminifers	TR	15	3
Calc. nannofossils	40	30	36
Radiolarians	–	TR	TR
Fish remains	–	TR	TR

[a] See Core 36 (*lithologic description)

ORGANIC CARBON AND CARBONATE (%):

	2, 70–73	4, 70–73
Organic carbon	–	–
Carbonate	50	41

SITE 612 HOLE CORE 56X CORED INTERVAL 511.5–521.0 m

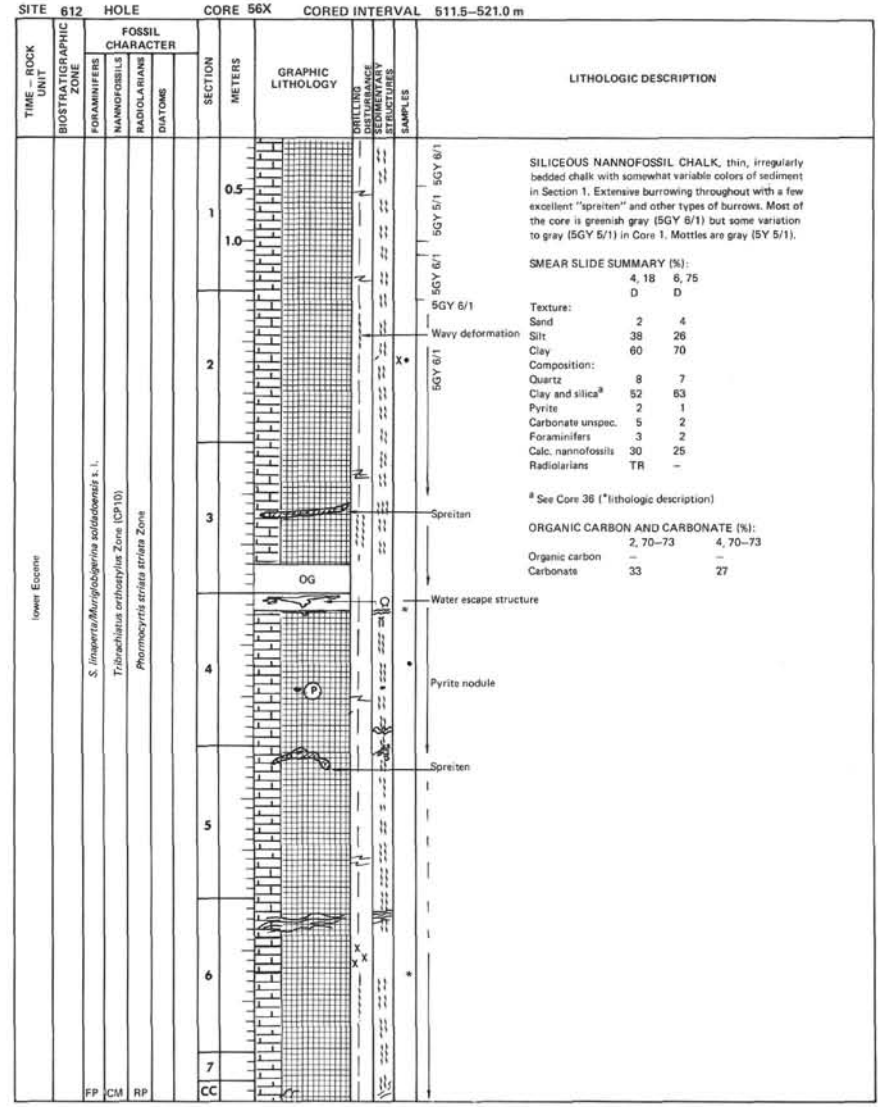

LITHOLOGIC DESCRIPTION

SILICEOUS NANNOFOSSIL CHALK, thin, irregularly bedded chalk with somewhat variable colors of sediment in Section 1. Extensive burrowing throughout with a few excellent "spreiten" and other types of burrows. Most of the core is greenish gray (5GY 6/1) but some variation to gray (5GY 5/1) in Core 1. Mottles are gray (5Y 5/1).

SMEAR SLIDE SUMMARY (%):

	4, 18	6, 75
	D	D
Texture:		
Sand	2	4
Silt	38	26
Clay	60	70
Composition:		
Quartz	8	7
Clay and silica[a]	52	63
Pyrite	2	1
Carbonate unspec.	5	2
Foraminifers	3	2
Calc. nannofossils	30	25
Radiolarians	TR	–

[a] See Core 36 (*lithologic description)

ORGANIC CARBON AND CARBONATE (%):

	2, 70–73	4, 70–73
Organic carbon	–	–
Carbonate	33	27

SITE 612 HOLE CORE 57X CORED INTERVAL 521.0–530.6 m

TIME – ROCK UNIT	BIOSTRATIGRAPHIC ZONE	FOSSIL CHARACTER: FORAMINIFERS	NANNOFOSSILS	RADIOLARIANS	DIATOMS	SECTION	METERS	GRAPHIC LITHOLOGY	DRILLING DISTURBANCE	SEDIMENTARY STRUCTURES	SAMPLES
lower Eocene	*M. aragonensis/S. linaperta* Tribrachiatus orthostylus Zone (CP10)	FP	AM	B		1, 2, 3, 4, 5, 6, CC	0.5, 1.0				X*

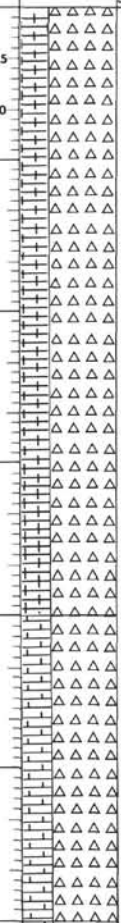

FORAMINIFERAL NANNOFOSSIL PORCELLANITE (Section 1 to Section 4) to NANNOFOSSIL PORCELLANITE (Section 5, 6, and Core Catcher).

Interlayered:
grayish yellow green (5GY 7/2)
light olive gray (5Y 5/2)

Interlayered:
even parallel/discontinuous, irregular thin laminated bedding

Bioturbation:
* numerous flattened burrows
* sporadic oblique or vertical burrows (Section 1, 120 and 135 cm; Section 2, 95 cm; Section 3, 15–25 cm; and Section 4, 30–40 cm) and pyritic nodules

SMEAR SLIDE SUMMARY (%):

	1, 100	5, 100
	D	D
Texture:		
Sand	TR	TR
Silt	30	40
Clay	70	60
Composition:		
Quartz	3	2
Clay and silica[a]	68	68
Pyrite	–	TR
Foraminifers	14	5
Calc. nannofossils	15	25

[a] See Core 36 (*lithologic description)

ORGANIC CARBON AND CARBONATE (%):

	2, 90–92	4, 80–82
Organic carbon	–	–
Carbonate	24	29

SITE 612 HOLE CORE 58X CORED INTERVAL 530.6–540.2 m

TIME – ROCK UNIT	BIOSTRATIGRAPHIC ZONE	FOSSIL CHARACTER: FORAMINIFERS	NANNOFOSSILS	RADIOLARIANS	DIATOMS	SECTION	METERS	GRAPHIC LITHOLOGY	DRILLING DISTURBANCE	SEDIMENTARY STRUCTURES	SAMPLES
lower Eocene	*M. subbotinae/M. aragonensis?* (P7) *Tribrachiatus orthostylus* Zone (CP10) *Burydella clinata* to *Bekoma bidartensis* Zone	FP	AM	FP		CC			X X		*

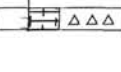

5GY 7/2 and 5Y 5/2

NANNOFOSSIL PORCELLANITE (Core Catcher)

Interlayered:
grayish yellow green (5GY 7/2)
light olive gray (5Y 5/2)

Interlayered:
even, parallel/discontinuous, irregular thin laminated bedding

SMEAR SLIDE SUMMARY (%):

	CC, 15
	D
Texture:	
Sand	TR
Silt	30
Clay	70
Composition:	
Quartz	7
Feldspar	
Clay and Silica[a]	65
Foraminifers	3
Calc. nannofossils	25

[a] See Core 36 (*lithologic description)

SITE 612 HOLE CORE 59X CORED INTERVAL 540.2–549.8 m

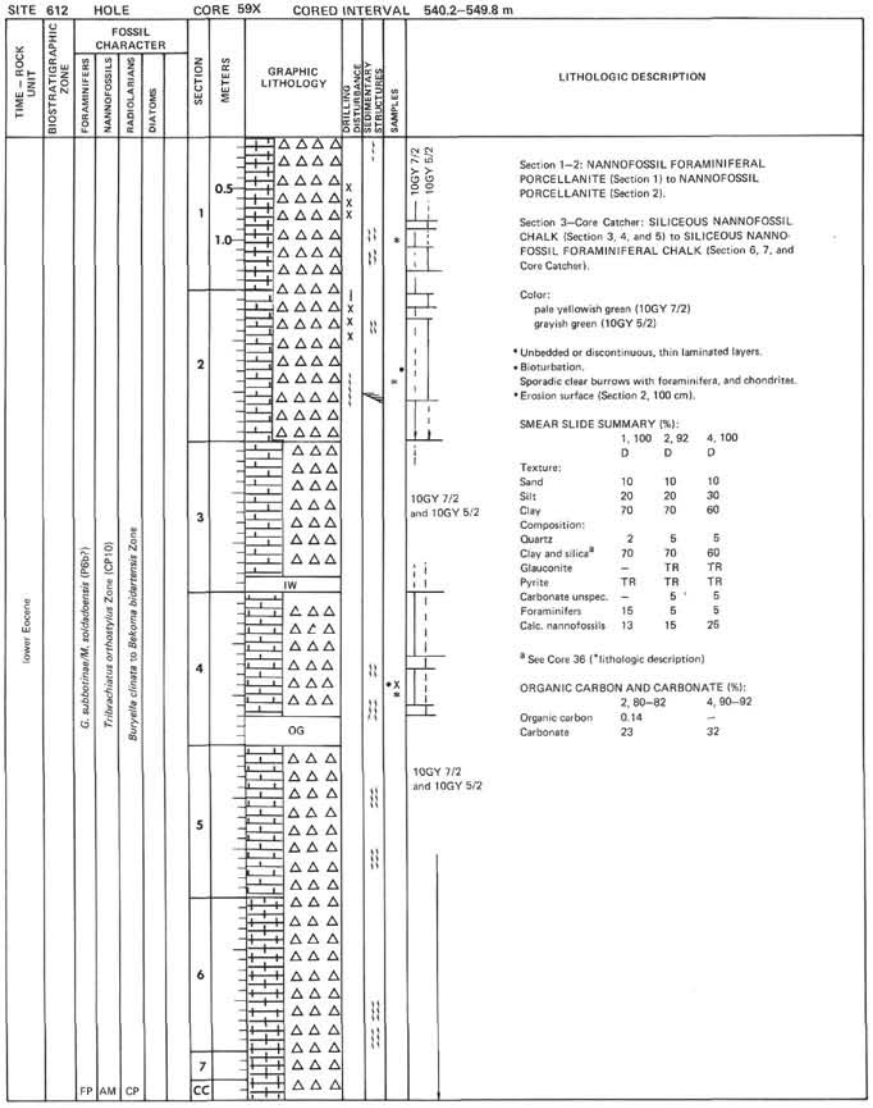

Section 1–2: NANNOFOSSIL FORAMINIFERAL PORCELLANITE (Section 1) to NANNOFOSSIL PORCELLANITE (Section 2).

Section 3–Core Catcher: SILICEOUS NANNOFOSSIL CHALK (Section 3, 4, and 5) to SILICEOUS NANNOFOSSIL FORAMINIFERAL CHALK (Section 6, 7, and Core Catcher).

Color:
pale yellowish green (10GY 7/2)
grayish green (10GY 5/2)

* Unbedded or discontinuous, thin laminated layers.
• Bioturbation.
Sporadic clear burrows with foraminifera, and chondrites.
• Erosion surface (Section 2, 100 cm).

SMEAR SLIDE SUMMARY (%):

	1, 100 D	2, 92 D	4, 100 D
Texture:			
Sand	10	10	10
Silt	20	20	30
Clay	70	70	60
Composition:			
Quartz	2	5	5
Clay and silica[a]	70	70	60
Glauconite	–	TR	TR
Pyrite	TR	TR	TR
Carbonate unspec.	–	5	5
Foraminifers	15	5	5
Calc. nannofossils	13	15	25

[a] See Core 36 (*lithologic description)

ORGANIC CARBON AND CARBONATE (%):

	2, 80–82	4, 90–92
Organic carbon	0.14	–
Carbonate	23	32

SITE 612 HOLE CORE 60X CORED INTERVAL 549.8–559.4 m

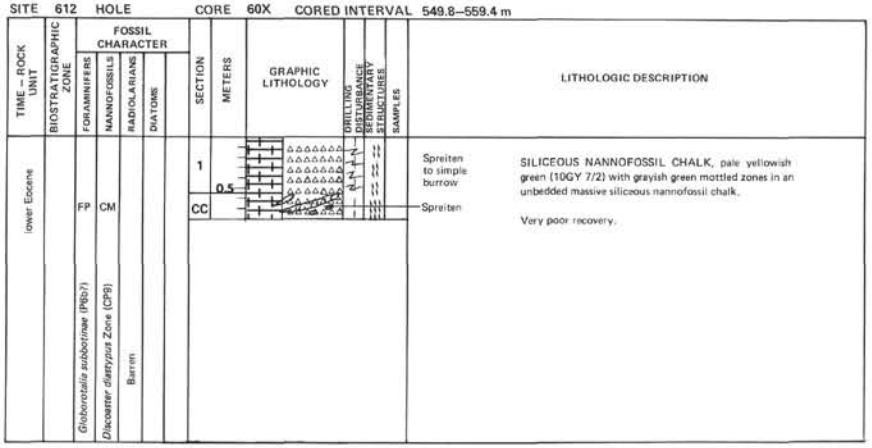

SILICEOUS NANNOFOSSIL CHALK, pale yellowish green (10GY 7/2) with grayish green mottled zones in an unbedded massive siliceous nannofossil chalk.

Very poor recovery.

SITE 612 HOLE CORE 61X CORED INTERVAL 559.4–569.0 m

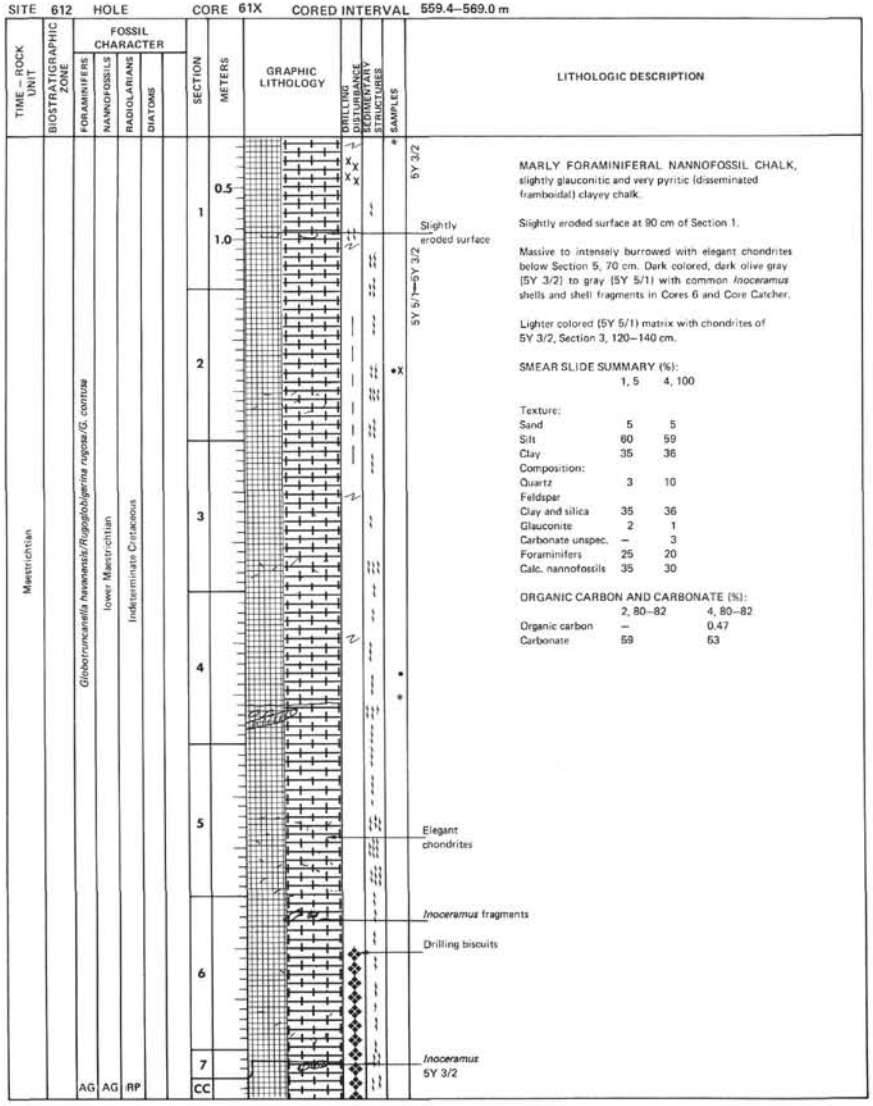

MARLY FORAMINIFERAL NANNOFOSSIL CHALK, slightly glauconitic and very pyritic (disseminated framboidal) clayey chalk.

Slightly eroded surface at 90 cm of Section 1.

Massive to intensely burrowed with elegant chondrites below Section 5, 70 cm. Dark colored, dark olive gray (5Y 3/2) to gray (5Y 5/1) with common *Inoceramus* shells and shell fragments in Cores 6 and Core Catcher.

Lighter colored (5Y 5/1) matrix with chondrites of 5Y 3/2, Section 3, 120–140 cm.

SMEAR SLIDE SUMMARY (%):

	1, 5	4, 100
Texture:		
Sand	5	5
Silt	60	59
Clay	35	36
Composition:		
Quartz	3	10
Feldspar		
Clay and silica	35	36
Glauconite	2	1
Carbonate unspec.	–	3
Foraminifers	25	20
Calc. nannofossils	35	30

ORGANIC CARBON AND CARBONATE (%):

	2, 80–82	4, 80–82
Organic carbon	–	0.47
Carbonate	59	53

SITE 612 HOLE CORE 62X CORED INTERVAL 569.0–578.6 m

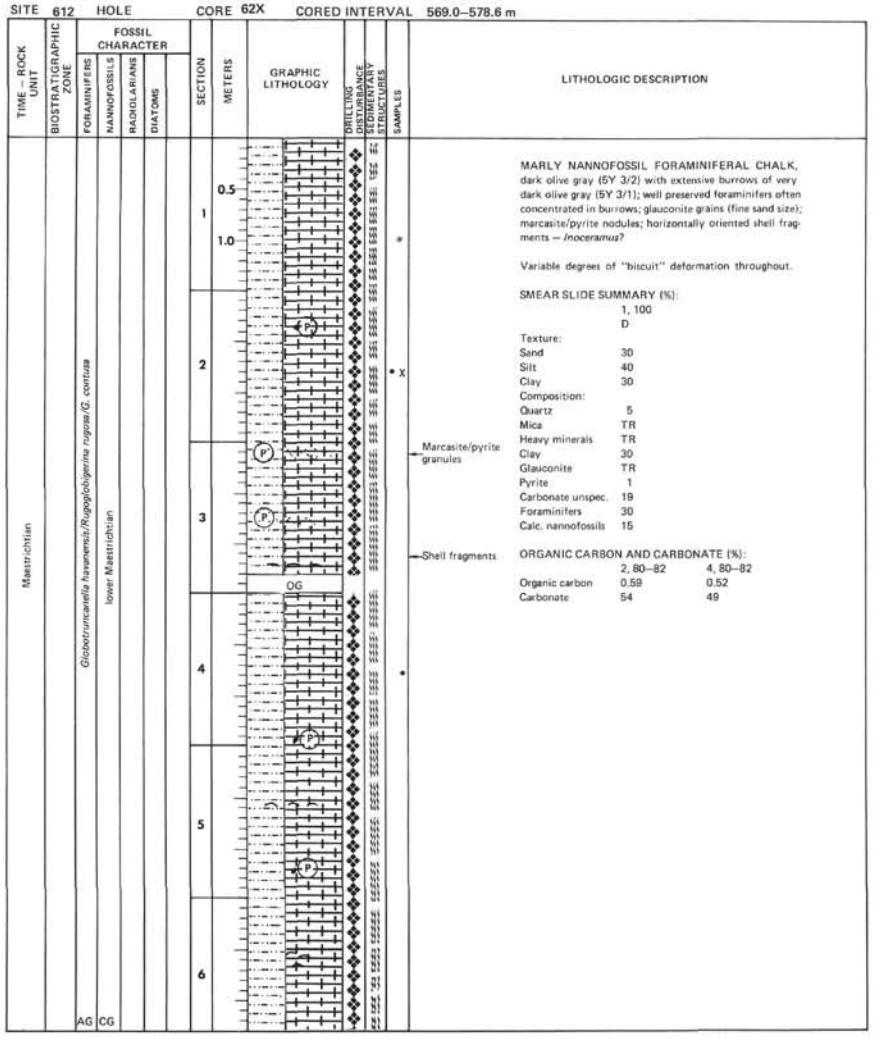

MARLY NANNOFOSSIL FORAMINIFERAL CHALK, dark olive gray (5Y 3/2) with extensive burrows of very dark olive gray (5Y 3/1); well preserved foraminifers often concentrated in burrows; glauconite grains (fine sand size); marcasite/pyrite nodules; horizontally oriented shell fragments – *Inoceramus*?

Variable degrees of "biscuit" deformation throughout.

SMEAR SLIDE SUMMARY (%):

	1, 100
	D
Texture:	
Sand	30
Silt	40
Clay	30
Composition:	
Quartz	5
Mica	TR
Heavy minerals	TR
Clay	30
Glauconite	TR
Pyrite	1
Carbonate unspec.	19
Foraminifers	30
Calc. nannofossils	15

ORGANIC CARBON AND CARBONATE (%):

	2, 80–82	4, 80–82
Organic carbon	0.59	0.52
Carbonate	54	49

SITE 612 HOLE CORE 63X CORED INTERVAL 578.6–588.3 m

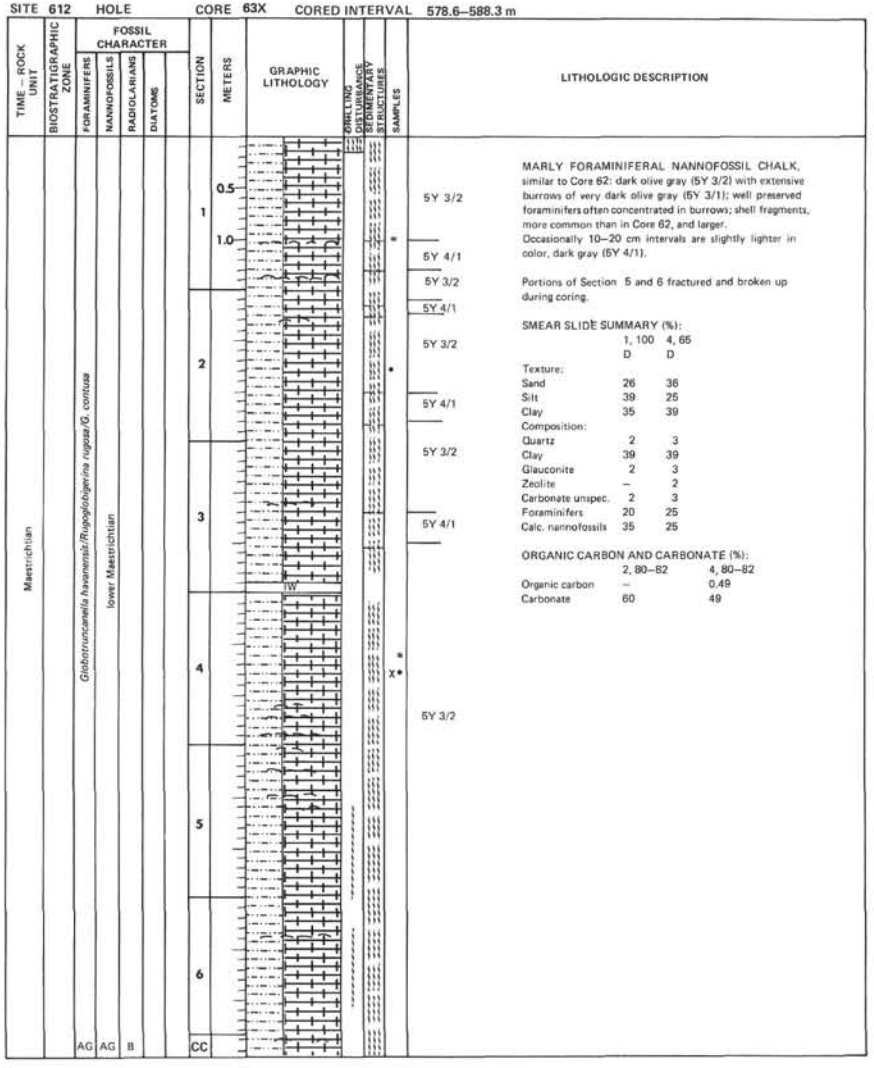

MARLY FORAMINIFERAL NANNOFOSSIL CHALK, similar to Core 62: dark olive gray (5Y 3/2) with extensive burrows of very dark olive gray (5Y 3/1); well preserved foraminifers often concentrated in burrows; shell fragments, more common than in Core 62, and larger. Occasionally 10–20 cm intervals are slightly lighter in color, dark gray (5Y 4/1).

Portions of Section 5 and 6 fractured and broken up during coring.

SMEAR SLIDE SUMMARY (%):

	1, 100	4, 65
	D	D
Texture:		
Sand	26	36
Silt	39	25
Clay	35	39
Composition:		
Quartz	2	3
Clay	39	39
Glauconite	2	3
Zeolite	–	2
Carbonate unspec.	2	3
Foraminifers	20	25
Calc. nannofossils	35	25

ORGANIC CARBON AND CARBONATE (%):

	2, 80–82	4, 80–82
Organic carbon	–	0.49
Carbonate	60	49

SITE 612 HOLE CORE 64X CORED INTERVAL 588.3–598.0 m

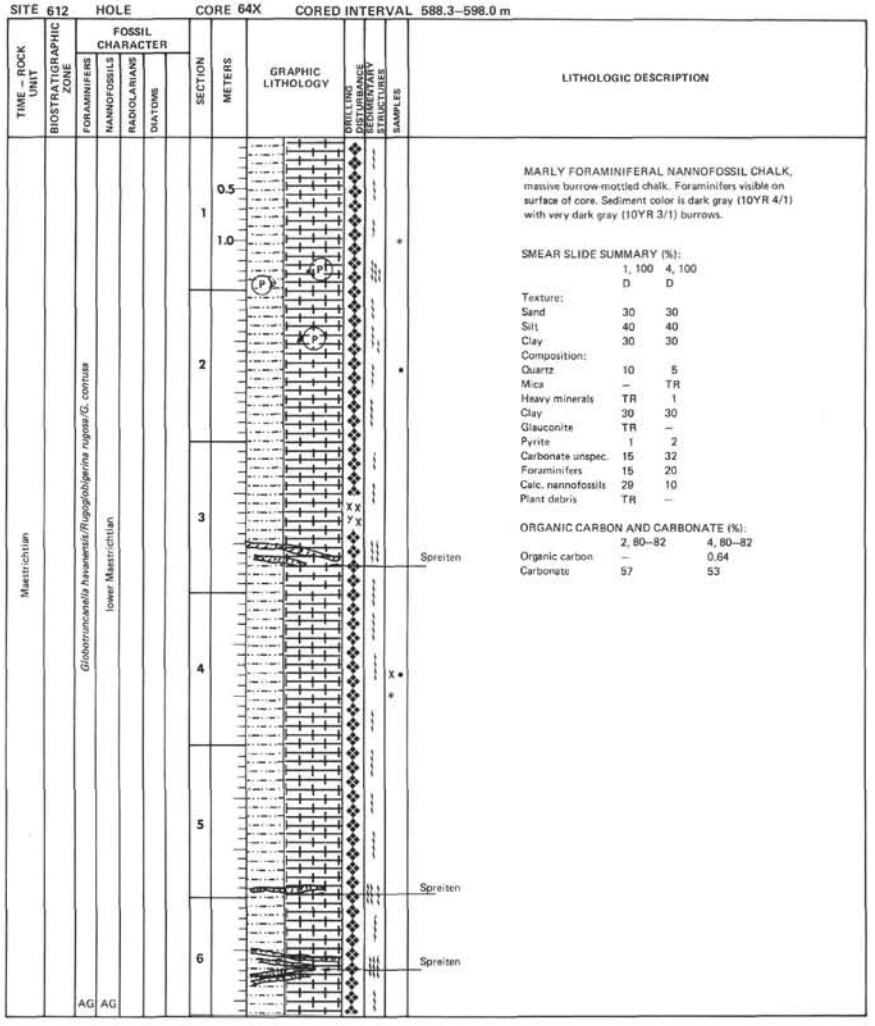

MARLY FORAMINIFERAL NANNOFOSSIL CHALK, massive burrow-mottled chalk. Foraminifers visible on surface of core. Sediment color is dark gray (10YR 4/1) with very dark gray (10YR 3/1) burrows.

SMEAR SLIDE SUMMARY (%):

	1, 100	4, 100
	D	D
Texture:		
Sand	30	30
Silt	40	40
Clay	30	30
Composition:		
Quartz	10	5
Mica	–	TR
Heavy minerals	TR	1
Clay	30	30
Glauconite	TR	–
Pyrite	1	2
Carbonate unspec.	15	32
Foraminifers	15	20
Calc. nannofossils	29	10
Plant debris	TR	–

ORGANIC CARBON AND CARBONATE (%):

	2, 80–82	4, 80–82
Organic carbon	–	0.64
Carbonate	57	53

SITE 612 HOLE CORE 65X CORED INTERVAL 598.0–607.7 m

TIME – ROCK UNIT	BIOSTRATIGRAPHIC ZONE	FOSSIL CHARACTER: FORAMINIFERS	NANNOFOSSILS	RADIOLARIANS	DIATOMS	SECTION	METERS	GRAPHIC LITHOLOGY	DRILLING DISTURBANCE	SEDIMENTARY STRUCTURES	SAMPLES	LITHOLOGIC DESCRIPTION
Maestrichtian	*Globotruncanella havanensis/Rugoglobigerina rugosa/G. gansseri/G. contusa*	AG	AG lower Maestrichtian			1, 2, CC	0.5, 1.0				*	10YR 4/1 (+10YR 5/1 and 10YR 3/1); 10YR 4/1

MARLY FORAMINIFERAL NANNOFOSSIL CHALK, main color is dark gray (10YR 4/1) with lighter gray (10YR 5/1) and very dark gray (10YR 3/1) streaks, mottles, and burrows. Arenitic shell fragments.

SMEAR SLIDE SUMMARY (%):

	1, 114 D
Texture:	
Sand	20
Silt	50
Clay	30
Composition:	
Quartz	4
Mica	TR
Heavy minerals	TR
Clay	30
Pyrite	1
Zeolite	TR
Carbonate unspec.	40
Foraminifers	10
Calc. nannofossils	15

SITE 612 HOLE CORE 66X CORED INTERVAL 607.7–617.3 m

TIME – ROCK UNIT	BIOSTRATIGRAPHIC ZONE	FOSSIL CHARACTER: FORAMINIFERS	NANNOFOSSILS	RADIOLARIANS	DIATOMS	SECTION	METERS	GRAPHIC LITHOLOGY	DRILLING DISTURBANCE	SEDIMENTARY STRUCTURES	SAMPLES	LITHOLOGIC DESCRIPTION
Maestrichtian	*Globotruncanella havanensis/Rugoglobigerina rugosa/G. contusa*	AG	AG	B lower Maestrichtian		1, 2, 3, 4, 5, 6, 7, CC	0.5, 1.0				*	10YR 4/1 (+10YR 5/1 and 10YR 3/1)

MARLY FORAMINIFERAL NANNOFOSSIL CHALK, dark gray (10YR 4/1), intensively burrowed. Burrows darker gray (10 YR 3/1) or light gray (10YR 5/1). Burrows are mainly diagonal spreiten and chondrites. Large *Inoceramus* shell fragments over all the core, sometimes concentrated in cm-thick layers as in Section 6 (10 cm). Frequent small pyrite and marcasite nodules.

SMEAR SLIDE SUMMARY (%):

	2, 74 M	4, 105 D
Texture:		
Sand	20	20
Silt	50	50
Clay	30	30
Composition:		
Quartz	5	5
Mica	TR	TR
Heavy minerals	TR	TR
Clay	30	30
Glauconite	TR	–
Pyrite	1	1
Zeolite	TR	1
Carbonate unspec.	34	33
Foraminifers	15	15
Calc. nannofossils	15	15
Plant debris	TR	–

ORGANIC CARBON AND CARBONATE (%):

	2, 70–73	4, 70–73
Organic carbon	0.50	0.73
Carbonate	55	46

SITE 612 HOLE CORE 67X CORED INTERVAL 617.3–626.9 m

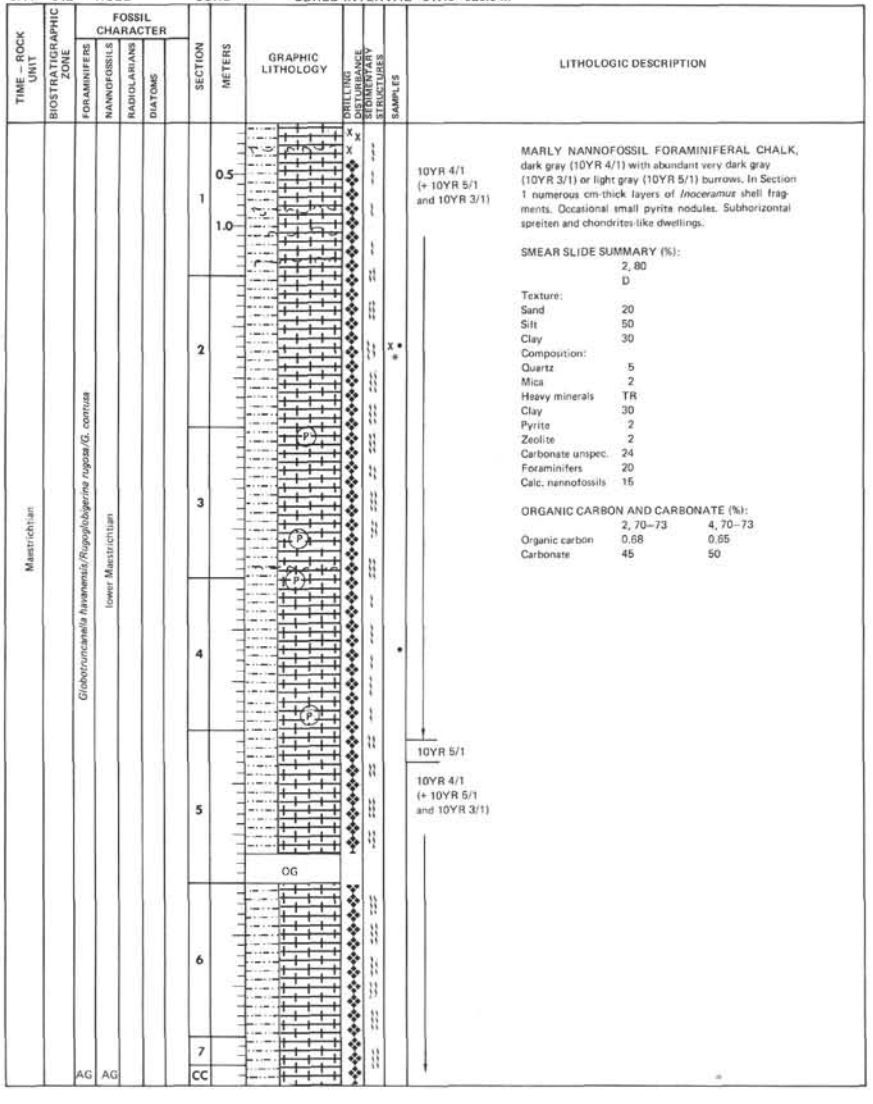

LITHOLOGIC DESCRIPTION

MARLY NANNOFOSSIL FORAMINIFERAL CHALK, dark gray (10YR 4/1) with abundant very dark gray (10YR 3/1) or light gray (10YR 5/1) burrows. In Section 1 numerous cm-thick layers of *Inoceramus* shell fragments. Occasional small pyrite nodules. Subhorizontal spreiten and chondrites-like dwellings.

SMEAR SLIDE SUMMARY (%):

	2, 80
	D
Texture:	
Sand	20
Silt	50
Clay	30
Composition:	
Quartz	5
Mica	2
Heavy minerals	TR
Clay	30
Pyrite	2
Zeolite	2
Carbonate unspec.	24
Foraminifers	20
Calc. nannofossils	15

ORGANIC CARBON AND CARBONATE (%):

	2, 70–73	4, 70–73
Organic carbon	0.68	0.65
Carbonate	45	50

SITE 612 HOLE CORE 68X CORED INTERVAL 626.9–636.5 m

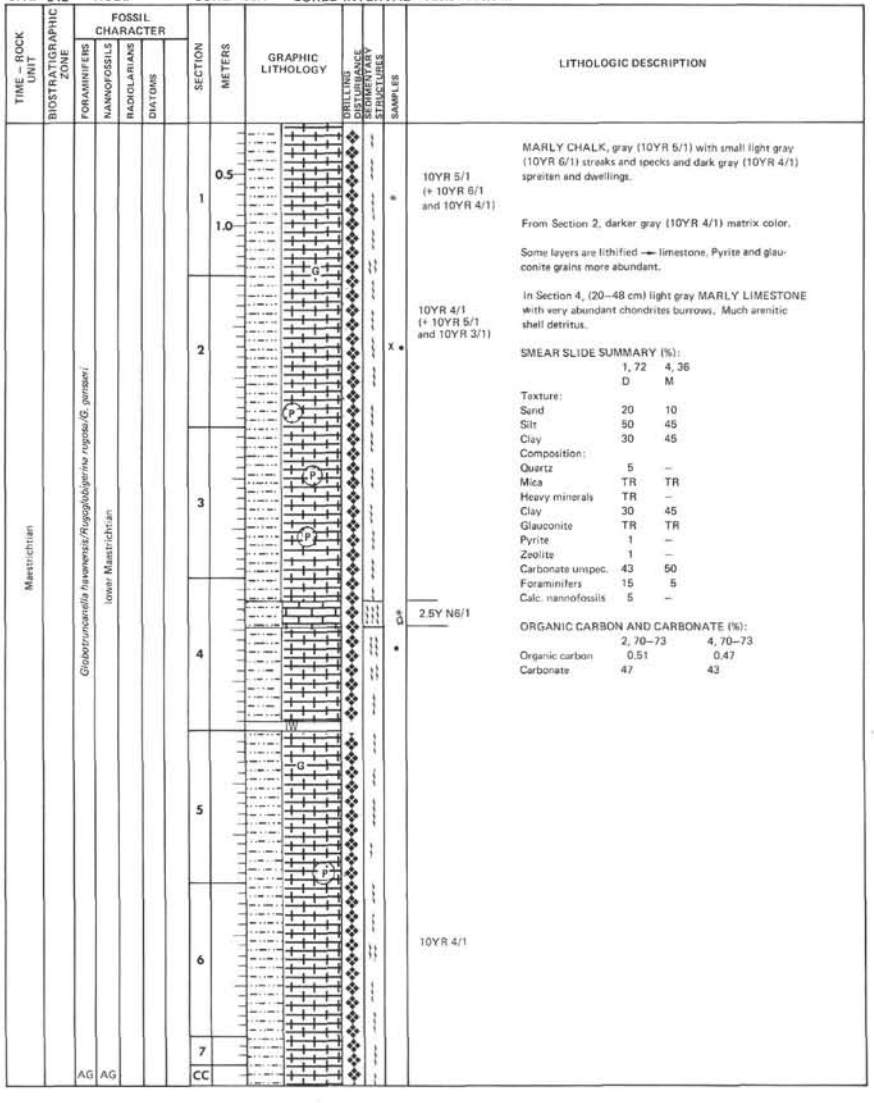

LITHOLOGIC DESCRIPTION

MARLY CHALK, gray (10YR 5/1) with small light gray (10YR 6/1) streaks and specks and dark gray (10YR 4/1) spreiten and dwellings.

From Section 2, darker gray (10YR 4/1) matrix color.

Some layers are lithified → limestone. Pyrite and glauconite grains more abundant.

In Section 4, (20–48 cm) light gray MARLY LIMESTONE with very abundant chondrites burrows. Much arenitic shell detritus.

SMEAR SLIDE SUMMARY (%):

	1, 72	4, 36
	D	M
Texture:		
Sand	20	10
Silt	50	45
Clay	30	45
Composition:		
Quartz	5	–
Mica	TR	TR
Heavy minerals	TR	–
Clay	30	45
Glauconite	TR	TR
Pyrite	1	–
Zeolite	1	–
Carbonate unspec.	43	50
Foraminifers	15	5
Calc. nannofossils	5	–

ORGANIC CARBON AND CARBONATE (%):

	2, 70–73	4, 70–73
Organic carbon	0.51	0.47
Carbonate	47	43

SITE 612 HOLE CORE 69X CORED INTERVAL 636.5–646.2 m

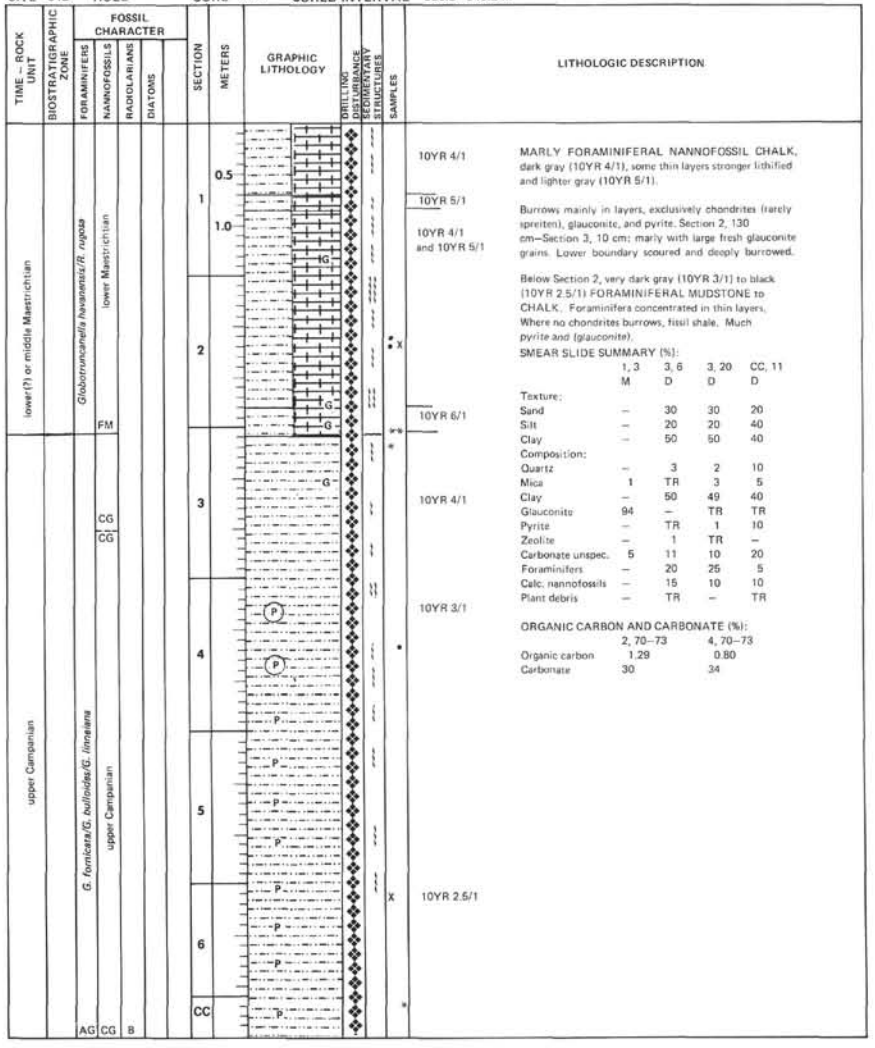

MARLY FORAMINIFERAL NANNOFOSSIL CHALK, dark gray (10YR 4/1), some thin layers stronger lithified and lighter gray (10YR 5/1).

Burrows mainly in layers, exclusively chondrites (rarely spreiten), glauconite, and pyrite. Section 2, 130 cm–Section 3, 10 cm: marly with large fresh glauconite grains. Lower boundary scoured and deeply burrowed.

Below Section 2, very dark gray (10YR 3/1) to black (10YR 2.5/1) FORAMINIFERAL MUDSTONE to CHALK. Foraminifera concentrated in thin layers. Where no chondrites burrows, fissil shale. Much pyrite and (glauconite).

SMEAR SLIDE SUMMARY (%):

	1, 3 M	3, 6 D	3, 20 D	CC, 11 D
Texture:				
Sand	–	30	30	20
Silt	–	20	20	40
Clay	–	50	50	40
Composition:				
Quartz	–	3	2	10
Mica	1	TR	3	5
Clay	–	50	49	40
Glauconite	94	–	TR	TR
Pyrite	–	TR	1	10
Zeolite	–	1	TR	–
Carbonate unspec.	5	11	10	20
Foraminifers	–	20	25	5
Calc. nannofossils	–	15	10	10
Plant debris	–	TR	–	TR

ORGANIC CARBON AND CARBONATE (%):

	2, 70–73	4, 70–73
Organic carbon	1.29	0.80
Carbonate	30	34

SITE 612 HOLE CORE 70X CORED INTERVAL 646.2–655.9 m

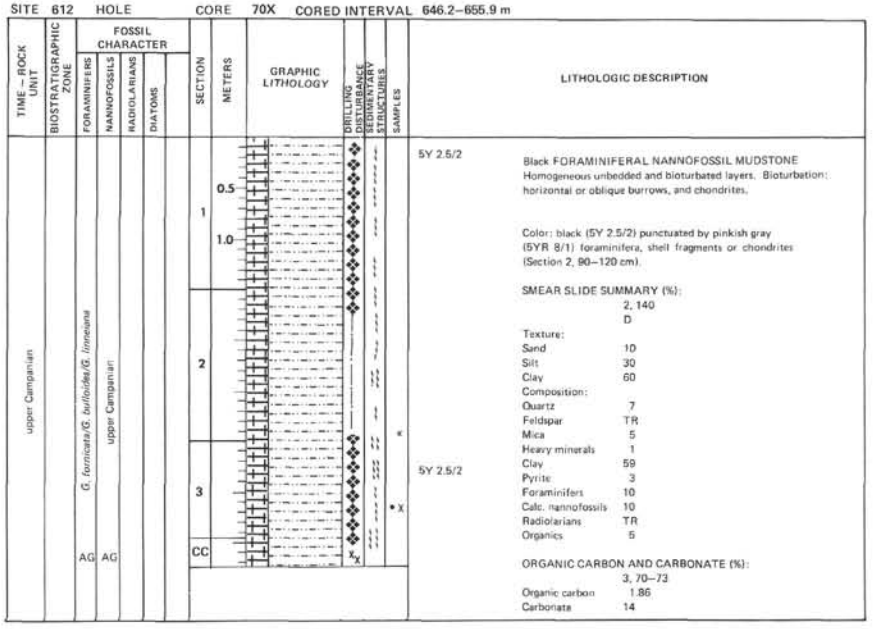

Black FORAMINIFERAL NANNOFOSSIL MUDSTONE
Homogeneous unbedded and bioturbated layers. Bioturbation: horizontal or oblique burrows, and chondrites.

Color: black (5Y 2.5/2) punctuated by pinkish gray (5YR 8/1) foraminifera, shell fragments or chondrites (Section 2, 90–120 cm).

SMEAR SLIDE SUMMARY (%):

	2, 140 D
Texture:	
Sand	10
Silt	30
Clay	60
Composition:	
Quartz	7
Feldspar	TR
Mica	5
Heavy minerals	1
Clay	59
Pyrite	3
Foraminifers	10
Calc. nannofossils	10
Radiolarians	TR
Organics	5

ORGANIC CARBON AND CARBONATE (%):

	3, 70–73
Organic carbon	1.86
Carbonate	14

SITE 612 HOLE CORE 71X CORED INTERVAL 655.9–665.6 m

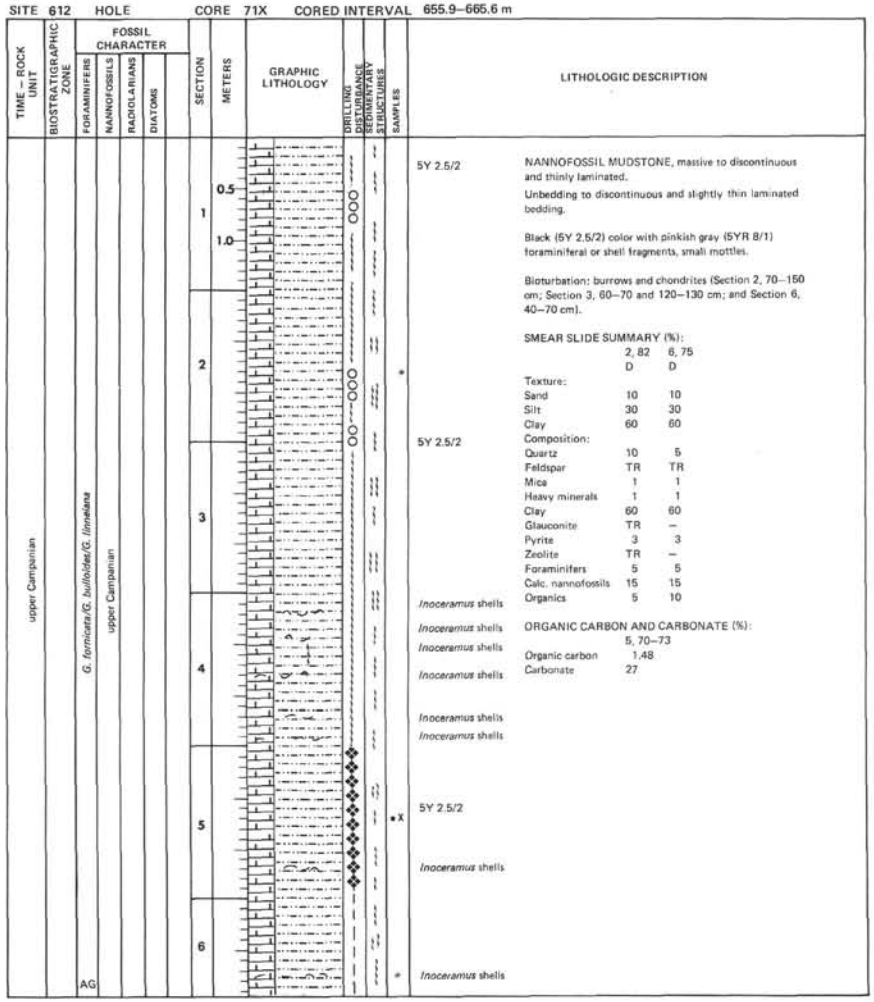

NANNOFOSSIL MUDSTONE, massive to discontinuous and thinly laminated.

Unbedding to discontinuous and slightly thin laminated bedding.

Black (5Y 2.5/2) color with pinkish gray (5YR 8/1) foraminiferal or shell fragments, small mottles.

Bioturbation: burrows and chondrites (Section 2, 70–150 cm; Section 3, 60–70 and 120–130 cm; and Section 6, 40–70 cm).

SMEAR SLIDE SUMMARY (%):

	2, 82	6, 75
	D	D
Texture:		
Sand	10	10
Silt	30	30
Clay	60	60
Composition:		
Quartz	10	5
Feldspar	TR	TR
Mica	1	1
Heavy minerals	1	1
Clay	60	60
Glauconite	TR	–
Pyrite	3	3
Zeolite	TR	–
Foraminifers	5	5
Calc. nannofossils	15	15
Organics	5	10

ORGANIC CARBON AND CARBONATE (%):

	5, 70–73
Organic carbon	1.48
Carbonate	27

SITE 612 HOLE CORE 72X CORED INTERVAL 665.6–675.3 m

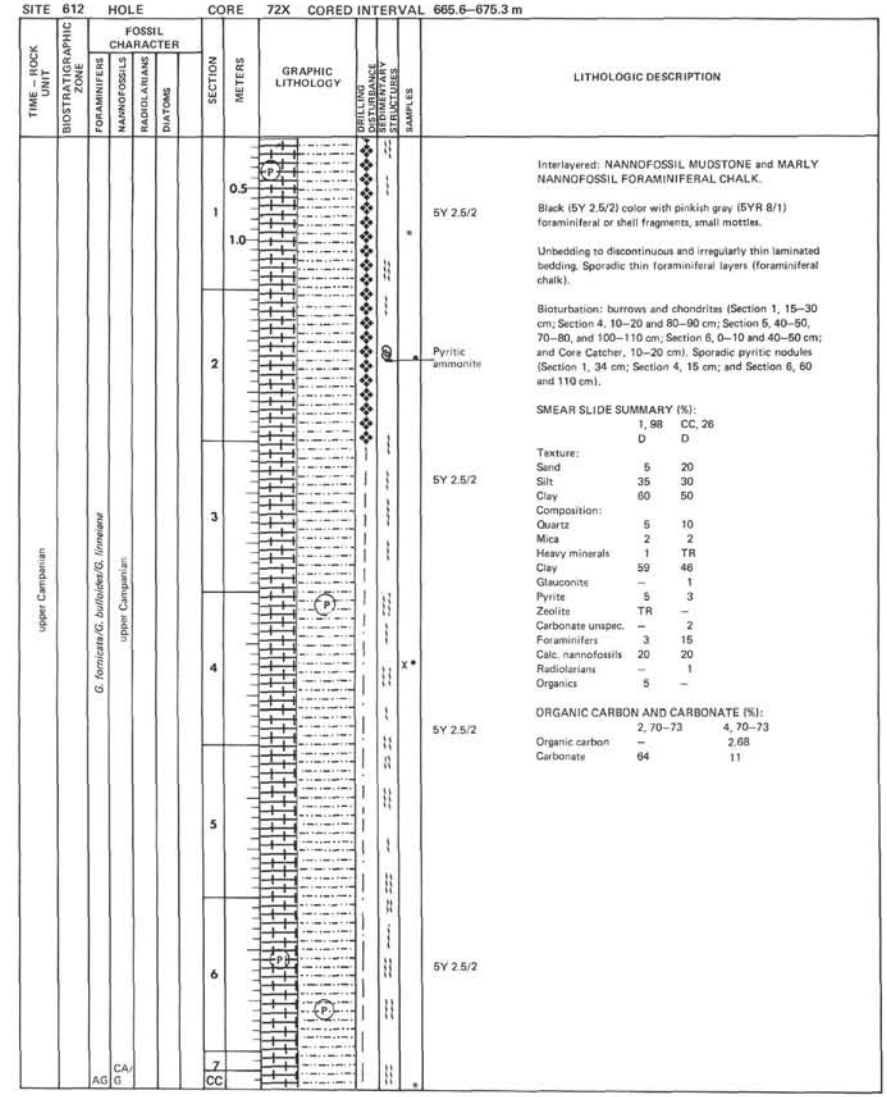

Interlayered: NANNOFOSSIL MUDSTONE and MARLY NANNOFOSSIL FORAMINIFERAL CHALK.

Black (5Y 2.5/2) color with pinkish gray (5YR 8/1) foraminiferal or shell fragments, small mottles.

Unbedding to discontinuous and irregularly thin laminated bedding. Sporadic thin foraminiferal layers (foraminiferal chalk).

Bioturbation: burrows and chondrites (Section 1, 15–30 cm; Section 4, 10–20 and 80–90 cm; Section 5, 40–50, 70–80, and 100–110 cm; Section 6, 0–10 and 40–50 cm; and Core Catcher, 10–20 cm). Sporadic pyritic nodules (Section 1, 34 cm; Section 4, 15 cm; and Section 6, 60 and 110 cm).

SMEAR SLIDE SUMMARY (%):

	1, 98	CC, 26
	D	D
Texture:		
Sand	5	20
Silt	35	30
Clay	60	50
Composition:		
Quartz	5	10
Mica	2	2
Heavy minerals	1	TR
Clay	59	46
Glauconite	–	1
Pyrite	5	3
Zeolite	TR	–
Carbonate unspec.	–	2
Foraminifers	3	15
Calc. nannofossils	20	20
Radiolarians	–	1
Organics	5	–

ORGANIC CARBON AND CARBONATE (%):

	2, 70–73	4, 70–73
Organic carbon	–	2.68
Carbonate	64	11

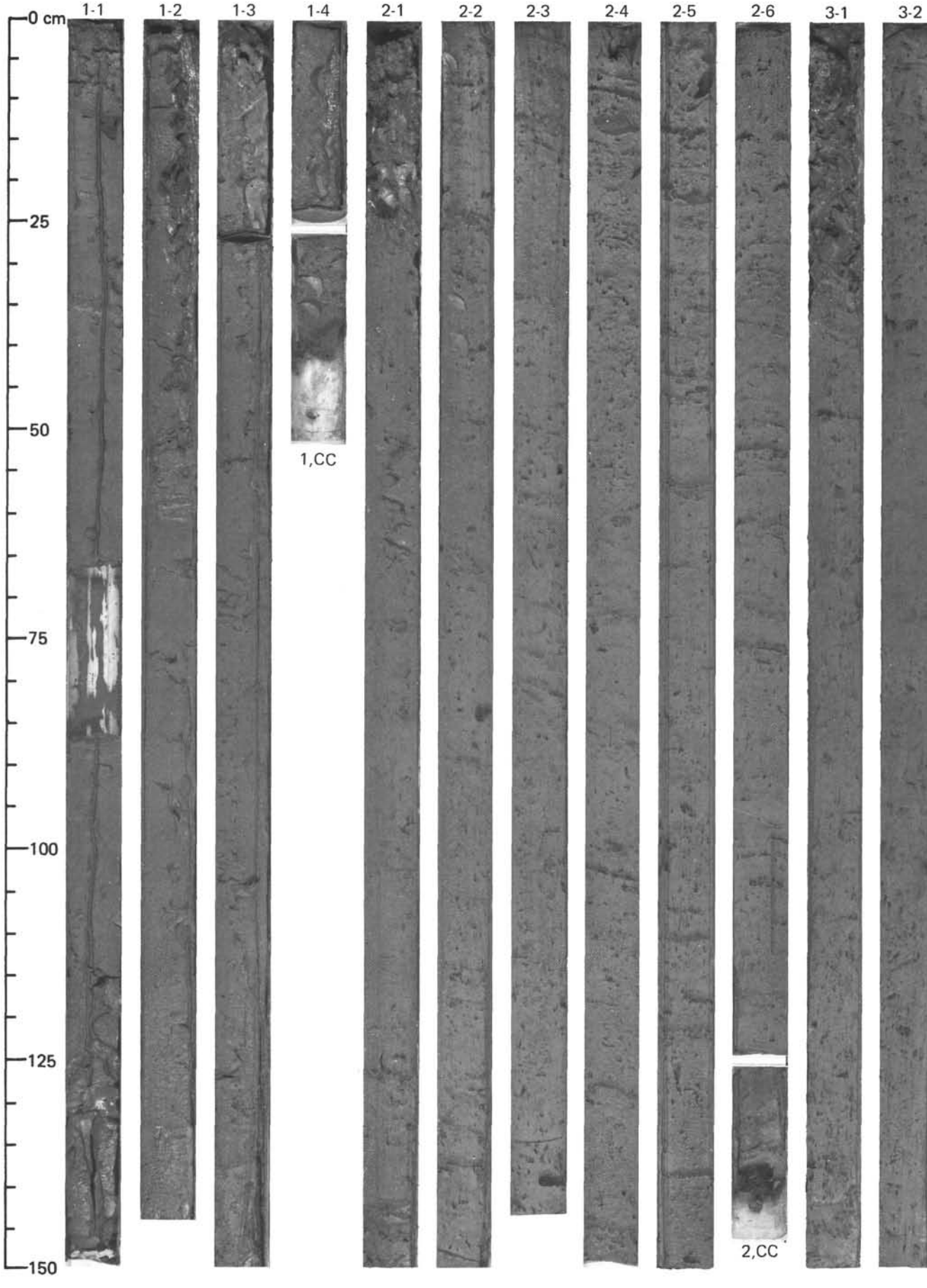
0 cm
25
50
75
100
125
150
1-1
1-2
1-3
1-4
1,CC
2-1
2-2
2-3
2-4
2-5
2-6
2,CC
3-1
3-2

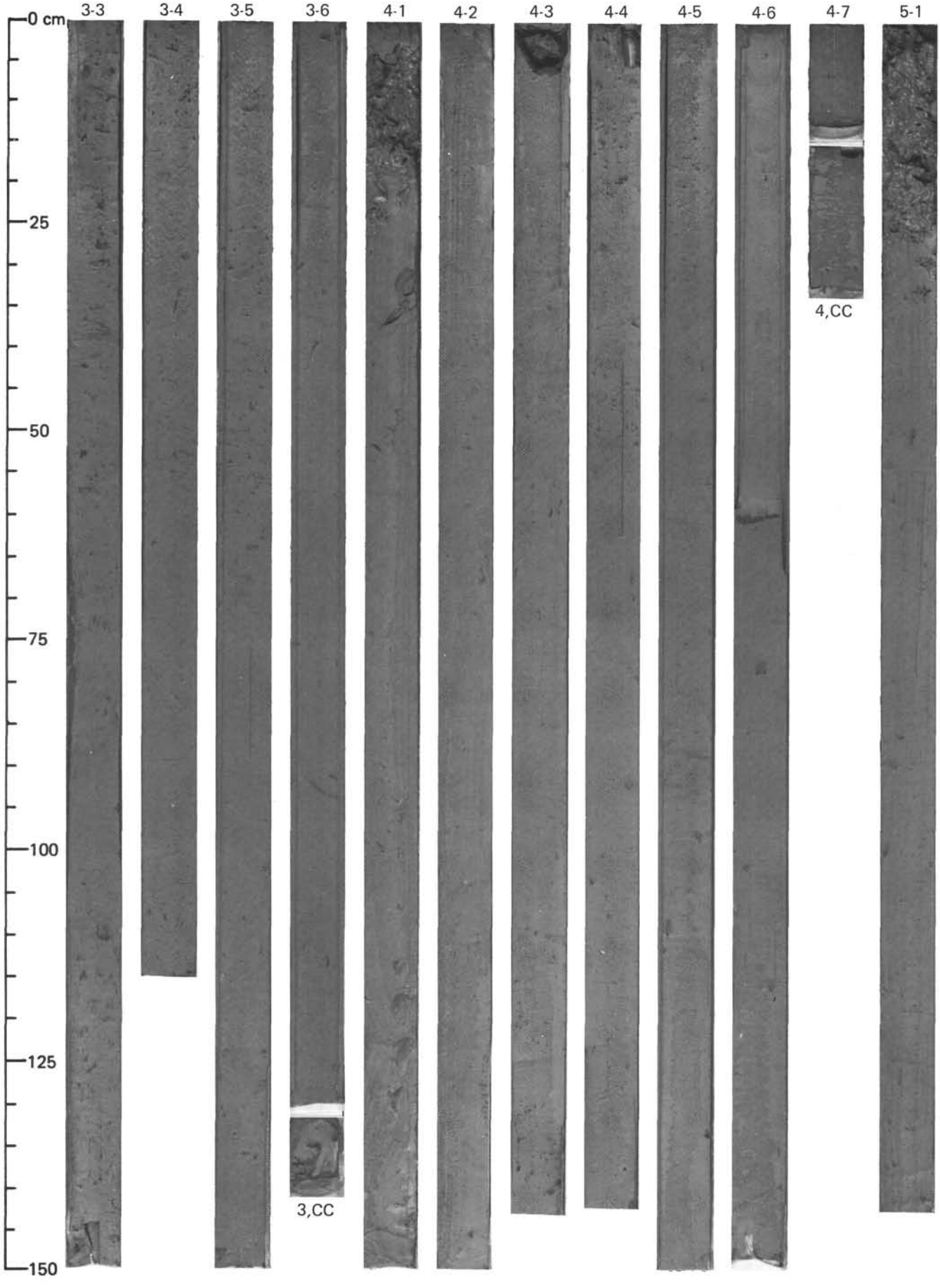
0 cm
25
50
75
100
125
150
3-3
3-4
3-5
3-6
3,CC
4-1
4-2
4-3
4-4
4-5
4-6
4-7
4,CC
5-1

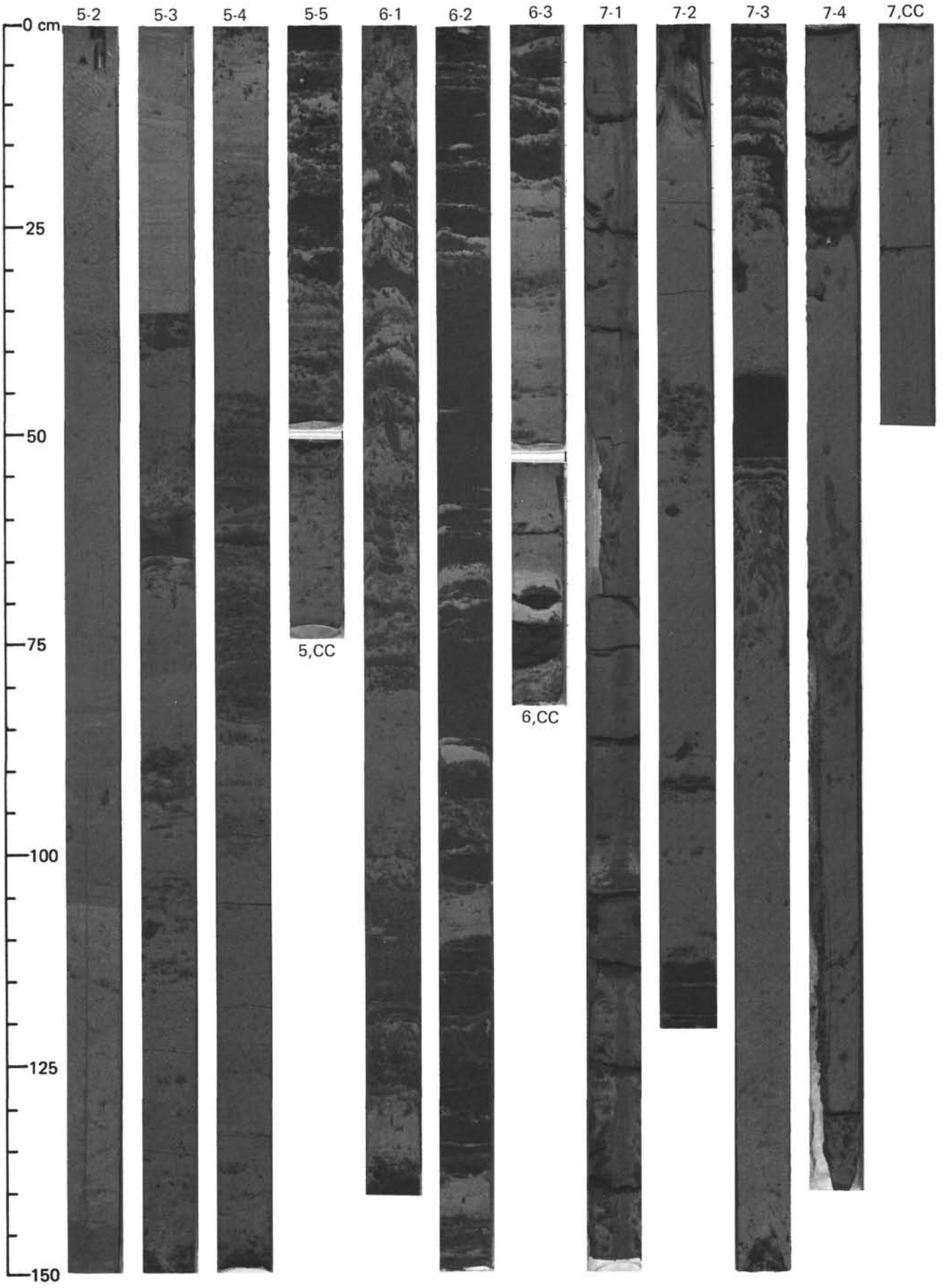
5-2
5-3
5-4
5-5
6-1
6-2
6-3
7-1
7-2
7-3
7-4
7,CC
0 cm
25
50
75
100
125
150
5,CC
6,CC

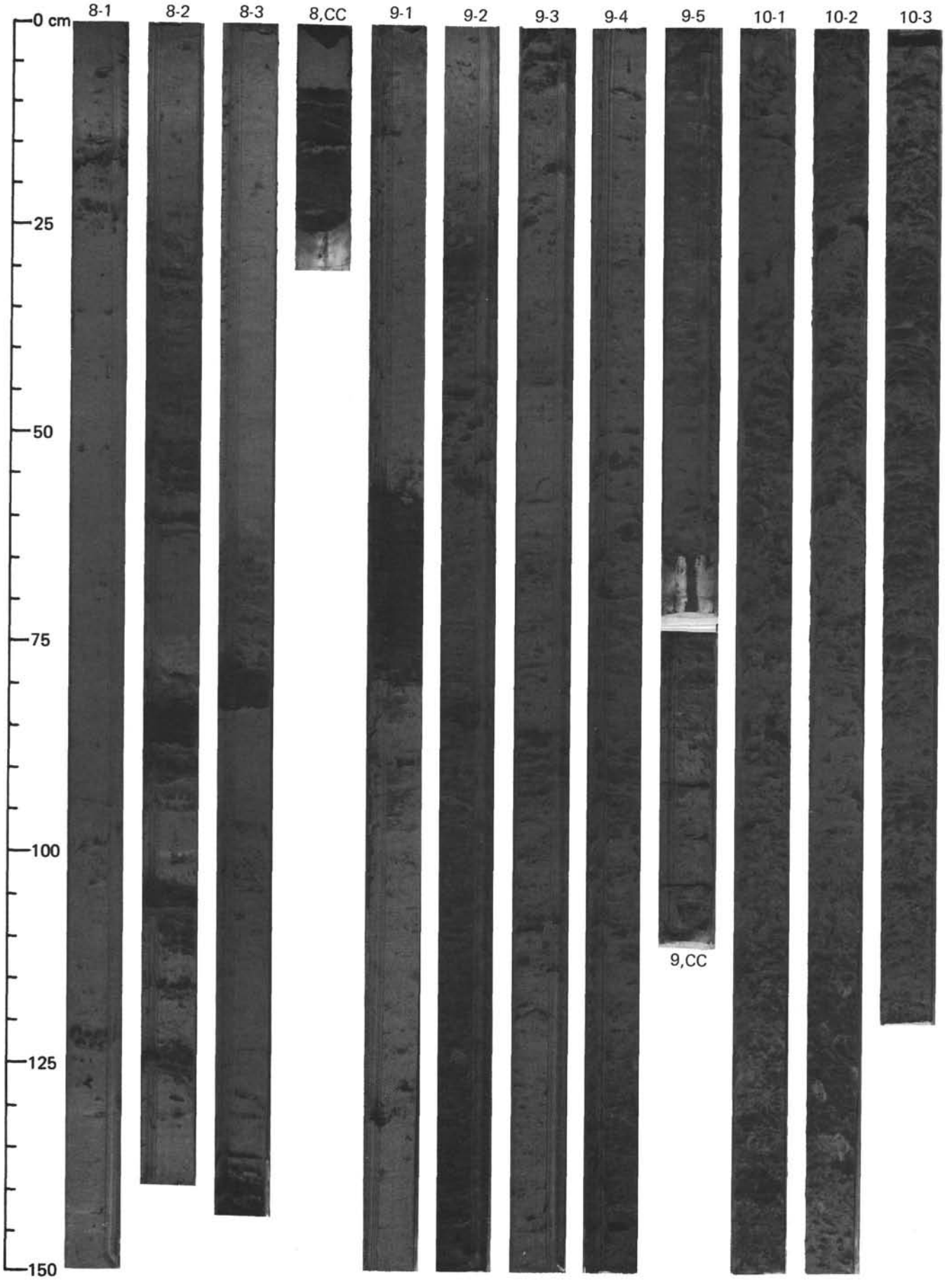
0 cm
25
50
75
100
125
150
8-1
8-2
8-3
8,CC
9-1
9-2
9-3
9-4
9-5
9,CC
10-1
10-2
10-3

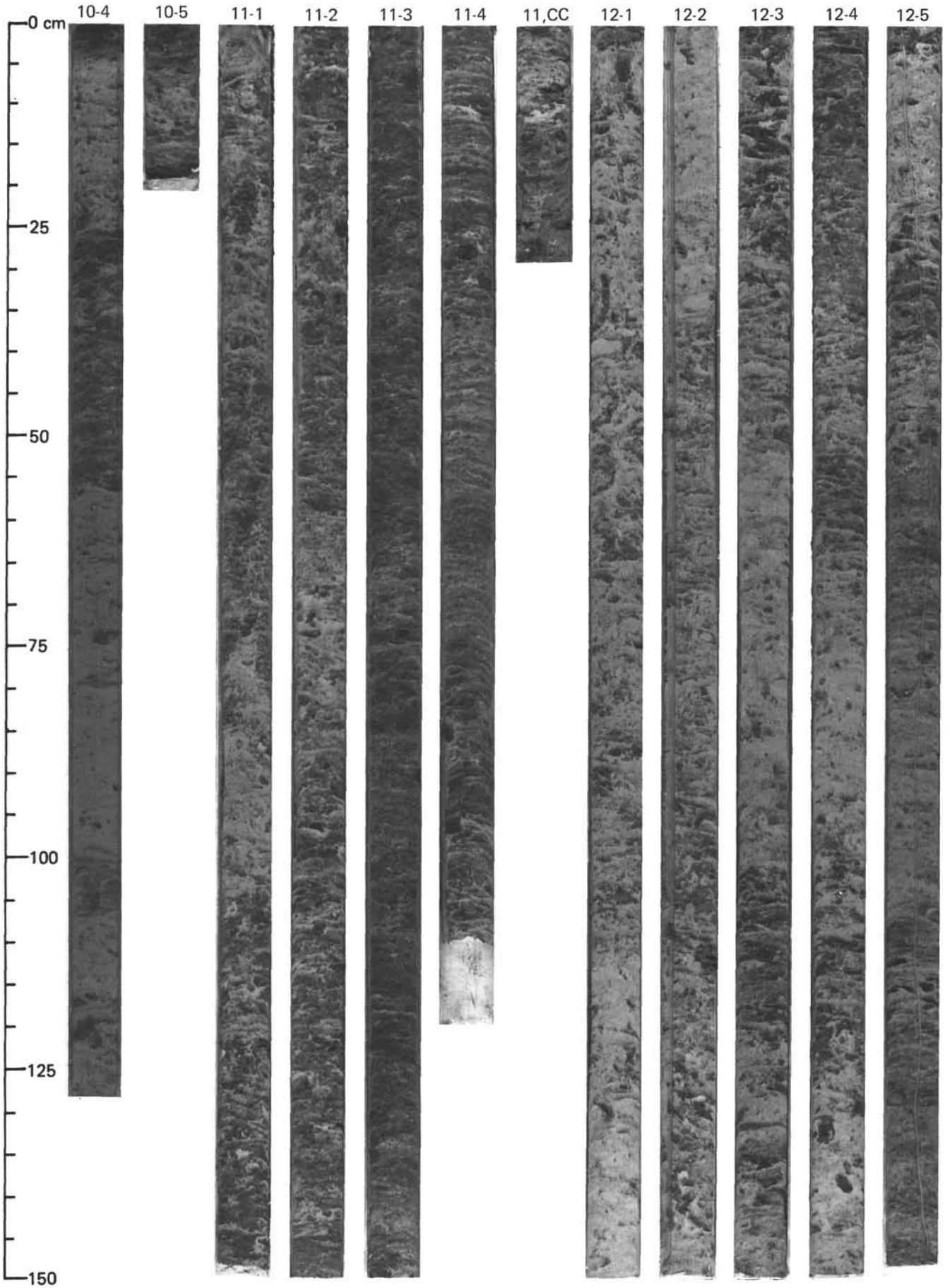
0 cm
25
50
75
100
125
150
10-4
10-5
11-1
11-2
11-3
11-4
11,CC
12-1
12-2
12-3
12-4
12-5

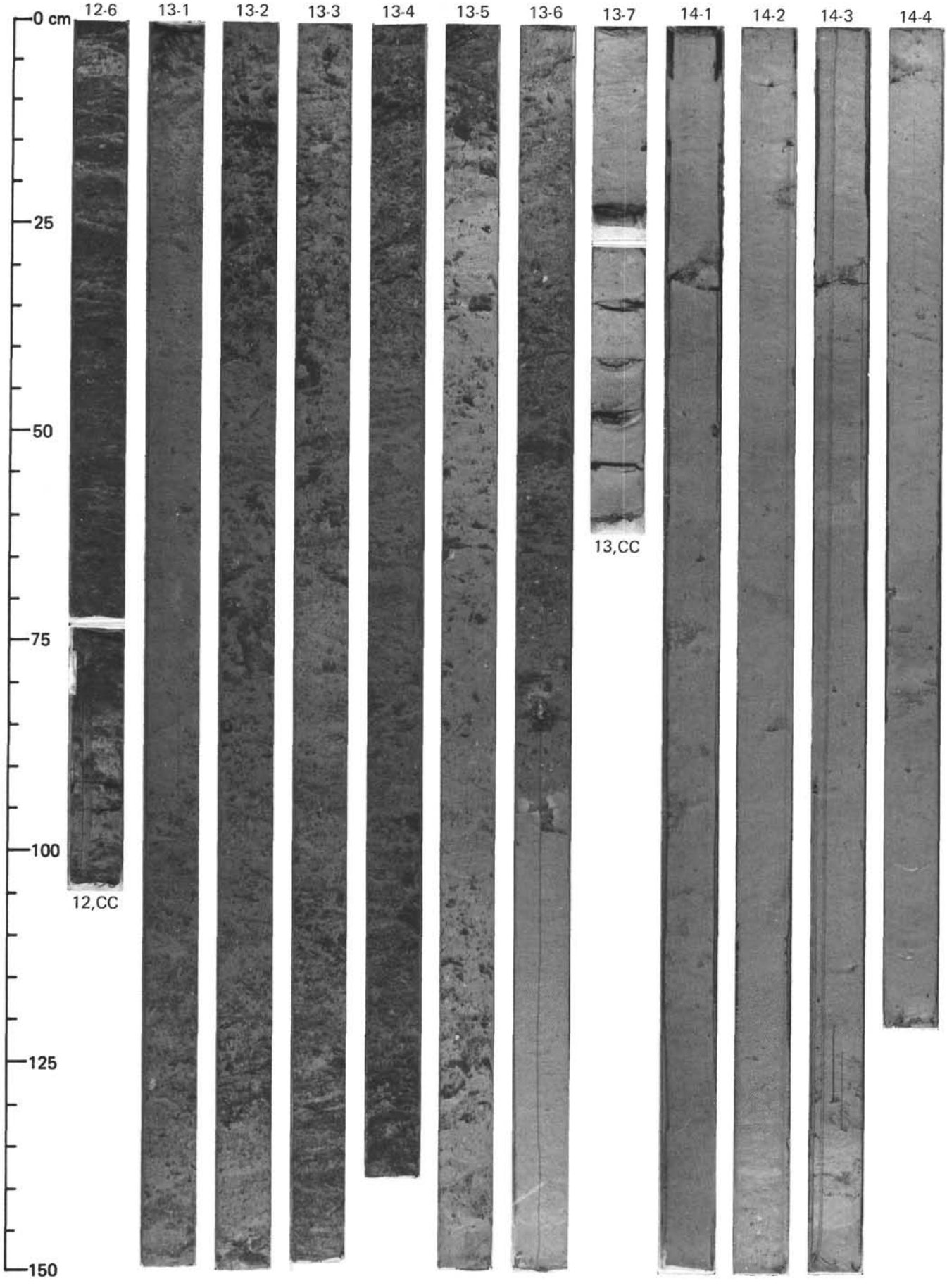
0 cm
25
50
75
100
125
150
12-6
12,CC
13-1
13-2
13-3
13-4
13-5
13-6
13-7
13,CC
14-1
14-2
14-3
14-4

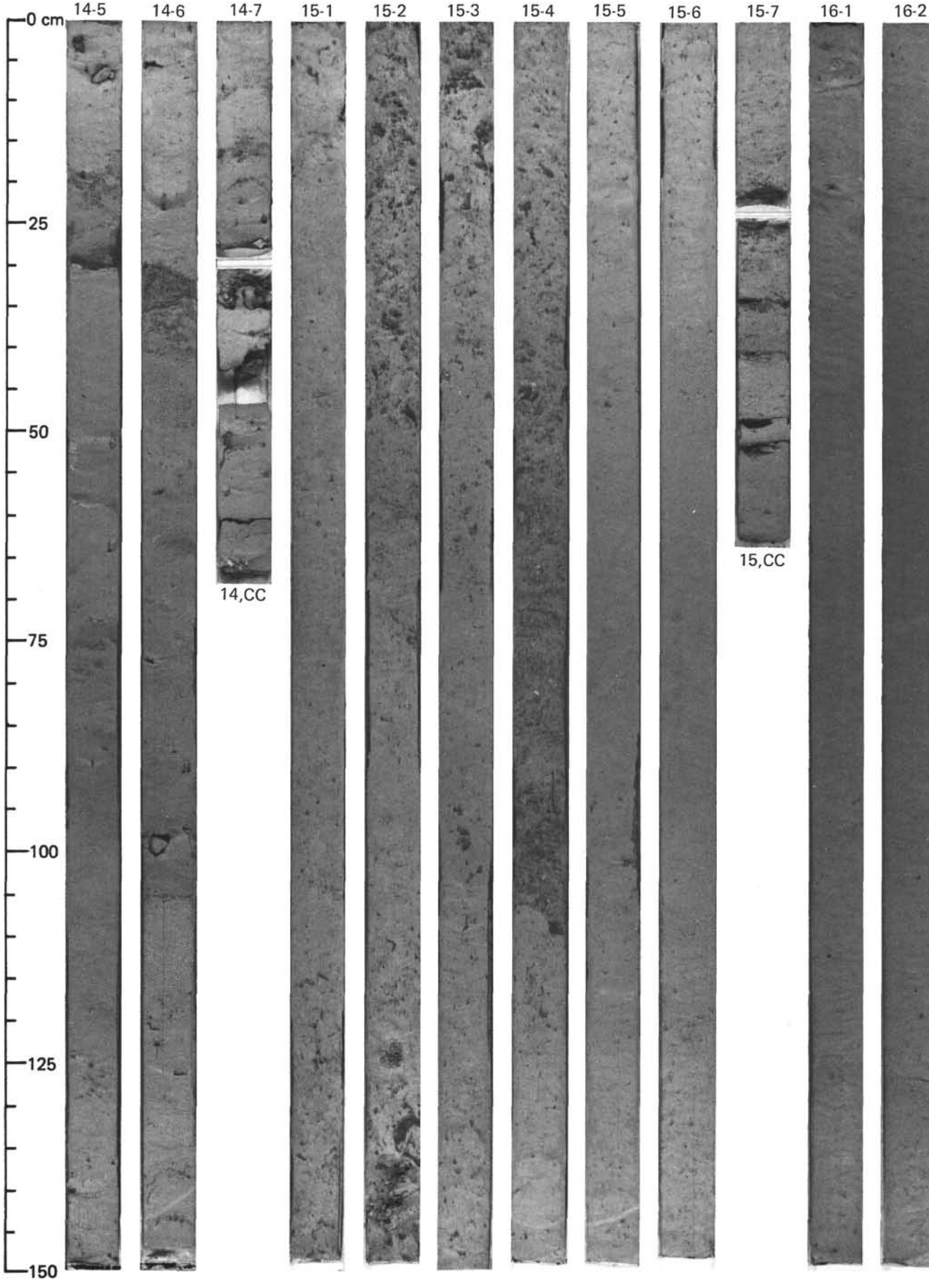
0 cm
25
50
75
100
125
150
14-5
14-6
14-7
14,CC
15-1
15-2
15-3
15-4
15-5
15-6
15-7
15,CC
16-1
16-2

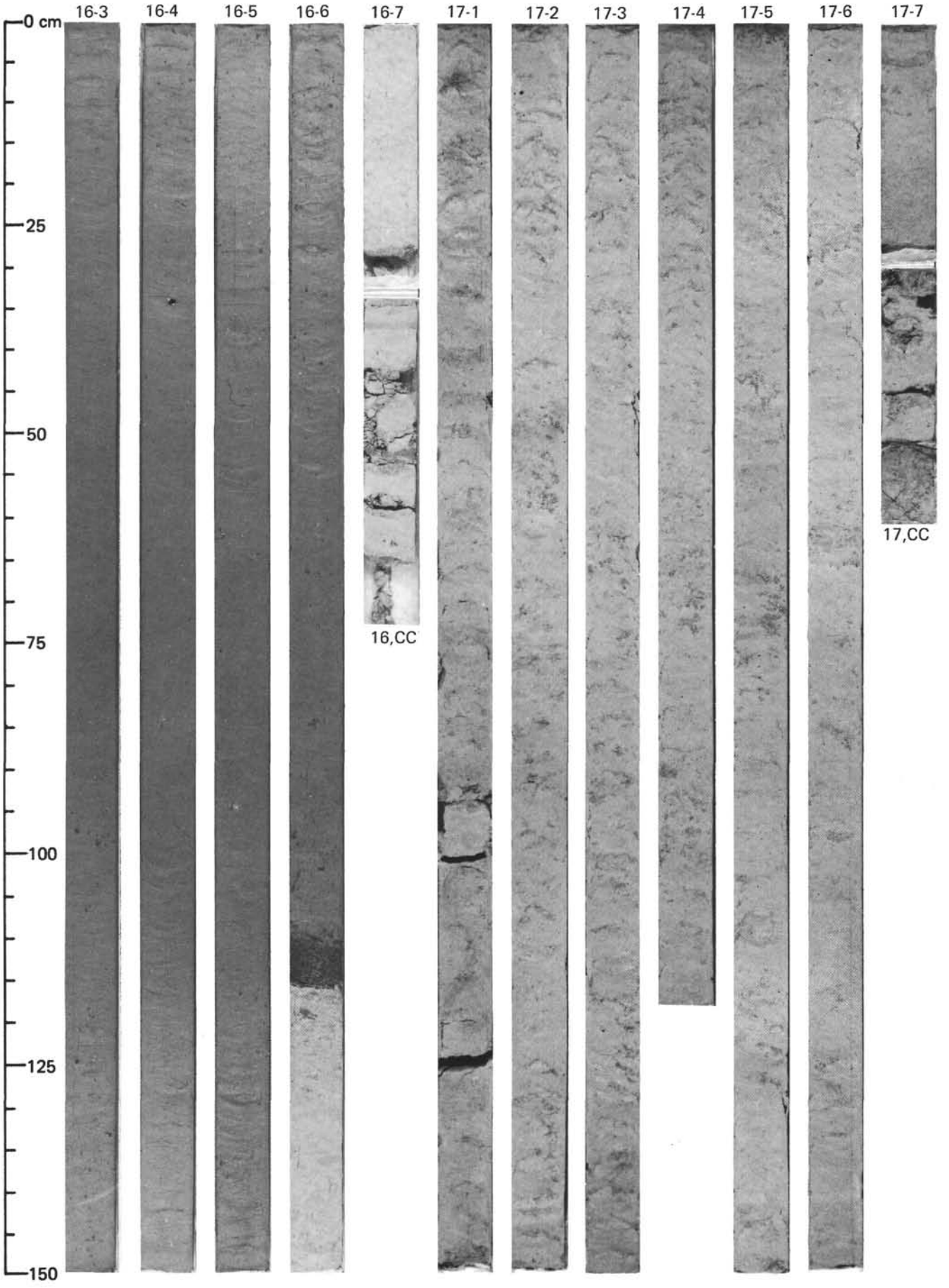
0 cm
25
50
75
100
125
150
16-3
16-4
16-5
16-6
16-7
16,CC
17-1
17-2
17-3
17-4
17-5
17-6
17-7
17,CC

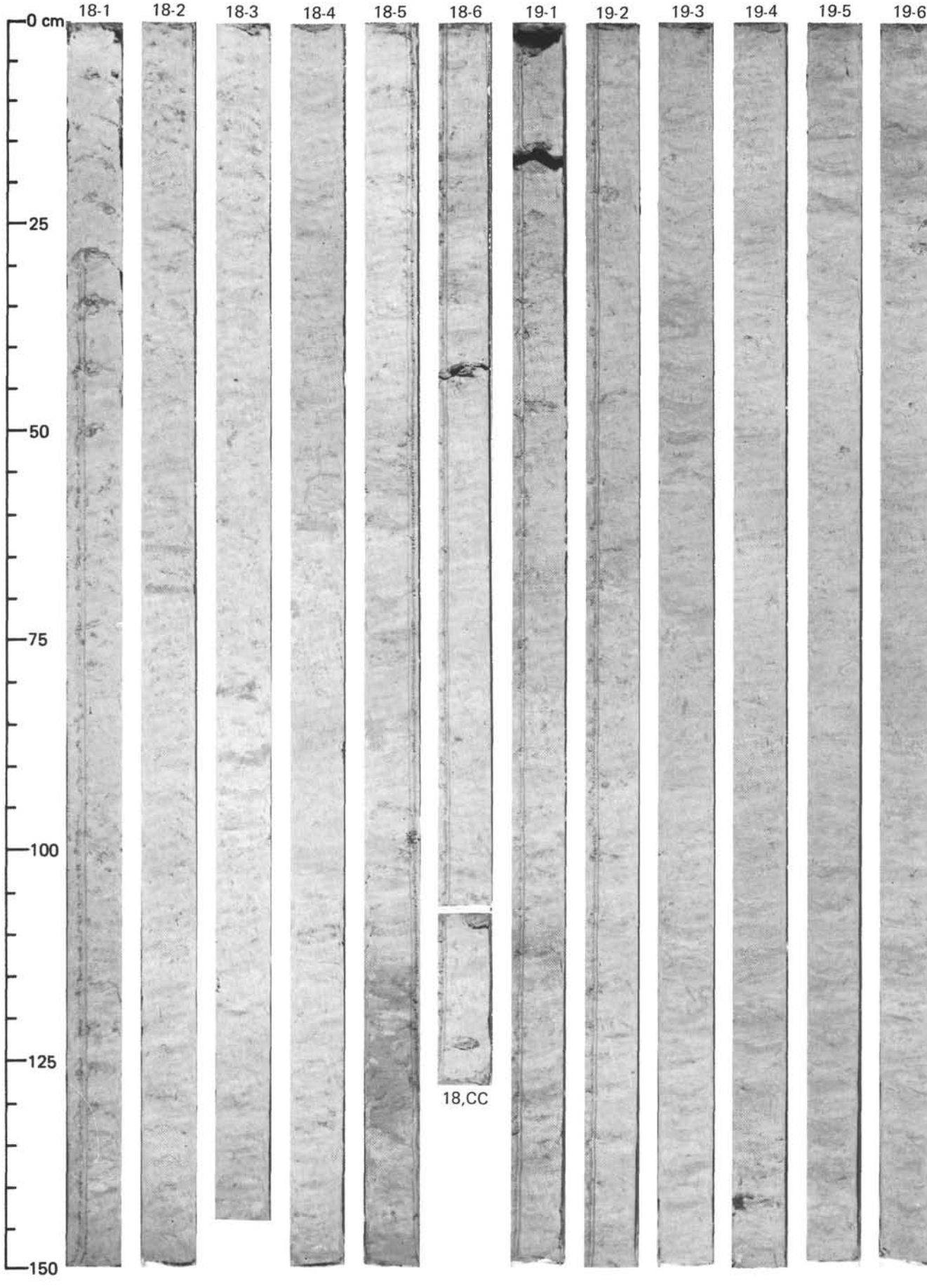
0 cm
25
50
75
100
125
150
18-1
18-2
18-3
18-4
18-5
18-6
18,CC
19-1
19-2
19-3
19-4
19-5
19-6

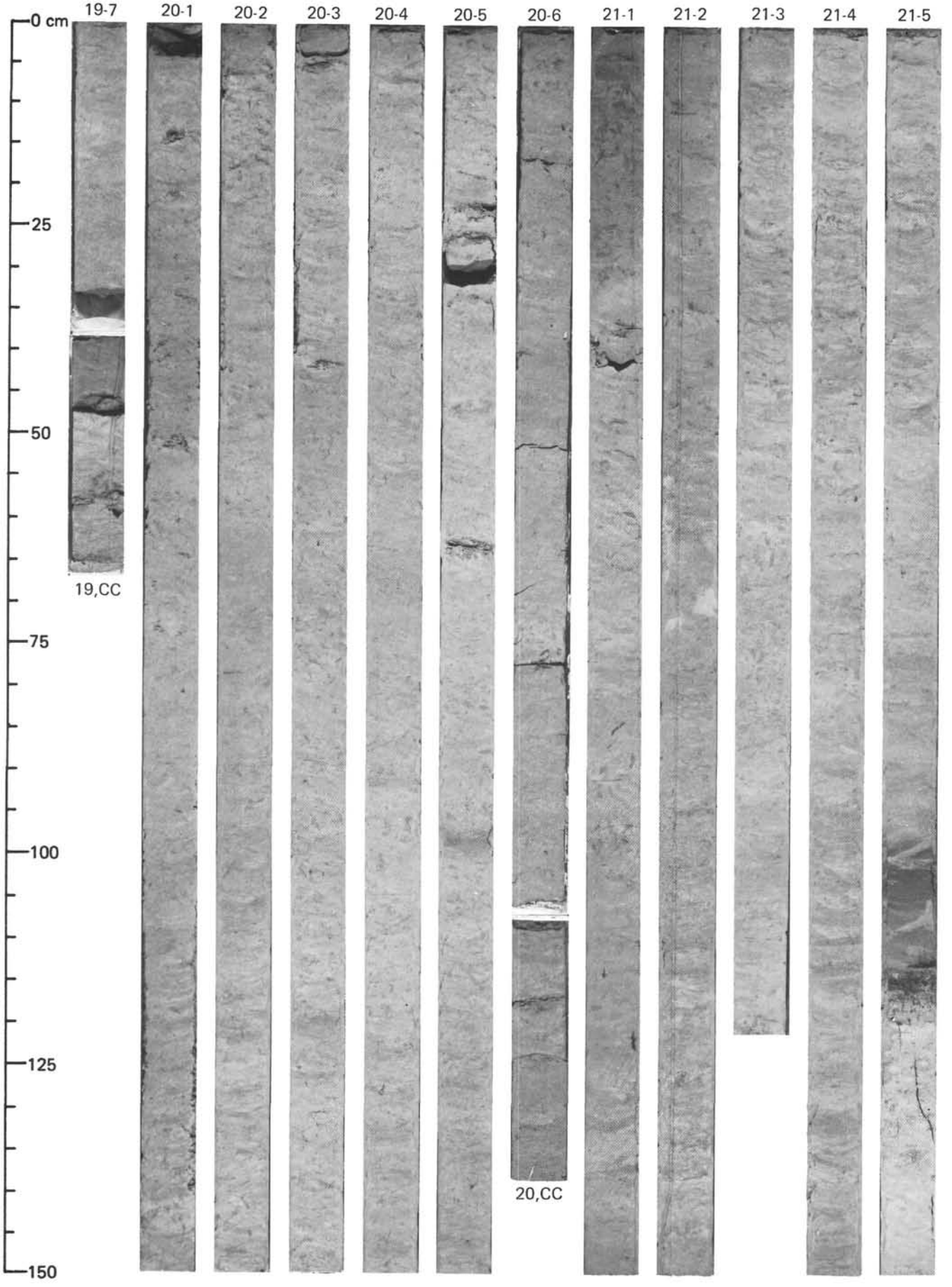
0 cm
25
50
75
100
125
150
19-7
19,CC
20-1
20-2
20-3
20-4
20-5
20-6
20,CC
21-1
21-2
21-3
21-4
21-5

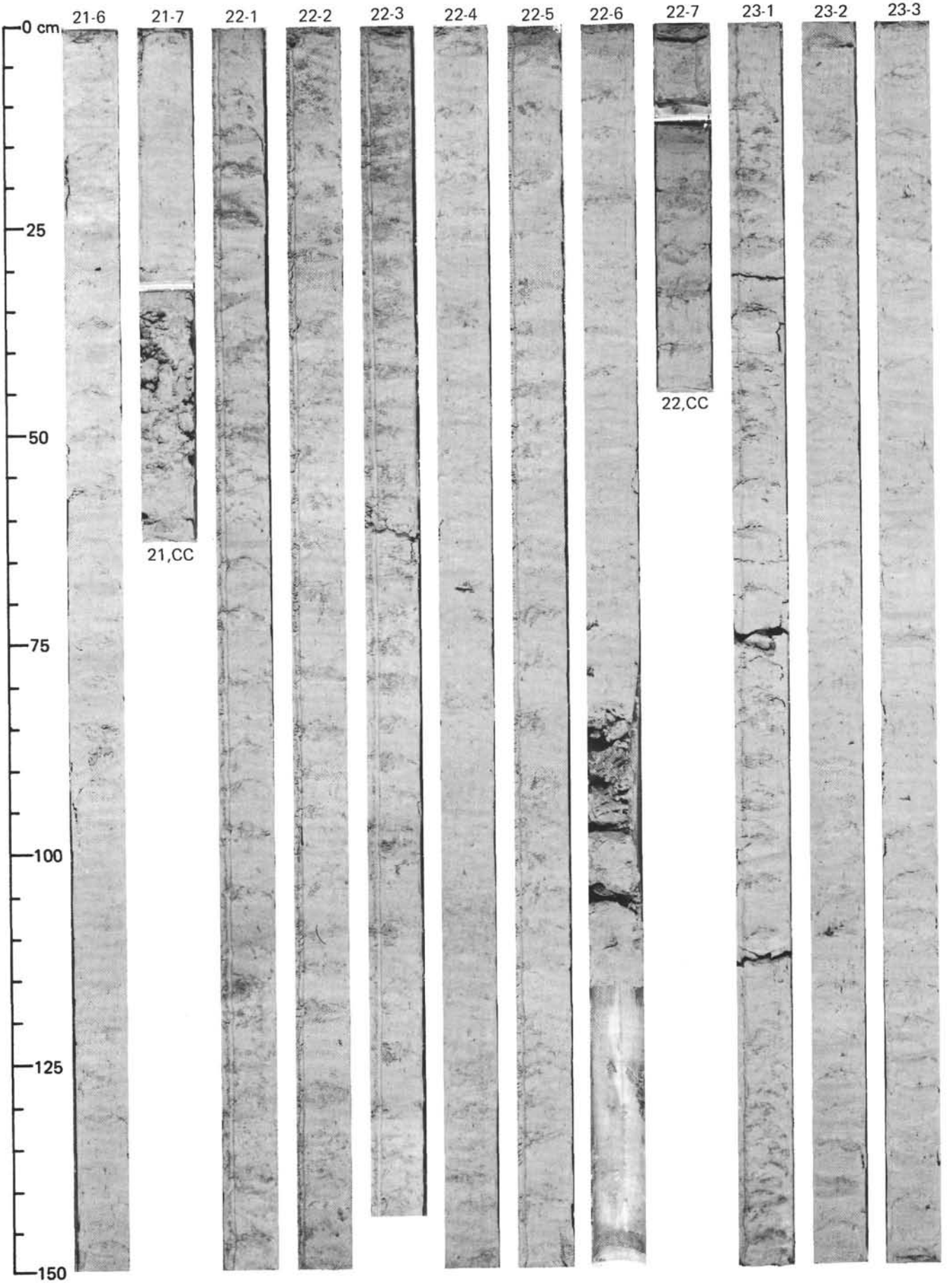
21-6
21-7
22-1
22-2
22-3
22-4
22-5
22-6
22-7
23-1
23-2
23-3
0 cm
25
50
75
100
125
150
21,CC
22,CC

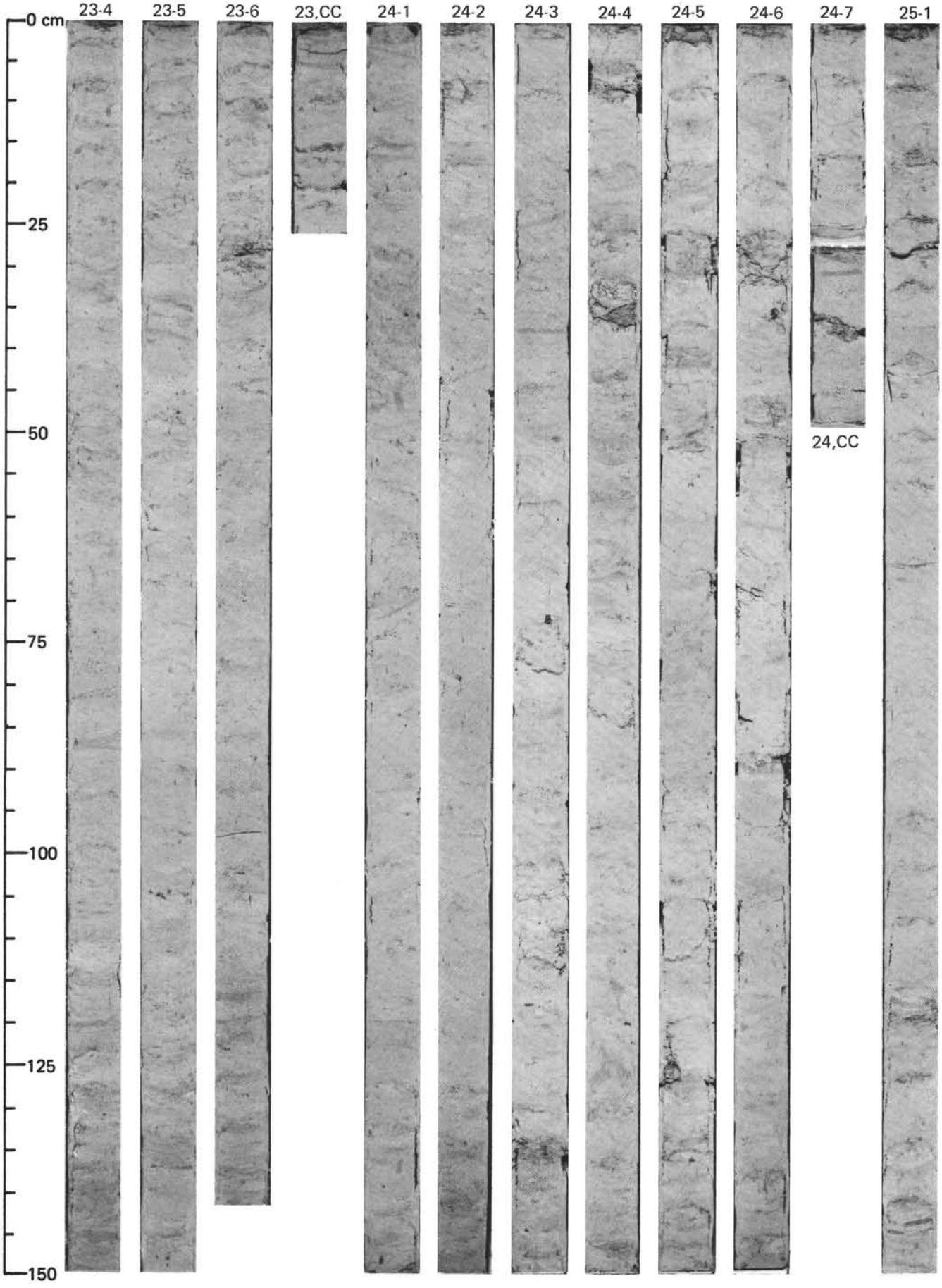
0 cm
25
50
75
100
125
150
23-4
23-5
23-6
23,CC
24-1
24-2
24-3
24-4
24-5
24-6
24-7
24,CC
25-1

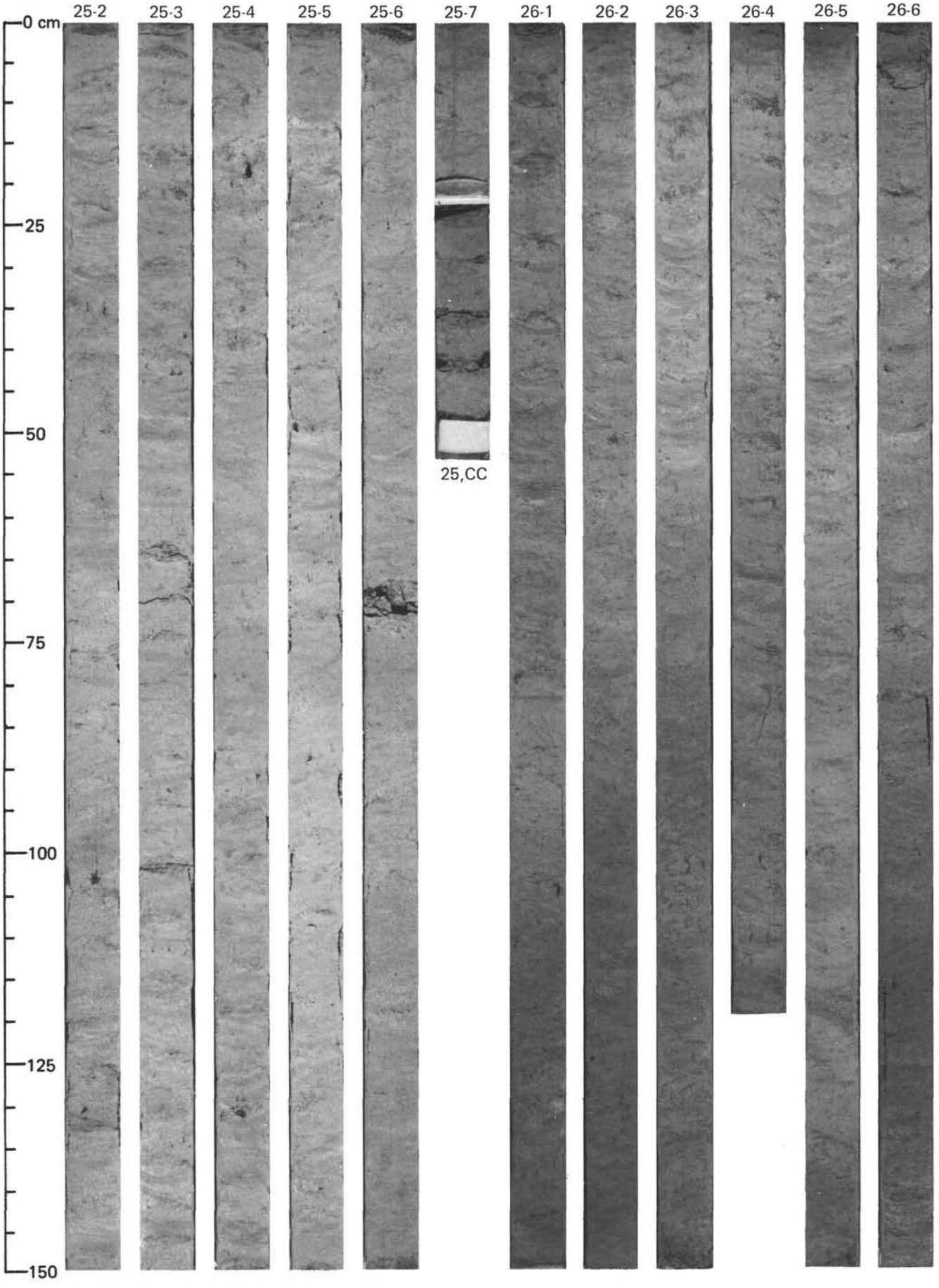
25-2
25-3
25-4
25-5
25-6
25-7
26-1
26-2
26-3
26-4
26-5
26-6
0 cm
25
50
75
100
125
150
25,CC

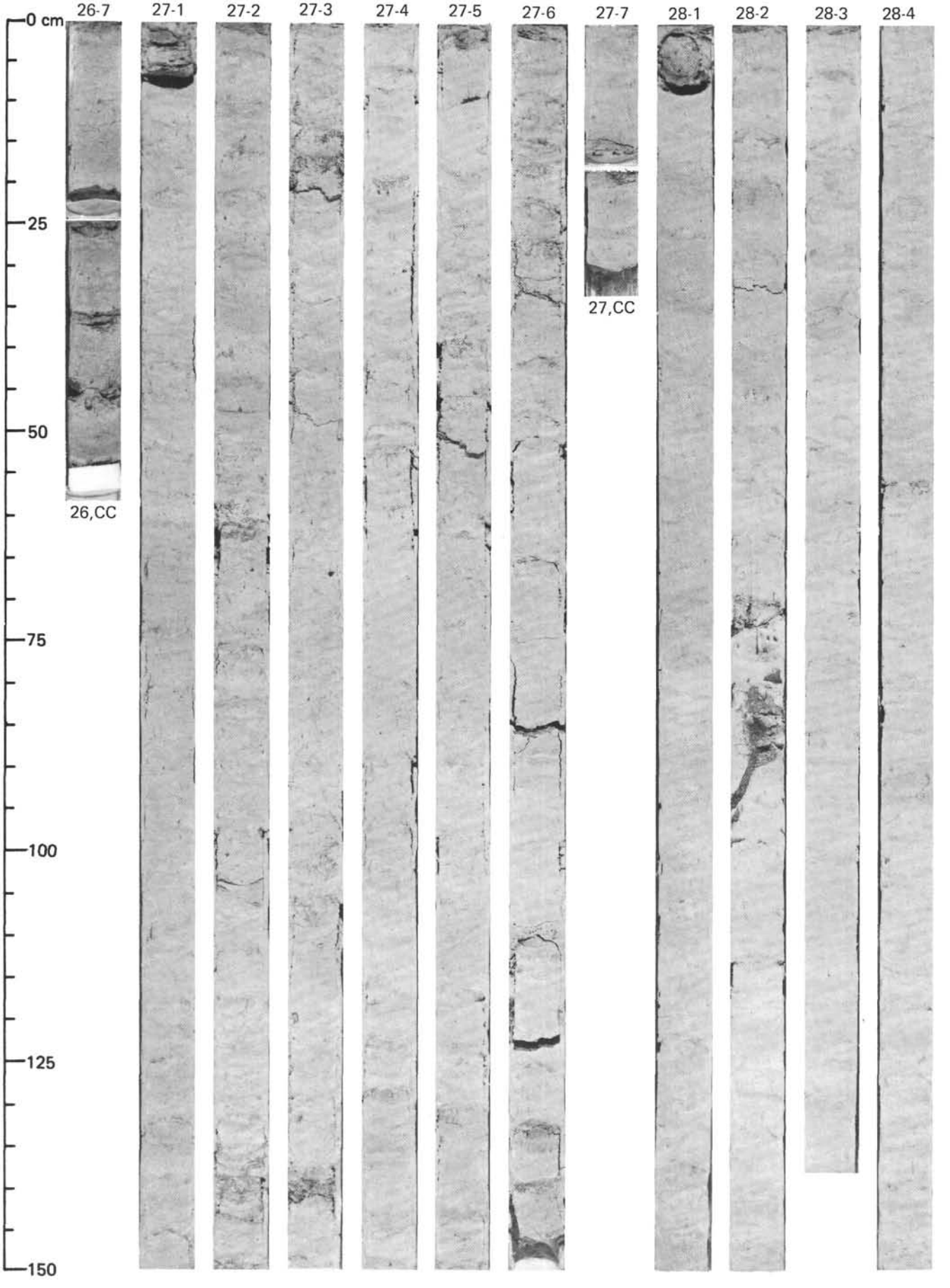
0 cm
25
50
75
100
125
150
26-7
26,CC
27-1
27-2
27-3
27-4
27-5
27-6
27-7
27,CC
28-1
28-2
28-3
28-4

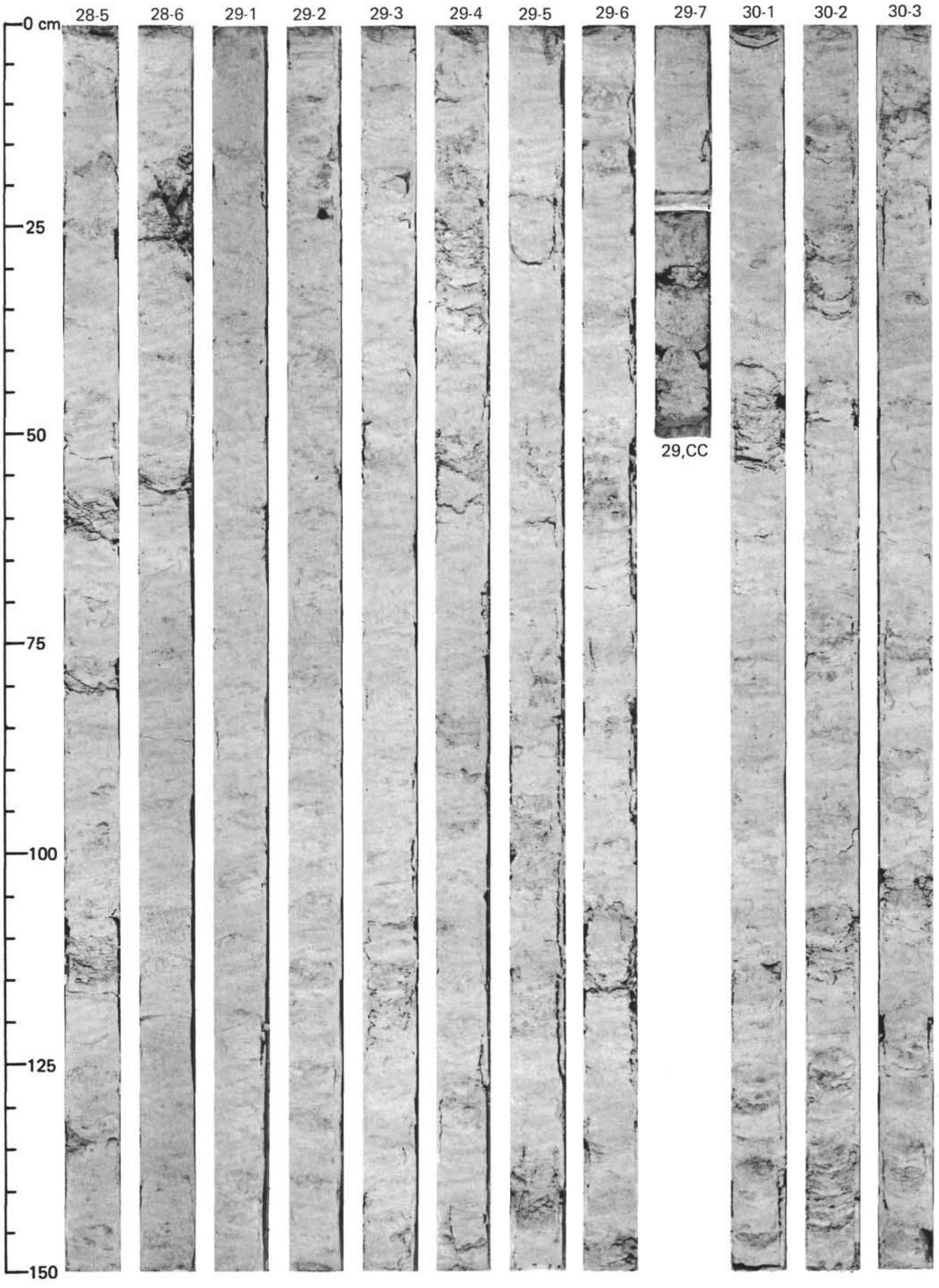
0 cm
25
50
75
100
125
150
28-5
28-6
29-1
29-2
29-3
29-4
29-5
29-6
29-7
30-1
30-2
30-3
29,CC

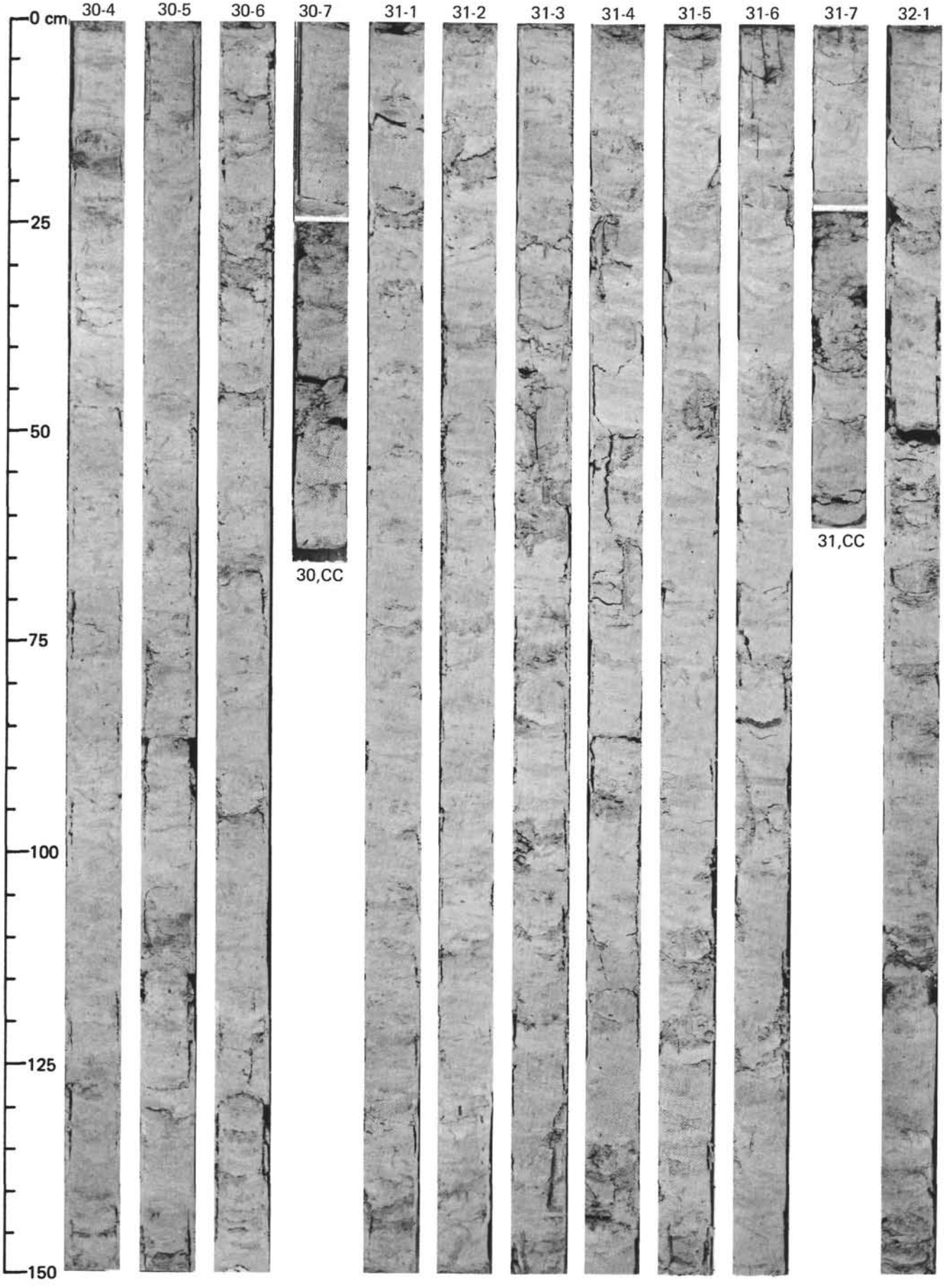
0 cm
25
50
75
100
125
150
30-4
30-5
30-6
30-7
30,CC
31-1
31-2
31-3
31-4
31-5
31-6
31-7
31,CC
32-1

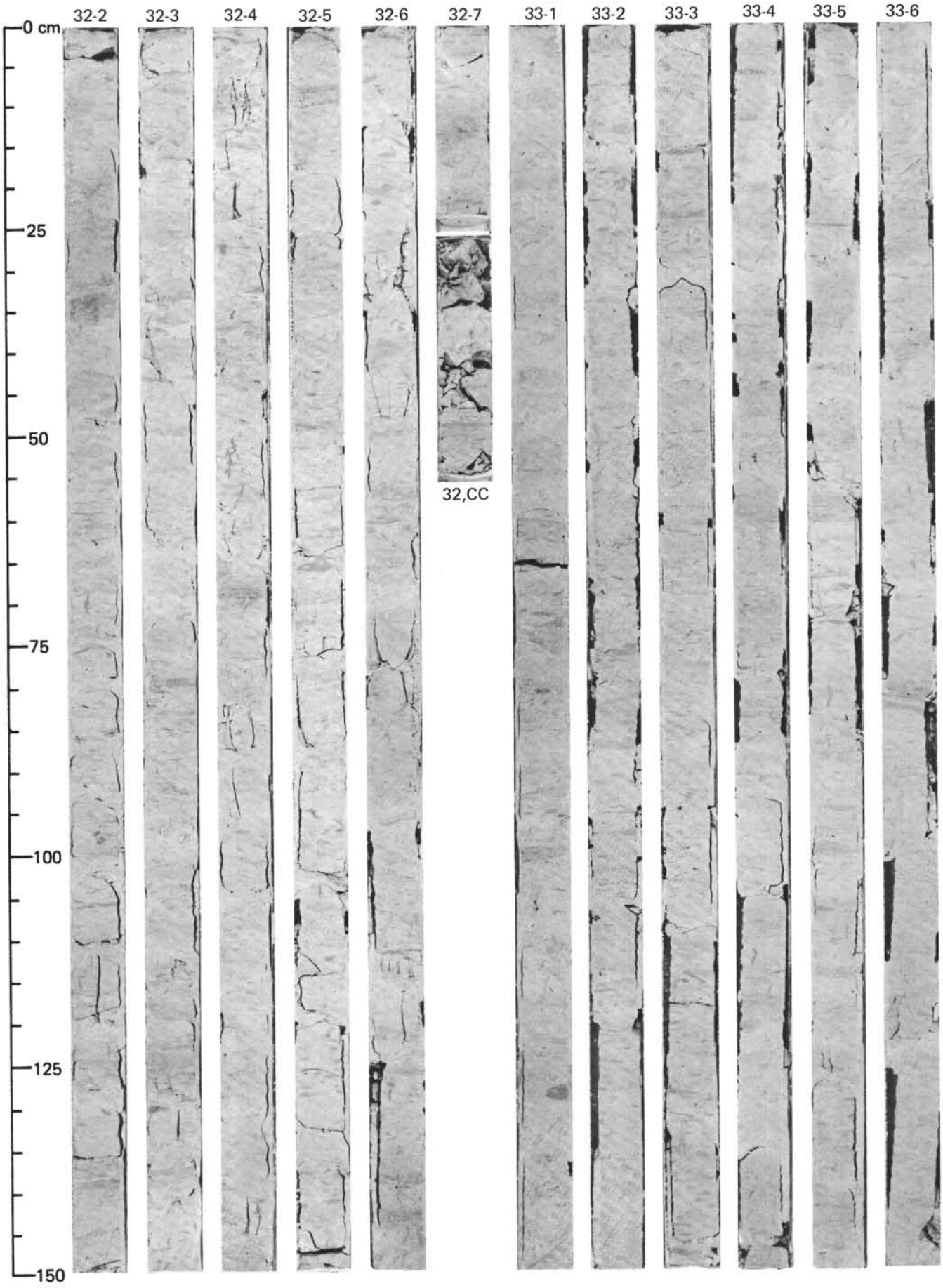
32-2
32-3
32-4
32-5
32-6
32-7
33-1
33-2
33-3
33-4
33-5
33-6
0 cm
25
50
75
100
125
150
32,CC

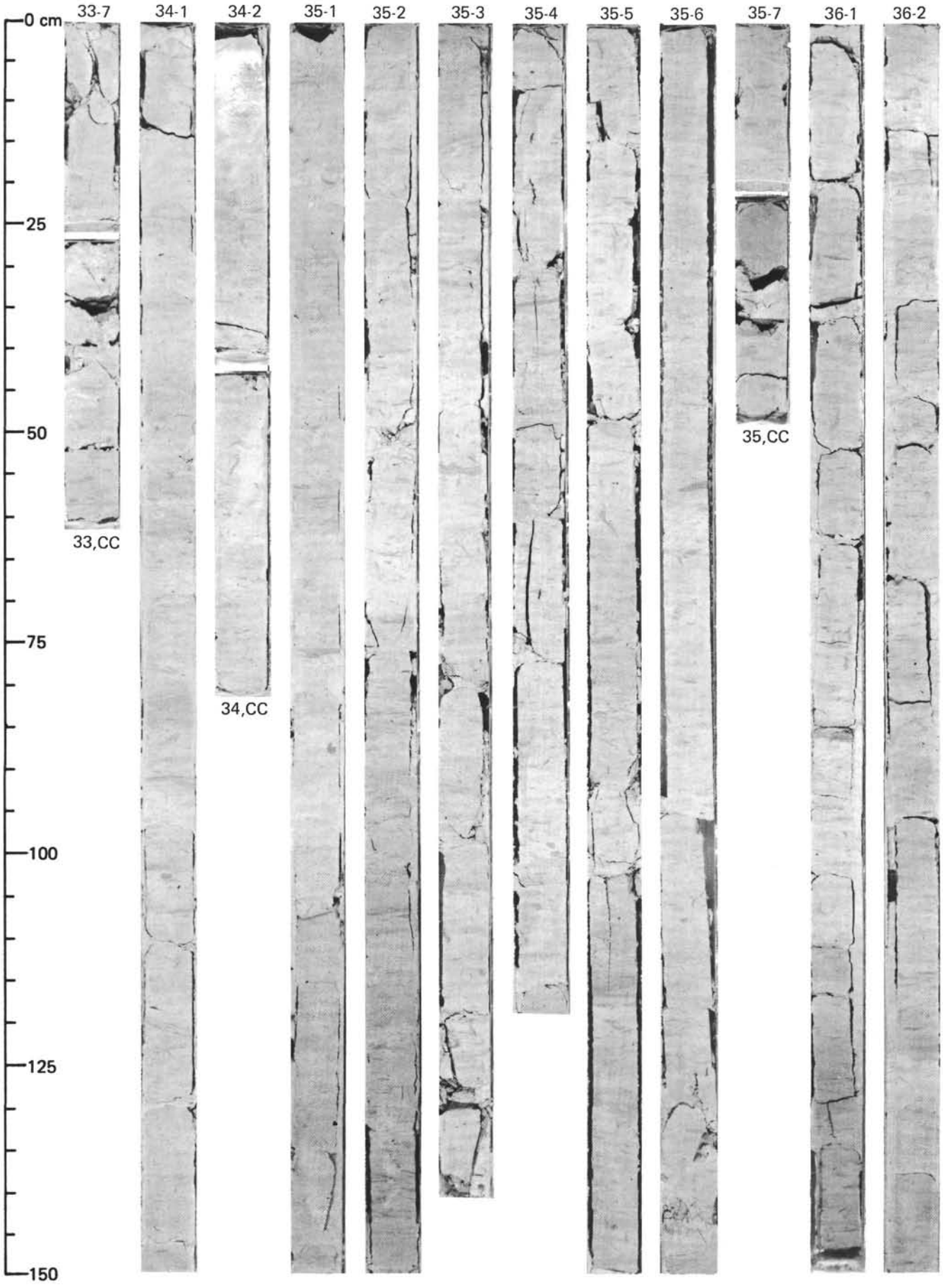
0 cm
25
50
75
100
125
150
33-7
33,CC
34-1
34-2
34,CC
35-1
35-2
35-3
35-4
35-5
35-6
35-7
35,CC
36-1
36-2

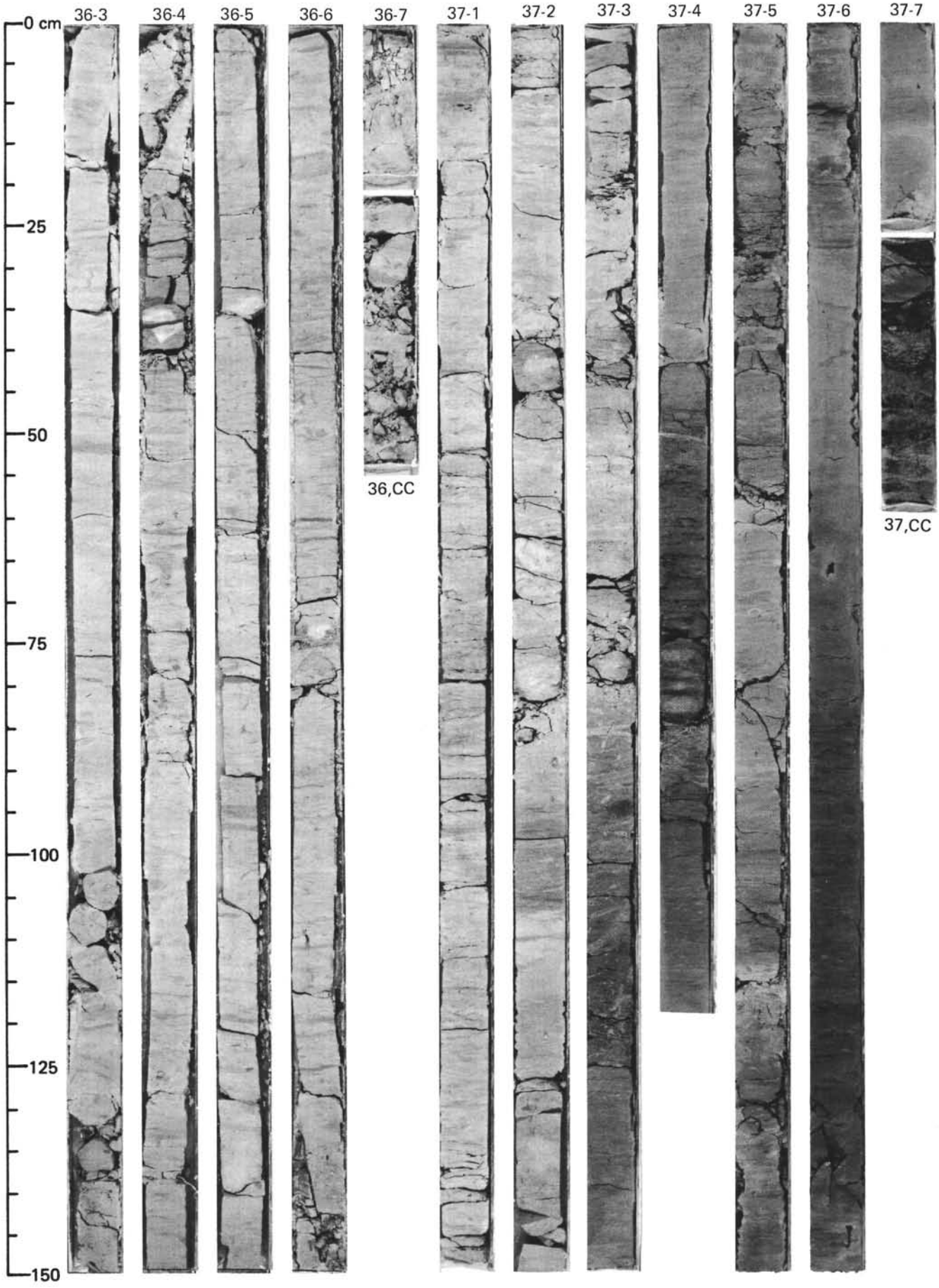
0 cm
25
50
75
100
125
150
36-3
36-4
36-5
36-6
36-7
36,CC
37-1
37-2
37-3
37-4
37-5
37-6
37-7
37,CC

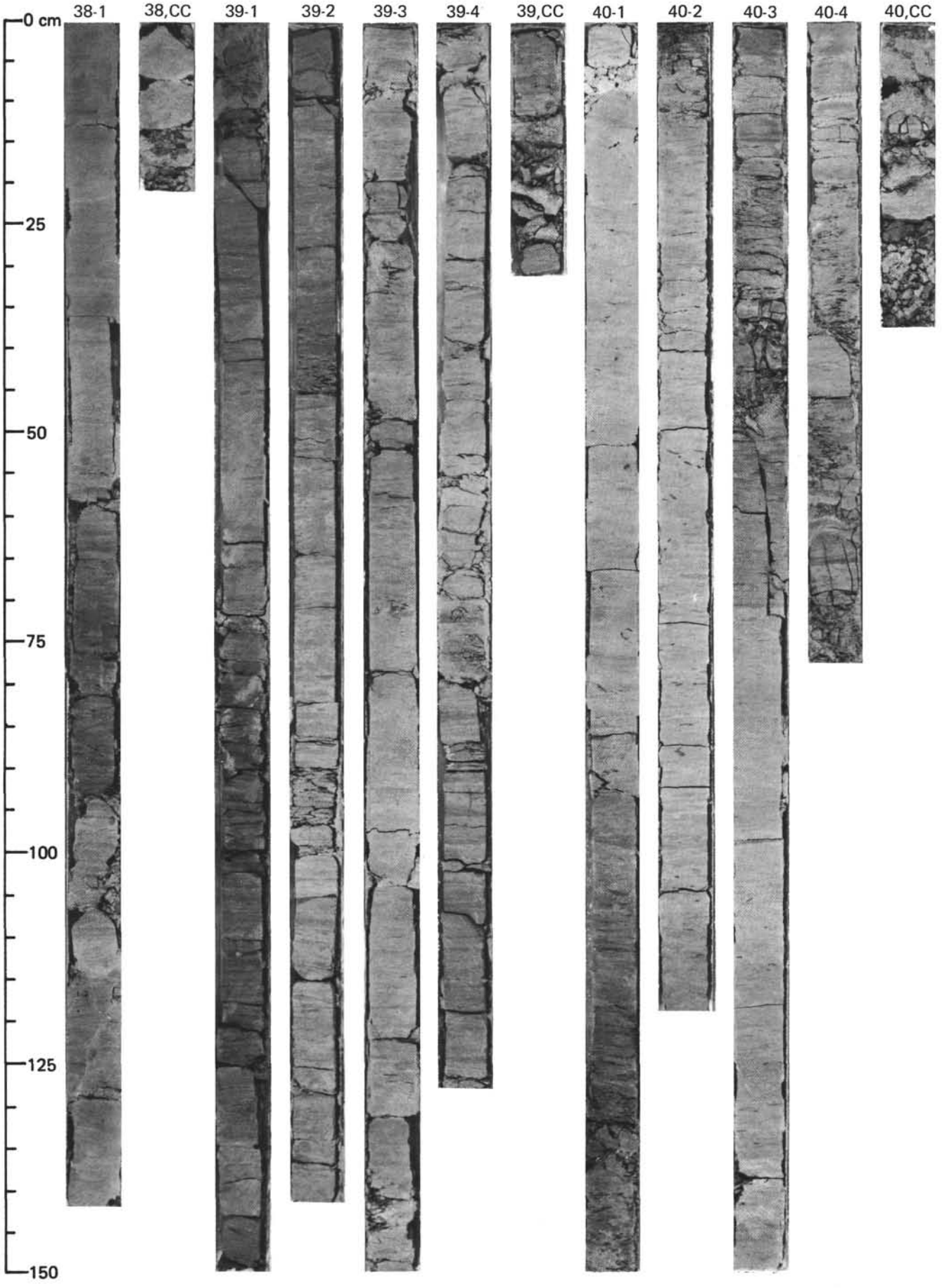
0 cm
25
50
75
100
125
150
38-1
38,CC
39-1
39-2
39-3
39-4
39,CC
40-1
40-2
40-3
40-4
40,CC

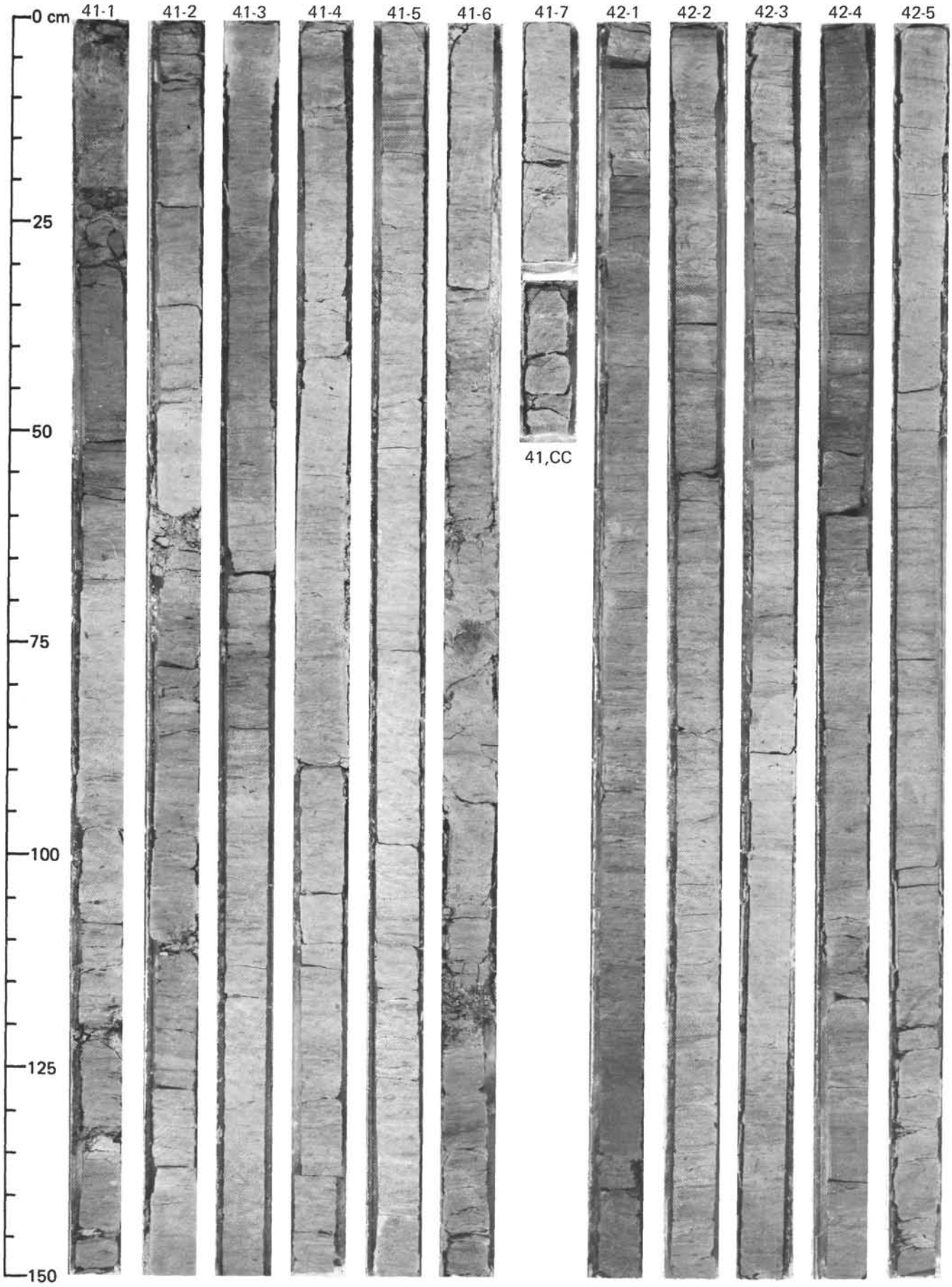
0 cm
25
50
75
100
125
150
41-1
41-2
41-3
41-4
41-5
41-6
41-7
41,CC
42-1
42-2
42-3
42-4
42-5

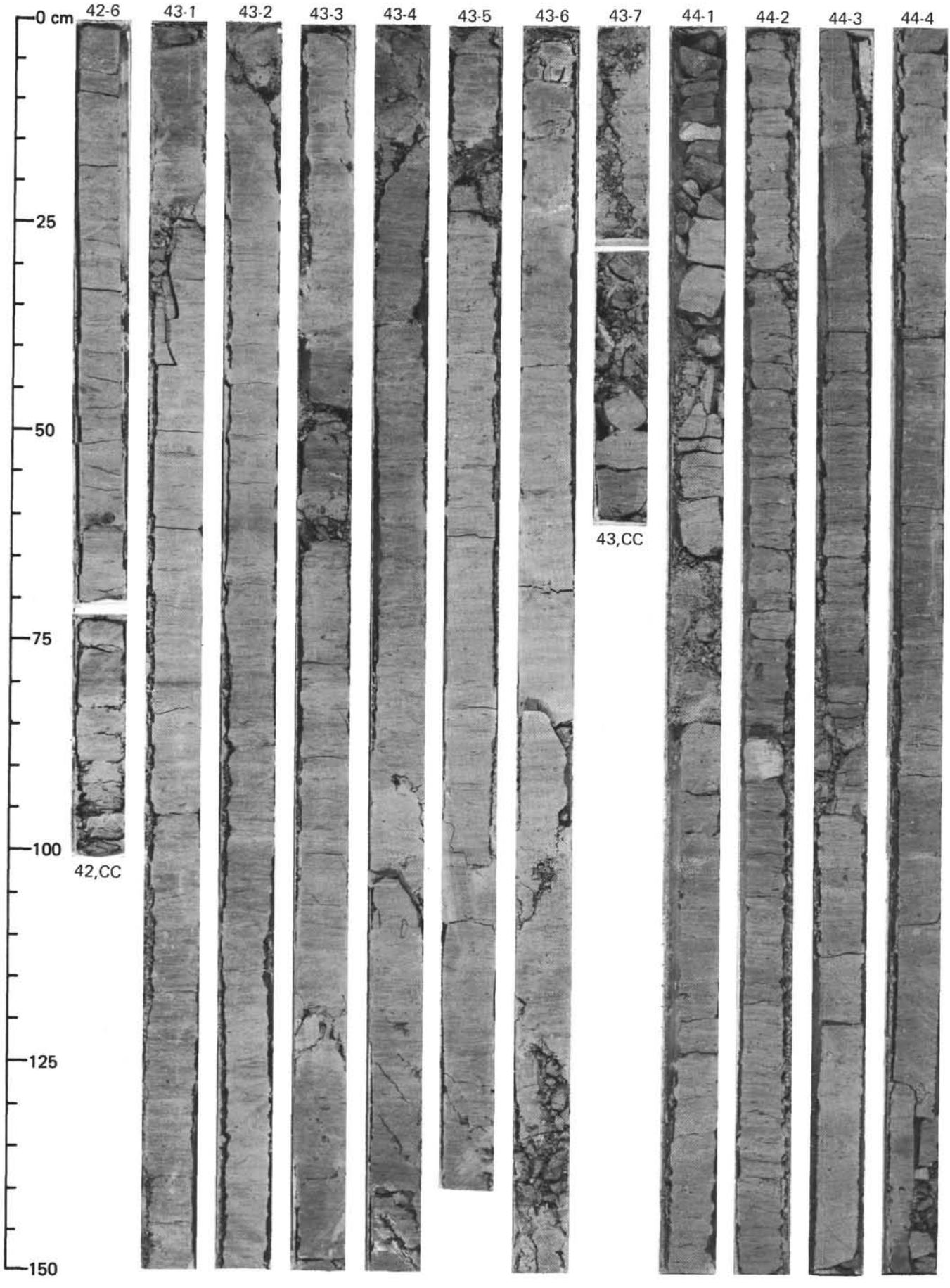
0 cm
25
50
75
100
125
150
42-6
42,CC
43-1
43-2
43-3
43-4
43-5
43-6
43-7
43,CC
44-1
44-2
44-3
44-4

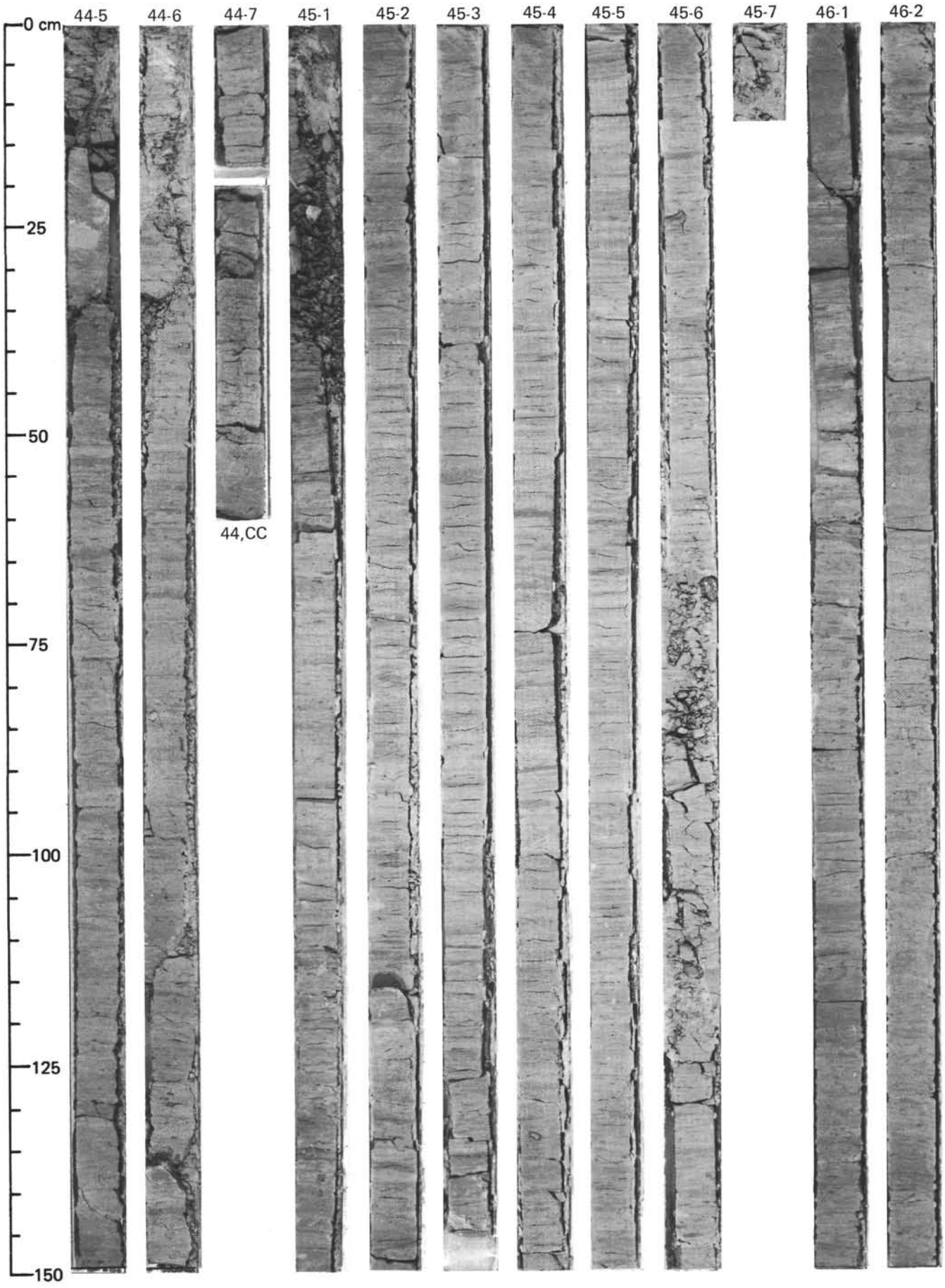
0 cm
25
50
75
100
125
150
44-5
44-6
44-7
44,CC
45-1
45-2
45-3
45-4
45-5
45-6
45-7
46-1
46-2

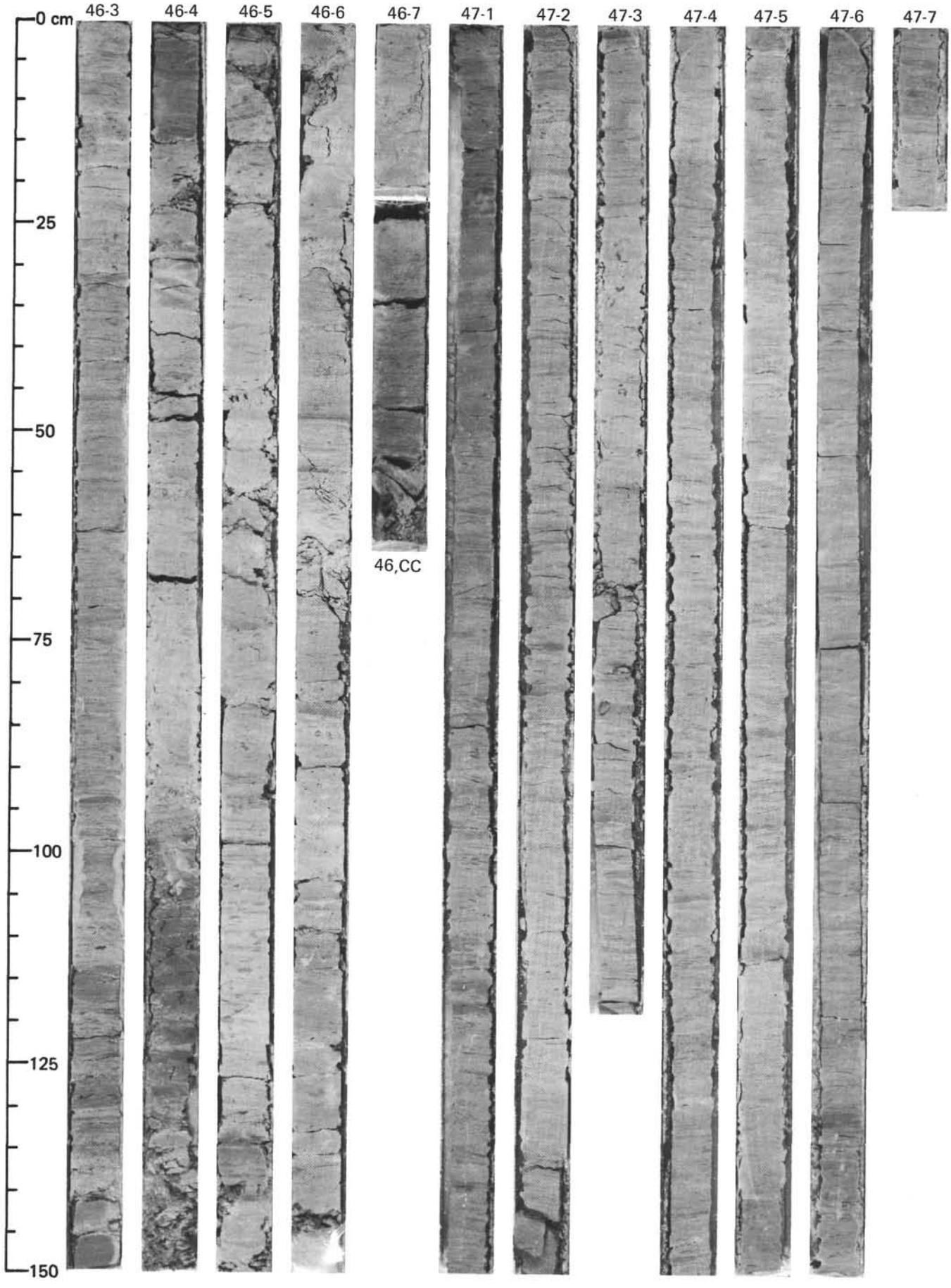
0 cm
25
50
75
100
125
150
46-3
46-4
46-5
46-6
46-7
46,CC
47-1
47-2
47-3
47-4
47-5
47-6
47-7

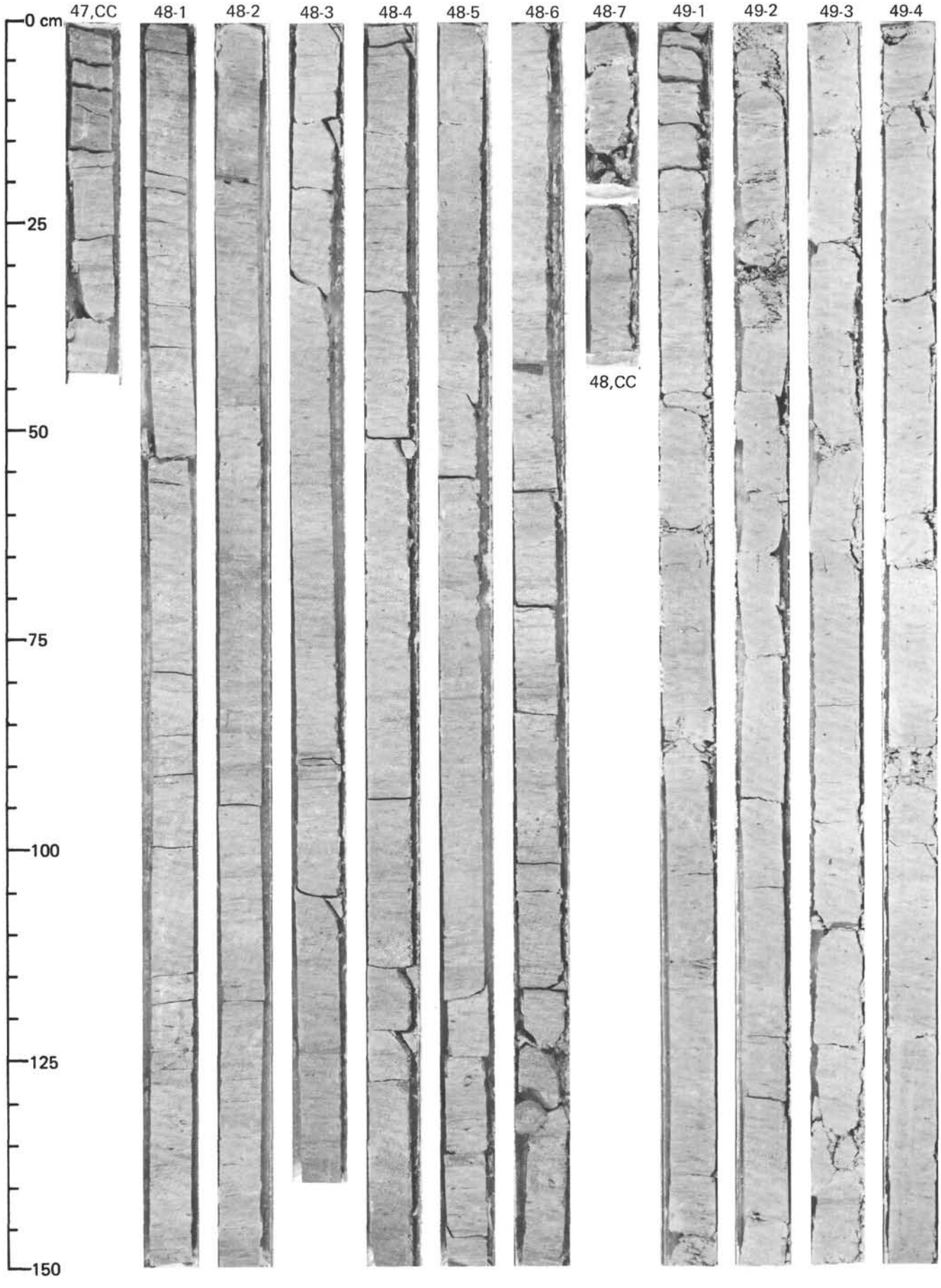
0 cm
25
50
75
100
125
150
47,CC
48-1
48-2
48-3
48-4
48-5
48-6
48-7
48,CC
49-1
49-2
49-3
49-4

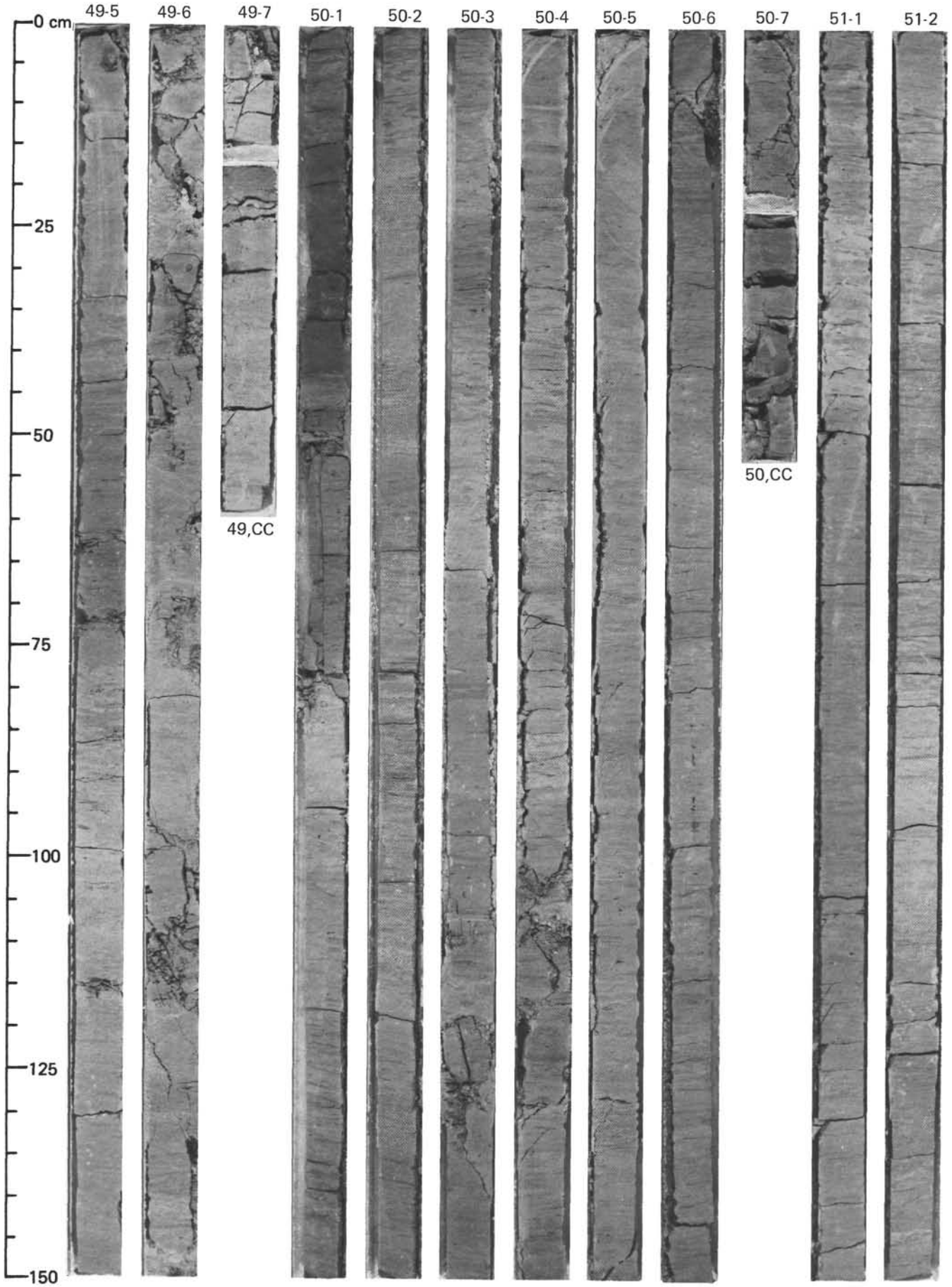
0 cm
25
50
75
100
125
150
49-5
49-6
49-7
49,CC
50-1
50-2
50-3
50-4
50-5
50-6
50-7
50,CC
51-1
51-2

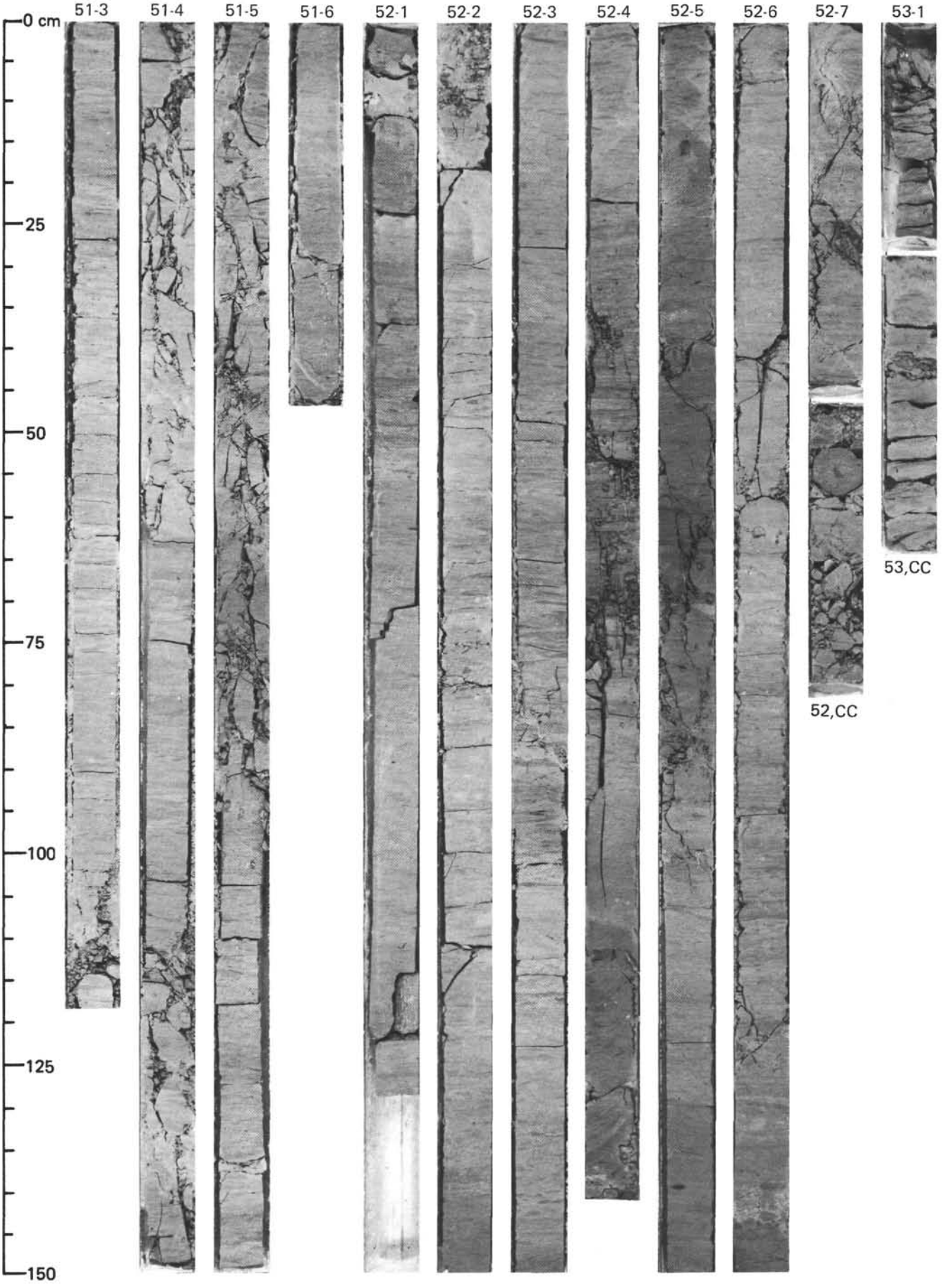
0 cm
25
50
75
100
125
150
51-3
51-4
51-5
51-6
52-1
52-2
52-3
52-4
52-5
52-6
52-7
53-1
53,CC
52,CC

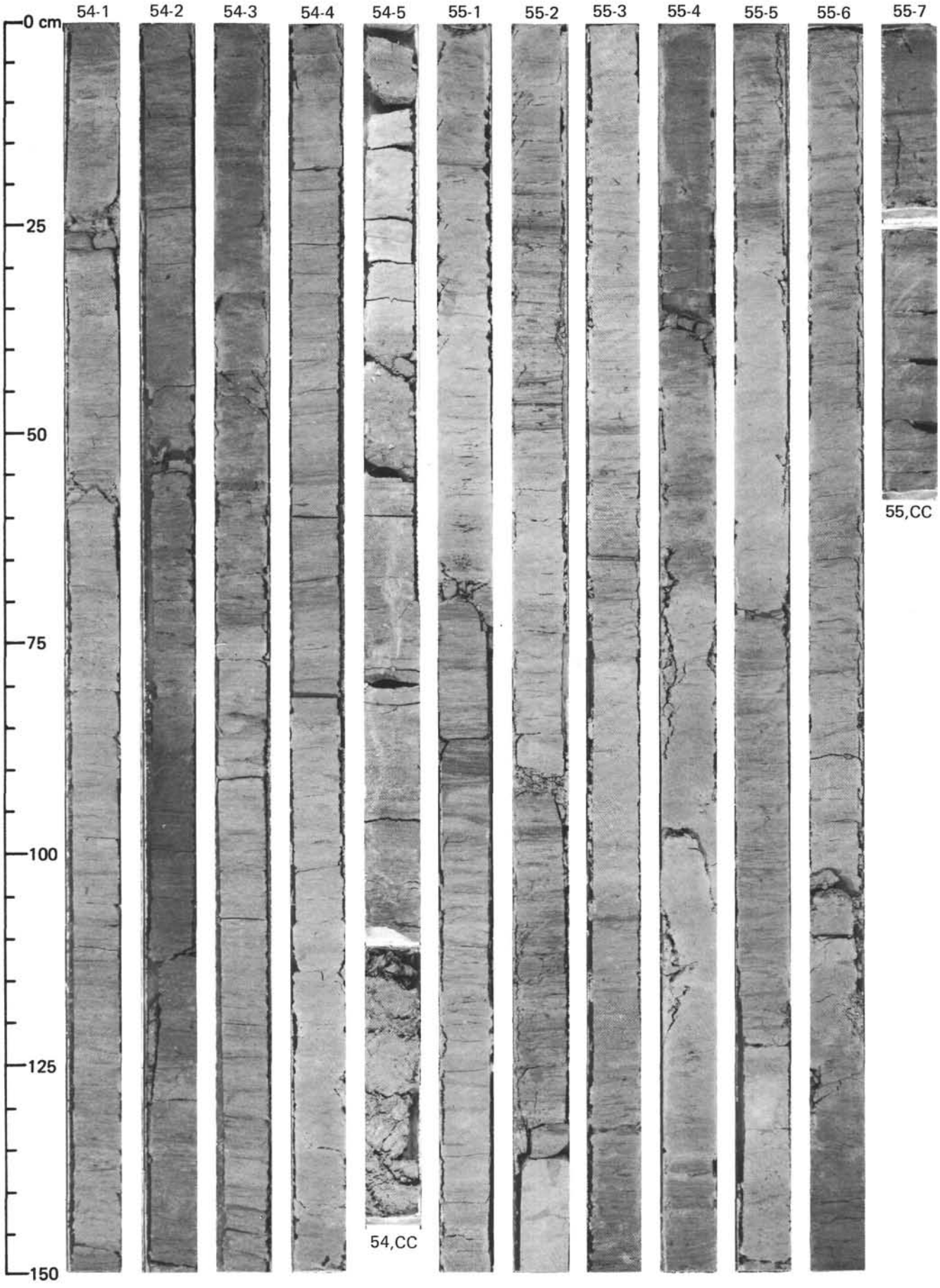
54-1
54-2
54-3
54-4
54-5
55-1
55-2
55-3
55-4
55-5
55-6
55-7
0 cm
25
50
75
100
125
150
54,CC
55,CC

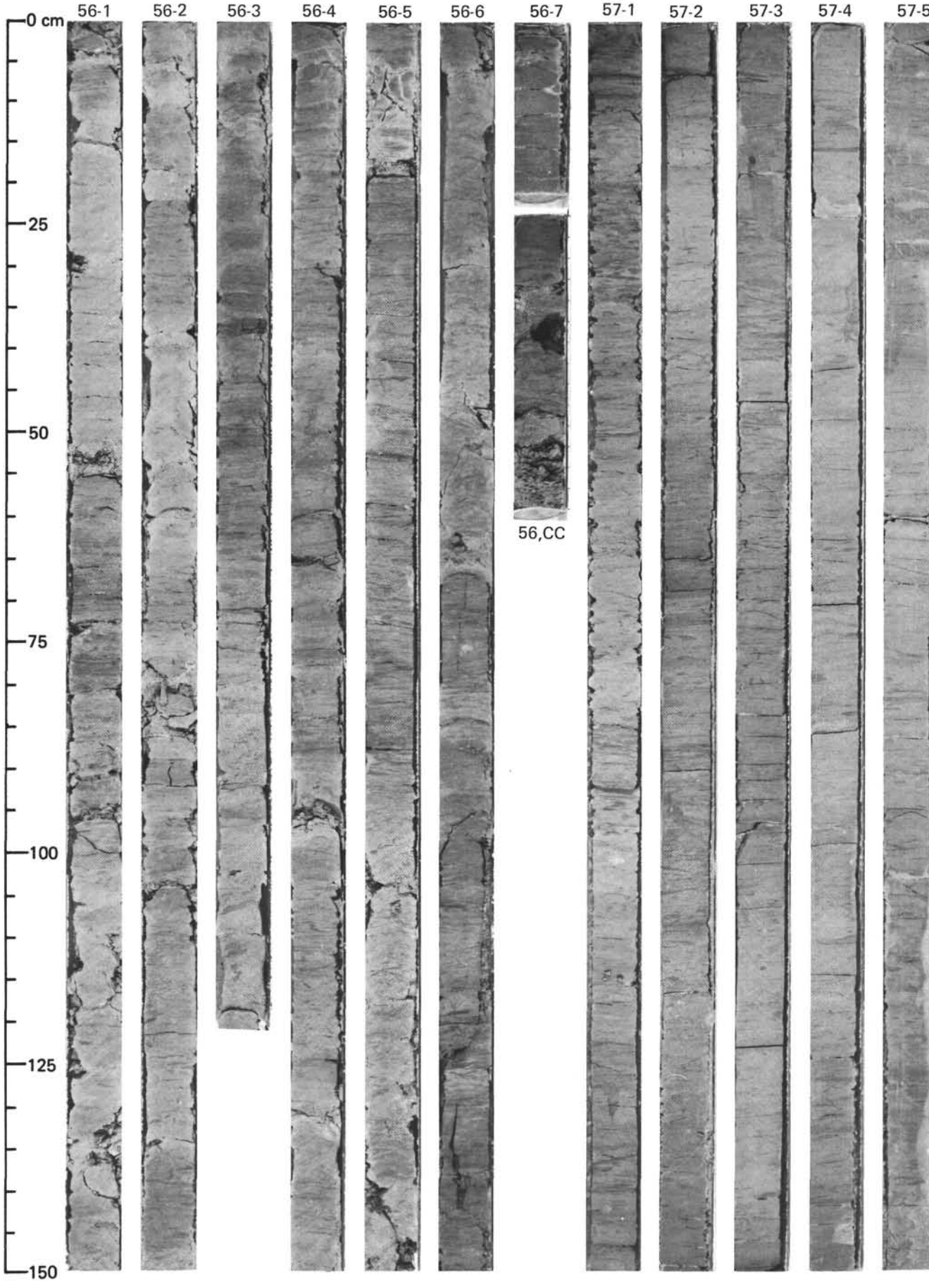
0 cm
25
50
75
100
125
150
56-1
56-2
56-3
56-4
56-5
56-6
56-7
56,CC
57-1
57-2
57-3
57-4
57-5

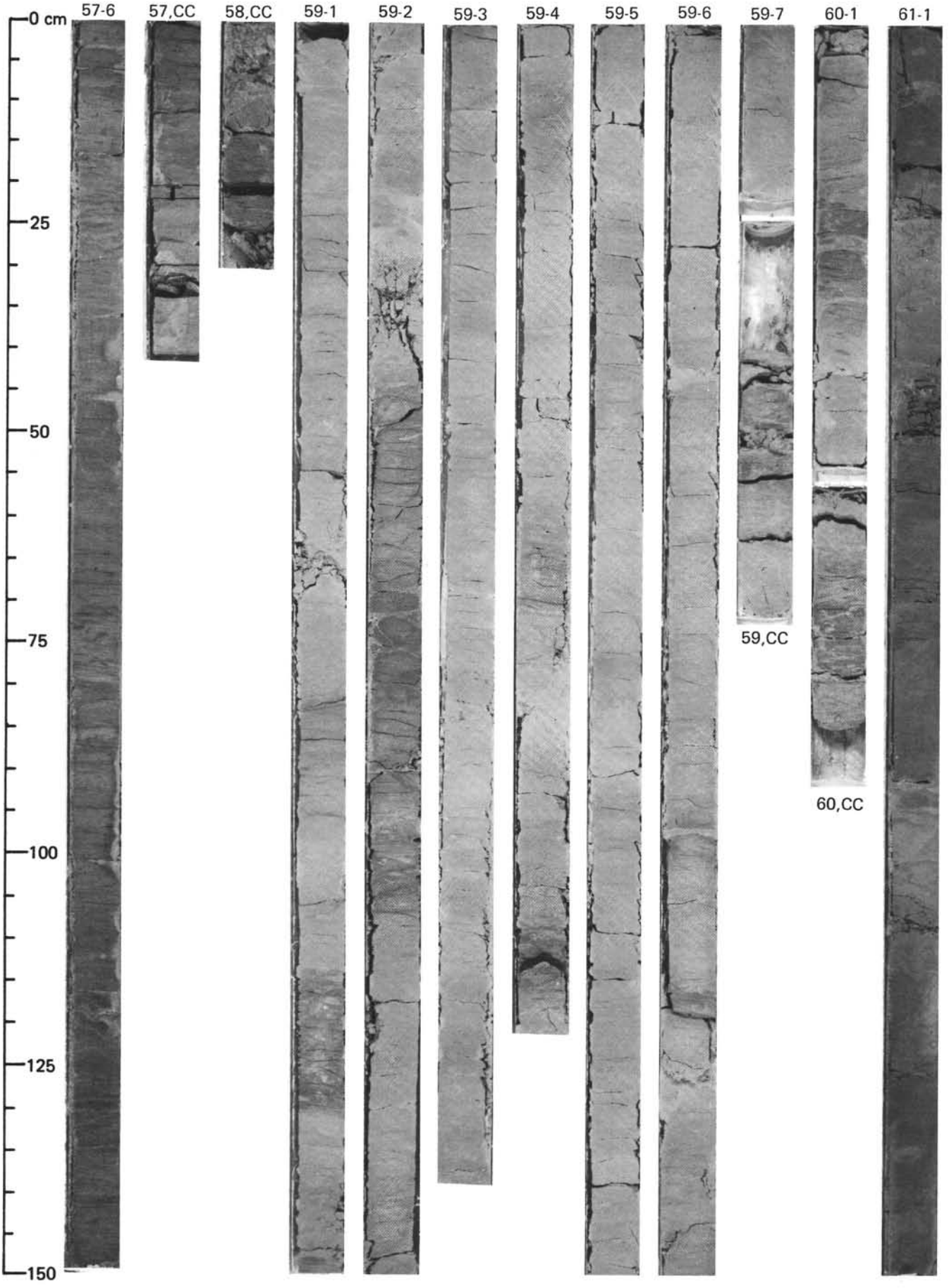
0 cm
25
50
75
100
125
150
57-6
57,CC
58,CC
59-1
59-2
59-3
59-4
59-5
59-6
59-7
59,CC
60-1
60,CC
61-1

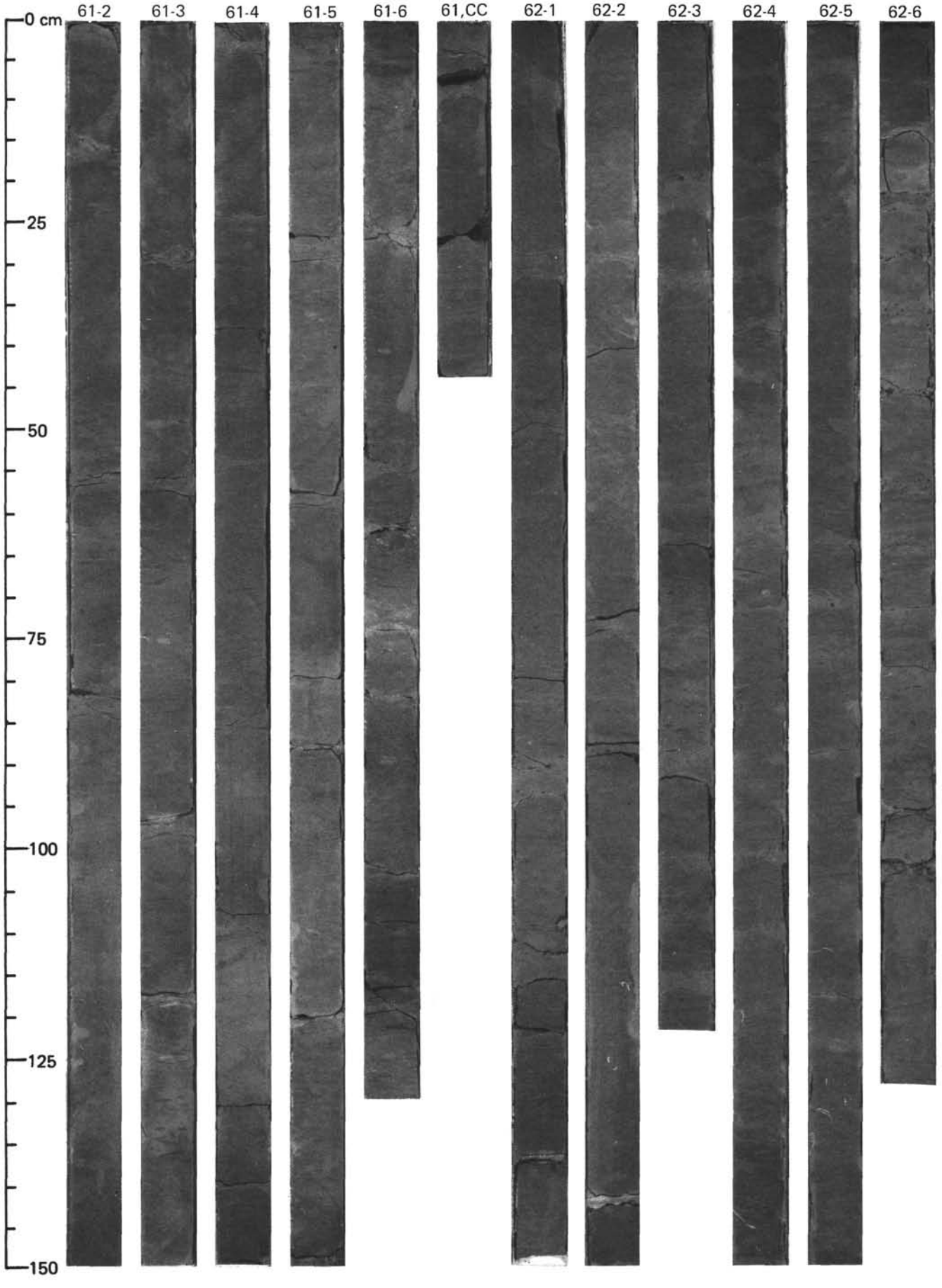
61-2
61-3
61-4
61-5
61-6
61,CC
62-1
62-2
62-3
62-4
62-5
62-6
0 cm
25
50
75
100
125
150

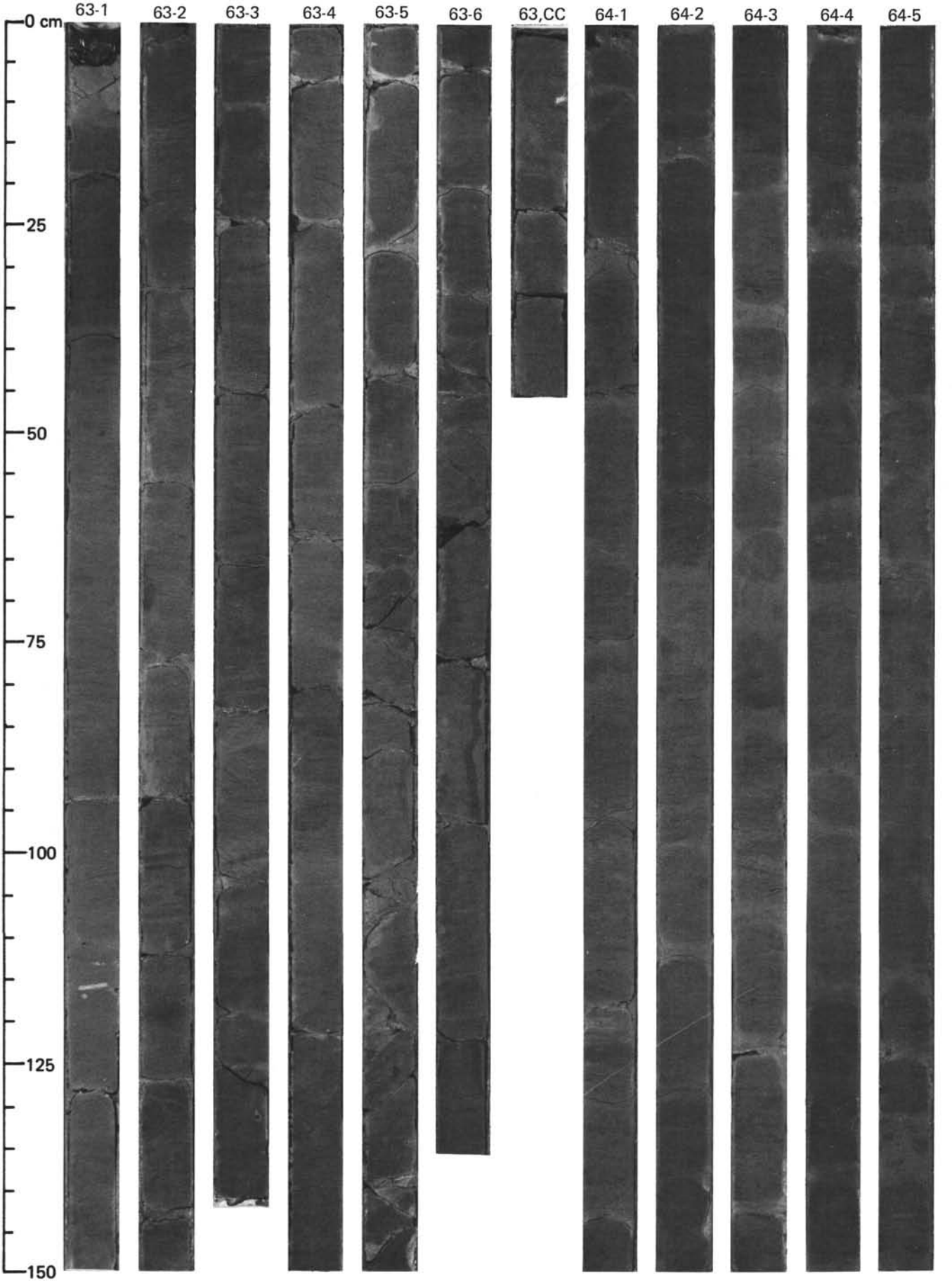
0 cm
25
50
75
100
125
150
63-1
63-2
63-3
63-4
63-5
63-6
63,CC
64-1
64-2
64-3
64-4
64-5

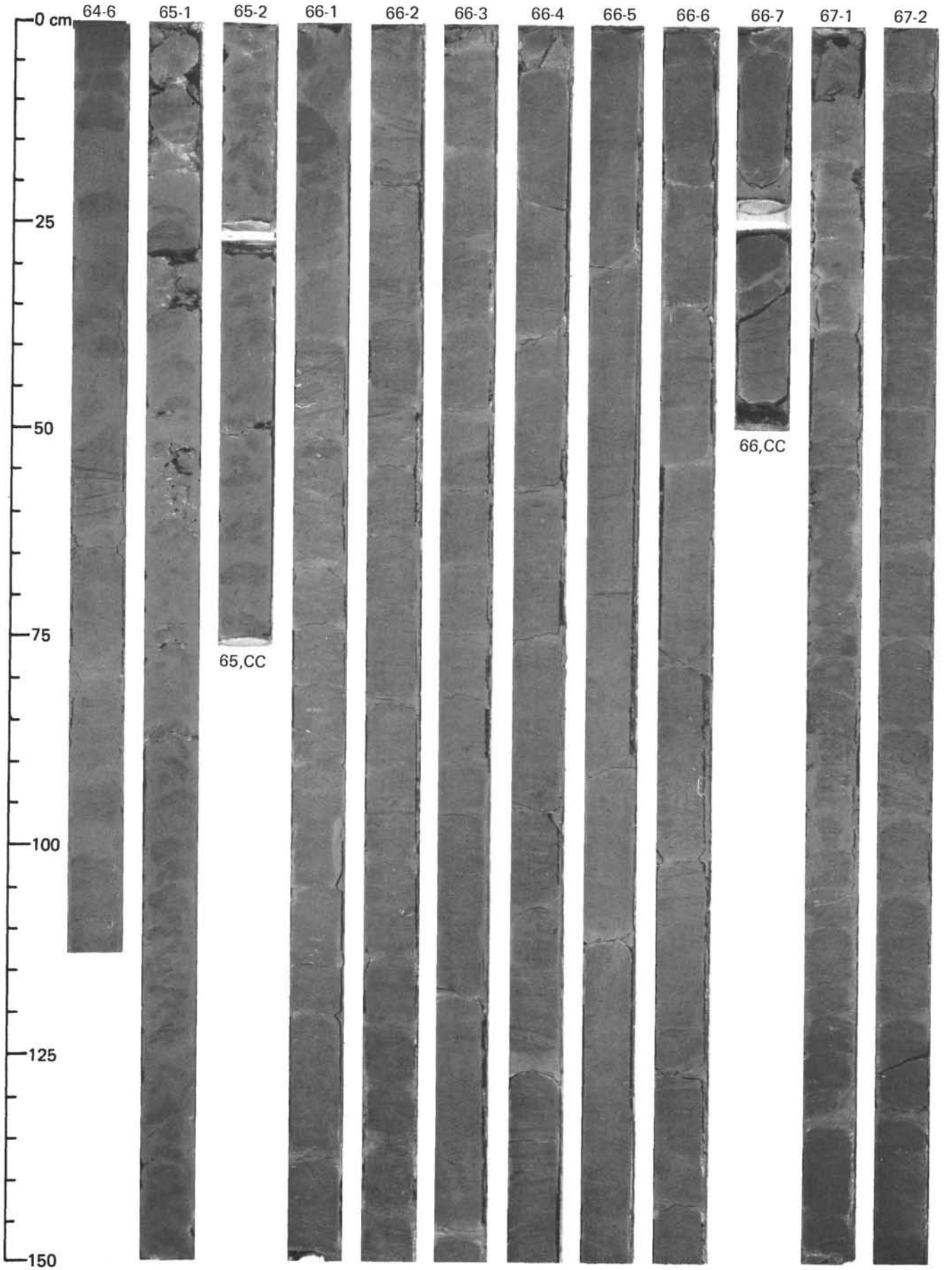
0 cm
25
50
75
100
125
150
64-6
65-1
65-2
65,CC
66-1
66-2
66-3
66-4
66-5
66-6
66-7
66,CC
67-1
67-2

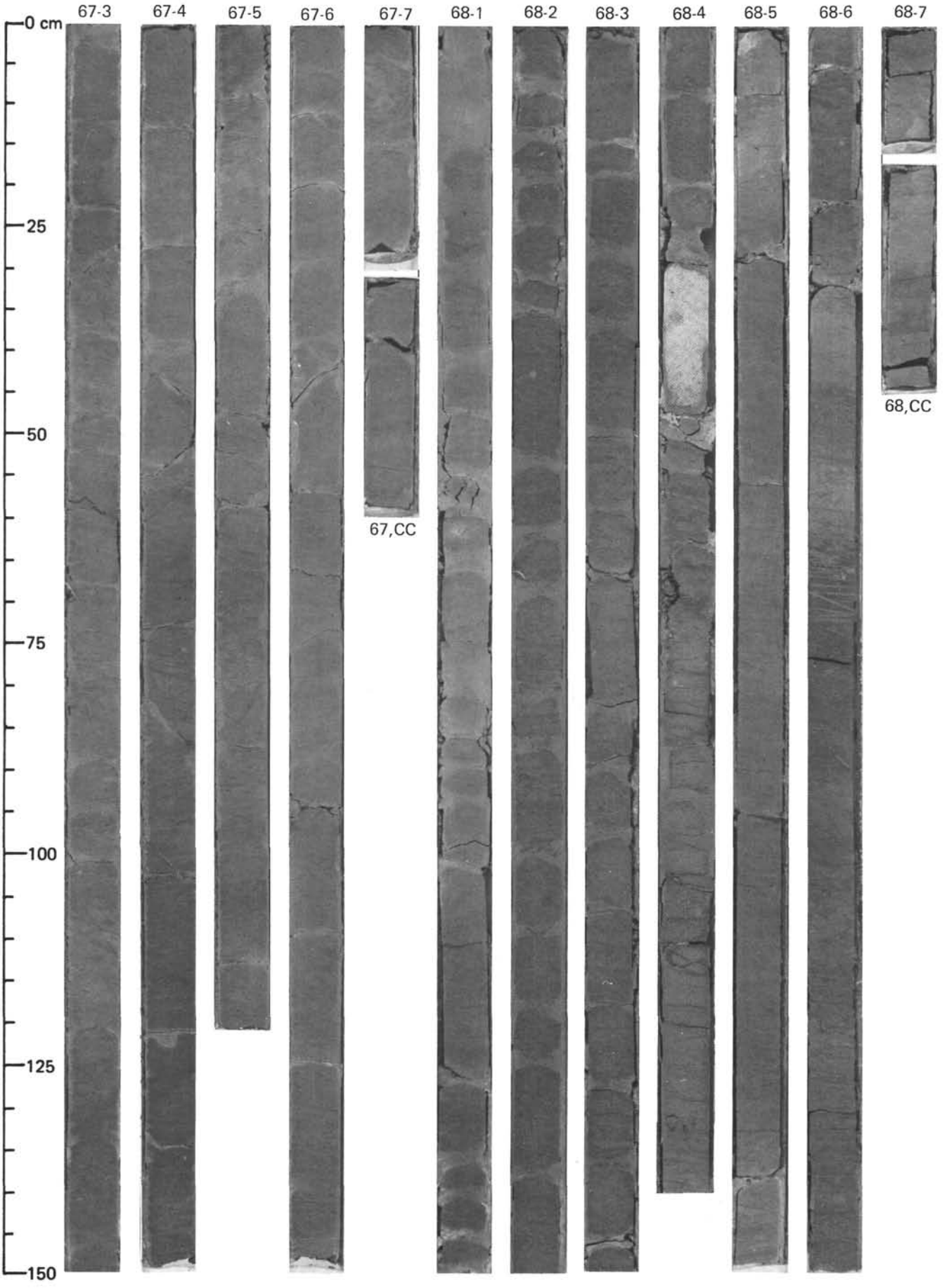
67-3
67-4
67-5
67-6
67-7
68-1
68-2
68-3
68-4
68-5
68-6
68-7
0 cm
25
50
75
100
125
150
67,CC
68,CC

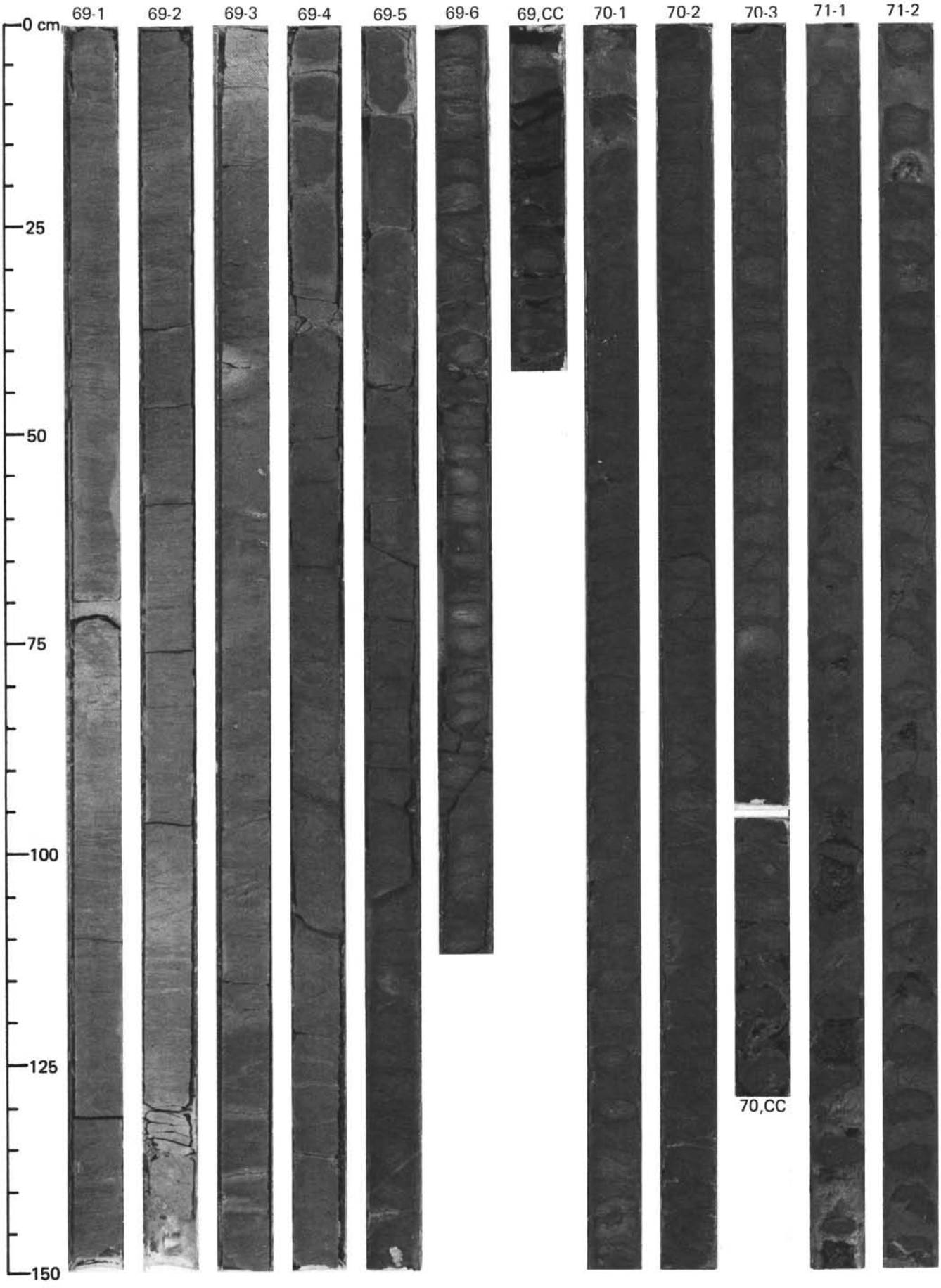
69-1
69-2
69-3
69-4
69-5
69-6
69,CC
70-1
70-2
70-3
71-1
71-2
0 cm
25
50
75
100
125
150
70,CC

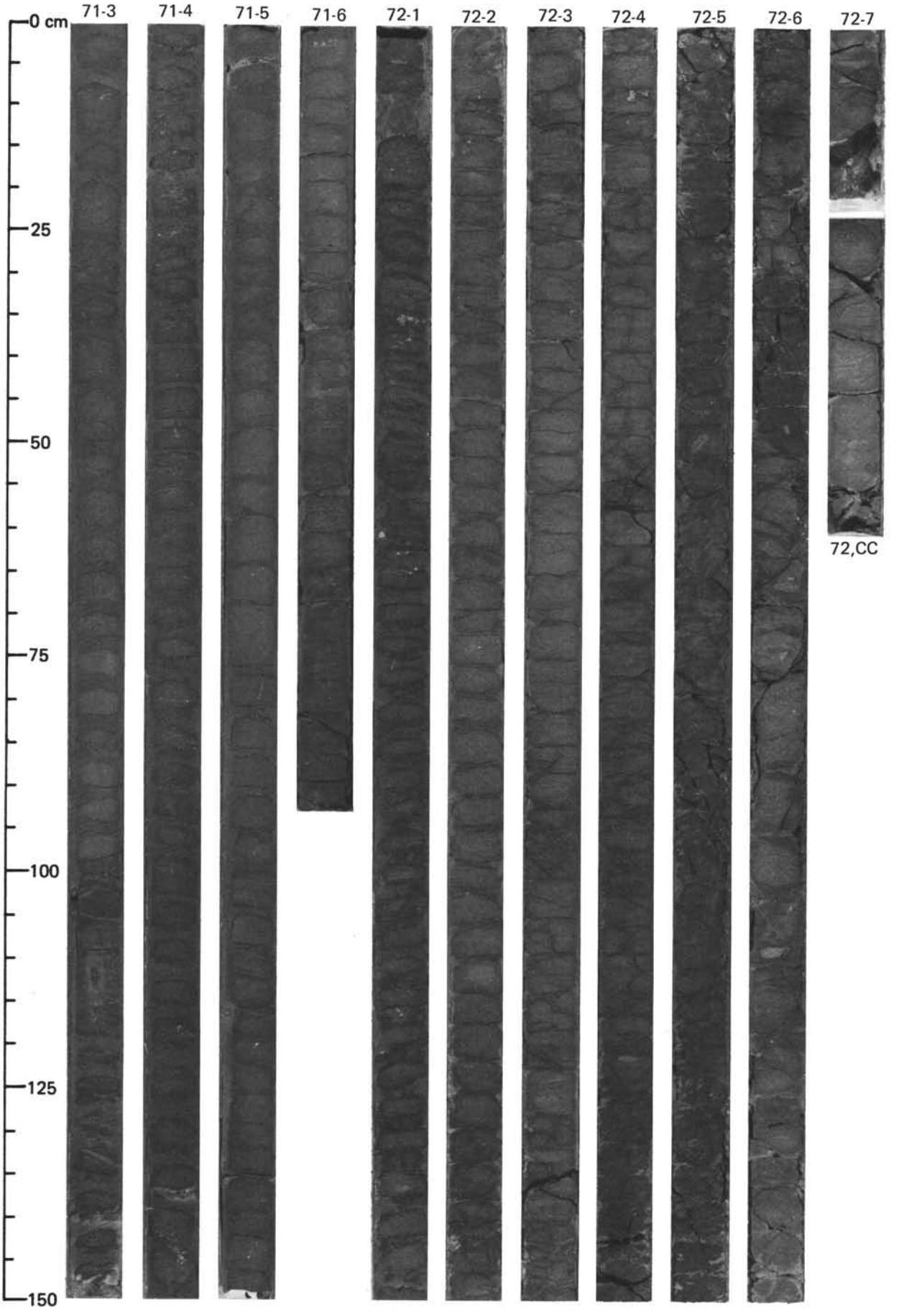
0 cm
25
50
75
100
125
150
71-3
71-4
71-5
71-6
72-1
72-2
72-3
72-4
72-5
72-6
72-7
72,CC